AMP-activated Protein Kinase and Muscle Metabolism

Tracy Leigh Scheffler

Dissertation submitted to the faculty of the Virginia Polytechnic Institute and State University in partial fulfillment of the requirements for the degree of

Doctor of Philosophy
In
Animal and Poultry Sciences

David E. Gerrard, Committee Chair
Jeffery Escobar
Madlyn I. Frisard
Matthew W. Hulver
Pablo Sobrado

July 11, 2012
Blacksburg, VA

Keywords: pork quality, skeletal muscle, mitochondria, calcium

AMP-activated Protein Kinase and Muscle Metabolism

Tracy Leigh Scheffler

ABSTRACT

AMP-activated protein kinase (AMPK) is a major regulator of skeletal muscle metabolism with relevance to agriculture and human health. During the conversion of muscle to meat, the rate and extent of postmortem metabolism and pH decline largely determine pork quality development. Pigs with the AMPKγ3 R200Q mutation generate pork with low ultimate pH (pH_u); this is attributed to high glycogen content, and greater "potential" to produce lactate and H^+. We hypothesized that decreasing muscle phosphocreatine and creatine would decrease ATP buffering capacity, resulting in earlier termination of glycolysis and pH decline. Dietary supplementation with the creatine analogue, β-GPA, decreased muscle total creatine but negatively affected performance. Another experiment was conducted using control or β-GPA diet and wild type and AMPKγ3^{R200Q} pigs in a 2×2 factorial design. The loss of muscle total creatine was important in maintenance of ATP levels in AMPKγ3^{R200Q} muscle early postmortem. Moreover, elevated glycogen did not affect pH_u, supporting that energetic modifications induced by feed restriction and β-GPA supplementation influence extent of pH decline. Next, we utilized a line of pigs selected for differences in pH_u. Another AMPKγ3 mutation (V199I), which is associated with higher pH_u and lower glycolytic potential, was prevalent. The 199II genotype increased pH_u in castrated males only. The wild type VV genotype increased glycolytic potential, but neither glycolytic potential nor lactate predicted pH_u.

In humans, AMPK activation is at least partly responsible for the beneficial effects of exercise on glucose transport and increased oxidative capacity in skeletal muscle. An inverse relationship

exists between skeletal muscle fiber cross-sectional area and oxidative capacity, which suggests muscle fibers hypertrophy at the expense of oxidative capacity. Therefore, we utilized pigs possessing mutations associated with increased oxidative capacity (AMP-activated protein kinase, AMPK$\gamma 3^{R200Q}$) or fiber hypertrophy (ryanodine receptor 1, RyR1^{R615C}) to determine if these events occur in parallel. RyR1^{R615C} increased muscle fiber size; AMPK$\gamma 3^{R200Q}$ increased oxidative capacity, evidenced by enhanced enzyme activity, mitochondrial function, and expression of mitochondrial proteins. Thus, pigs with both AMPK$\gamma 3^{R200Q}$ and RyR1^{R615C} possess increased fiber size and oxidative capacity, suggesting hypertrophy and oxidative capacity can occur simultaneously in skeletal muscle.

Acknowledgements

This has been quite a journey, and I cannot thank everyone enough for all the help and support along the way.

Many thanks to

Dr. Dave Gerrard, my advisor: for providing an escape route from my cubicle job to academic research. At the very beginning of grad school, I never intended to go into academia or become a science junkie, but sometimes it is better if I don't plan everything. I appreciate the advice, guidance, and opportunities; and for the debates and discussions about science.

Dr. Madlyn Frisard and Dr. Matt Hulver: your knowledge regarding mitochondria and muscle metabolism has been invaluable. Thank you for your suggestions and expertise which facilitated getting "piggy mito" assays up and running; and for letting me use your lab and equipment.

Dr. Pablo Sobrado: for your expertise in protein biochemistry, and for being a kind and genuine teacher.

Dr. Jeffery Escobar: for your input and suggestions, and for the wonders of Sigma Plot.

All of my Muscle Biology and Meat Science labmates: Jason Scheffler, Suny Park, Steve Kasten, Eric England, Kim Fisher, B-rad Reinholt, Greg van Eyk, Haibo 'Ben' Zhu, Christiaan Kapper, Sulaiman Matarneh. Thanks for many hours of help, particularly with sampling at the Meat Science Center, and for friendship in and out of Litton-Reaves. Thanks to all of you, I have many great memories from various adventures: golfing, Memorial Day BBQ, hiking…
Special thanks to: Jason, for listening, helping, and always reminding me to set a date; Suny, for being my mentor in the lab when I started my PhD – your personality and sense of humor always made work more fun than it should be.
Kim, for being a great officemate and friend, and for inside jokes and always having chocolate when needed (which was often).

Undergraduate lab workers: Erin Deliere, Amber Rosser, Jessie Gilbert, Caitlin Ray. These wonderful young ladies have provided much assistance with experiments and processing samples.

VT Meat Science Center –Mark Stevenson, for his expertise in harvesting; and Hengjian Wang, for assistance and use of his lab equipment; and to many others who helped with numerous harvests for projects.

VT Swine Center – Ryan Roberson and Mike Ashby, thank you for helping with the less glamorous parts of my research! Your willingness to assist with weighing pigs, getting tails, mixing feed, etc. was greatly appreciated. Ryan, thank you for your diligence and all the progress at the Swine Center.

Frisard/Hulver laboratory: for helping me with assays (particularly Ryan McMillan and Yaru Wu), and putting up with the extra person roaming around your lab.

Fellow graduate students, Hokie Hops, and friends: for your camaraderie and much-needed diversions.

Cindy Hixon: you always point me in the right direction, whether it is who to talk to, where something is, or where my advisor is. I admire your grit, and hope I don't ever get on the wrong side of it!

Ellie Stephens: for guidance enduring graduate school paperwork.

Pat Williams: before we even arrived at Virginia Tech, you were providing advice and assistance getting the lab equipped, and you have continued to be a tremendous resource during my time here. Thank you for taking over the ordering for our lab; it has been a huge help!

Family: for unconditional love and support. **Mom and Dad**: I can't express how grateful I am for all that you have done (and not done!) for me. Thank you for not making things too easy, yet always being there to provide encouragement.

Jason: it is only fitting that the person who puts up with me the most gets extra thanks…even then, I am fairly (ok, definitely) certain it is not enough. I don't know what I would do without you. I am glad it is *our* journey.

Table of Contents

Abstract ... ii

Acknowledgements ... iv

Table of Contents ... vi

List of Figures ... ix

List of Tables ... xii

Chapter 1. Introduction and Literature Review – Meat Quality ... 1

Introduction ... 1

Muscle metabolism ... 2

Conversion of muscle to meat ... 5

Lactic acidosis and pH ... 8

The evolution of the "Hampshire Effect", Rendement Napole (RN^-), and AMP-activated protein kinase (AMPK) ... 12

Summary ... 18

References ... 20

Chapter 2. Use of dietary supplementation with β-guanidinopropionic acid to alter phosphocreatine content, postmortem metabolism, and pork quality ... 24

Abstract ... 24

Introduction ... 25

Materials and Methods ... 26

Results and Discussion ... 30

Conclusions ... 37

References ... 49

Chapter 3. The creatine analog β-guanidinopropionic acid hastens postmortem muscle metabolism in pigs with AMP-activated protein kinase γ3 R200Q mutation ... 51

Abstract ... 51

Introduction ... 52

Materials and Methods ... 53

Results and Discussion ... 57

Conclusions....64
References....76

Chapter 4. High glycolytic potential does not predict low ultimate pH....79
Abstract....79
Introduction....80
Materials and Methods....81
Results and Discussion....83
Conclusions....89
References....101

Chapter 5. Introduction and Literature Review – Skeletal Muscle Metabolism and Growth....103
Introduction....103
Muscle phenotype....104
Mitochondria in skeletal muscle....107
Skeletal muscle plasticity....117
Muscle protein turnover....119
Protein synthesis....120
Protein degradation....123
Signaling pathways controlling muscle phenotype....128
Akt/mTOR....128
AMPK-PGC1α....130
Calcium....136
MAPK pathways....142
Nuclear factor-κB (NF-κB)....144
Antagonism between AMPK/PGC1α and Akt/mTOR....145
Summary....149
References....150

Chapter 6. Fiber hypertrophy and increased oxidative capacity can occur simultaneously in pig glycolytic skeletal muscle....166
Abstract....166

Introduction.....167
Materials and Methods.....169
Results.....175
Discussion.....182
References.....198

List of Figures

Chapter 1

Figure 1-1. Contribution of creatine kinase (CK) and adenylate kinase (AK) catalyzed reactions to ATP production....4

Figure 1-2. The glycogenolytic/glycolytic pathway 10

Chapter 2

Figure 2-1. Phosphocreatine, creatine, and total pool (PCr + Cr) in *longissimus* muscle of control and β-GPA treatments (1 wk or 2 wk). 38

Figure 2-2. Pork quality characteristics of pigs consuming control and β-GPA supplemented diets (1 or 2 wk). 39

Figure 2-3. Postmortem pH decline in *longissimus* muscle of control and β-GPA supplemented (1 or 2 wk) pigs 40

Figure 2-4. Postmortem changes in glycogen, glucose 6-phosphate, and lactate content of longissimus muscle of control and β-GPA supplemented (1 or 2 wk) pigs 41

Figure 2-5. Phosphocreatine, creatine, and total pool (PCr + Cr) in *longissimus* muscle of control, pair-fed (PF), and β-GPA (2 wk). 44

Figure 2-6. Pork quality characteristics of control, pair-fed (PF), or β-GPA supplemented diets (1 or 2 wk)....45

Figure 2-7. Postmortem pH decline in *longissimus* muscle of control, pair-fed (PF) and β-GPA supplemented pigs....46

Figure 2-8. Postmortem changes in glycogen and lactate content of *longissimus* muscle of control, pair-fed (PF) and β-GPA supplemented pigs 47

Figure 2-9. ATP, ADP, and ATP/ADP contents in *longissimus* muscle of control, pair-fed (PF) and β-GPA pigs. 48

Chapter 3

Figure 3-1. Phosphocreatine, creatine, and total pool (PCr + Cr) in longissimus muscle of AMPKγ3 and β-GPA supplemented pigs. 66

Figure 3-2. Postmortem changes in glycogen content of longissimus muscle of wild type (pooled control and β-GPA) and AMPKγ3R200Q (pooled AMPKγ3 and AMPKγ3+β-GPA) pigs. 67

Figure 3-3. Postmortem changes in glucose 6-phosphate (A) and glucose (B) content of longissimus muscle of wild type (pooled control and β-GPA) and AMPKγ3R200Q (pooled AMPKγ3 and AMPKγ3 + β-GPA) pigs. 68

Figure 3-4. Postmortem changes in lactate content of longissimus muscle of control, AMPKγ3, β-GPA, and AMPKγ3 + β-GPA pigs. 69

Figure 3-5. ATP content in *longissimus* muscle of control, AMPKγ3, β-GPA, and AMPKγ3 + β-GPA pigs. 70

Figure 3-6. Influence of diet (A) and genotype (B) on postmortem ADP contents in longissimus muscle 71

Figure 3-7. AMP contents in longissimus muscle of wild type (pooled control and β-GPA) and AMPKγ3R200Q (pooled AMPKγ3 and AMPKγ3 + β-GPA) pigs. 72

Figure 3-8. Postmortem IMP content in longissimus muscle. 73

Figure 3-9. Postmortem pH decline in longissimus muscle of control, AMPKγ3, β-GPA, and AMPKγ3 + β-GPA pigs. 74

Chapter 4

Figure 4-1. The pH of *longissimus* muscle at 45 min (A) and 24 h (pH_u; B) in AMPKγ3 199 genotypes. 93

Figure 4-2. Distribution of *longissimus* muscle glycolytic potential (GP) of AMPKγ3 199 genotypes 95

Figure 4-3. Relationship between *longissimus* muscle glycolytic potential (GP) and ultimate pH (pH_u) in AMPKγ3 199 genotypes. 96

Figure 4-4. Relationship between lactate and pH in *longissimus* muscle. 97

Figure 4-5. *Longissimus* muscle lactate content at 24 h postmortem in AMPKγ3 199 genotypes…98

Figure 4-6. Residual glycogen content (A), glucose 6-phosphate content (B), and glycolytic potential (GP; C) in *longissimus* muscle at 24 h postmortem 99

Figure 4-7. Ultimate pH (pH_u) and lactate content in *longissimus* muscle at 24 h postmortem..100

Chapter 5

Figure 5-1. Mitochondria fusion and fission 107

Figure 5-2. Peroxisome proliferator activated receptor γ coactivator 1α (PGC1α) regulation of gene transcription. 109

Figure 5-3. Electron transport chain in mitochondria. 112

Figure 5-4. Structure of AMPK. 130

Figure 5-5. Regulation of AMPK activity by upstream kinases, allosteric activation, and phosphatases 131

Figure 5-6. Role of AMP-activated protein kinase (AMPK) in regulation of metabolism 133

Chapter 6

Figure 6-1. RyR1 mutation increases cross-sectional area (CSA) of longissimus muscle fibers but does not necessarily increase total muscle area 190

Figure 6-2. AMPKγ3^{R200Q} increases activity of key oxidative enzymes in longissimus muscle. 191

Figure 6-3. AMPKγ3^{R200Q} increases state 3 respiration in isolated mitochondria 192

Figure 6-4. Mitochondrial DNA (mtDNA) content of longissimus muscle from control and AMPK^{R200Q} and RyR1^{R615C} mutant pigs 194

Figure 6-5. Transcript levels of key regulators of mitochondrial biogenesis and nuclear DNA- and mitochondrial DNA-encoded proteins. 195
Figure 6-6. Mitochondrial protein expression in longissimus muscle 196
Figure 6-7. Ratio of LC3-II to LC3-I in longissimus muscle from AMPKγ3 and RyR1 genotypes. 197

List of Tables

Chapter 2

Table 2-1. Performance during trial period for control and β-GPA (1 wk and 2 wk) treatments 42

Table 2-2. Performance during trial period for control, pair-fed (PF), and β-GPA treatments. 43

Chapter 3

Table 3-1. Performance during 2 wk trial period for control, AMPKγ3, β-GPA, and AMPKγ3 + β-GPA pigs 65

Table 3-2. Meat quality characteristics of AMPKγ3 and β-GPA supplemented pigs 75

Chapter 4

Table 4-1. Live weight and carcass characteristics of castrated male and female pigs 90

Table 4-2. Meat quality attributes of *longissimus* muscle 91

Table 4-3. Number and percentage (in parentheses) of pigs with different genotypes at the AMPK γ3 V199I substitution site.....92

Table 4-4. Meat quality characteristics of *longissimus* muscle by AMPKγ3 199 genotype and sex 94

Chapter 6

Table 6-1. Respiratory control ratio (RCR) values of isolated mitochondria from different pig genotypes 193

Chapter 1. Introduction and Literature Review – Meat Quality

Introduction

The rate and extent of postmortem pH decline during the conversion of muscle to meat significantly influence the development of fresh meat quality attributes. Classically, the rate and extent of postmortem pH decline are considered to follow postmortem glycolysis, with glycogen being converted to "lactic acid." About fifty years ago, it was recognized that hastened glycolysis contributed to high muscle temperature and acidity, and the development of pale, soft, and exudative (PSE) pork (Briskey and Wismer-Pedersen, 1961; Wismer-Pedersen and Briskey, 1961). More recently, Monin & Sellier (1985) suggested that animals with greater initial muscle glycogen content, or high "glycolytic potential," had an increased capacity for postmortem glycolysis, which would lead to an extended pH decline and lower ultimate pH. This was largely based on elevated muscle glycogen and low ultimate pH ("acid meat") observed in the Hampshire breed. These rapid and extended pH declines in postmortem muscle negatively impact protein characteristics, albeit by different mechanisms, and thus generate inferior pork. Subsequently, "early" and "ultimate" pH measurements have been embraced as indicators of meat quality, and undoubtedly, there are countless examples of experiments supporting this connection between pH decline and the development of pork color, texture, and water-holding properties.

Yet, despite the ability to predict and detect PSE, we still have little understanding of the mechanisms contributing to rapid or extended pH declines. Although pH decline is considered to follow glycolysis and accumulation of lactic acid, postmortem metabolism encompasses creatine

kinase and adenylate kinase-catalyzed reactions as well as glycolysis. This well-orchestrated network of reactions attempts to meet ATP demands despite removal of the oxygen supply. Meanwhile, products of these reactions may serve as allosteric effectors for other enzymes in the network, thus providing important 'feedback' or 'feed-forward' signals to alter flux through the pathways. This is further complicated by the heterogeneity of muscle fibers, meaning that variation in fiber properties, including metabolic capacity and metabolite level, may influence the regulation and course of postmortem metabolism. Therefore, it is necessary to reevaluate muscle energy metabolism as it relates to the conversion of muscle to meat.

Muscle metabolism

ATP is the "energy currency" of the cell. The hydrolysis of high energy phosphate bonds of ATP provides energy that can be utilized for mechanical (muscle contraction), chemical (biosynthesis and anabolism), and osmotic (active transport) work. The breakdown of ATP is balanced by energy producing pathways that catabolize stored nutrients, such as glycogen or fats, to generate ATP. Altogether, these functions keep the cell alive and allow it to maintain a stable internal environment or "homeostasis". In most cells, increasing ATP production to meet energy consumption is not problematic because changes in utilization may only be 2-3 fold. However, skeletal muscle energy turnover can increase greater than 100-fold during high intensity work (Meyer and Foley, 1996). In this case, if ATP (5-8 μmol/g muscle) was the sole source of energy, it would be exhausted in less than a second (Berg et al., 2002). Thus, muscle faces rather unique problems with regard to fuel homeostasis and metabolic regulation. In order to cope with various work intensities and durations, skeletal muscle possesses metabolic systems with

different capacities for generating ATP; these systems are also integrated via feedback and feed-forward control, in order to precisely match ATP demand with ATP consumption.

Under resting conditions, muscle has a low energy demand relative to other tissues, such as brain and liver. In fact, although skeletal muscle comprises approximately 40% of body mass, it is much less active at rest than other tissues on a per unit basis (Levine et al., 2000). Therefore, the ATP requirement for muscle at rest is easily met by aerobic (oxidative) metabolism. Glycogen (or glucose) is metabolized in glycolysis to pyruvate, which is converted to acetyl CoA; fats are broken down via β-oxidation to yield acetyl CoA. In the mitochondria, acetyl CoA units enter the TCA cycle to generate reducing equivalents (NADH and $FADH_2$) for use by the electron transport chain, which generates a proton gradient to power ATP synthesis. The maximum rate of oxidative phosphorylation is determined by an individual's ability to transport and utilize oxygen. The maximum oxygen utilization rate is far below the maximal ATP turnover rate in muscle, so oxidative metabolism is a "low power" system for regenerating ATP. However, oxidative metabolism can operate for long periods of time.

When muscle transitions from rest to work, ATP turnover may exceed oxygen utilization. This necessitates that muscle must be capable of quickly generating ATP in the absence of oxygen. Phosphocreatine (PCr), or the phosphagen system, serves as a temporal energy buffer; it is utilized to maintain ATP until other metabolic systems are activated and running. High creatine kinase (CK) activity in muscle promotes conversion of ADP and PCr to ATP and creatine (Cr) (Figure 1-1). This, along with the relatively high content (24 to 30 μmol/g muscle) of PCr compared to ATP, allows rapid generation of ATP, but it is only effective for brief periods (Meyer and Foley, 1996). Under circumstances of high work intensity, PCr may only last several seconds, leading to a decline in ATP content. Increased breakdown of ATP results in

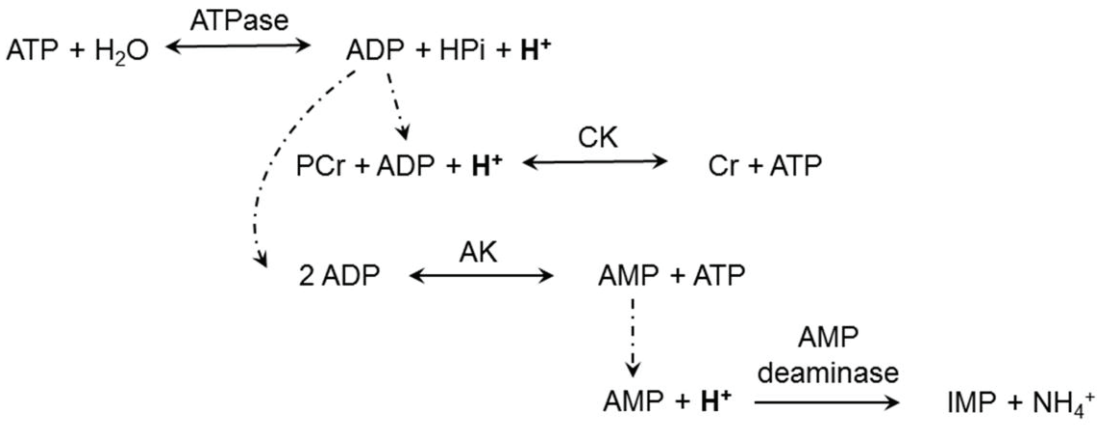

Figure 1-1. Contribution of creatine kinase (CK) and adenylate kinase (AK) catalyzed reactions to ATP production. AMP is deaminated to inosine monophosphate (IMP) to preserve high ATP/ADP and free energy of ATP hydrolysis. H+ are released by ATP hydrolysis, and H+ are consumed by CK and AMP deaminase reactions.

elevated levels of free ADP. Limiting ADP accumulation is important because the free energy released from ATP hydrolysis declines as the concentration of products, ADP and inorganic phosphate (Pi), increase, and/or substrate concentration (ATP) decreases. Adenylate kinase and AMP deaminase play important roles by limiting the accumulation of ADP when ATP turnover is high. Adenylate kinase utilizes 2 ADP to generate AMP and ATP. In turn, increases in AMP are limited by AMP deaminase, which irreversibly converts AMP to inosine monophosphate. Together, the adenylate kinase and AMP deaminase reactions preserve high ATP/ADP and free energy of ATP hydrolysis, at the cost of total adenine nucleotide pool. As a result of high ATP turnover and the adenylate kinase reaction, the AMP:ATP ratio increases. The AMP:ATP is a particularly sensitive indicator of cellular energy status or "energy charge." Moreover, increases in free AMP and ADP are important allosteric activators of key enzymes in the glycolytic pathway, thereby increasing flux through glycogenolysis and glycolysis in order to enhance ATP generation. Muscle glycogen is broken down and metabolized through glycolysis to pyruvate. When oxygen is limiting, pyruvate is reduced to lactic acid by lactate dehydrogenase; NAD^+ is

also regenerated to ensure that glycolysis can continue to operate under anaerobic conditions. Initiation of anaerobic glycolysis occurs fairly quickly, but anaerobic glycolysis cannot support maximal efforts nor can it be maintained at a high level for very long.

Conversion of muscle to meat

The metabolic pathways during the conversion of muscle to meat parallel those that occur in living muscle under anoxic or ischemic conditions. When the animal is harvested, exsanguination removes the blood supply, and hence the ability to deliver oxygen to the tissue. Metabolically active muscle must adapt to these circumstances to maintain homeostasis. ATP production is necessary to keep the muscle in the relaxed state, fuel active transport, and maintain ion gradients. Initially, the creatine kinase reaction supplies ATP. Once ~70% of the PCr pool has been degraded, ATP levels rapidly decline (Bendall, 1951). Meanwhile, the breakdown of ATP results in increasing ADP, which is utilized by the adenylate kinase reaction. Consequently, AMP increases and is deaminated to inosine monophosphate (IMP), which accumulates in postmortem muscle. Muscle glycogenolysis dominates the latter stages of postmortem metabolism, with glycogen being metabolized in anaerobic glycolysis to rephosphorylate ADP to ATP. Because there are no means to remove waste products, lactic acid accumulates. Whereas maximal ATP decrease in exercising muscle is 50% (Meyer and Foley, 1996), eventually all ATP will be depleted in postmortem muscle. As the breakdown of ATP exceeds its synthesis, less ATP is available to "relax" muscle; the formation of actomyosin crossbridges stiffens muscles, signaling the onset of rigor mortis. When ATP is depleted, crossbridges cannot be broken and muscle is relatively inextensible.

The rate and extent of postmortem pH decline are the main factors controlling pork quality development (Briskey, 1964; Monin and Sellier, 1985). Classically, pH decline is considered to follow postmortem glycolysis. As anaerobic glycolysis proceeds, glycogen is metabolized to lactic acid, which accumulates and decreases pH. Normally, pH of *longissimus* muscle declines gradually from 7.4 in living muscle to an ultimate pH of ~5.7 (Briskey, 1964). In the case of dark, firm, and dry (DFD) pork, postmortem muscle exhibits a gradual and subtle pH decline, with an ultimate pH greater than 6.0. This slight pH decline is associated with limited glycogen reserves, thus restricting the muscle's capacity for postmortem glycolysis. However, in the case of a rapid pH decline, muscles exhibit pH less than 6.0 during the first hour after slaughter. Rapid postmortem glycolysis and elevated muscle temperature are associated with a hastened pH decline and development of PSE pork. In contrast, muscles with an extended pH decline display normal rates of pH decline early postmortem but continue to a low ultimate pH of about 5.3 to 5.5, resulting in "acid meat." Monin and Sellier (1985) observed that Hampshire pigs generally exhibited higher muscle glycogen stores and lower ultimate pH; they suggested that elevated initial muscle glycogen content resulted in an increased capacity for postmortem glycolysis, which would lead to an extended pH decline and low ultimate pH. Hence, the muscle metabolites glycogen, glucose, glucose 6-phosphate and lactate were combined into a single measure to reflect all the compounds in muscle capable of being converted to lactate; this "glycolytic potential" indicated the muscle's capacity for postmortem glycolysis (Monin and Sellier, 1985).

Subsequently, meat scientists have relied heavily on glycogen, lactic acid, and glycolytic potential to explain postmortem metabolism and pH decline. Certainly, there is a significant relationship between muscle glycolysis and pH postmortem. In the case of DFD meat, the

muscle exhibits little postmortem metabolism because substrate and energy reserves are limiting. In "acid meat", high initial muscle glycogen is well correlated with low ultimate pH. Using this wide breadth of observations, a strong correlation between glycogen and ultimate pH was established. This has perpetuated the use of "glycolytic potential" to predict ultimate pH. However, using these correlations does not establish a cause and effect relationship. Although muscle glycogen content accounts for 40-60% of the variation in ultimate pH (Huff-Lonergan et al., 2002; Maribo et al., 1999), the relationship between glycogen content and ultimate pH is not linear. Residual glycogen is highly variable at low pH and pH values may plateau in the presence of residual glycogen (Immonen and Puolanne, 2000; van Laack and Kauffman, 1999). Glycogen alone does not determine the extent of postmortem metabolism.

Lactic acid is commonly used as an indicator of postmortem metabolism and muscle pH. Again, a correlation can be established using a wide range of lactic acid values observed in DFD and normal meat, but this does not necessarily show a cause and effect relationship. Since the introduction of "glycolytic potential" it has been misconstrued and oversimplified to mean that higher amounts muscle glycogen result in greater amounts of lactic acid and lower meat pH. Even some of the earliest observations of Hampshire muscle acknowledge that "increased glycogen disappearance was not completely accounted for by 24 h lactic acid content or ultimate pH of the muscle" (Sayre et al., 1963). Moreover, the original research article proposing glycolytic potential conveyed that Hampshire pigs possessed low ultimate *longissimus* muscle pH compared to Large White pigs, but fully recognized that lactic acid values were similar at 24-48 h and thus lactic acid could not be the cause of low ultimate pH (Monin and Sellier, 1985).

Lactic acidosis and pH

The accuracy of using 'lactic acidosis' and 'lactic acid' to explain the pH decline observed in postmortem muscle, as well as in exercising muscle, should be questioned. In the field of exercise physiology, "lactic acidosis" – the theory that during oxygen deprivation, lactic acid builds up in muscle and causes fatigue – has been a dogma since the 1920s. Early observations indicated associations between oxygen deprivation, lactic acid accumulation, and muscle fatigue, but did not establish direct causality. Within the past several years, new theories have ignited a fervent debate challenging the notion of lactic acidosis (Brooks, 2010; Kemp, 2005; Robergs, 2011; Robergs et al., 2004). This current debate, along with the parallels between anoxic or ischemic muscle and postmortem muscle, provides an excellent opportunity to reevaluate our understanding of postmortem metabolism and pH development.

Much criticism regarding the 'lactic acidosis' construct lies in the lactate dehydrogenase reaction. Because lactic acid is a weak acid with a pKa of 3.86, production of lactic acid at the pHs observed in exercising muscle or fresh meat would cause the release of a proton (H^+) and result in the acid salt lactate as the final product. This release of H^+ and lactate generated from the LDH reaction is the basis for lactic acidosis. However, evidence supports that lactate production is actually advantageous (Robergs et al., 2004). First, the LDH reaction utilizes two electrons and a proton from NADH, and a proton from solution, to promote reduction of pyruvate to lactate. This consumption of protons means that the LDH reaction is not acidifying as "lactic acidosis" suggests; rather it is a buffering reaction that delays acidosis. Moreover, the LDH reaction regenerates cytosolic NAD^+, which is required by the glyceraldehyde-3 phosphate dehydrogenase reaction. Regeneration of NAD^+ ensures that glycolysis, and hence ATP production, may continue. In exercising muscle, lactate may facilitate the removal of H^+ from the

cell; both can be transported out of the cell via symport by monocarboxylate transporters. In total, this suggests lactic acid is not responsible for acidifying the cell; thus other reactions must be the source of net H^+ production and pH decline.

ATP hydrolysis is proposed to be the major source of proton load during anaerobic muscle metabolism (Gevers, 1977; Hochachka and Mommsen, 1983). ATP hydrolysis generates a proton ($ATP + H_2O \rightarrow ADP + Pi + H^+$). Anytime ATP is broken down by ATPases, or used by enzymes in the energy investment phase of glycolysis, H^+ are generated. The Pi produced in ATP hydrolysis can also function as a buffer for H^+. Pi can have between 0 and 3 OH groups, with pK values of 2.2, 6.8, and 12.4. One oxygen can take up a proton at physiological pH, causing the Pi to be converted from HPO_4^{-2} to $H_2PO_4^{-1}$. Pi accumulation in the cell, however, does not mirror ATP hydrolysis. Free Pi, as well as ADP, are used as substrates in glycolysis, which means the H^+ must either be buffered, transported out of the cell, or left to accumulate.

Several reactions in anaerobic metabolism influence proton balance, and hence, may play a role in "metabolic acidosis". The creatine kinase reaction consumes a proton in the direction of PCr breakdown. This proton consumption is alkalinizing to the cell, and in fact, a brief alkaline shift of ~0.1 pH units can be observed at the onset of exercise (Meyer and Foley, 1996). AMP deaminase also consumes a proton while converting AMP to IMP and NH_4^+. The substrate for glycolysis is either glucose or glycogen (postmortem muscle) (Figure 1-2). ATP is required to phosphorylate glucose to glucose 6-phosphate, generating one H^+. In contrast, breakdown of glycogen involves using Pi to generate glucose-1 phosphate, which is isomerized to glucose 6-phosphate; Pi is consumed and no H^+ are generated. The phosphofructokinase and glyceraldehyde 3 phosphate dehydrogenase reactions produce significant H^+, whereas the pyruvate kinase and LDH reactions consume H^+. According to the calculations of Robergs et al.

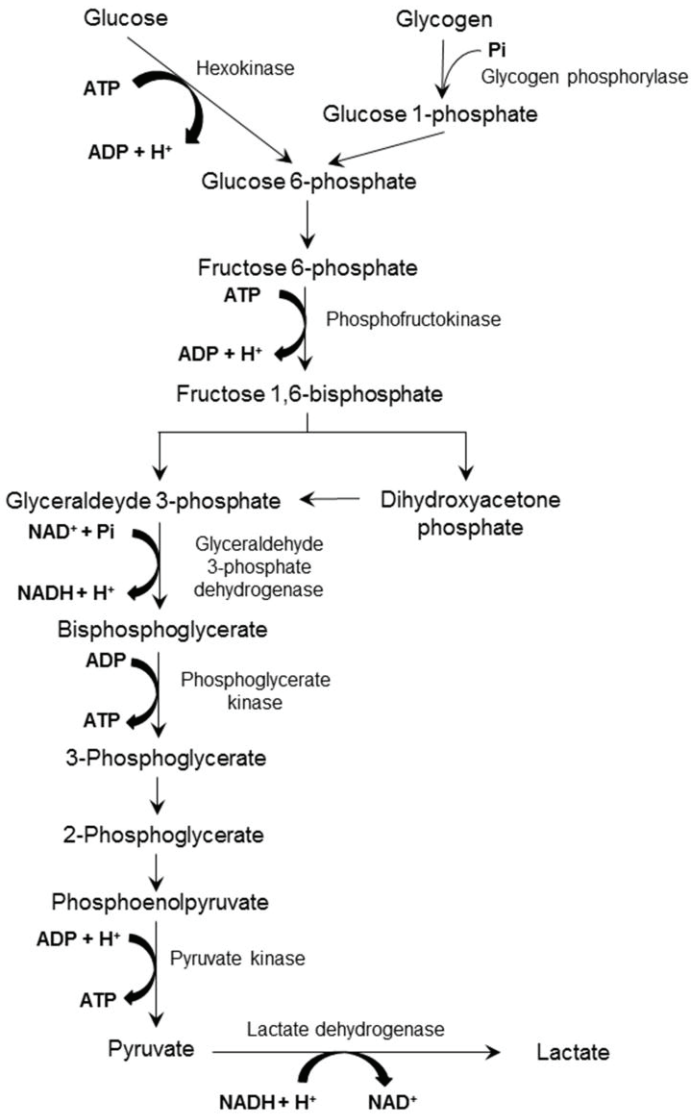

Figure 1-2. The glycogenolytic/glycolytic pathway. Glucose or glycogen is metabolized via glycolysis. Under anaerobic conditions the final product, pyruvate, is converted to lactate. H+ are released during the early steps when ATP is "invested" and in the reaction catalyzed by glyceraldehyde 3-phosphate dehydrogenase; H+ are consumed during the ATP-harvesting step catalyzed by pyruvate kinase and in the production of lactate.

(2004), for every 2 pyruvate synthesized from glycogenolysis, there would be 1 H^+ generated. Kemp et al. (2006) clarified that, when coupled with the LDH reaction (1 H^+ absorbed per pyruvate to lactate), glycogenolysis to lactate would consume one net H^+. Taking this a step

further, the 3 ATP generated by glycogenolysis do not accumulate, but are used by ATPases, resulting in 3 H^+ from ATP hydrolysis and a net of 2 H^+ produced from 2 lactate.

Classically, glycolysis is considered to generate H^+ and lactate at 1:1 ratio (Hochachka and Mommsen, 1983) but this does not necessarily mean the H^+ is coming from the dissociation of lactic acid. Recently, Marcinek, Kushmerick, & Conley (2010) utilized an ischemic mouse hindlimb model to test if glycolytic H^+ production matched lactate generation in a physiological pH range (6.7-7.0). While ATP levels remained similar under ischemia, lactate and H^+ production were near 1:1, which was considered consistent with the concept of "lactate acidosis." However, as Robergs et al. (2004) contends, a stable ATP level does not imply that there is not ATP turnover, and thus it cannot be ruled out that ATP hydrolysis is the source of H^+, not lactic acid (dissociated to lactate and H^+). Vinnakota, Rusk, Palmer, Shankland, & Kushmerick (2010) constructed mathematical models and simulations of pH and lactate using parameters of reactions involved in anaerobic metabolism. Their metabolite values were obtained using transient anoxia to eliminate oxidative phosphorylation as an energy source and perturb steady state energy metabolism. These simulations indicate that during glycolytic flux, the net H^+ production of the reactions in the glycogenolytic and glycolytic pathway is zero; and that ATPase is the major source of H^+ production and CK dominates H^+ consumption, whereas glycolytic flux yields lactate anion at the LDH reaction. These results support the concept that lactate is beneficial and does not contribute to acidosis.

More interestingly, Marcinek et al. (2010) pointed out that the 1:1 association between lactate and H^+ is likely to fail when PCr is depleted, thereby perturbing cellular ATP levels. The increase in ATP hydrolysis relative to supply is expected to generate H^+ independent of glycolysis and uncouple the 1:1 relationship between H^+ and lactate. Although this would be an

extreme situation for exercising muscle, it is certainly applicable to postmortem muscle. First, this suggests there is some credibility to using lactate as an indicator of pH decline, but at some point the relationship fails. Perhaps this may be related to the similar lactate values, yet different ultimate pH, observed in Hampshire versus Large White pigs (Monin and Sellier, 1985). Moreover, maintaining PCr appears to be key to protecting cellular ATP and preventing H^+ accumulation from net ATP hydrolysis. This highlights the importance of looking beyond glycogen and lactate when evaluating the course of postmortem metabolism and pH decline.

The evolution of the "Hampshire Effect", Rendement Napole (RN^-), and AMP-activated protein kinase (AMPK)

As early as 1960s, it was noted that Hampshire pigs possessed elevated muscle glycogen compared to other breeds (Sayre et al., 1963). Hampshire pigs, along with their "normal" and "rapid" metabolizing cohorts, were used as models to understand postmortem metabolism and meat quality. Subsequently, when Monin & Sellier (1985) established the association between high muscle glycogen stores and low ultimate pH in meat from Hampshire pigs, they referred to it as the "Hampshire effect" to distinguish it from the PSE meat produced from a rapid pH decline. Moreover, using "glycolytic potential" to predict ultimate pH seemed logical provided the strong correlations between glycogen and pH found in DFD versus normal meat. These early observations regarding meat quality, pH decline, and postmortem metabolism were influential and formative, but progression of techniques and knowledge dictate that we continue to refine and reevaluate previous work. Although there is a consistent association between high glycogen content and low ultimate pH in RN^- or AMPK $\gamma3^{R200Q}$ pigs (those with the "Hampshire effect"), recent work has established that there are many other metabolic factors that are altered in this

mutated tissue. These factors may be relevant during postmortem metabolism and the conversion of muscle to meat.

Since the introduction of glycolytic potential, knowledge regarding the basis of the "Hampshire effect" phenotype has grown astronomically. Leroy, Naveau, Elsen, & Sellier (1990) reported a major gene affecting cured-cooked ham processing yield – the 'Rendement Napole' technological yield – and suspected this was due to the Hampshire influence in the breeding stock. There are two alleles: the dominant allele (RN^{-}), associated with elevated muscle glycogen and reduced RN technological yield, and the wild-type recessive allele (rn^{+}). The RN^{-} mutation is a single nucleotide polymorphism resulting in a non-conservative R200Q substitution in the PRKAG3 gene (Milan et al., 2000). This gene encodes for the muscle specific γ-3 regulatory subunit of AMP-activated protein kinase (AMPK). Besides increasing glycogen content, $\gamma 3^{R200Q}$ has major effects on other parameters of skeletal muscle metabolism. This is largely due to effect of this mutation on protein function, as well as the significance of AMPK to muscle metabolism.

AMPK, dubbed the "fuel gauge" of the cell, is a major regulator of skeletal muscle metabolism. AMPK is a heterotrimeric serine-threonine kinase composed of a catalytic α subunit and a regulatory β and γ subunit. Phosphorylation of Thr-172 on the α-subunit is considered critical for activity (Stein et al., 2000). The β subunit functions as a scaffold and contains a glycogen binding domain (Polekhina et al., 2003) whereas the γ subunit possesses binding sites for the allosteric activator, AMP. Because AMP competes with ATP for the binding site, AMPK is able to detect increases in AMP:ATP caused by cellular stresses. As mentioned earlier (Section 2), the AMP:ATP ratio is a sensitive indicator of cellular "energy charge". Binding of

AMP allosterically activates AMPK and protects it from dephosphorylation. AMPK signaling is involved in short-term (protein modification) events, as well as gene transcription and adaption.

Activated AMPK stimulates energy producing pathways and down-regulates energy consuming pathways in order to preserve cellular ATP. Increased AMPK activity induced by the AMP analog AICAR promotes translocation of the GLUT4 transporter to the cell membrane and thus promotes glucose uptake (Jorgensen et al., 2004; Kurth-Kraczek et al., 1999). AMPK also enhances lipid oxidation by inactivating acetyl CoA-carboxylase. The resulting reduction in malonyl-CoA relieves inhibition of carnitine palmitoyl transferase-1, which promotes fatty acid uptake into the mitochondria for oxidation. Thus, AMPK increases lipid oxidation for greater energy production. AMPK also facilitates longer lasting effects on metabolism by influencing gene transcription, protein expression, and adaptation. Chronic activation of AMPK increases GLUT4 transcription (Zheng et al., 2001), hexokinase and GLUT4 protein content and muscle glycogen (Holmes et al., 1999), and mitochondrial biogenesis (Zong et al., 2002). Jager, Handschin, St.-Pierre, & Spiegelman (2007) extended these observations by demonstrating that AMPK directly phosphorylates peroxisome proliferator activated receptor γ coactivator 1α (PGC1α), which initiates many of AMPK's effects on gene regulation and promotes oxidative metabolism. Further, AMPK mediates the exercise induced transformation of muscle to a more oxidative phenotype (Rockl et al., 2007).

The γ3 subunit significantly affects AMPK activity in skeletal muscle. Initial reports noted that $\gamma3^{R200Q}$ pigs had decreased AMPK activity (Milan et al., 2000). However, a similar mutation in the γ1 subunit, R70Q, results in constitutive AMPK activity and loss of AMP dependence (Adams et al., 2004; Hamilton et al., 2001). Further, Costford et al. (2007) identified $\gamma3^{R225W}$ in humans, which is homologous to R200Q. Differentiated satellite cells from $\gamma3^{R225W}$

carriers possess nearly a two-fold increase in basal and AMP-activated AMPK activity. We have also found increased AMPK activity in $\gamma3^{R200Q}$ pigs (Park et al., 2009a). This, along with the dominant nature of the mutation, is convincing evidence that $\gamma3^{R200Q}$ is an activating mutation. In particular, the γ3 subunit is specific to skeletal muscle and is more highly expressed in fast "white" muscles (Mahlapuu et al., 2004). This corroborated earlier observations that swine with $\gamma3^{R200Q}$ possess a 70% increase in glycogen in muscle, but not in liver and heart (Milan et al., 2000).

Despite elevated glycogen, γ3 subunit mutations are associated with a more oxidative muscle phenotype. AMPK$\gamma3^{R200Q}$ pigs exhibit higher activity of enzymes involved in the TCA cycle and fatty acid breakdown (citrate synthase and β-hydroxyacyl coenzyme A dehydrogenase, respectively) (Lebret et al., 1999). AMPK $\gamma3^{R200Q}$ pigs also possess a greater proportion of 'slower' myosin heavy chain isoform (Park et al., 2009b). The mutation increases oxidative capacity in glycolytic skeletal muscle by increasing mitochondrial biogenesis, which is associated with increased expression of PGC1α and several transcription factors that regulate mitochondrial proteins (Garcia-Roves et al., 2008). Further, Barnes et al. (2004) demonstrated that $\gamma3^{R225Q}$ mice maintain higher rates of fatty acid oxidation when exposed a high fat diet, thereby protecting them against triglyceride accumulation and insulin resistance. This suggests that γ3 regulates fuel repartitioning and muscle adaptation to facilitate lipid oxidation, which may allow for more glucose to be directed toward glycogen synthesis. In total, this evidence supports that $\gamma3^{R225Q}$ not only increases muscle glycogen, but also remodels the metabolic and contractile machinery toward a more oxidative phenotype.

The ability of $\gamma3^{R200Q}$ mutant pigs to "prolong" pH decline may be related to an improved ability to buffer ATP levels or maintain ATP levels longer during the postmortem period.

Unfortunately, the factors reported early postmortem are typically limited to lactate, glycogen, and pH; these only "scratch the surface" in terms of understanding energy status. Regardless, the early rate of pH decline for Hampshire, RN^{-}, or AMPK $\gamma 3^{R200Q}$ pigs is considered "normal". Mutant and wild type pigs exhibit similar glycogen degradation during exercise (Andersson, 2003; Granlund et al., 2010) and early postmortem (Copenhafer et al., 2006; Monin and Sellier, 1985). There is some disagreement as to whether glycogen phosphorylase activity is unaltered in mutant pigs (Estrade, Ayoub, Talmant, & Monin, 1994) or increased (Granlund et al., 2010; Sayre et al., 1963). Interestingly, AMPK $\gamma 3^{R200Q}$ pigs possess higher phosphocreatine than wild type pigs at 0 and 30 min after exsanguination (Copenhafer et al., 2006). The higher PCr may be the result of an overall increase in the PCr+Cr pool, an altered creatine kinase equilibrium, and/or different rate of PCr utilization. Decreased PCr:Cr leads to increased AMPK activity, which results in a subsequent decrease in creatine kinase activity (Ponticos et al., 1998). Inactivation of creatine kinase by active AMPK may be an energy conservation mechanism to prevent CK from consuming ATP for rephosphorylation of creatine. This would be consistent with a lower rate of PCr utilization.

Given the role of PCr as an ATP buffer, increased PCr would be expected to preserve ATP levels and delay postmortem glycolysis. Early postmortem, improved PCr status is associated with maintenance of ATP levels (Copenhafer et al., 2006; Kastenschmidt et al., 1968). Accordingly, dietary supplementation with Cr monohydrate has been used to increase muscle PCr+Cr stores. Pigs fed Cr possess *longissimus* muscle with increased pH early postmortem, although there appears to be some animal or breed variation in the capacity for Cr uptake into muscle (Lindahl et al., 2006; Young et al., 2005). In contrast, others (Maddock et al., 2002; Stahl et al., 2001) have shown no improvements in *longissimus* pH early postmortem, but muscle PCr

or Cr values were not indicated, making it difficult to draw definitive conclusions from these studies.

Other alleles in AMPKγ3 are associated with changes in muscle metabolism and meat quality. In particular, a V199I substitution is linked to decreased glycogen and lactate content and higher ultimate pH (Ciobanu et al., 2001). The Berkshire breed, which is typically recognized for superior meat quality attributes, including color, pH, marbling, and eating quality, has a high frequency (0.74) of the II genotype, while the frequency in Duroc and Large White is much lower (0.17 and 0.07, respectively) (Ciobanu et al., 2001). The effect of the $\gamma3^{V199I}$ substitution on phenotype is much smaller in magnitude compared to the RN^{-} $\gamma3^{R200Q}$ substitution. Further, the II genotype represents a low percentage of the population and sample sizes are generally small. Nonetheless, others have attempted to evaluate effects of $\gamma3^{V199I}$ on meat quality. Lindahl et al. (2004a; 2004b) reported that pigs with II or IV genotype produced pork with similar pH at 24 h, but higher pH at 48 h and 3d in *longissimus* muscle. In contrast, Fontanesi et al. (2008) demonstrated that II genotype was associated with higher pH at 2h in *semimembranosus* muscle, but did not detect any differences between genotypes in glycogen, lactate, glycolytic potential, and 24 h pH.

Regardless, the association of the AMPKγ3 199 II genotype with improved meat quality and lower glycogen content suggests that the isoleucine substitution has a disparate effect on AMPK compared to the $\gamma3^{R200Q}$ substitution. Given that isoleucine and valine are both non-polar and are similar in structure and size, it is somewhat surprising that this substitution alters phenotype. However, because AMPK is a significant player in regulation of energy metabolism, small differences in its activity or regulation could alter metabolism and meat quality. Using transfected cells, Barnes et al. (2004) demonstrated AMPK activity in $\gamma3^{V199I}$ heterotrimers is not

sensitive to changes in [AMP] but maintains similar basal AMPK activity as wild type. Thus, diminished AMP dependence of AMPK could reduce the capacity of $\gamma3^{V199I}$ muscle to adapt to short- and long-term energy insults, thereby altering energy metabolism. Unfortunately, more detailed information about the energy status of $\gamma3^{V199I}$ muscle is lacking. It is particularly interesting that the $\gamma3^{V199I}$ substitution immediately precedes the amino acid coded by the "RN" site. Curiously, 199I is always found with 200R (rn^{+}), and 200Q (RN^{-}) is always found with 199V; 199V may be with either 200R or 200Q (Milan et al., 2000). Thus, Ciobanu et al. (2001) suggested that the RN phenotype may be a result of combined effect of the 199V-200Q haplotype.

The paradox of high glycogen and high oxidative capacity in AMPK $\gamma3^{R200Q}$ pigs is intriguing and casts doubt on glycogen as a direct player in postmortem pH decline. The increased mitochondria, glucose uptake and myriad of other changes that occur in mutated muscle imply that it has essentially adapted to be more efficient and more prepared to deal with an energy insult. Mitochondria content, enzyme content and activity, regulation by metabolites, and the interactions of these factors could all play roles in modifying the course of postmortem metabolism in these pigs. Although the RN or $\gamma3^{R200Q}$ pig is a unique model of postmortem metabolism, we expect that understanding energetics and metabolism in this model may be useful in explaining the variation in pH decline and ultimate pH observed in the general population.

Summary

Although there is an association between high glycogen content and low ultimate pH in $\gamma3^{R200Q}$ or RN^{-} pigs, the direct cause and effect relationship should be challenged. Traditionally,

the increased glycogen in $\gamma3^{R200Q}$ pig muscle is inferred to generate more "lactic acid" postmortem, which is thought to lower ultimate pH. However, lactate values may be similar despite different ultimate pH, and as those in exercise physiology have suggested, the validity of "lactic acidosis" is questionable. Lactate may actually be beneficial and buffer H^+ accumulation. Moreover, increased glycogen is only one of the many metabolic properties that is quite different in $\gamma3^{R200Q}$ pig versus "normal" muscle. Enzyme content and activity, fiber type, and energy status all contribute to maintenance and turnover of ATP, and hence the course and extent of postmortem metabolism. Fortunately, a wide range of techniques and animal models are available to investigate the complex and fascinating nature of muscle bioenergetics and its role in meat quality development.

References

Adams, J., Z. P. Chen, B. J. Van Denderen, C. J. Morton, M. W. Parker, L. A. Witters, D. Stapleton, and B. E. Kemp. 2004. Intrasteric control of AMPK via the γ1 subunit AMP allosteric regulatory site. Protein Sci. 13: 155-165.

Andersson, L. 2003. Identification and characterization of AMPK γ3 mutations in the pig. Biochem. Soc. Trans. 31: 232-235.

Barnes, B. R., S. Marklund, T. L. Steiler, M. Walter, G. Hjalm, V. Amarger, M. Mahlapuu, Y. Leng, C. Johansson, D. Galuska, K. Lindgren, M. Abrink, D. Stapleton, J. R. Zierath, and L. Andersson. 2004. The 5'-AMP-activated protein kinase γ3 isoform has a key role in carbohydrate and lipid metabolism in glycolytic skeletal muscle. J. Biol. Chem. 279: 38441-38447.

Bendall, J. R. 1951. The shortening of rabbit muscles during rigor mortis: its relation to the breakdown of adenosine triphosphate and creatine phosphate and to muscular contraction. J. Physiol. 114: 71-88.

Berg, J. M., J. L. Tymoczko, and L. Stryer (Editors). 2002. Biochemistry. W.H. Freeman and Company, New York.

Briskey, E. J. 1964. Etiological status and associated studies of pale, soft, exudative porcine musculature Adv. Food Res. 13: 89-178.

Briskey, E. J., and J. Wismer-Pedersen. 1961. Biochemistry of pork muscle structure. I. Rate of anaerobic glycolysis and temperature change versus the apparent structure of muscle tissue. J. Food Sci. 26: 297-305.

Brooks, G. A. 2010. What does glycolysis make and why is it important? J. Appl. Physiol. 108: 1450-1451.

Ciobanu, D., J. Bastiaansen, M. Malek, J. Helm, J. Woollard, G. Plastow, and M. Rothschild. 2001. Evidence for new alleles in the protein kinase adenosine monophosphate-activated γ3-subunit gene associated with low glycogen content in pig skeletal muscle and improved meat quality. Genetics 159: 1151-1162.

Copenhafer, T. L., B. T. Richert, A. P. Schinckel, A. L. Grant, and D. E. Gerrard. 2006. Augmented postmortem glycolysis does not occur early postmortem in AMPKγ3-mutated porcine muscle of halothane positive pigs. Meat Sci. 73: 590-599.

Costford, S. R., N. Kavaslar, N. Ahituv, S. N. Chaudhry, W. S. Schackwitz, R. Dent, L. A. Pennacchio, R. McPherson, and M. E. Harper. 2007. Gain-of-function R225W mutation in human AMPKγ3 causing increased glycogen and decreased triglyceride in skeletal muscle. PLoS ONE 2: e903.

Fontanesi, L., R. Davoli, L. Nanni Costa, F. Beretti, E. Scotti, M. Tazzoli, F. Tassone, M. Columbo, L. Buttazzoni, and V. Russo. 2008. Investigation of candidate genes for glycolytic potential of porcine skeletal muscle: association with meat quality and production traits in Italian Large White pigs. Meat Sci. 80: 780-787.

Garcia-Roves, P. M., M. E. Osler, M. H. Holmstrom, and J. R. Zierath. 2008. Gain-of-function R225Q mutation in AMP-activated protein kinase γ3 subunit increases mitochondrial biogenesis in glycolytic skeletal muscle. J. Biol. Chem. 283: 35724-35734.

Gevers, W. 1977. Generation of Protons by Metabolic Processes in Heart-Cells. J. Mol. Cell. Cardiol. 9: 867-874.

Granlund, A., O. Kotova, B. Benziane, D. Galuska, M. Jensen-Waern, A. V. Chibalin, and B. Essén-Gustavsson. 2010. Effects of exercise on muscle glycogen synthesis signalling and enzyme activities in pigs carrying the PRKAG3 mutation. Exp. Physiol. 95: 541-549.

Hamilton, S. R., D. Stapleton, J. B. O'Donnell, J. T. Kung, S. R. Dalal, B. E. Kemp, and L. A. Witters. 2001. An activating mutation in the γ1 subunit of the AMP-activated protein kinase. FEBS Lett. 500: 163-168.

Hochachka, P. W., and T. P. Mommsen. 1983. Protons and anaerobiosis. Science 219: 1391-1397.

Holmes, B. F., E. J. Kurth-Kraczek, and W. W. Winder. 1999. Chronic activation of 5'-AMP-activated protein kinase increases GLUT-4, hexokinase, and glycogen in muscle. J. Appl. Physiol. 87: 1990-1995.

Huff-Lonergan, E., T. J. Baas, M. Malek, J. C. Dekkers, K. Prusa, and M. F. Rothschild. 2002. Correlations among selected pork quality traits. J. Anim. Sci. 80: 617-627.

Immonen, K., and E. Puolanne. 2000. Variation of residual glycogen-glucose concentration at ultimate pH values below 5.75. Meat Sci. 55: 279-283.

Jager, S., C. Handschin, J. St.-Pierre, and B. M. Spiegelman. 2007. AMP-activated protein kinase (AMPK) action in skeletal muscle via direct phosphorylation of PGC-1α. Proc. Natl. Acad. Sci. USA 104: 12017-12022.

Jorgensen, S. B., B. Viollet, F. Andreelli, C. Frosig, J. B. Birk, P. Schjerling, S. Vaulont, E. A. Richter, and J. F. P. Wojtaszewski. 2004. Knockout of the α2 but not α1 5'-AMP-activated protein kinase isoform abolishes 5-aminoimidazole-4-carboxamide-1-β-4-ribofuranoside but not contraction-induced glucose uptake in skeletal muscle. J. Biol. Chem. 279: 1070-1079.

Kastenschmidt, L. L., W. G. Hoekstra, and E. J. Briskey. 1968. Glycolytic intermediates and co-factors in "fast-" and "slow-glycolyzing" muscles of the pig. J. Food Sci. 33: 151-158.

Kemp, G. 2005. Lactate accumulation, proton buffering, and pH change in ischemically exercising muscle. Am. J. Physiol. Regul. Integr. Comp. Physiol. 289: R895-R901.

Kemp, G., D. Boning, R. Beneke, and N. Maassen. 2006. Explaining pH change in exercising muscle: lactic acid, proton consumption, and buffering vs. strong ion difference. Am. J. Physiol. Regul. Integr. Comp. Physiol. 291: R235-237; author reply R238-239.

Kurth-Kraczek, E. J., M. F. Hirshman, L. J. Goodyear, and W. W. Winder. 1999. 5' AMP-activated protein kinase activation causes GLUT4 translocation in skeletal muscle. Diabetes 48: 1667-1671.

Lebret, B., P. Le Roy, G. Monin, L. Lefaucheur, J. C. Caritez, A. Talmant, J. M. Elsen, and P. Sellier. 1999. Influence of the three RN genotypes on chemical composition, enzyme activities, and myofiber characteristics of porcine skeletal muscle. J. Anim. Sci. 77: 1482-1489.

Leroy, P., J. Naveau, J. M. Elsen, and P. Sellier. 1990. Evidence for a new major gene influencing meat quality in pigs. Genet. Res. 55: 33-40.

Levine, J. A., W. T. Donahoo, and E. L. Melanson. 2000. Cellular and Whole-Animal Energetics. In: M. H. Stipanuk (ed.) Biochemical, Physiological, and Molecular Aspects of Human Nutrition. p 593-617. Saunders, Philadelpha.

Lindahl, G., A.-C. Enfält, G. v. Seth, Å. Joseli, I. Hedebro-Velander, H. J. Andersen, M. Braunschweig, L. Andersson, and K. Lundström. 2004a. A second mutant allele (V199I) at the PRKAG3 (RN) locus--II. Effect on colour characteristics of pork loin. Meat Sci. 66: 621-627.

Lindahl, G., A. C. Enfalt, G. von Seth, A. Josell, I. Hedebro-Velander, H. J. Andersen, M. Braunschweig, L. Andersson, and K. Lundstrom. 2004b. A second mutant allele (V199I) at the PRKAG3 (RN) locus- I. Effect on technological meat quality of pork loin. Meat Sci. 66: 609-619.

Lindahl, G., J. F. Young, N. Oksbjerg, and H. J. Andersen. 2006. Influence of dietary creatine monohydrate and carcass cooling rate on colour characteristics of pork loin from different pure breeds. Meat Sci. 72: 624-634.

Maddock, R. J., B. S. Bidner, S. N. Carr, F. K. McKeith, E. P. Berg, and J. W. Savell. 2002. Creatine monohydrate supplementation and the quality of fresh pork in normal and halothane carrier pigs. J. Anim. Sci. 80: 997-1004.

Mahlapuu, M., C. Johansson, K. Lindgren, G. Hjalm, B. R. Barnes, A. Krook, J. R. Zierath, L. Andersson, and S. Marklund. 2004. Expression profiling of the γ-subunit isoforms of AMP-activated protein kinase suggests a major role for γ3 in white skeletal muscle. Am. J. Physiol. Endocrinol. Metab. 286: E194-200.

Marcinek, D. J., M. J. Kushmerick, and K. E. Conley. 2010. Lactic acidosis in vivo: testing the link between lactate generation and H^+ accumulation in ischemic mouse muscle. J. Appl. Physiol. 108: 1479-1486.

Maribo, H., S. Stoier, and P. F. Jorgensen. 1999. Procedure for determination of glycolytic potential in porcine m. longissimus dorsi. Meat Sci. 1999: 191-193.

Meyer, R. A., and J. M. Foley. 1996. Cellular processes integrating the metabolic response to exercise Handbook of Physiology. p 841-869.

Milan, D., J.-T. Jeon, C. Looft, V. Amarger, A. Robic, M. Thelander, C. Rogel-Gaillard, S. Paul, N. Iannuccelli, L. Rask, H. Ronne, K. Lundstrom, N. Reinsch, J. Gellin, E. Kalm, P. L. Roy, P. Chardon, and L. Andersson. 2000. A mutation in PRKAG3 associated with excess glycogen content in pig skeletal muscle. Science 288: 1248-1251.

Monin, G., and P. Sellier. 1985. Pork of low technological quality with a normal rate of muscle pH fall in the immediate post-mortem period: the case of the Hampshire breed. Meat Sci. 13: 49-63.

Park, S., T. L. Scheffler, A. M. Gunawan, H. Shi, C. Zeng, K. M. Hannon, A. L. Grant, and D. E. Gerrard. 2009a. Chronic elevated calcium blocks AMPK-induced GLUT-4 expression in skeletal muscle. Am. J. Physiol. Cell Physiol. 296: C106-115.

Park, S. K., A. M. Gunawan, T. L. Scheffler, A. L. Grant, and D. E. Gerrard. 2009b. Myosin heavy chain isoform content and energy metabolism can be uncoupled in pig skeletal muscle. J. Anim. Sci. 87: 522-531.

Polekhina, G., A. Gupta, B. J. Michell, B. van Denderen, S. Murthy, S. C. Feil, I. G. Jennings, D. J. Campbell, L. A. Witters, M. W. Parker, B. E. Kemp, and D. Stapleton. 2003. AMPK β subunit targets metabolic stress sensing to glycogen. Curr. Biol. 13: 867-871.

Ponticos, M., Q. L. Lu, J. E. Morgan, D. G. Hardie, T. A. Partridge, and D. Carling. 1998. Dual regulation of the AMP-activated protein kinase provides a novel mechanism for the control of creatine kinase in skeletal muscle. EMBO J. 17: 1688-1699.

Robergs, R. A. 2011. Counterpoint: Muscle lactate and H^+ production do not have a 1:1 association in skeletal muscle. J. Appl. Physiol. 110: 1489-1491; discussion 1498.

Robergs, R. A., F. Ghiasvand, and D. Parker. 2004. Biochemistry of exercise-induced metabolic acidosis. Am. J. Physiol. Regul. Integr. Comp. Physiol. 287: R502-516.

Rockl, K. S., M. F. Hirshman, J. Brandauer, N. Fujii, L. A. Witters, and L. J. Goodyear. 2007. Skeletal muscle adaptation to exercise training: AMP-activated protein kinase mediates muscle fiber type shift. Diabetes 56: 2062-2069.

Sayre, R. N., E. J. Briskey, and W. G. Hoekstra. 1963. Comparison of muscle characteristics and post-mortem glycolysis in three breeds of swine. J. Anim. Sci. 22: 1012-1020.

Stahl, C. A., G. L. Allee, and E. P. Berg. 2001. Creatine monohydrate supplemented in swine finishing diets and fresh pork quality: II. Commercial applications. J. Anim. Sci. 79: 3081-3086.

Stein, S. C., A. Woods, N. A. Jones, M. D. Davison, and D. Carling. 2000. The regulation of AMP-activated protein kinase by phosphorylation. Biochem. J. 345: 437-443.

van Laack, R. L. J. M., and R. G. Kauffman. 1999. Glycolytic potential of red, soft, exudative pork longissimus muscle. J. Anim. Sci. 77: 2971-2973.

Vinnakota, K. C., J. Rusk, L. Palmer, E. Shankland, and M. J. Kushmerick. 2010. Common phenotype of resting mouse extensor digitorum longus and soleus muscles: equal ATPase and glycolytic flux during transient anoxia. J. Physiol. (London) 588: 1961-1983.

Wismer-Pedersen, J., and E. J. Briskey. 1961. Rate of anaerobic glycolysis versus structure in pork muscle. Nature 189: 318-320.

Young, J. F., H. C. Bertram, K. Rosenvold, G. Lindahl, and N. Oksbjerg. 2005. Dietary creatine monohydrate affects quality attributes of Duroc but not Landrace pork. Meat Sci. 70: 717-725.

Zheng, D., P. S. MacLean, S. C. Pohnert, J. B. Knight, A. L. Olson, W. W. Winder, and G. L. Dohm. 2001. Regulation of muscle GLUT4 transcription by AMP-activated protein kinase. J. Appl. Physiol. 91: 1073-1083.

Zong, H., J. M. Ren, L. H. Young, M. Pypaert, J. Mu, M. J. Birnbaum, and G. I. Shulman. 2002. AMP kinase is required for mitochondrial biogenesis in skeletal muscle in response to chronic energy deprivation. Proc. Natl. Acad. Sci. USA 99: 15983-15987.

Chapter 2. Use of dietary supplementation with β-guanidinopropionic acid to alter phosphocreatine content, postmortem metabolism, and pork quality

Abstract

Rate and extent of postmortem glycolysis are the main factors controlling pork quality development. Our objective was to evaluate the role of the phosphagen system (phosphocreatine, PCr; and creatine, Cr) on postmortem metabolism and pork quality attributes. Phosphocreatine and creatine content of muscle were manipulated by feeding pigs the creatine analogue, β-guanidinopropionic acid (β-GPA). In experiment 1, animals received a standard (control) diet or β-GPA supplemented (2%) diet (1 wk or 2 wk). Supplementation with β-GPA for 2 wk resulted in a 20% decrease in total Cr (PCr+Cr) ($P = 0.02$) but reduced feed intake ($P = 0.003$) and growth performance ($P = 0.007$). β-GPA supplementation for 2 wk was also associated with improved pork color, indicated by decreased reflectance ($P = 0.003$). In order to better separate the effects of reduced muscle Cr and restricted growth on pork quality, a second experiment was conducted with control, pair-fed, and 2-wk β-GPA supplementation. Neither treatment influenced pork quality attributes. Immediately postmortem, muscle from control pigs exhibited higher ATP/ADP compared to pair-fed ($P < 0.05$); subsequently, ATP/ADP of control muscle decreased and was similar to pair-fed and β-GPA at 20 min. Loss of the phosphagen system and growth restriction differentially influence early postmortem energy metabolism.

Introduction

Pale, soft, and exudative (PSE) pork is a major industry concern due to its undesirable appearance and reduced functionality. Pork quality development is largely governed by rate and extent of postmortem glycolysis (Briskey, 1964; Monin and Sellier, 1985). Hastened postmortem glycolysis generates heat and causes a rapid accumulation of lactate and hydrogen ions. This combination of high carcass temperature at relatively low muscle pH results in the denaturation of sarcoplasmic and myofibrillar proteins (Honikel and Kim, 1986; Warner et al., 1997). Conversely, 'acid meat' or meat with a low ultimate pH (pH_u), is generally considered to result from increased muscle glycogen stores; this is suggested to allow greater glycolysis and a low ultimate pH. There is certainly a relationship between glycogen and ultimate pH at extreme pH values; for example, dark, firm and dry meat is the result of limiting substrate resulting in minimal postmortem glycolysis. However, glycogen alone does not fully explain differences in pH_u (Scheffler et al., 2011).

An improved ability to buffer ATP levels in postmortem muscle may contribute to increased glycolytic capacity. After exsanguination, muscle attempts to maintain homeostasis by generating ATP. The most immediate means of buffering ATP is via the phosphagen system; creatine kinase catalyzed transfer of phosphate from phosphocreatine (PCr) to ADP yields ATP and creatine. Continued contraction or utilization of ATP by other ATP-dependent enzymes results in depletion of PCr and accumulation of ADP. Additional ATP can be readily generated by the myokinase reaction ($2ADP \leftrightarrow AMP + ATP$). Subsequently, AMP is deaminated to IMP by AMP deaminase. The combined efforts of myokinase and AMP deaminase maintain ATP/ADP ratio during high energy demands and prevent muscle fatigue (Meyer and Foley, 1996; Sahlin et al., 1990). Increases in AMP and ADP stimulate anaerobic degradation of

glycogen, resulting in lactate and H^+. Hydrolysis of ATP ($ATP + H_2O \leftrightarrow ADP + Pi + H^+$) via any number of reactions in muscle cells also generates H^+. Thus, the capacity to generate ATP may influence H^+ accumulation and pH decline, thereby impacting meat quality development.

Our previous work (Copenhafer et al., 2006) showed that, in addition to elevated glycogen, pigs with the Rendement Napole mutation (or AMP-activated protein kinase γ3 R200Q) possess greater PCr levels immediately postmortem. This elevated PCr indicates an enhanced capacity to buffer ATP, which may promote extended glycolysis. Along these same lines, reduced PCr should result in a reduced capacity to buffer ATP. Therefore, the objective of our study was to reduce PCr content of muscle and determine its effect on postmortem metabolism and meat quality development. The creatine analogue, β-guanidinopropionic acid (β-GPA), competes with Cr for transport into muscle cells, resulting in depletion of PCr and Cr in a time-dependent manner (Tullson et al., 1996). Phosphorylated β-GPA is a much poorer substrate for creatine kinase and cannot substitute for PCr (Chevli and Fitch, 1979). We, therefore, hypothesized that the reduced PCr pool in muscle from β-GPA fed animals would result in a reduced capacity to buffer ATP, necessitating that glycogen would be metabolized earlier postmortem in order to maintain ATP levels.

Materials and Methods

Animals. All procedures with animals were conducted in accordance and with prior approval of the Virginia Tech Animal Care and Use Committee. *Experiment 1:* Twelve castrated male pigs (Yorkshire/Large White × Duroc) were obtained from Murphy Brown, LLC (Waverly, VA). Pigs were individually housed in 1.44 m^2 pens at the Litton Reaves Animal Facility at Virginia Tech. Animals were blocked by initial weight and assigned to control or treatment diet (1 wk or

2 wk). Treatment diet consisted of a standard (control) swine diet supplemented with 2% β-GPA. At initiation of the experiment, pigs in the 2 wk group (n = 4) were provided with treatment diet, while remaining pigs (n=8) were given the control diet. After 1 wk, 4 pigs in the control group were switched to the treatment diet. Feed and water were provided ad libitum. *Experiment 2:* Castrated male and female pigs were obtained from Murphy Brown, LLC and individually penned at the Virginia Tech Swine Center. Animals were blocked by sex and assigned to control, pair-fed, or treatment (2 wk of 1% β-GPA supplementation). Treatment pigs were also offered access to flavored beverage (Kool-Aid ® sweetened with glucose) supplemented with 1% β-GPA, while control and pair-fed pigs received the flavored beverage without β-GPA. Experiments 1 and 2: At the end of the 2 wk trial period, pigs were transported to the Virginia Tech Meat Science Center and harvested. Pigs were electrically stunned and exsanguinated. Exsanguination was considered time 0.

Muscle sampling. Muscle samples (~5 g) were collected from the lumbar region of the *longissimus* muscle at 0, 20, and 45 min and 24 h postmortem; sampling at 90 min time point was added for experiment 2. Samples were immediately frozen in liquid nitrogen and stored at –80 °C until analysis.

Meat quality characteristics. At 24h postmortem, carcasses were ribbed between the 10th and 11th costae. Two 2.54-cm thick chops were removed from the carcass anterior to the cut surface at the 10th rib and trimmed to remove excess backfat and connective tissue. Subjective color, marbling (NPPC, 2000) and firmness (NPPC, 1991) were evaluated by five individuals at the cut surface of the *longissimus* at the 10^{th} rib. On the same surface, objective color measurements were determined using a portable Minolta CR300 colorimeter (Ramsey, NJ, USA). Mean L

(lightness), a (redness), and b (yellowness) values were collected from three separate locations on the surface of the chop. Water holding capacity was determined on the adjacent chop using the drip loss method (Rasmussen and Andersson, 1996). Briefly, muscle samples were collected from one chop using a coring device and placed in drip loss tubes. After 24h at 4°C, the drip loss containers plus samples were weighed. Muscle samples were removed and containers were reweighed with exudates. Percentage drip loss was calculated and recorded.

Muscle metabolite analysis and pH measurements. Muscle glucose 6-phosphate (G6P), glycogen, and lactate concentrations were determined using enzyme analytical methods (Bergmeyer, 1974) modified to a 96-well configuration (Hammelman et al., 2003). For pH determination, ~1 g of frozen muscle was homogenized in 10 ml of 5mM iodoacetate. The pH of the homogenate was determined using a ROSS electrode attached to an Orion pH meter (Thermo Fisher Scientific, Beverly, MA, USA).

Adenosine nucleotides and IMP. Adenosine triphosphate and adenosine diphosphate, were detected using high performance liquid chromatography (HPLC; Agilent Technologies, Santa Clara, CA, USA) with modifications (Bernocchi et al., 1994; Williams et al., 2008). Muscle samples were homogenized in 0.5 M perchloric acid and neutralized with $KHCO_3$; extracts were filtered (0.2 μm) prior to injection. Separation was accomplished using a C_{18} 2.6-μm reversed-phase column (0.46 x 5 cm) (Kinnetex Phenomenex, Torrance, CA, USA). The mobile phase consisted of a gradient; buffer A was composed of 0.1 M KH_2PO_4, 5 mM tetrabutylammonium hydrogen sulfate (TBAHS), and 2.5% acetonitrile (v/v) (pH 6.0), while the second buffer (B) consisted of 0.1 M KH_2PO_4, 5 mM TBAHS and 25% acetonitrile (pH 5.5). The column was eluted for 2 min with buffer A, for 2 min with buffers A and B (increasing to 11%), and for 4

min with increase to 45% buffer B, and lastly, reequilibrated for 15 min with 100% buffer A. Flow was 2.0 ml/min and separation was performed at room temperature. Adenosine nucleotides and IMP were detected at 254 nm and were quantified by using peak areas and retention times of external standards.

Phosphocreatine and creatine. Phosphocreatine was determined using neutralized muscle extracts analyzed by a standard sequential enzyme assay (Passonneau and Lowry, 1993). Creatine was determined using a kit (BioVision, Milpitas, CA, USA) according to the manufacturer's instructions. Total Cr was determined by adding PCr (enzyme analysis) and Cr (kit) values.

Statistical analysis. Relationships between GPA administration and meat quality development were analyzed using PROC MIXED procedure of SAS. The model included the effect of treatment (experiment 1: control, 1 wk, or 2 wk; experiment 2: control, PF, or β-GPA). The 'repeated' statement was used for pH and metabolite measurements made at multiple time points; time, treatment, and time by treatment interaction were included in the model. The slices statement was used to determine treatment effects at individual time points; for significant treatment differences at a particular time point, differences were determined by using contrasts with adjustments for multiple comparisons (Bonferroni method). For variables that did not include 'time' as a factor (ie, color or total Cr), Tukey's adjustment for multiple comparisons was used to compare least square means.

Results and Discussion

Creatine kinase catalyzes the reaction PCr + ADP + H^+ $\leftrightarrow$ Cr + ATP, and thus prevents decreases in intracellular ATP/ADP. Dietary β-GPA competes with creatine for uptake into skeletal muscle, resulting in a time-dependent decrease in PCr and Cr. Phosphorylated β-GPA (P-β-GPA) is a much poorer substrate for creatine kinase (Chevli and Fitch, 1979), and gradual depletion of high energy phosphate prompts adaptations in muscle energy metabolism (Shoubridge et al., 1985) and myosin isoform composition (Moerland et al., 1989). In order to decrease PCr and Cr and minimize alterations in metabolic enzymes, we limited the treatment period to1 or 2 wk.

We did not detect differences in individual PCr or Cr pools due to β-GPA treatment; however, dietary β-GPA influenced total Cr pool (PCr + Cr) in *longissimus* muscle (Figure 2-1). There was a linear trend for loss in total Cr and time on β-GPA diet, but only 2 wk β-GPA supplementation decreased ($P < 0.05$) total Cr compared to control levels. Although we did not detect differences in individual PCr and Cr pools, the reduction in total Cr pool was primarily manifested as a loss in PCr. In agreement, short duration (1-3 wk) of β-GPA treatment dramatically reduces PCr compared to Cr in rat muscle (Tullson et al., 1996). Yet, typical resting levels of PCr in fast-twitch muscle are around 20 μmol/g (Bendall, 1973); because utilization of PCr results in Cr production, the shift in PCr/Cr indicates that PCr is already partly depleted immediately postmortem. Thus, variation in proportion of PCr and Cr content also reflects differences in energy status at harvest.

Dietary β-GPA was associated with considerable improvements in meat quality attributes. Two-wk treatment with β-GPA decreased reflectance (lower L values; $P=0.003$; Figure 2-2A) and yellowness (b value; $P=0.03$, Figure 2-2B). Similarly, 2 wk β-GPA

supplementation resulted in more reddish-pink meat color, as evidenced by increased subjective color scores (P=0.004; Figure 2-2C). Importantly, differences in subjective color between treatments were relatively large; a '2' score represents pinkish gray, while '3' is reddish pink. Moreover, β-GPA treatment tended to decrease drip loss (P=0.10; Figure 2-2D), indicating increased water-holding capacity.

Because pork quality development is closely associated with the rate and extent of pH decline, we evaluated pH at early and 'ultimate' (24 h or 1440 min) time points. Overall, β-GPA supplementation tended to increase pH (main effect, treatment P=0.10) and pH over time (treatment × time, P=0.09; Figure 2-3). Initial pH (0 min) was similar between treatments; thereafter, β-GPA supplementation was associated with numerically higher pH early postmortem (0 to 45 min), although there were not significant differences between treatments at these time points. At 24 h, 2 wk β-GPA supplementation resulted in increased pH compared to control.

Next, we aimed to understand how β-GPA supplementation and reduced muscle Cr pool may influence pH decline and augment meat quality. Initially, we had expected that the reduction in PCr and Cr due to β-GPA supplementation would reduce the muscle's capacity to buffer ATP, necessitating that glycogen would be metabolized earlier postmortem in order to maintain ATP levels. In contrast, the superior meat quality attributes and tendency toward increased pH suggested that β-supplementation actually slows postmortem metabolism and/or limits extent of pH decline. Glycogen content was numerically but not significantly decreased in muscle from β-GPA treated animals; glycogen degradation over time was not affected by β-GPA supplementation (Figure 2-4A). During anaerobic glycolysis, glycogen phosphorylase cleaves the outer chains of glycogen, generating glucose 1-phosphate, which is isomerized to glucose 6-phosphate. Glycogen debranching enzyme breaks the α-1,6 linkages, releasing free glucose,

which accumulates in postmortem muscle. At 20 min postmortem, G6P was increased in muscle from control compared to 2 wk β-GPA treatment ($P<0.05$; Figure 2-4B). Increased G6P may suggest that glycogen breakdown is greater in control muscle compared to β-GPA muscle; glycogenolysis may be slowed or delayed in β-GPA muscle. Lactate is the end product of anaerobic glycolysis and thus its accumulation can be indicative of the rate of postmortem metabolism. β-GPA treatment did tend to influence lactate production over time (treatment × time, $P=0.10$; Figure 2-4C). At 45 min, lactate was highest in control pigs; in conjunction with the lower 45 min pH observed, this suggests more rapid postmortem metabolism in the control group.

Creatine kinase and PCr have important roles in muscle energetics. Coupling of ATP hydrolysis and the creatine kinase reaction results in the net equation: $PCr + \beta H^+ \rightarrow Cr + P_i$. Creatine kinase helps prevent increases in ADP_{free}, and consumes H^+ (β is pH dependent), which contributes to a brief alkaline shift at the beginning of contraction (Meyer and Foley, 1996). Muscle from β-GPA treated animals must have additional means to offset the loss of ATP buffering capacity by PCr as well as prevent local decreases in pH. During contraction in fast-twitch white muscle of β-GPA fed rats, deamination of AMP is initiated sooner, resulting in increased inosine monophosphate (IMP) formation (Tullson et al., 1996). Whereas 'normal' muscle has PCr to buffer adenine nucleotide levels, β-GPA muscle must compensate by increasing AMP deaminase activity in order to blunt the increases in AMP and ADP that occur with greater ATP hydrolysis. Because both AMP and ADP are allosteric stimulators of glycolytic enzymes, including glycogen phosphorylase, delaying their accumulation would slow glycolytic metabolism postmortem. However, we did not find increased IMP levels in β-GPA muscle.

Alternatively, P_i generated from the coupling of ATP hydrolysis and creatine kinase may be important for stimulating glycolysis. In muscle of control and β-GPA fed rats, 5 Hz stimulation resulted in two-fold greater acid accumulation in control muscle; this was associated with a nearly two-fold increase in lactate (Meyer et al., 1986). Additionally, β-GPA muscle degraded ~33% less glycogen during stimulation and contained lower levels of P_i. The dramatic increase in glycolytic metabolism in muscle of control rats was attributed largely to P_i generated from hydrolysis of PCr, which potently stimulates glycogen phosphorylase and thus glycogenolysis. Thus, reducing available PCr may decrease glycolytic flux and slow postmortem metabolism.

β-GPA-induced changes in muscle metabolism that may relate to ultimate pH are less clear. Traditionally, ultimate pH is considered to be a function of 'glycolytic potential' (GP) (Monin and Sellier, 1985). In muscle from β-GPA supplemented pigs, glycogen is available (~45 μmol/g) and thus is not limiting glycolysis; in fact, virtually all glycogen appears to be broken down in the 24h postmortem period. Lactate values at 24h were similar between treatments and did not parallel differences in ultimate pH. While direct effects of β-GPA impact total Cr and maintenance of ATP during early metabolism, this likely has indirect effects on course of postmortem metabolism. Glycolytic enzymes are subject to allosteric regulation by adenine nucleotides, IMP, and H^+, among others; thus, altering the production or proportion of key metabolites could alter the overall course of metabolism. Moreover, β-GPA supplementation for several (6-10) weeks decreases activity of glycogen phosphorylase and phosphofructokinase and increases activity of oxidative enzymes in fast-twitch muscles (Shoubridge et al., 1985). Thus, muscle tries to adapt to loss of immediate ATP-buffering capacity by increasing its ATP generating capacity. Although we chose a shorter treatment period to limit adaptation of

metabolic and contractile proteins, it is plausible that β-GPA influenced metabolic properties of muscle. These metabolic properties may also be influenced by growth performance. Although initial weights were similar and feed was offered ad libitum, pigs on the treatment diet consumed less feed (P=0.008, P=0.002; Table 2-1) and thus weighed less (P=0.04) at the end of the trial. Reduced performance is most likely due to undesirable flavor (bitterness) of β-GPA. Overall, pigs exposed to 2 wk β-GPA maintained weight during the trial period. Pigs assigned to 1 wk β-GPA treatment gained weight while on the control diet, but after being switched to the treatment diet, consumed less feed than control pigs. Reduced energy intake and growth rate in β-GPA pigs would be expected to increase oxidative metabolism, which could contribute to differences in postmortem metabolism and meat quality.

Experiment 2

In the first experiment, β-GPA supplementation for 2 wk contributed to a significant reduction in the total Cr pool in muscle. Yet, β-GPA supplementation also reduced feed consumption and hence limited growth. In order to separate the contribution of reduced feed intake and decreased Cr pool on postmortem muscle metabolism, we utilized a pair-fed group along with ad libitum control and 2 wk β-GPA supplementation groups. Final weight was similar across treatment groups (Table 2-2). During the treatment period, pair-fed and β-GPA pigs gained approximately 50% less than control pigs (P=0.002).

Similar to experiment 1, we did not detect differences in individual PCr or Cr pools due to β-GPA supplementation; however, total Cr pool was decreased in β-GPA supplemented pigs compared to control and pair-fed groups (Figure 2-5). The 20% reduction in the Cr pool was consistent with that observed in the 2 wk β-GPA group in the first study. In this instance,

differences in total Cr appear to be primarily due to Cr, not PCr. This suggests there may be greater utilization of PCr in the control and pair-fed compared to the β-GPA group.

Neither pair-fed nor β-GPA treatment was associated with discernible changes in meat quality attributes (Figure 2-6). Lightness, yellowness, subjective color and drip loss were similar amongst all groups. Early postmortem pH decline and ultimate pH were also similar across treatments (Figure 2-7). With respect to postmortem glycolysis, treatment did not influence glycogen, although there was a trend indicating treatments differed in glycogen degradation over time (treatment × time, P=0.14; Figure 2-8). There was little glycogen degradation in muscle from PF animals during the first 45 min postmortem, and greater glycogen degradation thereafter. Muscle from control and β-GPA fed animals exhibited a more consistent and linear rate of glycogen degradation. Lactate accumulation mirrored glycogen degradation. Treatment had no effect (P=0.95) on lactate, and initial and final lactate levels were similar between treatments. Treatment tended to alter lactate accumulation over time (treatment × time, P=0.10). The majority of lactate accumulation in muscle from pair-fed animals occurred between 45 and 90 min, whereas lactate accumulation was more linear in the β-GPA group.

Initially, postmortem metabolism is driven largely by ATP demand. In turn, the ability to maintain ATP during the postmortem period is a function of both ATP utilization and ATP production. Creatine kinase and myokinase ($2ADP \leftrightarrow AMP + ATP$) catalyzed reactions consume ADP_{free} and generate ATP, thereby preserving high ATP/ADP. ATP was similar among treatments and declined similarly with time postmortem (treatment, P=0.67; treatment × time, P=0.95; Figure 2-9). Treatment did not alter ADP over time either (treatment × time, P=0.29). Because ATP may remain stable despite large changes in metabolic flux, we also evaluated ATP/ADP ratio. Treatment altered ATP/ADP ratio depending on the time postmortem

(treatment × time, P=0.03). ATP/ADP decreased from 0 to 20 min in control and β-GPA (P<0.05), but remained similar in PF. The detectable decrease in ATP/ADP in control and β-GPA muscle early postmortem is likely the consequence of PCr depletion; this could lead to increases in ADP, and declining levels of ATP. Moreover, in β-GPA muscle, the total Cr pool is compromised, and this would be expected to decrease initial ATP/ADP; although ATP/ADP was numerically lower in β-GPA compared to control at time 0, it was not significant. However, at time 0, ATP/ADP was lower (P<0.05) in muscle from PF pigs compared controls. At first glance, this would suggest compromised energy status in PF muscle; curiously, ATP levels in PF muscle are similar to control, and PF muscle does not exhibit indications of rapid postmortem metabolism or accelerated ATP decline. Potentially, these alterations are related to reduced feed intake and growth, and may actually represent an effort to conserve energy. Decreasing ATP/ADP in living muscle would stimulate energy-producing pathways, and in particular, enhancing oxidative metabolism would be a more efficient means of maintaining energy production with less resources. Moreover, ATP/ADP remained similar from 0 to 20 min in muscle from PF pigs, indicating an increased capacity to buffer ATP levels, and/or decreased ATP demand.

For both experiments, dietary supplementation with β-GPA for 2 wk resulted in a 20% reduction in the total Cr pool in muscle. This is consistent with muscle creatine turnover rate of roughly 2% per day (Picou et al., 1976), and time-course studies in rats (Tullson et al., 1996). In the first study, 2 wk β-GPA supplementation was associated with obvious improvements in pork quality, but also contributed to decreased feed intake and poor performance. For the second experiment, we lowered β-GPA content in the diet from 2% to 1% and also offered sweetened, flavored water supplemented with β-GPA in order to increase feed consumption without

sacrificing β-GPA intake. Further, we added a pair-fed group to better discern differences caused by feed consumption or growth versus reduced muscle Cr. While pig performance improved in the second study, weight gain was still only 50% of control, and there were no detectable improvements in meat quality attributes. It is possible the discrepancies in meat quality between experiments are due to metabolic differences relating to weight maintenance (experiment 1) versus growth (experiment 2) in β-GPA treatment groups.

Conclusions

Dietary supplementation with β-GPA for 2 wk reduces total Cr pool in pig *longissimus* muscle but also reduces feed intake and growth performance. Despite reduced capacity to generate ATP via the phosphagen system, β-GPA supplementation does not accelerate early postmortem pH decline or glycolysis. In the first study, β-GPA supplemented pigs maintained weight and produced higher quality pork, whereas in the second study, β-GPA supplemented pigs exhibited limited weight gain and generated similar quality pork as control pigs. β-GPA supplementation results in time-dependent changes in gene and protein expression. Moreover, restricted growth also influences adaptive mechanisms that alter enzyme activity and/or ATP turnover. Thus, the dramatic differences in pork quality in the first study may be due to synergistic effects of β-GPA and growth restriction.

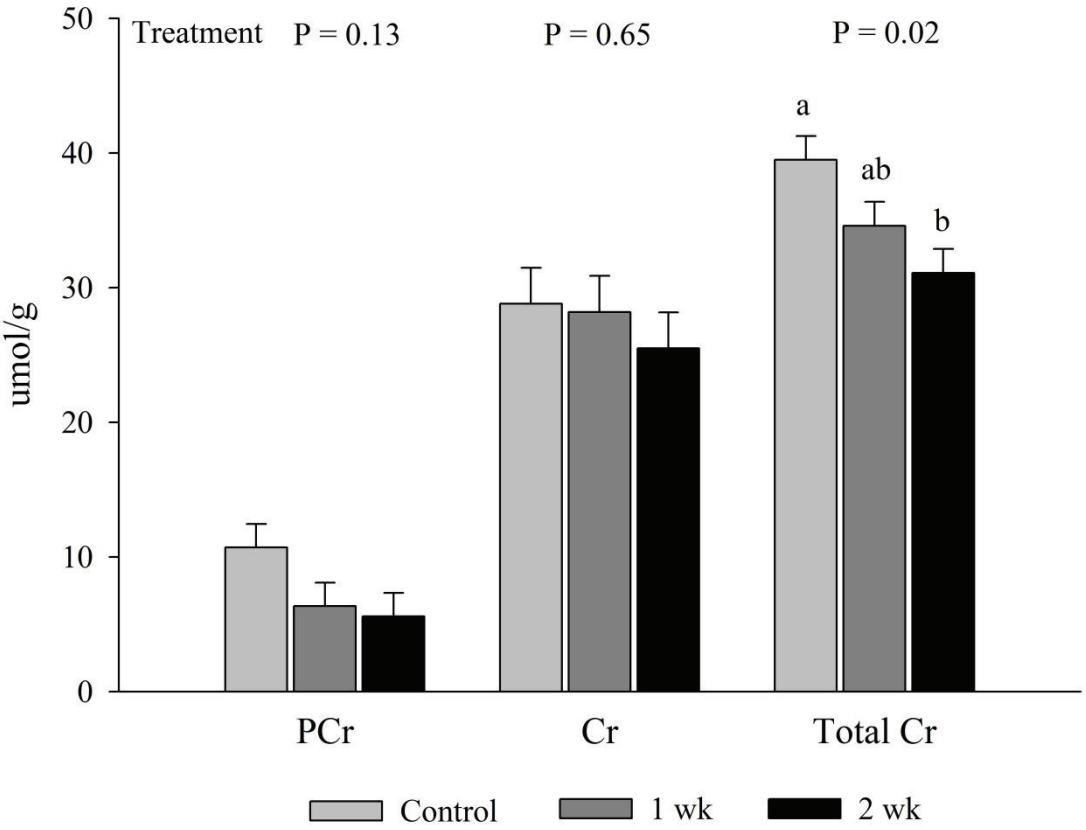

Figure 2-1. Phosphocreatine, creatine, and total pool (PCr + Cr) in *longissimus* muscle of control and β-GPA treatments (1 wk or 2 wk). Data are LS means ± SE. Different subscripts (a,b) indicate significant differences (P<0.05) between treatments. P-values are for main effects of treatment.

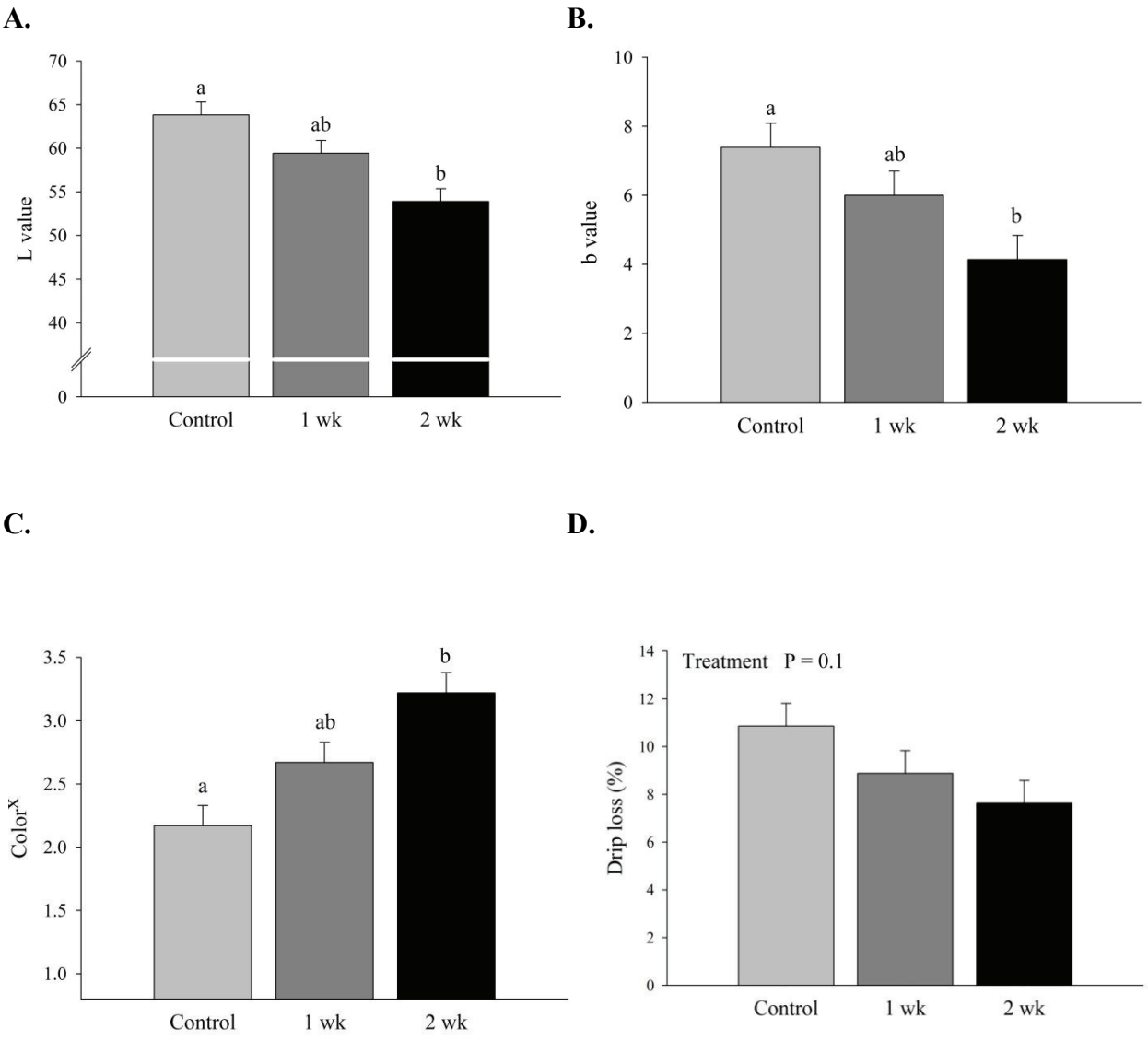

Figure 2-2. Pork quality characteristics of pigs consuming control and β-GPA supplemented diets (1 or 2 wk). Lightness or L-value (A), yellowness or b-value (B), subjective color score (C), and drip loss (D) of *longissimus* muscle. Data are LS means ± SE. Different subscripts (a,b) indicate significant differences (P<0.05) between treatments.
[x] Subjective color: 1 = pale, pinkish gray to white and 6 = dark purplish red

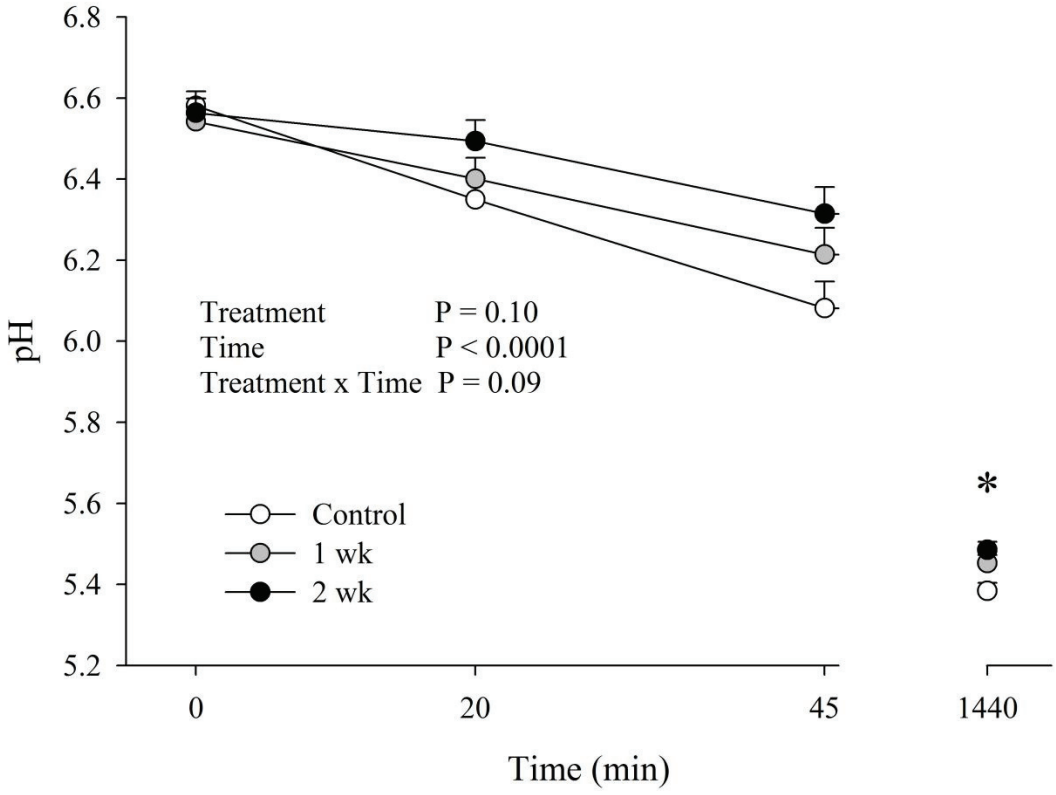

Figure 2-3. Postmortem pH decline in *longissimus* muscle of control and β-GPA supplemented (1 or 2 wk) pigs. Data are LS means ± SE. *2 wk β-GPA is different from control (P<0.05).

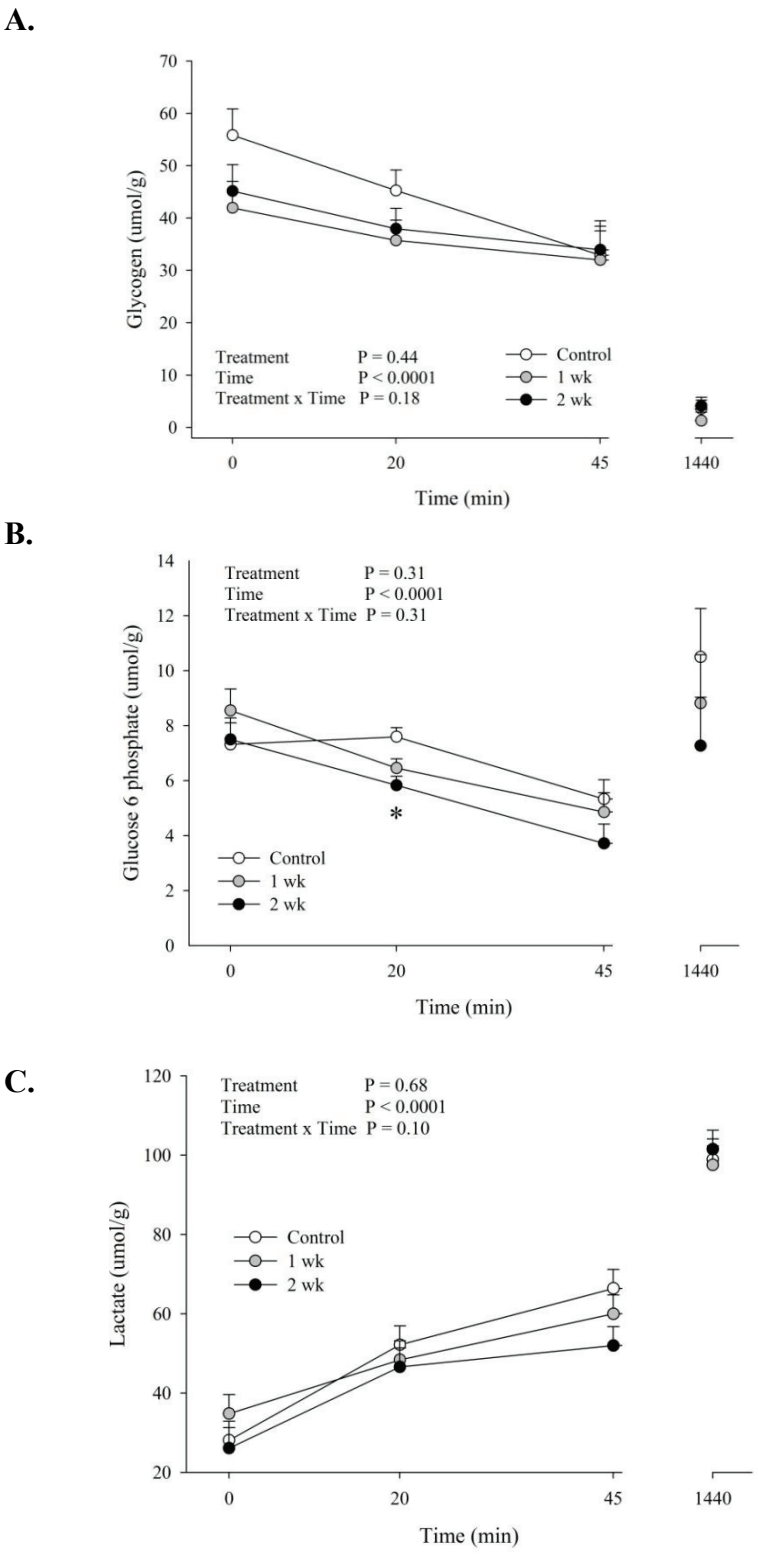

Figure 2-4. Postmortem changes in glycogen, glucose 6-phosphate, and lactate content of longissimus muscle of control and β-GPA supplemented (1 or 2 wk) pigs. Data are LS means ± SE. *2 wk β-GPA is different from control (P<0.05)

Variable	Control	1 wk	2 wk	SE	Significance
Initial weight, kg	83.3	82.9	87.0	3.1	NS
1 wk weight, kg	93.1	92.2	87.6	3.0	NS
Final weight, kg	98.9 [a]	89.3 [b]	88.0 [b]	2.9	0.04
Weight gain, kg					
Wk 0 – 1	9.3 [a]	9.8 [a]	0.6 [b]	0.9	<0.0001
Wk 1 – 2	5.8 [a]	-2.8 [b]	0.3 [b]	0.9	0.0004
Feed disappearance, kg					
Wk 0 – 1	9.8 [a]	10.5 [a]	5.0 [b]	0.7	0.0008
Wk 1 – 2	16.0 [a]	6.9 [b]	6.1 [b]	1.5	0.002

Table 2-1. Performance during trial period for control and β-GPA (1 wk and 2 wk) treatments. [a,b] LS means within a row that do not have a common subscript (a, b) differ P<0.05

Variable	Control	PF	β-GPA	Significance
Initial weight, kg	89.5 ± 2.6	91.9 ± 2.2	92.3 ± 2.2	NS
Final weight, kg	100.2 ± 3.2	97.1 ± 2.6	97.5 ± 2.6	NS
Weight gain, kg	10.6 ± 1.2 [a]	5.1 ± 1.0 [b]	5.2 ± 1.0 [b]	0.002

Table 2-2. Performance during trial period for control, pair-fed (PF), and β-GPA treatments. [a,b] LS means within a row that do not have a common subscript (a, b) differ $P<0.05$

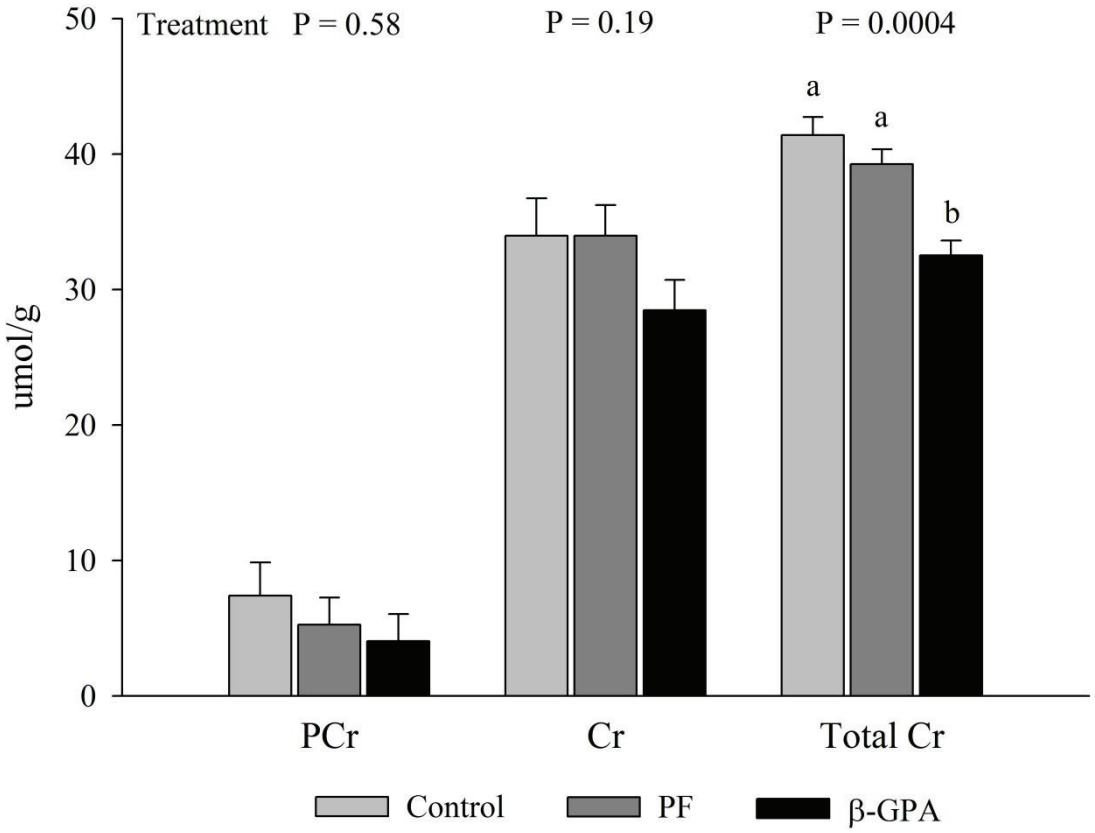

Figure 2-5. Phosphocreatine, creatine, and total pool (PCr + Cr) in *longissimus* muscle of control, pair-fed (PF), and β-GPA (2 wk). Data are LS means ± SE. Different subscripts (a,b) indicate significant differences (P<0.05) between treatments. P-values are for main effects of treatment.

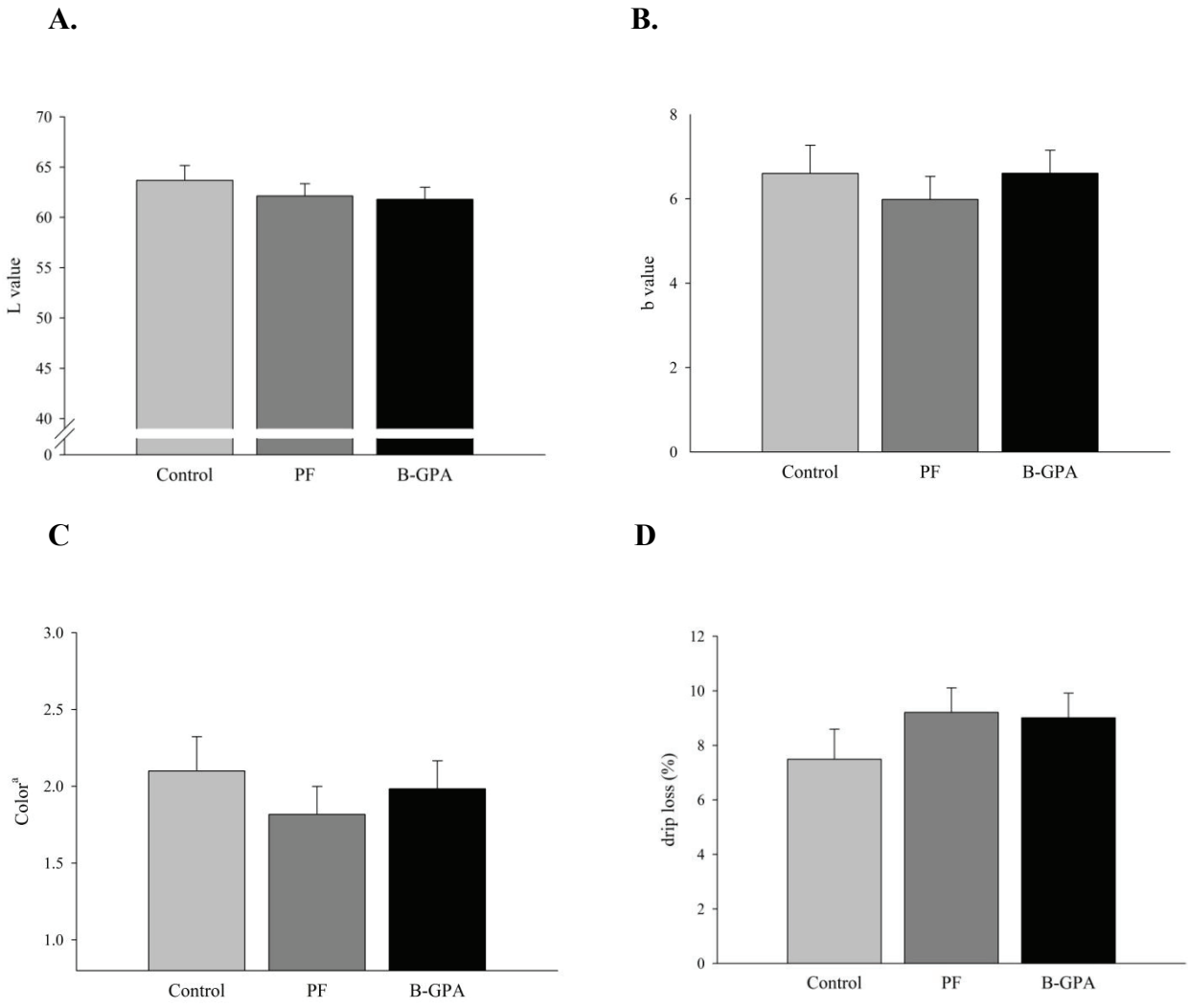

Figure 2-6. Pork quality characteristics of control, pair-fed (PF), or β-GPA supplemented diets (1 or 2 wk). Lightness or L-value (A), yellowness or b-value (B), subjective color score (C), and drip loss (D) of *longissimus* muscle. Data are LS means ± SE.
[a] Subjective color: 1 = pale, pinkish gray to white and 6 = dark purplish red

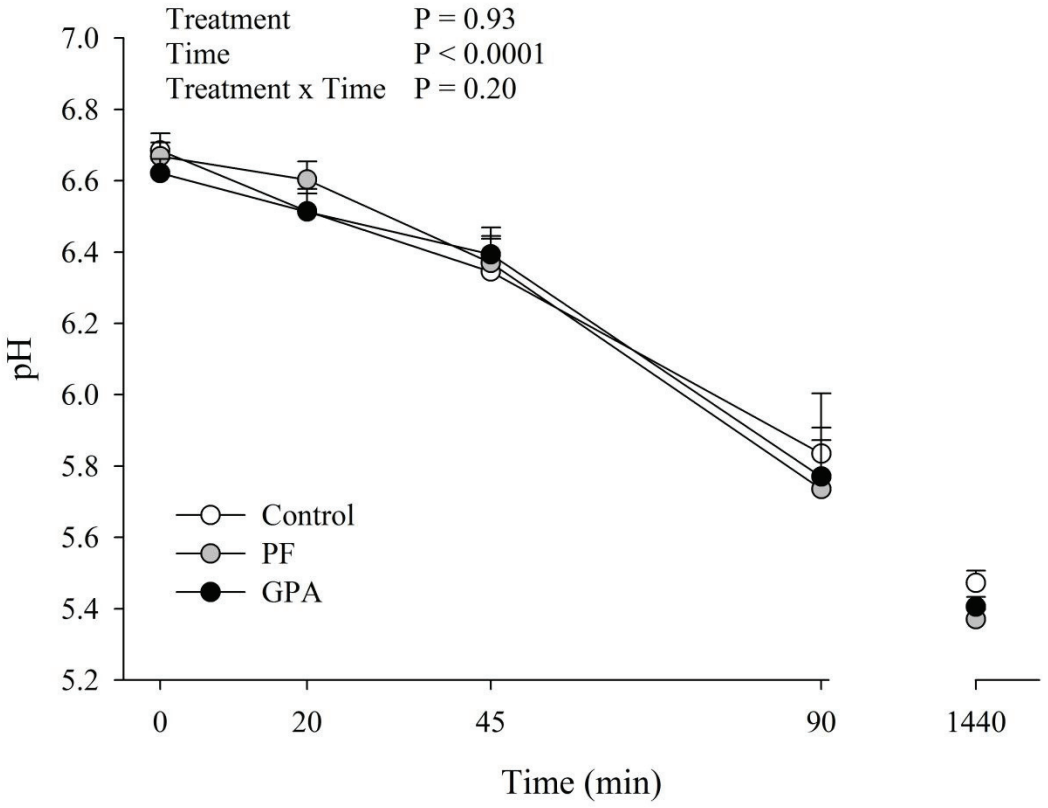

Figure 2-7. Postmortem pH decline in *longissimus* muscle of control, pair-fed (PF) and β-GPA supplemented pigs. Data are LS means ± SE.

A.

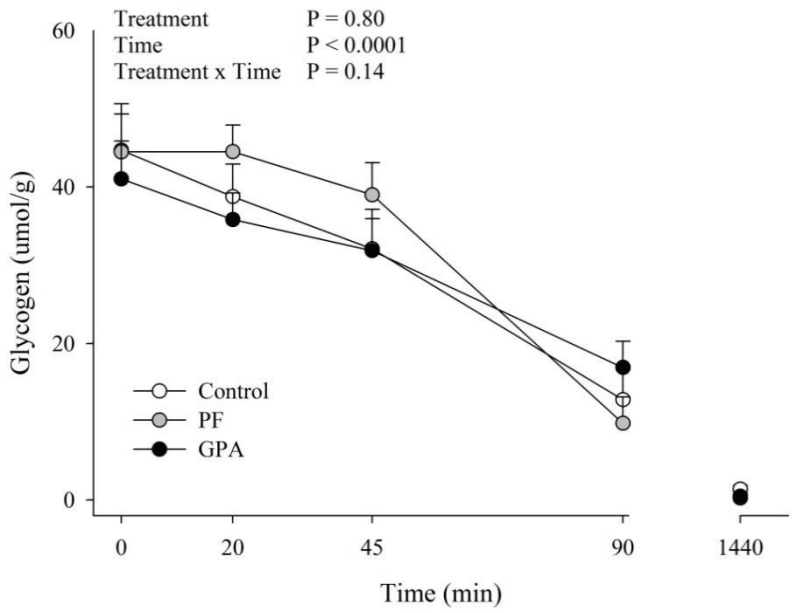

B.

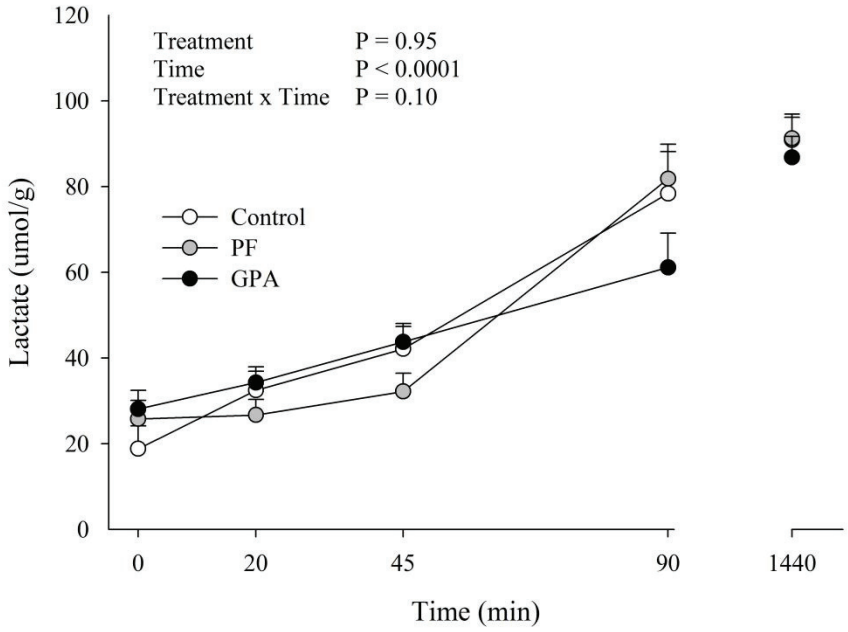

Figure 2-8. Postmortem changes in glycogen and lactate content of *longissimus* muscle of control, pair-fed (PF) and β-GPA supplemented pigs. Data are LS means ± SE.

Time (min)	0	20	45	90
ATP (μmol/g)				
Control	5.73 ± 0.33	4.77 ± 0.41	3.95 ± 0.71	0.90 ± 0.63
PF	5.90 ± 0.20	5.31 ± 0.33	4.62 ± 0.58	1.17 ± 0.51
β-GPA	5.75 ± 0.20	5.07 ± 0.33	4.04 ± 0.58	1.40 ± 0.51
ADP (μmol/g)				
Control	0.50 ± 0.07	0.84 ± 0.10	0.83 ± 0.07	0.46 ± 0.16
PF	0.71 ± 0.04	0.72 ± 0.08	0.79 ± 0.06	0.58 ± 0.13
β-GPA	0.64 ± 0.04	0.92 ± 0.08	0.86 ± 0.06	0.73 ± 0.13

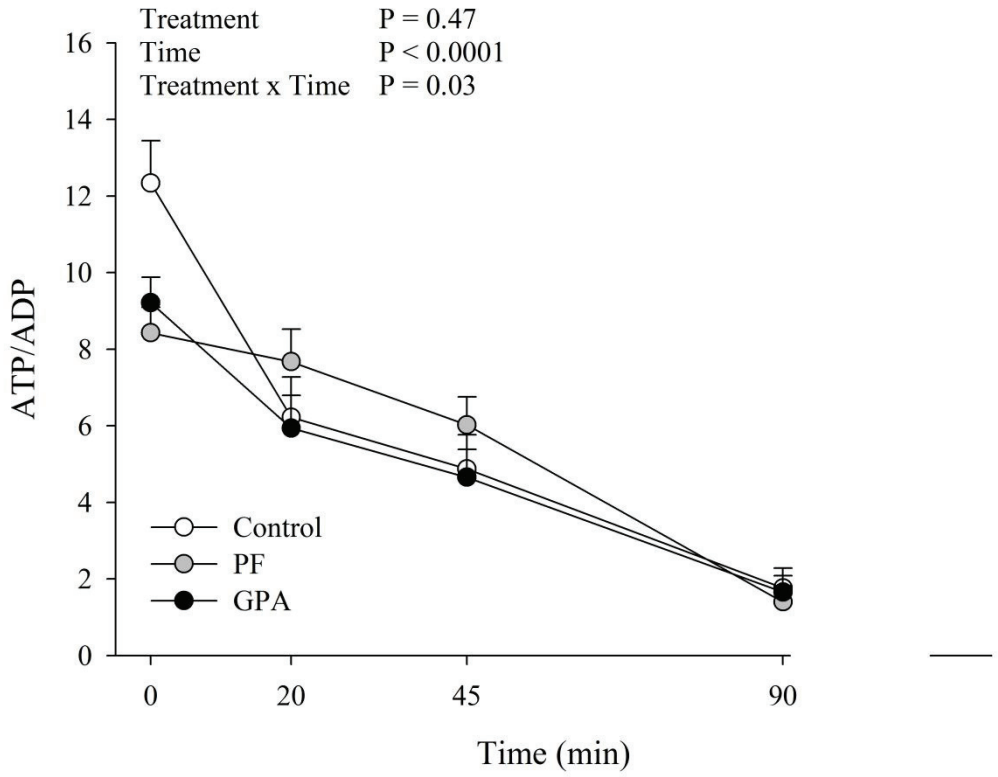

Figure 2-9. ATP, ADP, and ATP/ADP contents in *longissimus* muscle of control, pair-fed (PF) and β-GPA pigs. Data are means ± SE.

References

Bendall, J. R. 1973. Post mortem changes in muscle. In: G. H. Bournes (ed.) The structure and function of muscle. p 227-274. Academic Press, New York.

Bergmeyer, H. U. 1974. Methods of enzymatic analysis. Academic Press, New York.

Bernocchi, P., C. Ceconi, A. Cargnoni, P. Pedersini, S. Curello, and R. Ferrari. 1994. Extraction and assay of creatine phosphate, purine, and pyridine nucleotides in cardiac tissue by reversed-phase high-performance liquid chromatography. Anal. Biochem. 222: 374-379.

Briskey, E. J. 1964. Etiological status and associated studies of pale, soft, exudative porcine musculature Adv. Food Res. 13: 89-178.

Chevli, R., and C. D. Fitch. 1979. β-Guanidinopropionic acid and phosphorylated β-guanidinopropionic acid are substrates for creatine kinase. Biochemical Medicine 21: 162-167.

Copenhafer, T. L., B. T. Richert, A. P. Schinckel, A. L. Grant, and D. E. Gerrard. 2006. Augmented postmortem glycolysis does not occur early postmortem in AMPKγ3-mutated porcine muscle of halothane positive pigs. Meat Sci. 73: 590-599.

Hammelman, J. E., B. C. Bowker, A. L. Grant, J. C. Forrest, A. P. Schinckel, and D. E. Gerrard. 2003. Early postmortem electrical stimulation simulates PSE pork development. Meat Sci. 63: 69-77.

Honikel, K. O., and C. J. Kim. 1986. Causes of the development of PSE pork. Fleischwirtsch. 66: 349-353.

Meyer, R. A., T. R. Brown, B. L. Krilowicz, and M. J. Kushmerick. 1986. Phosphagen and intracellular pH changes during contraction of creatine-depleted rat muscle. Am. J. Physiol., Cell Physiol. 250: C264-274.

Meyer, R. A., and J. M. Foley. 1996. Cellular processes integrating the metabolic response to exercise Handbook of Physiology. p 841-869.

Moerland, T. S., N. G. Wolf, and M. J. Kushmerick. 1989. Administration of a creatine analogue induces isomyosin transitions in muscle. Am. J. Physiol. 257: C810-816.

Monin, G., and P. Sellier. 1985. Pork of low technological quality with a normal rate of muscle pH fall in the immediate post-mortem period: the case of the Hampshire breed. Meat Sci. 13: 49-63.

NPPC. 1991. Procedures for evaluating market hogs. National Pork Producers Council, Des Moines, IA.

NPPC. 2000. Pork composition and quality assessment procedures. National Pork Producers Council, Des Moines, IA.

Passonneau, J. V., and O. H. Lowry. 1993. Enzymatic analysis: A practical guide. Humana Press, Totowa, NJ.

Picou, D., P. J. Reeds, A. Jackson, and N. Poulter. 1976. The measurement of muscle mass in children using [15N]creatine. Pediatr. Res. 10: 184-188.

Rasmussen, A., and M. Andersson. 1996. New method for determination of drip loss in pork muscles. In: Proc. 42nd Int. Congr. Meat Sci. Technol., Lillehammer, Norway. p 286-287.

Sahlin, K., J. Gorski, and L. Edstrom. 1990. Influence of ATP turnover and metabolite changes on IMP formation and glycolysis in rat skeletal muscle. Am. J. Physiol. 259: C409-412.

Scheffler, T. L., S. Park, and D. E. Gerrard. 2011. Lessons to learn about postmortem metabolism using the AMPKgamma3(R200Q) mutation in the pig. Meat Sci. 89: 244-250.

Shoubridge, E. A., R. A. Challiss, D. J. Hayes, and G. K. Radda. 1985. Biochemical adaptation in the skeletal muscle of rats depleted of creatine with the substrate analogue β-guanidinopropionic acid. Biochem. J. 232: 125-131.

Tullson, P. C., K. W. Rundell, R. L. Sabina, and R. L. Terjung. 1996. Creatine analogue β-guanidinopropionic acid alters skeletal muscle AMP deaminase activity. Am. J. Physiol. 270: C76-85.

Warner, R. D., R. G. Kauffman, and M. L. Greaser. 1997. Muscle protein changes post mortem in relation to pork quality traits. Meat Sci. 45: 339-352.

Williams, J. H., S. E. Vidt, and J. Rinehart. 2008. Measurement of sarcoplasmic reticulum Ca^{2+} ATPase activity using high-performance liquid chromatography. Anal. Biochem. 372: 135-139.

Chapter 3. The creatine analog β-guanidinopropionic acid hastens postmortem muscle metabolism in pigs with AMP-activated protein kinase γ3 R200Q mutation

Abstract

Pigs with the AMP-activated protein kinase γ3 R200Q mutation (AMPKγ3^{R200Q}) generate pork with low ultimate pH (pH_u). Muscle total creatine content, which includes creatine (Cr) and phosphocreatine (PCr), can be reduced by dietary supplementation with the Cr analogue, β-guanidinopropionic acid (β-GPA). We hypothesized that reducing muscle Cr and PCr may accelerate postmortem glycolysis and ATP loss, and prevent extended pH decline in AMPKγ3^{R200Q} pigs. Wild type and AMPKγ3^{R200Q} pigs were assigned to control or β-GPA supplemented (1%) diet for 2 wk. Regardless of genotype, β-GPA reduced muscle PCr ($P=0.006$) and total Cr ($P<0.0001$). β-GPA supplementation did not influence glycogen breakdown, but genotype and diet affected lactate accumulation over time (genotype × diet × time, $P=0.03$). In general, AMPKγ3^{R200Q} + β-GPA exhibited more rapid metabolism than control, AMPKγ3^{R200Q}, β-GPA treatments; this was evidenced by more rapid loss of ATP, more rapid increase in IMP, and decreased pH during the first 90 min postmortem. Overall, pH_u was similar despite elevated glycogen (AMPKγ3^{R200Q}), reduced total Cr (β-GPA) or both (AMPKγ3^{R200Q} + β-GPA). Although total Cr did not affect pH_u, it is particularly important in maintenance of ATP levels in AMPKγ3^{R200Q} muscle early postmortem. Moreover, elevated glycogen did not affect pH_u, supporting that factors other than glycogen content are important for determining pH_u in pork.

Introduction

Pork quality development is largely determined by the rate and extent of postmortem metabolism and pH decline. The Halothane mutation and acute stress accelerate ATP hydrolysis, anaerobic glycolysis, and accumulation of lactate and H^+, resulting in pale, soft, and exudative (PSE) pork. Conversely, the AMP-activated protein kinase γ3 R200Q mutation (AMPKγ3^{R200Q}) results in pork with low ultimate pH (pH_u) or "acid meat" (Monin and Sellier, 1985). Abnormally low pH_u contributes to PSE development by reducing net charge of myofibrillar proteins and myofilament spacing (Irving et al., 1989) and decreasing sarcoplasmic protein solubility (Joo et al., 1999). Moreover, low pH_u is particularly detrimental to processing yield; pigs with AMPKγ3^{R200Q} were originally referred to as Rendement Napole (RN-) due to the negative effect of the mutant allele on cured and cooked ham yield, as determined by the Rendement Napole laboratory method.

Prior to availability of DNA sequencing and genotyping procedures, pigs predisposed to developing "acid meat" were identified on basis of "glycolytic potential". AMPKγ3^{R200Q} increases muscle glycogen content by 70% (Milan et al., 2000), thus enhancing glycolytic potential and capacity for extended postmortem glycolysis (Monin and Sellier, 1985). However, glycolysis stops in the presence of residual glycogen, and lactate levels may be similar despite variation in ultimate pH (Monin and Sellier, 1985). Further, the AMPKγ3^{R200Q} mutation not only alters glycogen, but also enhances muscle oxidative capacity (Estrade et al., 1994; Lebret et al., 1999), suggesting other mechanisms may be responsible for low pH_u.

Extended postmortem metabolism in AMPKγ3^{R200Q} pigs may be associated with an enhanced ability to maintain ATP levels postmortem. In addition to anaerobic glycolysis, creatine kinase and adenylate kinase are involved in ATP production. Creatine kinase can

rapidly generate ATP from phosphocreatine (PCr): PCr + ADP + $H^+ \leftrightarrow$ ATP + creatine (Cr). Because resting PCr levels are typically much greater than ATP (~24 versus ~6 μmol/g), the phosphagen system provides an immediate means of buffering ATP levels. However, with high energy demand, creatine kinase may only produce enough ATP to last a few seconds (Meyer and Foley, 1996). Myokinase (2 ADP $\leftrightarrow$ ATP + AMP) and glycolysis generate additional ATP. Previously, we determined that pigs possessing AMPKγ3^{R200Q} had higher PCr levels immediately postmortem (Copenhafer et al., 2006). Higher PCr levels indicate increased ability to maintain ATP levels postmortem, or alternatively, suggest a larger total Cr pool. Enhanced ability to maintain ATP via the phosphagen system may contribute to extended pH decline and low pHu. Thus, decreasing the Cr pool may reduce the capacity to maintain ATP, and could prevent extended pH decline. Therefore, our objective was to decrease the Cr pool in order to understand the contribution of the phosphagen system to postmortem metabolism in wild type and AMPKγ3^{R200Q} pigs.

Materials and Methods

Animals. All procedures with animals were conducted in accordance and with prior approval of the Virginia Tech Animal Care and Use Committee. Animals used for this study were reared at the Virginia Tech Swine Center. A total of 24 animals were utilized in a 2 × 2 factorial arrangement. Animals selected for the experiment were moved to a different building, penned in groups of three in approximately 7.5 m^2 pens, and allowed 3 d before for adjustment prior to initiation of the experiment. Pigs possessing wild type or AMPKγ3^{R200Q} mutation (carriers and homozygous mutant) were randomly assigned to control or treatment diet (weight range 77-105 kg, mean = 90 kg). Treatment diet consisted of a standard (control) swine diet supplemented

with 1% β-GPA. Because β-GPA negatively affects feed intake, we also included molasses (both diets) to improve palatability. Because β-GPA reduces feed intake even when provided ad libitum, we provided β-GPA diet ad libitum but restricted feed to pigs assigned to the control diet. At the end of the 2 wk treatment period, pigs were transported to the Virginia Tech Meat Science Center and harvested. Pigs were electrically stunned and exsanguinated. Exsanguination was considered time 0.

Genotype determination. Genotypes were determined using polymerase chain reaction restriction fragment length polymorphism technique. DNA was isolated from tissue and used for PCR amplification. For determination of AMPKγ3^{R200Q} genotype, the primers were (5' → 3') AAATGTGCAGACAAGGATCTC (Forward) and CCCACGAAGCTCTGCTT (Reverse). AMPKγ3^{R200Q} genotype was determined using restriction enzyme BsrBI; the single nucleotide polymorphism (G→A) deletes the restriction enzyme recognition site. PCR products were digested with enzyme overnight and fragments were separated on an agarose gel stained with ethidium bromide for visualization.

Muscle sampling. Muscle samples (~5 g) were collected from the lumbar region of the *longissimus* muscle at 0, 20, 45, and 90 min and 24 h (1440 min) postmortem. Samples were immediately frozen in liquid nitrogen and stored at –80 °C until analysis.

Meat quality characteristics. At 24 h postmortem, carcasses were ribbed between the 10th and 11th costae. Two 2.54-cm thick chops were removed from the carcass anterior to the cut surface at the 10th rib and trimmed to remove excess backfat and connective tissue. At the cut surface of the *longissimus* at the 10th rib, objective color measurements were determined using a portable

Minolta CR300 colorimeter (Ramsey, NJ, USA). Mean L (lightness), a (redness), and b (yellowness) values were collected from three separate locations on the surface of the chop. Water holding capacity was determined on the adjacent chop using the drip loss method (Rasmussen and Andersson, 1996). Briefly, muscle samples were collected from one chop using a coring device and placed in drip loss tubes. After 24 h at 4°C, the drip loss containers plus samples were weighed. Muscle samples were removed and containers were reweighed with exudates. Percentage drip loss was calculated and recorded.

Muscle metabolite analysis and pH measurements. Muscle glucose, glucose 6-phosphate (G6P), glycogen, and lactate concentrations were determined using enzyme analytical methods (Bergmeyer, 1974) modified to a 96-well configuration (Hammelman et al., 2003). For pH determination, ~1 g of frozen muscle was homogenized in 10 ml of 5mM iodoacetate. The pH of the homogenate was determined using a ROSS electrode attached to an Orion pH meter (Thermo Fisher Scientific, Beverly, MA, USA).

Adenosine nucleotides and IMP. Adenosine triphosphate, adenosine diphosphate, adeonosine monophosphate, and inosine monophosphate were detected using high performance liquid chromatography (HPLC; Agilent Technologies, Santa Clara, CA, USA) with modifications (Bernocchi et al., 1994; Williams et al., 2008). Muscle samples were homogenized in 0.5 M perchloric acid and neutralized with $KHCO_3$; extracts were filtered (0.2 µm) prior to injection. Separation was accomplished using a C_{18} 2.6-µm reversed-phase column (0.46 x 5 cm) (Kinnetex Phenomenex, Torrance, CA, USA). The mobile phase consisted of a gradient; buffer A was composed of 0.1 M KH_2PO_4, 5 mM tetrabutylammonium hydrogen sulfate (TBAHS), and 2.5% acetonitrile (v/v) (pH 6.0), while the second buffer (B) consisted of 0.1 M KH_2PO_4, 5 mM TBAHS and 25% acetonitrile (pH 5.5). The column was eluted for 2 min with buffer A, for 2

min with buffers A and B (increasing to 11%), and for 4 min with increase to 45% buffer B, and lastly, reequilibrated for 15 min with 100% buffer A. Flow was 2.0 ml/min and separation was performed at room temperature. Adenosine nucleotides and IMP were detected at 254 nm and were quantified by using peak areas and retention times of external standards.

Phosphocreatine and creatine. Sample PCr was determined using neutralized muscle extracts analyzed by a standard sequential enzyme assay (Passonneau and Lowry, 1993). Creatine was determined using a kit (BioVision, Milpitas, CA, USA) according to the manufacturer's instructions. Total Cr is the sum of PCr (enzyme analysis) and Cr (kit) values.

Statistical analysis. Relationships between GPA administration and meat quality development were analyzed using proc mixed procedure of SAS. Three animals were excluded from statistical analysis due to poor performance on the β-GPA diet (1 wild type pig and 2 AMPKγ3 pigs). The model included the effect of diet (control or β-GPA supplementation), AMPKγ3 genotype (wild type or carrier and mutant), and the diet × genotype interaction. The 'repeated' statement was used for pH and metabolite measurements made at multiple time points; time, diet, genotype, and the 2-way and 3-way interactions were included in the model. The slices statement was used to determine diet, genotype or diet × genotype effects at individual time points; for interactions with significant differences at a particular time point, differences were determined using contrasts with adjustments for multiple comparisons. For variables that did not include 'time' as a factor (ie, total Cr), Tukey's adjustment for multiple comparisons was used to compare least square means.

Results and Discussion

Our objective for this study was to manipulate total Cr in muscle of wild type and AMPK$\gamma3^{R200Q}$ mutant pigs in order to better understand the role of the phosphagen system in postmortem metabolism and pH decline. Dietary supplementation with β-GPA reduces muscle total Cr, but also decreases feed intake and growth (Scheffler, unpublished observations). Because reduced energy intake influences metabolism, we opted to provide 1% β-GPA diet ad libitum but limit fed control pigs. Initial and final weights were similar between all groups. However, β-GPA supplementation reduced weight gain (main effect: diet, P = 0.006; Table 3-1) during the 2 wk trial period. Expected weight gain for pigs fed ad libitum would be approximately 0.8 kg/d, which results in 11 kg in a 2 wk period. Although we do not have a direct ad libitum comparison, this is consistent with weight gain observed in two other experiments we conducted with a 2 wk trial period (Scheffler, unpublished observations). In the current experiment, pigs on the control diet gained about 6 kg in a 2 wk period, which corresponds to nearly a 50% decrease in weight gain.

Because the proportion of PCr versus Cr can be influenced by energy demand early postmortem, total Cr (PCr + Cr) is the most reliable indicator of the "success" of β-GPA supplementation. β-GPA supplementation decreased (P < 0.0001; Figure 3-1) muscle total Cr. There was a tendency (P=0.10) for elevated total Cr in AMPK$\gamma3^{R200Q}$ compared to control pigs, but total Cr levels were similar in β-GPA fed pigs regardless of genotype (genotype × diet interaction, P=0.04). Supplementation with β-GPA for 2 wk resulted in a 15 to 20% decrease in total Cr, which is consistent with our preliminary experiments, yet smaller than that observed in rodents (Tullson et al., 1996). Specifically, β-GPA supplementation reduced muscle PCr (P = 0.006). In agreement, β-GPA supplementation primarily affects PCr first, then Cr content

(Tullson et al., 1996). Although we have observed greater PCr content in longissimus muscle of AMPKγ3^{R200Q} mutant pigs immediately postmortem (Copenhafer et al., 2006), genotype did not affect PCr in this experiment.

Next, we aimed to determine the influence of β-GPA and AMPKγ3 genotype on the course of postmortem glycolysis. As expected, AMPKγ3^{R200Q} dramatically increased (~60%) muscle glycogen ($P < 0.0001$; Figure 3-2), but neither genotype nor β-GPA treatment influenced glycogen degradation over time. Thus, the total amount of glycogen metabolized and its rate of breakdown over time are similar even though glycogen content is much greater in AMPKγ3^{R200Q} muscle. During anaerobic glycolysis, glycogen phosphorylase cleaves the outer chains of glycogen, generating glucose 1-phosphate, which is isomerized to G6P. Genotype also influenced G6P ($P=0.002$, Figure 3-3A) and G6P levels over time ($P=0.007$). G6P was similar between genotypes at 20 min, but at 45 min and after, G6P was greater in AMPKγ3^{R200Q} muscle. Elevated G6P in AMPKγ3^{R200Q} muscle has been reported elsewhere (Copenhafer et al., 2006; Monin and Sellier, 1985) and suggests enhanced activity of glycogen phosphorylase relative to subsequent steps in glycolysis. Glycogen degradation is also facilitated by glycogen debranching enzyme. This enzyme breaks α-1,6 linkages and releases free glucose, which accumulates in postmortem muscle. Genotype affected glucose accumulation over time (genotype × time, $P=0.0006$, Figure 3-3B). In general, AMPKγ3^{R200Q} decreased glucose levels initially, but at 90 min and 24 h, glucose was greater ($P<0.05$) in mutant pigs. Decreased glucose levels immediately postmortem may reflect greater glucose uptake and efficient conversion to G6P by hexokinase in AMPKγ3^{R200Q} muscle. Thus, initial G6P in AMPKγ3^{R200Q} muscle may be from the hexokinase reaction, whereas G6P in wild type muscle would be primarily from glycogenolysis. The final product of anaerobic glycolysis is lactate. Although initial and final

lactate levels were similar across groups, the combined influence of genotype and diet was dependent on time (P=0.03, Figure 3-4). The greatest difference in lactate was at 90 min; while β-GPA or AMPKγ3^{R200Q} alone were numerically similar or less than control, β-GPA + AMPKγ3^{R200Q} resulted in the highest lactate levels. Therefore, the combination of β-GPA and AMPK mutation enhances conversion of glycogen to lactate by 90 min postmortem.

Glycolysis is closely associated with rate and extent of postmortem metabolism. However, ATP levels are a more direct indicator of balance between energy demand and energy production. Moreover, partial loss of total Cr due to β-GPA supplementation can be expected to reduce immediate ATP buffering capacity because creatine kinase, along with myokinase (2ADP ↔AMP+ATP), utilize ADP_{free} to generate ATP, thus maintaining a high ATP/ADP and preventing loss of ΔG_{ATP}. Dietary β-GPA supplementation did not alter ATP, but in combination with AMPKγ3^{R200Q}, altered ATP disappearance over time (P=0.03, Figure 3-5). ATP levels were similar at 0 min, but AMPKγ3^{R200Q} + β-GPA exacerbated ATP loss at 20 min. At 45 and 90 min, AMPKγ3^{R200Q} + β-GPA muscle also had numerically lower ATP content, reflected in the tendency (P=0.07) toward genotype × diet interaction.

During postmortem metabolism, ADP levels may accumulate due to greater ATP hydrolysis relative to ATP production. Diet influenced ADP accumulation in a time-dependent manner (P=0.01, Figure 3-6A). Regardless of AMPK genotype, β-GPA supplementation tended to increase ADP at 0 min, and by 20 min, ADP was greater in muscle from β-GPA pigs. Thereafter, ADP was similar between dietary treatments. Increased ADP in β-GPA supplemented muscle is most likely due to partial loss of PCr and thus reduced capacity to remove ADP early postmortem. Conversely, genotype influenced muscle ADP levels at 90 and 1440 min postmortem (genotype × time, P=0.003, Figure 3-6B). Curiously, at 90 min, ADP was

much lower in AMPK$\gamma3^{R200Q}$ muscle relative to wild type and remained lower at 1440 min. Compared to other treatments, the combination of AMPK$\gamma3^{R200Q}$ + β-GPA seems to increase postmortem metabolism, yet ADP levels remain low. This could be due to near-completion of postmortem metabolism and greater depletion of all adenine nucleotides. Yet, AMPK$\gamma3^{R200Q}$ muscle exhibits similar glycolysis and ATP levels as control and β-GPA muscle, substantiating that low ADP levels at 90 min are indeed a genotype-related phenomena.

Increased myokinase activity could promote conversion of ADP to ATP and AMP, thereby maintaining low ADP. Genotype affected AMP at 90 min (P=0.02, Figure 3-7); however, AMPK$\gamma3^{R200Q}$ was associated with lower AMP. AMP is converted to IMP by AMP deaminase, and combined flux through myokinase and AMP deaminase would result in greater IMP accumulation. β-GPA + AMPK$\gamma3^{R200Q}$ tended to (P=0.10) increase IMP relative to other groups (Figure 3-8A), particularly from 20 to 90 min postmortem (diet × genotype × time, P=0.03). β-GPA supplementation influenced IMP early but not late postmortem (P=0.04; Figure 3-8B). In fact, β-GPA elevated IMP at 0 min (P<0.05) and tended to (P=0.07) increase IMP at 20 min. In contrast, genotype exerted a stronger influence on IMP later postmortem (genotype × time, P=0.03; Figure 3-8C). Relative to wild type, IMP was higher (P<0.05) in AMPK$\gamma3^{R200Q}$ muscle at 90 min and lower at 1440 min. Therefore, combined flux through myokinase and AMP deaminase may partly explain lower ADP levels at 90 min in pigs possessing AMPK$\gamma3^{R200Q}$. Overall, increased IMP accumulation in β-GPA + AMPK$\gamma3^{R200Q}$ muscle is consistent with loss of ATP and more rapid glycolysis.

Rate and extent of metabolism is closely associated with pH decline and pork quality development. Genotype and diet combination affected pH decline over time (P=0.05, Figure 3-9). While pH was similar at 0 min across all treatments, AMPK$\gamma3^{R200Q}$ + β-GPA muscle

exhibited numerically lower pH from 20 to 90 min postmortem and contributed to an overall tendency (P=0.10) for lower pH (genotype × diet, P=0.10). Typically, AMPKγ3^{R200Q} contributes to low pH_u (<5.3). However, mean pH_u values were quite similar between all treatments (<0.10 pH unit difference).

In general, diet and genotype had little impact on meat quality attributes. Redness (a value), yellowness (b value), and drip loss were not affected by AMPKγ3 genotype or β-GPA supplementation (Table 3-2). Curiously, a genotype × diet interaction (P=0.05) was observed for reflectance (L value or lightness). Whereas muscle from AMPKγ3^{R200Q} + β-GPA pigs had similar reflectance as control, β-GPA and AMPKγ3^{R200Q} muscle had decreased reflectance. AMPKγ3^{R200Q} usually increases reflectance (Copenhafer et al., 2006; Hamilton et al., 2000; Lundström et al., 1996), likely due to the low pH_u typically observed in this genotype. However, others have reported decreased reflectance (Bidner et al., 2004). We observed similar pH_u in wild type and AMPKγ3^{R200Q} muscle and this likely explains why reflectance was not increased in this study. Increased rate of postmortem metabolism, characterized by pH < 6.0 at 1h, also generates pork with pale color and increased reflectance. Postmortem metabolism and pH decline are relatively "normal" in different treatment groups. AMPKγ3^{R200Q} + β-GPA muscle exhibited the most rapid pH decline but likely had pH $\geq$ 6 at 1h. In total, the combination of normal rates of postmortem pH decline and similar pH_u are consistent with relatively similar quality attributes across treatments.

Our primary objective was to use dietary supplementation with β-GPA to decrease total Cr in wild type and AMPKγ3^{R200Q} muscle. We hypothesized that decreasing total Cr in AMPKγ3^{R200Q} muscle would prevent extended glycolysis. Supplementation with β-GPA reduced PCr and total Cr, but overall, pH_u was similar across treatments. AMPKγ3^{R200Q} muscle

possessed elevated glycogen and considerable residual glycogen, but AMPK$\gamma3^{R200Q}$ genotype alone did not result in lower pH_u. Thus, if high glycogen content or glycolytic potential was primarily responsible for determining pH_u, AMPK$\gamma3^{R200Q}$ genotype should have decreased pH_u. However, pH decline stopped in the presence of available glycogen, supporting that other factors promote extended glycolysis.

In preliminary experiments, pigs on β-GPA diet consumed less feed and gained less weight. We attempted to offset growth differences by restricting feed provided to pigs on the control diet. While we limited weight gain by ~50% in pigs on the control diet, these pigs still gained more weight than β-GPA supplemented pigs. Thus, it is possible some differences in β-GPA muscle are related to feed intake and growth. Yet, in general, β-GPA alone did not dramatically influence glycogen degradation, ATP breakdown, or pH. Instead, the most profound differences in metabolism were observed in pigs with both AMPK$\gamma3^{R200Q}$ + β-GPA; muscle from these pigs exhibited more rapid postmortem metabolism during the first 90 min.

It is not evident why the β-GPA induced reduction in total Cr had a greater influence on metabolism in AMPK$\gamma3^{R200Q}$ versus wild type pigs. Long term (6 to 8 wk) β-GPA exposure decreases ATP:ADP and activates AMPK (Williams et al., 2009; Zong et al., 2002). Increased AMPK activity may contribute to rapid postmortem metabolism (Shen et al., 2006a; Shen et al., 2006b; Shen et al., 2007). Although phosphagen depletion triggers adaptation by enhancing AMPK activity (Zong et al., 2002), AMPK$\gamma3^{R200Q}$ results in constitutive AMPK activity (Adams et al., 2004; Woods et al., 2000). Thus, increased AMPK activity could be expected in AMPK$\gamma3^{R200Q}$, β-GPA, and AMPK$\gamma3^{R200Q}$ + β-GPA muscle. Thus, it seems unlikely that AMPK activity explains rapid metabolism in AMPK$\gamma3^{R200Q}$ + β-GPA pigs relative to other treatments.

Notably, several adaptations observed in Cr-depleted muscle are similar to characteristics of AMPK$\gamma 3^{R200Q}$ muscle. Exposure to β-GPA induces numerous changes in gene and protein expression, enzyme activity, and metabolic capacity. Phosphagen depletion increases mitochondrial biogenesis and oxidative capacity (Williams et al., 2009; Zong et al., 2002); glucose transporter expression, glucose transport, and glycogen storage (Ren et al., 1993); as well as fatty acid transporter content and fatty acid oxidation (Pandke et al., 2008). Supplementation with β-GPA supplementation also reduces creatine kinase and phosphofructokinase activity (Shoubridge et al., 1985) and decreases AMP deaminase activity, although changes in AMP deaminase do not appear to limit IMP accumulation (Tullson et al., 1996). In order to limit adaptation, our trial period lasted only 2 wk. Certain characteristics induced by β-GPA feeding, such as increased glycogen, were clearly not observed in our study; however, other attributes, such as AMP deaminase activity, begin to decline within 1 wk (Tullson et al., 1996) and thus could be relevant to postmortem metabolism.

Alternatively, the loss of Cr and PCr could be particularly stressful in AMPK$\gamma 3^{R200Q}$ muscle. Cytosolic creatine kinase is positioned near myosin ATPases, sarcoplasmic reticulum calcium ATPases, and membrane ATPases, so it can more directly channel ATP to sites of utilization. It is not clear if phosphagen depletion affects localization of cytosolic creatine kinase, particularly if expression is decreased. However, loss of Cr and PCr is particularly detrimental in slow muscle because it is associated with oxidative damage to mitochondrial creatine kinase, which renders it nonfunctional (O'Gorman et al., 1997; Schlattner et al., 2006). Mitochondrial creatine kinase has important roles in preventing free radical generation and oxidative damage within the mitochondria (Meyer et al., 2006) and protecting against mitochondrial-induced mechanisms of cell death (Dolder et al., 2003). Thus, loss of PCr and Cr

could have different consequences in "normal" glycolytic longissimus compared to more oxidative AMPKγ3^{R200Q} muscle. Thus, we speculate that AMPKγ3^{R200Q} may make muscle more sensitive to cellular energy stress induced by phosphagen depletion, but further research will be necessary to confirm this.

Conclusions

The phosphagen system contributes to ATP buffering capacity early postmortem, and we anticipated that decreasing total Cr in muscle of AMPKγ3^{R200Q} pigs may prevent extended glycolysis. Although total Cr does not appear to affect pH_u, it seems to have particular significance in maintenance of ATP early postmortem in AMPKγ3^{R200Q} muscle. Moreover, regardless of β-GPA supplementation, AMPKγ3^{R200Q} increased glycogen. Yet, total glycogen degradation was similar across treatments, and paralleled by similar final lactate and pH_u. This supports that glycogen content does not directly cause extended pH decline and thus other factors besides glycogen are important for determining pH_u of pork.

Variable	Control	AMPKγ3	β-GPA	AMPKγ3 +β-GPA	Signficance		
					Genotype	Diet	Genotype × Diet
Initial weight, kg	94.8 ± 4.1	88.5 ± 2.9	90.6 ± 3.7	91.0 ± 4.1	NS	NS	NS
Final weight, kg	100.6 ± 4.4	94.4 ± 3.1	91.1 ± 3.9	94.7 ± 4.4	NS	NS	NS
Weight gain, kg	5.8 ± 1.3	5.9 ± 1.0	0.5 ± 1.2	3.6 ± 1.3	NS	0.006	NS

Table 3-1. Performance during 2 wk trial period for control, AMPKγ3, β-GPA, and AMPKγ3 + β-GPA pigs. Data are LS means ± SE. NS = Not significant.

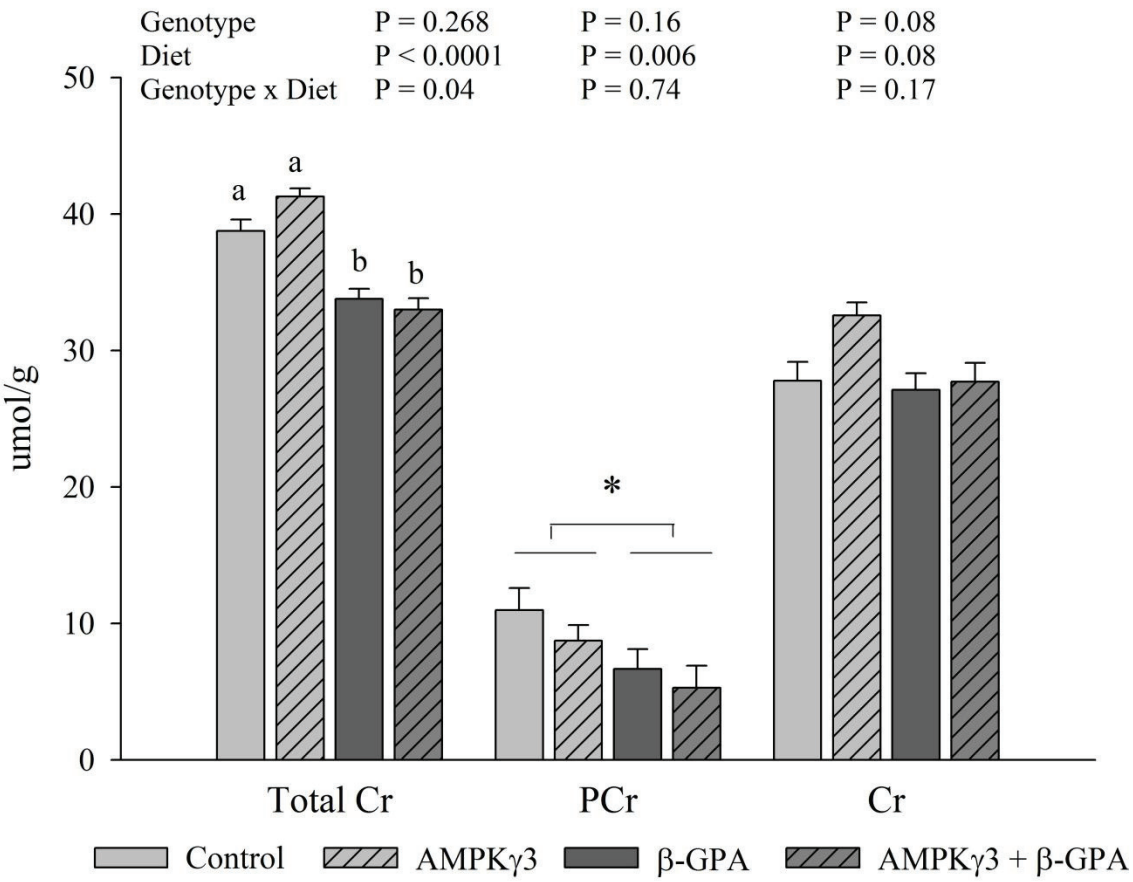

Figure 3-1. Phosphocreatine, creatine, and total pool (PCr + Cr) in longissimus muscle of AMPKγ3 and β-GPA supplemented pigs. Data are LS means ± SE. Different subscripts (a,b) indicate significant differences (P<0.05) between treatments. * Indicates significant difference for main effect between control fed (control and AMPKγ3) and β-GPA fed (β-GPA and β-GPA+ AMPKγ3) pigs. P-values are for main effects and interactions.

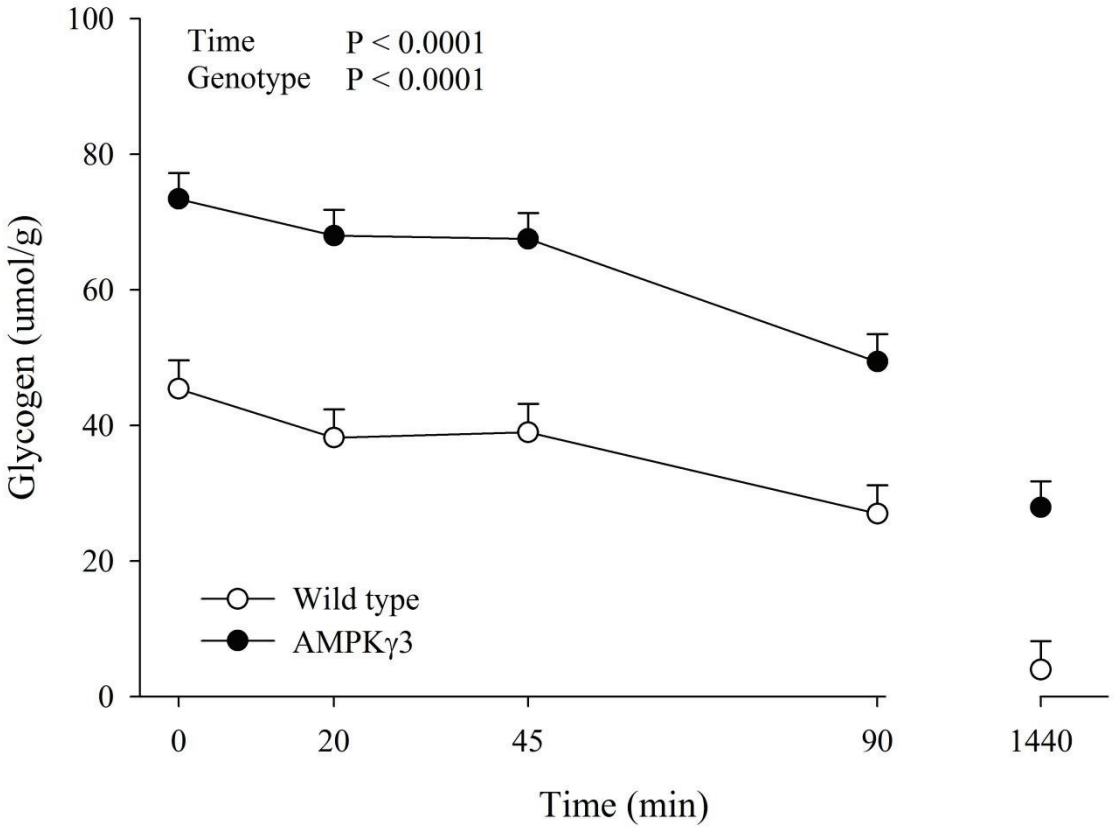

Figure 3-2. Postmortem changes in glycogen content of longissimus muscle of wild type (pooled control and β-GPA) and AMPKγ3R200Q (pooled AMPKγ3 and AMPKγ3+β-GPA) pigs. Data are LS means ± SE. P-values are for main effects.

A.

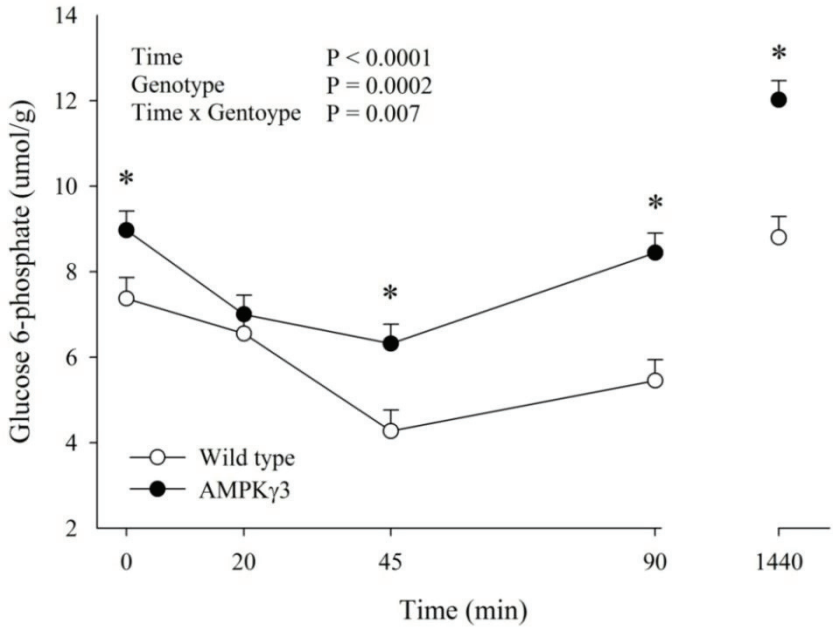

B.

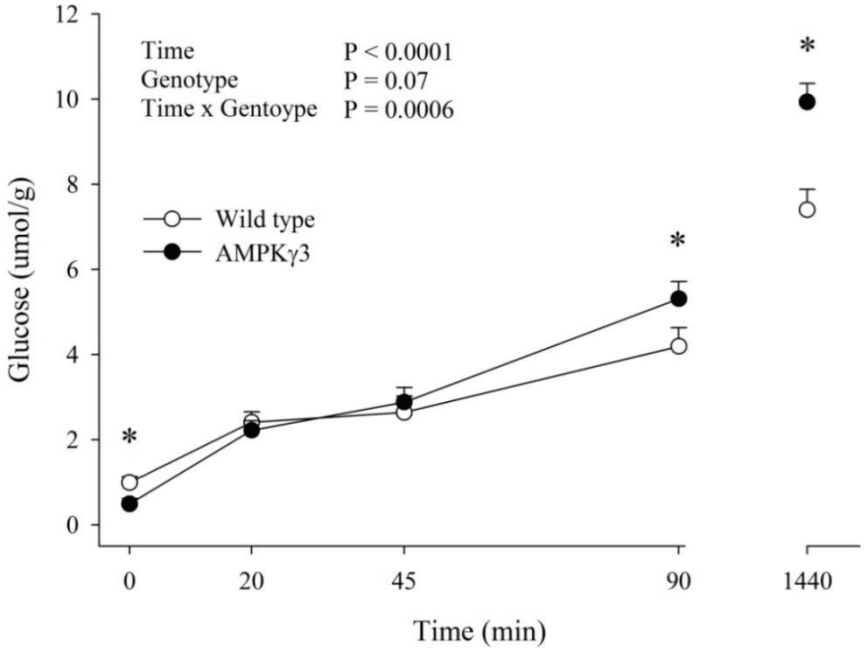

Figure 3-3. Postmortem changes in glucose 6-phosphate (A) and glucose (B) content of longissimus muscle of wild type (pooled control and β-GPA) and AMPKγ3R200Q (pooled AMPKγ3 and AMPKγ3 + β-GPA) pigs. Data are LS means ± SE. P-values are for main effects and interactions. * Indicates significant difference between wild type and AMPKγ3^{R200Q} within a time point.

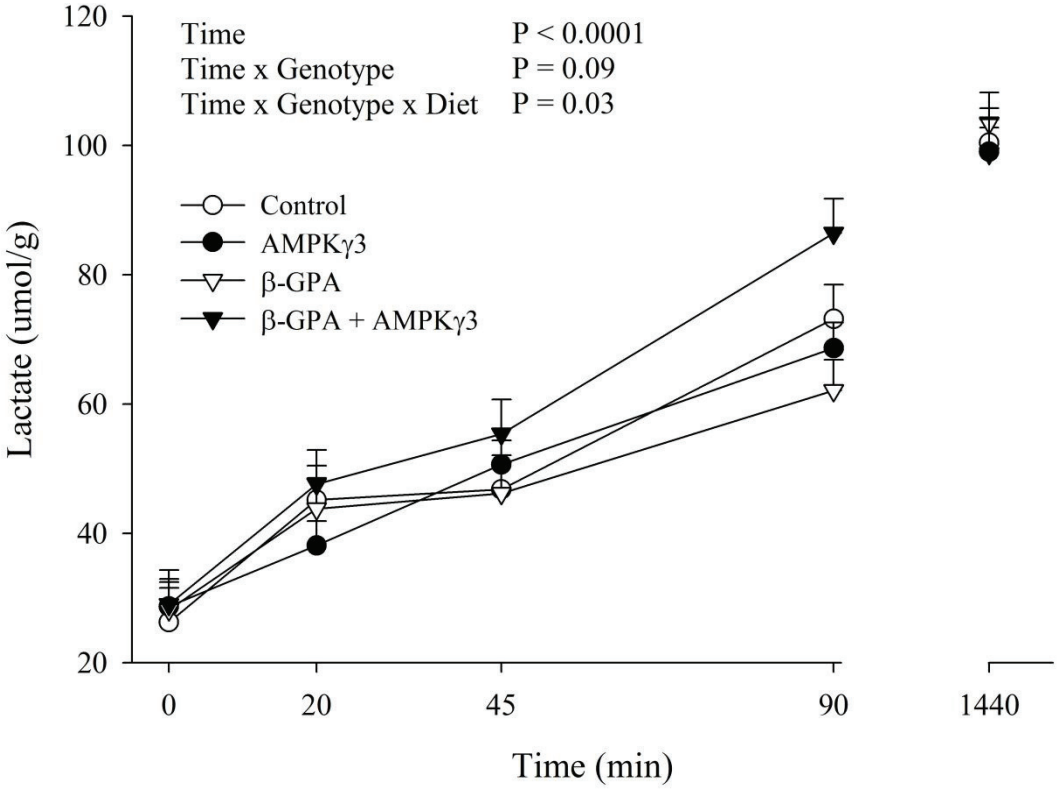

Figure 3-4. Postmortem changes in lactate content of longissimus muscle of control, AMPKγ3, β-GPA, and AMPKγ3 + β-GPA pigs. Data are LS means ± SE. P-values are for main effects and interactions.

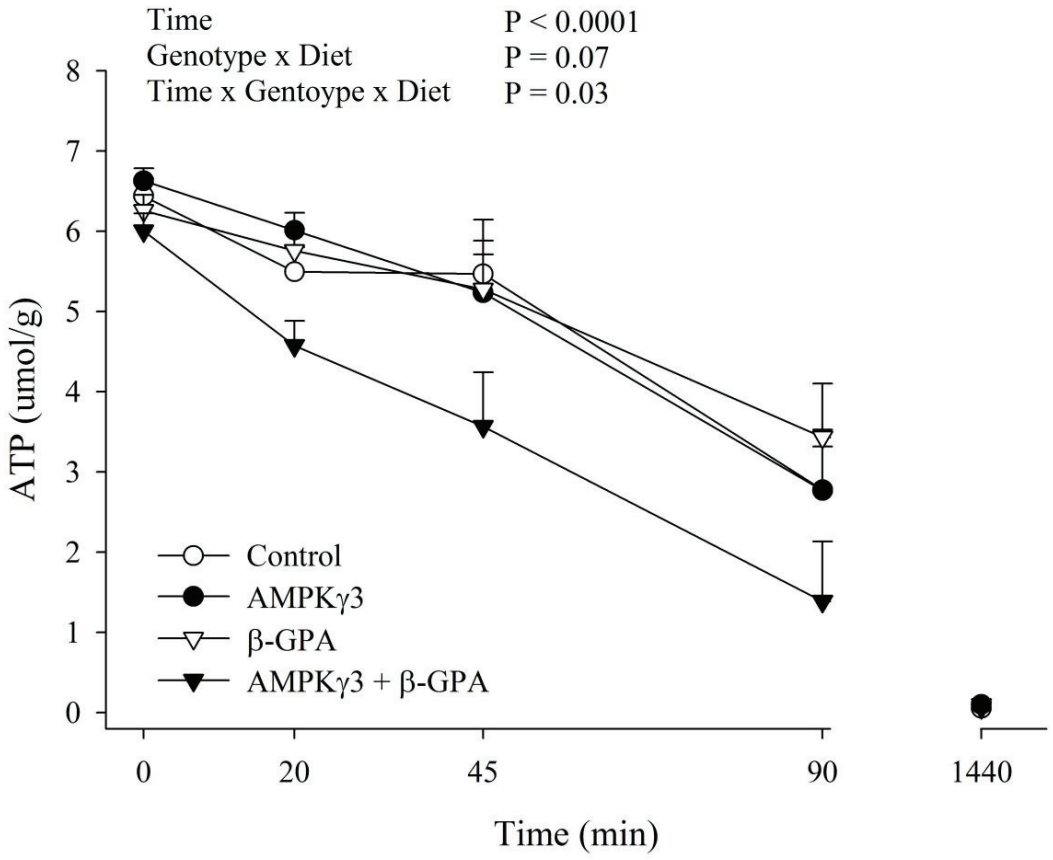

Figure 3-5. ATP content in *longissimus* muscle of control, AMPKγ3, β-GPA, and AMPKγ3 + β-GPA pigs. Data are LS means ± SE. P-values are for main effects and interactions.

A.

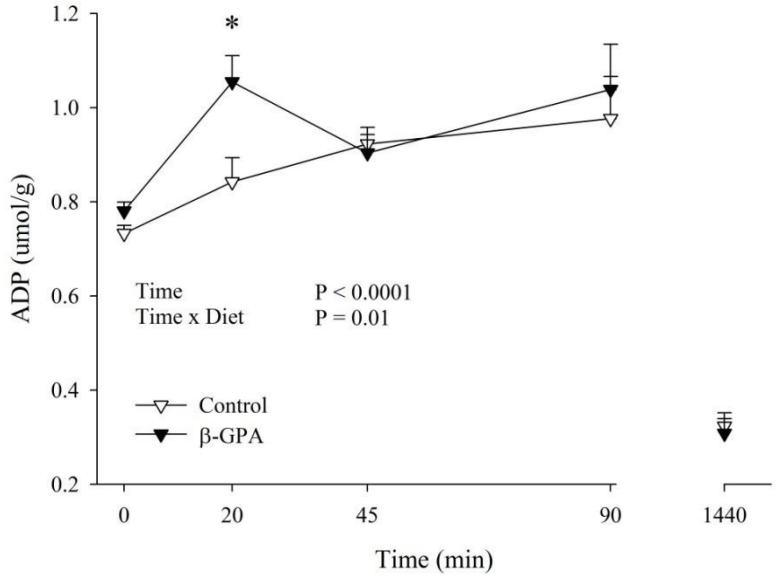

B.

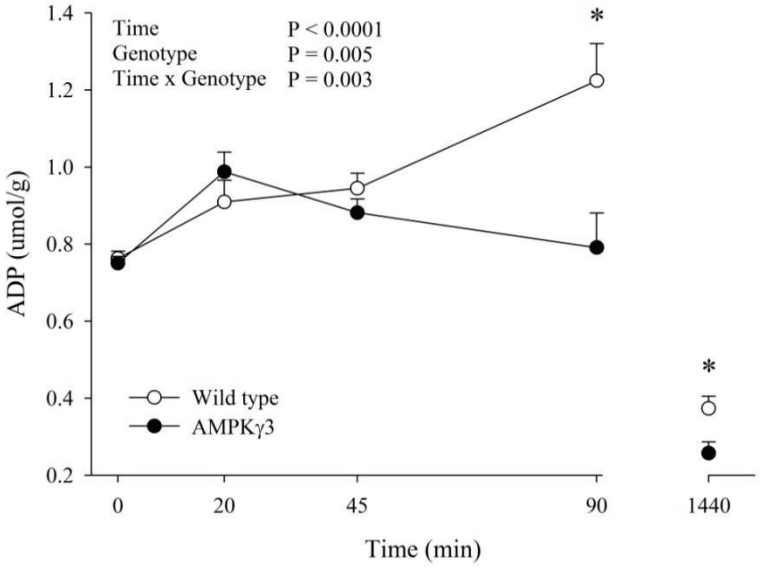

Figure 3-6. Influence of diet (A) and genotype (B) on postmortem ADP contents in longissimus muscle. (A) ADP content of pigs fed control diet (pooled control and AMPKγ3R200Q) and β-GPA supplemented diet (pooled β-GPA and AMPKγ3R200Q + β-GPA). (B) ADP content of pigs of wild type (pooled control and β-GPA) and AMPKγ3R200Q (pooled AMPKγ3 and AMPKγ3 + β-GPA) pigs. Data are LS means ± SE. P-values are for main effects and interactions. * Indicates significant difference (within time point) between (A) control and β-GPA fed, or (B) wild type and AMPKγ3R200Q pigs.

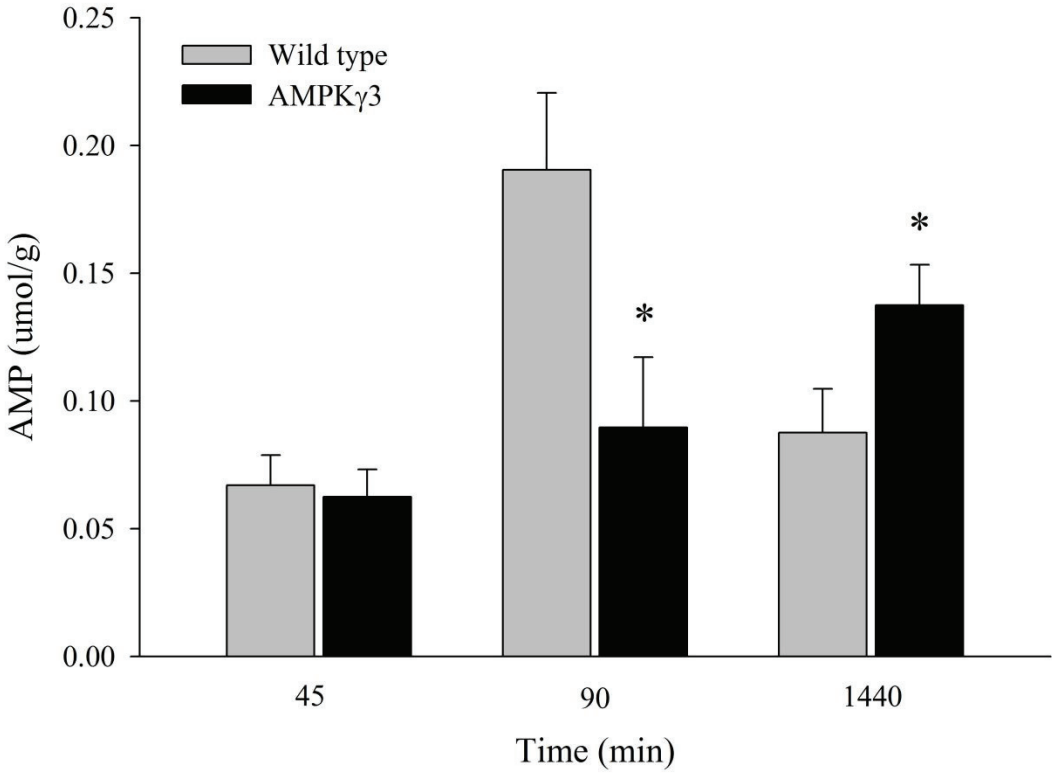

Figure 3-7. AMP contents in longissimus muscle of wild type (pooled control and β-GPA) and AMPKγ3R200Q (pooled AMPKγ3 and AMPKγ3 + β-GPA) pigs. * Indicates significant difference between wild type and AMPKγ3R200Q within a time point.

A.

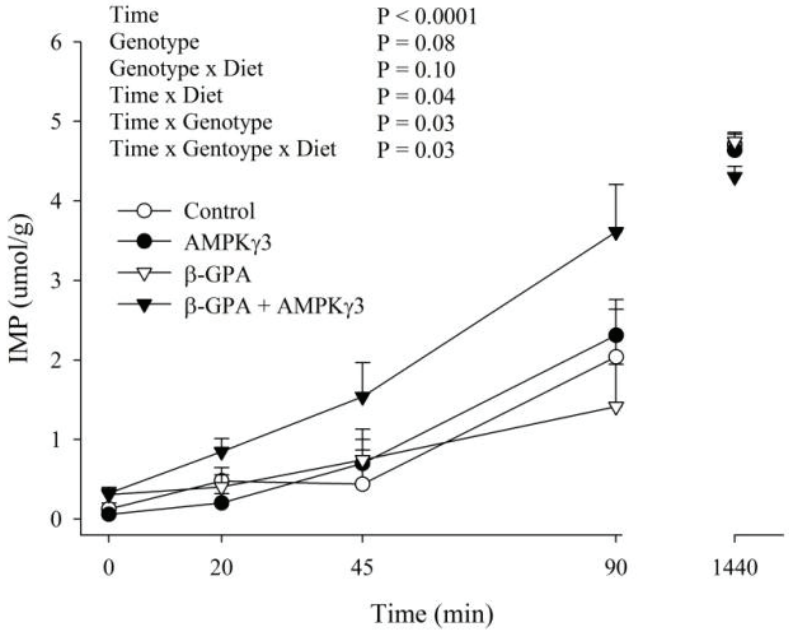

B.

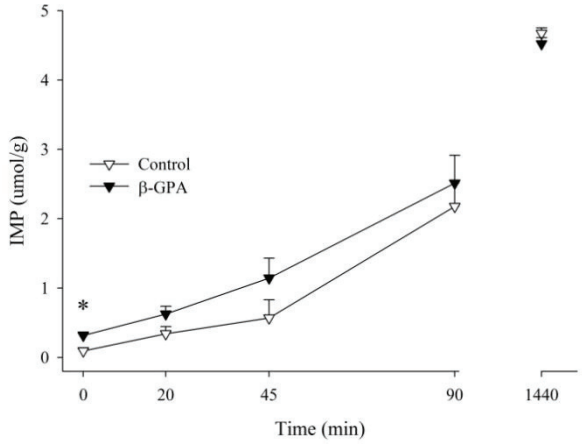

C.

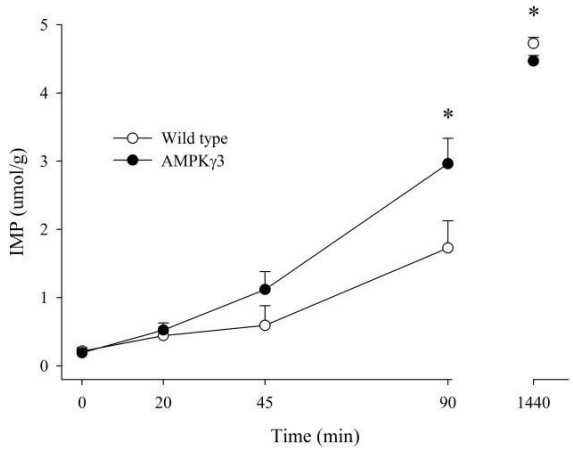

Figure 3-8. Postmortem IMP content in longissimus muscle. (A) IMP contents of control, AMPKγ3, β-GPA, and AMPKγ3 + β-GPA pigs (B) Influence of diet on IMP content: pigs fed control diet (pooled control and AMPKγ3R200Q) and β-GPA supplemented diet (pooled β-GPA and AMPKγ3R200Q + β-GPA). (C) Influence of genotype on IMP content: wild type (pooled control and β-GPA) and AMPKγ3R200Q (pooled AMPKγ3 and AMPKγ3 + β-GPA) pigs. Data are LS means ± SE. P-values are for main effects and interactions. * Indicates significant difference (within time point) between control and β-GPA fed (A), or wild type and AMPKγ3R200Q (B) pigs.

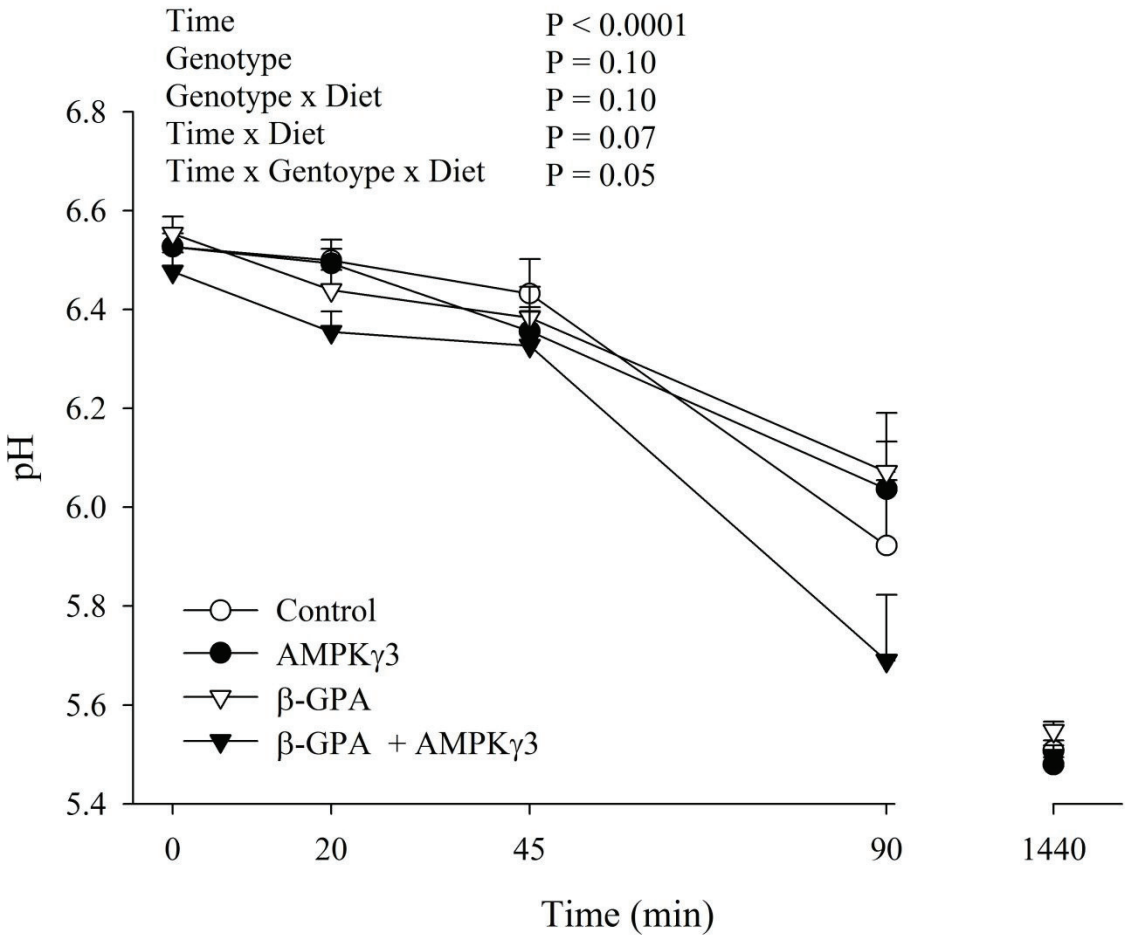

Figure 3-9. Postmortem pH decline in longissimus muscle of control, AMPKγ3, β-GPA, and AMPKγ3 + β-GPA pigs. Data are LS means ± SE. P-values are for main effects and interactions.

Variable	Control	AMPKγ3	β-GPA	AMPKγ3 +β-GPA	Signficance		
					Genotype	Diet	Genotype × Diet
L value	57.7 ± 1.2	54.6 ± 0.9	54.6 ± 0.9	57.7 ± 1.2	NS	NS	0.05
a value	10.84 ± 0.82	10.56 ± 0.58	10.20 ± 0.73	10.80 ± 0.82	NS	NS	NS
b value	6.48 ± 0.68	5.63 ± 0.48	6.23 ± 0.61	7.07 ± 0.68	NS	NS	NS
Drip loss, %	7.89 ± 1.2	6.50 ± 0.8	7.48 ± 1.1	7.19 ± 1.2	NS	NS	NS

Table 3-2. Meat quality characteristics of AMPKγ3 and β-GPA supplemented pigs. Reflectance or lightness (L-value), redness (a-value), yellowness (b-value), and drip loss of *longissimus* muscle. Data are LS means ± SE. NS = Not significant.

References

Adams, J., Z. P. Chen, B. J. Van Denderen, C. J. Morton, M. W. Parker, L. A. Witters, D. Stapleton, and B. E. Kemp. 2004. Intrasteric control of AMPK via the γ1 subunit AMP allosteric regulatory site. Protein Sci. 13: 155-165.

Bergmeyer, H. U. 1974. Methods of enzymatic analysis. Academic Press, New York.

Bernocchi, P., C. Ceconi, A. Cargnoni, P. Pedersini, S. Curello, and R. Ferrari. 1994. Extraction and assay of creatine phosphate, purine, and pyridine nucleotides in cardiac tissue by reversed-phase high-performance liquid chromatography. Anal. Biochem. 222: 374-379.

Bidner, B. S., M. Ellis, D. P. Witte, S. N. Carr, and F. K. McKeith. 2004. Influence of dietary lysine level, pre-slaughter fasting, and rendement napole genotype on fresh pork quality. Meat Sci. 68: 53-60.

Copenhafer, T. L., B. T. Richert, A. P. Schinckel, A. L. Grant, and D. E. Gerrard. 2006. Augmented postmortem glycolysis does not occur early postmortem in AMPKγ3-mutated porcine muscle of halothane positive pigs. Meat Sci. 73: 590-599.

Dolder, M., B. Walzel, O. Speer, U. Schlattner, and T. Wallimann. 2003. Inhibition of the mitochondrial permeability transition by creatine kinase substrates. Requirement for microcompartmentation. J. Biol. Chem. 278: 17760-17766.

Estrade, M., S. Ayoub, A. Talmant, and G. Monin. 1994. Enzyme activities of glycogen metabolism and mitochondrial characteristics in muscles of RN- carrier pigs (Sus scrofa domesticus). Comp. Biochem. Physiol. B. Biochem. Mol. Biol. 108B: 295-301.

Hamilton, D. N., M. Ellis, K. D. Miller, F. K. McKeith, and D. F. Parrett. 2000. The effect of the Halothane and Rendement Napole genes on carcass and meat quality characteristics of pigs. J. Anim. Sci. 78: 2862-2867.

Hammelman, J. E., B. C. Bowker, A. L. Grant, J. C. Forrest, A. P. Schinckel, and D. E. Gerrard. 2003. Early postmortem electrical stimulation simulates PSE pork development. Meat Sci. 63: 69-77.

Irving, T. C., H. J. Swatland, and B. M. Millman. 1989. X-Ray-Diffraction Measurements of Myofilament Lattice Spacing and Optical Measurements of Reflectance and Sarcomere-Length in Commercial Pork Loins. J. Anim. Sci. 67: 152-156.

Joo, S. T., R. G. Kauffman, B. C. Kim, and G. B. Park. 1999. The relationship of sarcoplasmic and myofibrillar protein solubility to colour and water-holding capacity in porcine longissimus muscle. Meat Sci. 52: 291-297.

Lebret, B., P. Le Roy, G. Monin, L. Lefaucheur, J. C. Caritez, A. Talmant, J. M. Elsen, and P. Sellier. 1999. Influence of the three RN genotypes on chemical composition, enzyme activities, and myofiber characteristics of porcine skeletal muscle. J. Anim. Sci. 77: 1482-1489.

Lundström, K., A. Andersson, and I. Hansson. 1996. Effect of the RN gene on technological and sensory meat quality in crossbred pigs with Hampshire as terminal sire. Meat Sci. 42: 145-153.

Meyer, L. E., L. B. Machado, A. P. Santiago, W. S. da-Silva, F. G. De Felice, O. Holub, M. F. Oliveira, and A. Galina. 2006. Mitochondrial creatine kinase activity prevents reactive oxygen species generation: antioxidant role of mitochondrial kinase-dependent ADP re-cycling activity. J. Biol. Chem. 281: 37361-37371.

Meyer, R. A., and J. M. Foley. 1996. Cellular processes integrating the metabolic response to exercise Handbook of Physiology. p 841-869.

Milan, D., J.-T. Jeon, C. Looft, V. Amarger, A. Robic, M. Thelander, C. Rogel-Gaillard, S. Paul, N. Iannuccelli, L. Rask, H. Ronne, K. Lundstrom, N. Reinsch, J. Gellin, E. Kalm, P. L. Roy, P. Chardon, and L. Andersson. 2000. A mutation in PRKAG3 associated with excess glycogen content in pig skeletal muscle. Science 288: 1248-1251.

Monin, G., and P. Sellier. 1985. Pork of low technological quality with a normal rate of muscle pH fall in the immediate post-mortem period: the case of the Hampshire breed. Meat Sci. 13: 49-63.

O'Gorman, E., K. H. Fuchs, P. Tittmann, H. Gross, and T. Wallimann. 1997. Crystalline mitochondrial inclusion bodies isolated from creatine depleted rat soleus muscle. J. Cell Sci. 110 (Pt 12): 1403-1411.

Pandke, K. E., K. L. Mullen, L. A. Snook, A. Bonen, and D. J. Dyck. 2008. Decreasing intramuscular phosphagen content simultaneously increases plasma membrane FAT/CD36 and GLUT4 transporter abundance. Am. J. Physiol. Regul. Integr. Comp. Physiol. 295: R806-813.

Passonneau, J. V., and O. H. Lowry. 1993. Enzymatic analysis: A practical guide. Humana Press, Totowa, NJ.

Rasmussen, A., and M. Andersson. 1996. New method for determination of drip loss in pork muscles. In: Proc. 42nd Int. Congr. Meat Sci. Technol., Lillehammer, Norway. p 286-287.

Ren, J. M., C. F. Semenkovich, and J. O. Holloszy. 1993. Adaptation of muscle to creatine depletion: effect on GLUT-4 glucose transporter expression. Am. J. Physiol. 264: C146-150.

Schlattner, U., M. Tokarska-Schlattner, and T. Wallimann. 2006. Mitochondrial creatine kinase in human health and disease. BBA-Molecular Basis of Disease 1762: 164-180.

Shen, Q. W., W. J. Means, S. A. Thompson, K. R. Underwood, M. J. Zhu, R. J. McCormick, S. P. Ford, and M. Du. 2006a. Pre-slaughter transport, AMP-activated protein kinase, glycolysis, and quality of pork loin. Meat Sci. 74: 388-395.

Shen, Q. W., W. J. Means, K. R. Underwood, S. A. Thompson, M. J. Zhu, R. J. McCormick, S. P. Ford, M. Ellis, and M. Du. 2006b. Early post-mortem AMP-activated protein kinase (AMPK) activation leads to phosphofructokinase-2 and -1 (PFK-2 and PFK-1) phosphorylation and the development of pale, soft, and exudative (PSE) conditions in porcine longissimus muscle. J. Agric. Food Chem. 54: 5583-5589.

Shen, Q. W., K. R. Underwood, W. J. Means, R. J. McCormick, and M. Du. 2007. The halothane gene, energy metabolism, adenosine monophosphate-activated protein kinase, and glycolysis in postmortem pig longissimus dorsi muscle. J. Anim. Sci. 85: 1054-1061.

Shoubridge, E. A., R. A. Challiss, D. J. Hayes, and G. K. Radda. 1985. Biochemical adaptation in the skeletal muscle of rats depleted of creatine with the substrate analogue β-guanidinopropionic acid. Biochem. J. 232: 125-131.

Tullson, P. C., K. W. Rundell, R. L. Sabina, and R. L. Terjung. 1996. Creatine analogue β-guanidinopropionic acid alters skeletal muscle AMP deaminase activity. Am. J. Physiol. 270: C76-85.

Williams, D. B., L. N. Sutherland, M. R. Bomhof, S. A. Basaraba, A. B. Thrush, D. J. Dyck, C. J. Field, and D. C. Wright. 2009. Muscle-specific differences in the response of

mitochondrial proteins to β-GPA feeding: an evaluation of potential mechanisms. Am. J. Physiol. Endocrinol. Metab. 296: E1400-1408.

Williams, J. H., S. E. Vidt, and J. Rinehart. 2008. Measurement of sarcoplasmic reticulum Ca^{2+} ATPase activity using high-performance liquid chromatography. Anal. Biochem. 372: 135-139.

Woods, A., D. Azzout-Marniche, M. Foretz, S. C. Stein, P. Lemarchand, P. Ferre, F. Foufelle, and D. Carling. 2000. Characterization of the role of AMP-activated protein kinase in the regulation of glucose-activated gene expression using constitutively active and dominant negative forms of the kinase. Mol. Cell. Biol. 20: 6704-6711.

Zong, H., J. M. Ren, L. H. Young, M. Pypaert, J. Mu, M. J. Birnbaum, and G. I. Shulman. 2002. AMP kinase is required for mitochondrial biogenesis in skeletal muscle in response to chronic energy deprivation. Proc. Natl. Acad. Sci. USA 99: 15983-15987.

Chapter 4. High glycolytic potential does not predict low ultimate pH

Abstract

The extent of postmortem pH decline influences meat quality development and processing functionality. In order to better understand determination of pH_u, we utilized castrated males and females from a line of pigs selected for different pH_u. The Rendement Napole (RN-) mutation in AMP-activated protein kinase γ3 subunit (AMPKγ3200Q), which is associated with low pH, was not present. Another mutation in AMPKγ3 (199I) is linked to improved ultimate pH; all three genotypes (II, IV and VV) were present in both sexes. The mutant 199II genotype increased pH_u, but only in castrated males (genotype × sex, P = 0.04). Genotype affected glycolytic potential (P = 0.03); wild type 199VV genotype resulted in a wide distribution (~100 to 200 umol/g) of glycolytic potential. Both GP and 24 h lactate content were weakly associated with pH_u. Moreover, AMPKγ3 199 genotype did not affect lactate (P = 0.50). Next, a subset of animals was selected based on low (n = 9, -Gly) and high (n = 5, +Gly) residual glycogen content, and compared with AMPKγ3 200Q. Both +Gly and 200Q muscle contained sufficient substrate (undigested glycogen and glucose 6 phosphate) at 24 h; however muscle with 200Q generated low ultimate pH (P = 0.003) and greater lactate (P = 0.001) compared to +Gly. In addition –Gly and +Gly groups exhibited similar pH_u (P = 0.50) despite a large difference in GP (~100 versus 150 μmol/g; P = 0.0005). Thus, high GP does not appear to be directly responsible for extended pH decline.

Introduction

The rate and extent of postmortem pH decline during the conversion of muscle to meat largely influence development of pork quality attributes. Classically, the rate and extent of pH decline are considered to follow postmortem glycolysis, with glycogen being converted to lactate and H^+. Typically, pH of longissimus muscle declines gradually from 7.4 in living muscle to an ultimate pH (pH_u) of about 5.5. In contrast, dark, firm, and dry (DFD) pork exhibits a subtle pH decline and pH_u greater than 6.0; relatively low muscle glycogen contents are thought to limit postmortem glycolysis and hence pH decline. Conversely, muscle with an extended pH decline demonstrates a normal rate of pH decline early postmortem, but continues to a low ultimate pH around 5.3. Low pH_u reduces net charge on muscle proteins, which decreases sarcoplasmic protein solubility as well as myofilament spacing, and contributes to development of pale, soft, and exudative (PSE) characteristics. Pork with low pH_u is often referred to as "acid meat" to distinguish it from PSE meat caused by rapid glycolysis. Monin & Sellier (1985) suggested that greater initial muscle glycogen content confers an increased capacity for postmortem glycolysis, or high "glycolytic potential," that in turn, extends pH decline. This concept was largely based on elevated muscle glycogen and low ultimate pH commonly observed in the Hampshire breed.

Using extremes of DFD and "acid meat" from Hampshire pigs provides a correlation between glycolytic potential, lactate, and pH_u. Yet, in their original research article, Monin and Sellier (1985) recognized that lactate values were similar at 24-48 h in Hampshire and control pigs, and thus lactic acid could not be the cause of low ultimate pH. Subsequently, the "Hampshire effect" has been recognized as a single nucleotide polymorphism that leads to glutamine being substituted for arginine (R200Q) in AMP-activated protein kinase (AMPK) γ3 subunit (Milan et al., 2000). This mutation not only results in elevated muscle glycogen, but also

increases mitochondrial content and oxidative capacity (Barnes et al., 2005; Barnes et al., 2004; Garcia-Roves et al., 2008). Thus, metabolism in AMPKγ3^{R200Q} mutant pigs is quite different than control pigs, suggesting that other metabolic factors influence determination of pH_u in AMPKγ3^{R200Q} muscle. Moreover, the mutation in ryanodine receptor 1 (RyR1^{R615C}), which increases the rate of postmortem pH decline, may also result in lower pHu (Hamilton et al., 2000) and greater 24 h lactate levels (Monin and Sellier, 1985), yet this mutation does not dramatically alter glycolytic potential.

Genetic selection against both the Halothane and AMPKγ3 R200Q mutations has dramatically reduced the prevalence of these mutations, particularly in commercial herds. Regardless, there is still tremendous variation in early and ultimate pH. Differences in pH are not explained by enhanced glycolytic enzyme capacity (Allison et al., 2003). Glycolytic enzymes can accommodate rapid flux, and metabolic enzymes appear active even at low ultimate pH. Moreover, postmortem glycolysis stops in the presence of residual glycogen (Copenhafer et al., 2006; Immonen and Puolanne, 2000; van Laack and Kauffman, 1999), indicating other factors may limit the course of postmortem metabolism and pH decline. Our objective was to evaluate postmortem energy metabolism and glycolysis in relation to pH decline in a line of pigs selected for pH_u.

Materials and Methods

Animals. Animals for this study were obtained from a Synthetic Duroc line developed by Pig Improvement Company (PIC; Hendersonville, TN). Castrated male (n = 20) and female (n = 40) pigs were transported to Virginia Tech and allowed a minimum 6 d acclimation period prior to harvest. Pigs designated AMPKγ3 200Q were raised at the Virginia Tech Swine Center. Pigs

were harvested at the Virginia Tech Meat Science Center. Pigs were rendered unconscious by electrical stunning and exsanguinated. Exsanguination was considered time 0.

Muscle sampling. Muscle samples (~5-10 g) were collected from the lumbar region of the longissimus muscle at 0 and 45 min and 24 h after exsanguination. Samples were immediately frozen in liquid nitrogen and stored at -80°C until further analysis.

Meat quality characteristics. At 24 h postmortem, carcasses were ribbed between the 10^{th} and 11^{th} costae. Subjective color scores (NPPC, 2000) were evaluated at the cut surface of the longissimus at the 10^{th} rib. Two- 2.54 cm thick chops were removed anterior to the 10^{th} rib and trimmed to excess backfat and connective tissue. One chop was used to determine objective color (L, a, and b) using the mean of values collected from three separate locations on the chop surface using a portable Minolta colorimeter.

Genotype determination. Genotypes were determined using polymerase chain reaction (PCR) restriction fragment length polymorphism technique. DNA was isolated from blood or tissue and used for PCR amplification. For AMPKγ3 genotyping, the primers were (5' – 3') AAATGTGCAGACAAGGATCTC (Forward) and CCCACGAAGCTCTGCTT (Reverse). PCR products were digested with restriction enzyme overnight (AMPKγ3^{V199I}, BsaHI; AMPKγ3^{R200Q}, BsrBI) and fragments were separated on an agarose gel stained with ethidium bromide for visualization.

Glycogen, glucose, glucose-6-phosphate, and lactate. For glycogen analysis, frozen muscle was powdered in liquid nitrogen and subjected to acid hydrolysis at 95C. Another portion of frozen muscle was homogenized in perchloric acid, centrifuged, and the resulting supernatant was used for glucose, glucose-6-phosphate, and lactate analysis. Muscle glucose (free glucose and glucose resulting from glycogen hydrolysis), glucose-6-phosphate, and lactate concentrations were determined using enzyme analytical methods (Bergmeyer, 1974) adapted to a 96-well plate assay (Hammelman et al., 2003). These metabolite concentrations were used to calculate glycolytic potential according to the formula proposed by Monin and Sellier (1985): Glycolytic potential (μmol/g) = 2*(glucose + glucose-6-phosphate + glycogen) + lactate.

Statistical analysis. Relationships between genotype and meat quality development were analyzed using PROC MIXED procedure of SAS. The model included the effect of genotype (wild type, VV; carrier, IV; or mutant, II), sex, and genotype × sex interaction; if the interaction was not significant, it was excluded from the model. The PROC REG function was used to determine relationships between continuous variables, such as lactate and pH_u. For comparisons based on glycogen content, the model included the main effect of glycogen group (low residual glycogen, high residual glycogen, or AMPKγ3 200Q). Tukey's adjustment for multiple comparisons was used to compare least square means between groups.

Results and Discussion

In order to understand energy metabolism in relation to pH decline, we utilized castrated male and female pigs from a population selected for variation in pH_u and pork quality. Females were heavier than castrated males ($P < 0.001$; Table 4-1) and possessed less 10^{th} rib fat ($P <$

0.001); females also exhibited larger longissimus muscle area ($P < 0.001$), even if muscle area was adjusted for weight. There was considerable variation in early (pH_{45min}) and pH_u of longissimus muscle (Table 4-2). Because this line is noted for relatively high pH_u, the pH_u we observed were lower than expected, particularly when pH > 5.3 is considered "normal". In part, this may be due to differences in commercial versus small-scale processing conditions, and most likely is related to chilling and cooling rate of carcasses. Moreover, our data were collected during the summer months, when environmental conditions are most likely to have a negative impact on pork quality (Mancini and Hunt, 2005). Along with the wide range in pH, objective and subjective parameters of meat quality were also quite variable.

Because pigs possessed different genetic propensities for high pH_u, we considered genetic factors related to postmortem energy metabolism. To date, single nucleotide polymorphisms in RyR1 (halothane gene) and AMPKγ3 (RN gene) are the only major mutations well-documented to impact pH decline and pork quality; however, our experimental pigs did not possess these mutations. Additional single nucleotide polymorphisms in AMPKγ3 and mutations in genes encoding glycolytic enzymes have been associated with altered metabolism and pork quality development (Ciobanu et al., 2001; Fontanesi et al., 2003; Otto et al., 2007; Reiner et al., 2002). In particular, another mutation in AMPKγ3 which results in a different amino acid substitution (V199I), is associated with higher pH_u and improved meat quality (Ciobanu et al., 2001; Lindahl et al., 2004) and may also contribute to higher pH early postmortem (Fontanesi et al., 2008). All AMPKγ3 199 genotypes (VV, IV, and II) were present in pigs used in this study, and similar genotype frequencies were observed in castrated males and females (Table 4-3). According to Ciobanu et al. (2001), the frequency of the genotype (II) for improved pork quality varies greatly, from about 2% in Landrace to 74% in Berkshire. In this study, frequencies of II, IV, and

VV genotypes were 15, 55, and 30%, respectively, which is similar to frequencies observed in other Duroc and Duroc synthetic breeds.

The rate and extent of pH decline impact pork quality development. Accordingly, pH at 45 min and pH_u explained ~20 to 40% of the variation in objective color measurements. AMPKγ3 199 genotype tended (P = 0.07) to influence pH at 45 min (Figure 4-1A). Early pH was numerically higher in 199 VV and IV genotypes compared to 199 II. In contrast, others (Fontanesi et al., 2008) indicated AMPKγ3 199 II is associated with higher pH early postmortem. For pH_u, the influence of AMPKγ3 199 genotype was dependent on gender (genotype × gender, P = 0.04; Figure 4-1B). Ultimate pH was greater in castrated males with genotype 199II compared to all females regardless of genotype, and castrated males with genotype VV. The improvement in pH due to genotype was ~0.10 pH unit, which is consistent with Ciobanu et al. (2001). Nonetheless, it is unclear why genotype affected pH_u in castrated males but not females. In general, color attributes followed trends in pH_u (Figure 4-4). Females exhibited similar L, a, and b values regardless of genotype. Within castrated males, those possessing AMPKγ3 199 II were most different from VV genotype, although only redness (a value) was significantly lower in 199 II and IV castrated males, as compared to wild type (VV). Lindahl et al.(2004) also reported that 199I allele decreased reflectance, redness, and yellowness color.

AMPKγ3 199 II genotype is proposed to improve pH_u by decreasing the capacity for postmortem glycolysis, evidenced by lower glycolytic potential due to lower residual glycogen content as well as lower lactate content at 24 h (Ciobanu et al., 2001). Genotype influenced (P = 0.03) glycolytic potential (Figure 4-2A). Wild type (VV genotype) possessed numerically greater GP than other genotypes, but was only significantly (P < 0.05) greater than the

heterozygotes. Curiously, GP of genotype 199 VV ranged from about 100 to almost 200 μmol/g lactate equivalents whereas the range and maximum values for GP for genotypes IV and II were much less (approximately 100 to 140 μmol/g; Figure 4-2B). In fact, GP values near 200 are comparable those of pigs that possess a 200Q allele (RN^-). If the highest GP value was considered an outlier and excluded from analysis, genotype still tended (P = 0.10) to influence GP. The 199V allele may enhance the capacity for glycogen storage relative to 199I. This is consistent with the concept that RN^- phenotype may be due to combined effect of the 199V-200Q haplotype (Ciobanu et al., 2001). Due to the close proximity of the alleles and more recent evolution of 200Q, the 200Q allele is always found with 199V, while 200R (rn^+) may be found with either 199I or 199V. It is unclear how 199V-200R contributes to enhanced glycogen storage in comparison to 199I-200R.

Due to the range in glycogen and GP values, we also examined the relationship between GP and pH_u. GP was not related to pH_u (r^2=0.00, P =0.89; Figure 4-3). Removing two influential points made the relationship between GP and pH_u significant (P = 0.005) but the association remained rather low (r^2 = 0.18). Intriguingly, two samples with the highest GP produced two of the higher pH_u; moreover, several samples possessed low pH_u despite relatively normal GP values. This contradicts the idea that high GP causes low pH_u; this notion is based largely on high GP (>200 μmol/g) and low pH_u (<5.3) observed in pigs with the 200Q allele. In the absence of 200Q, GP does not appear to be strongly associated with pH decline, and low pH_u can occur in "normal" pigs.

During postmortem metabolism, glycogen is broken down to lactate and H^+; thus, lactate accumulation is associated with pH decline. While high pH_u (> 6.0) is associated with limited glycolysis and lower lactate levels, extended glycolysis is assumed to generate higher lactate

levels. When a wide range of pH and lactate values (including both 45 min and 24 h) are considered, there is a strong relationship between lactate production and pH ($r^2 = 0.96$, $P < 0.0001$; Figure 4-4A). When only 24 h values are considered, the relationship between lactate and pH is significant but weak (figure 3B; $r^2 = 0.12$, $P = 0.007$; Figure 4-4B). Moreover, lactate levels at 24 h are not related to AMPKγ3 199 genotype ($P = 0.50$; Figure 4-5).

While AMPKγ3 199 genotype influences glycolytic potential, the capacity for glycolysis does not explain pH_u. AMPK is a major regulator of energy metabolism in skeletal muscle; the γ3 200Q allele influences enzyme activity, gene and protein expression, fiber type, and mitochondrial biogenesis (Witczak et al., 2008), whereas little is known regarding the effect of γ3 199 on muscle metabolism. Therefore, the positive association of the 199I allele with pork quality may be more highly related to energetic status and metabolic properties and not necessarily glycogen content per se. Moreover, increased glycolytic potential in AMPKγ3 199 VV does not result in lower pH_u. Specifically, two GP values were quite high but were also some of the highest pH_u observed in this group. Admittedly, these are only two observations including very high GP in absence of 200Q, but it highlights the importance of 200Q in determining the extent of postmortem pH decline. Thus, the 200Q allele consistently generates low pH_u, and 200Q is associated with high glycolytic potential, but high glycolytic potential does not necessarily equate to low pH_u.

Clearly, low glycogen reserves can limit glycolysis and are associated with $pH_u > 6.0$. Yet, once glycogen content surpasses some threshold, glycogen likely has no direct effect on glycolysis or pH decline. In support, glycolysis stops in the presence of residual glycogen. During postmortem metabolism, glycogen is broken down by glycogen phosphorylase and glycogen debranching enzyme. Glycogen phosphorylase cleaves the outer chains of glycogen,

generating glucose 1-phosphate, which is isomerized to glucose 6-phosphate. Glycogen debranching enzyme breaks α-1,6 linkages, releasing free glucose. Free glucose and G6P, as well as lactate, are the main metabolites from glycolysis that are found in muscle at rigor; some undigested glycogen may also remain. Therefore, we identified a subset of samples from this group according to high (n = 5, + Gly) and low residual (n = 9, - Gly) glycogen content, and added a small set (n=3) of pigs with AMPKγ3 200Q. Although pigs with 200Q were from a different population, they were harvested with the other group and thus were subjected to the same environmental conditions.

Residual glycogen represents undigested glycogen content in muscle at 24 h postmortem. The +Gly and AMPKγ3 200Q groups possessed greater glycogen than -Gly group ($P = 0.003$; Figure 4-6A). Moreover, -Gly group contained low levels of G6P at 24 h, whereas +Gly group was intermediate to 200Q carriers, with all groups differing from each other ($P<0.05$; Figure 4-6B). Both +Gly and AMPKγ3 200Q groups possessed ample G6P and glycogen at 24 h, supporting that glycolysis stops in the presence of available substrate. Glycolytic potential followed a similar pattern as G6P; with –Gly exhibiting the lowest GP and AMPKγ3 200Q possessing the highest GP (Figure 4-6C). Even though muscle with +Gly had a relatively high GP, this group possessed greater pH_u than AMPKγ3 200Q ($P = 0.003$; Figure 4-7A) and similar pH_u ($P = 0.9$) to the -Gly group. Lactate content was elevated in AMPKγ3 200Q relative to –Gly ($P < 0.0001$) and +Gly ($P = 0.001$) groups. Greater accumulation of lactate indicates that greater amount of substrate is completely converted to lactate and H^+, which may contribute to decreased pH. However, this may not always be the case; as similar lactate levels have been reported in 200Q and wild type muscle (Copenhafer et al., 2006; Monin and Sellier, 1985).

Both +Gly and AMPKγ3 200Q muscle contains sufficient substrate for glycolysis, but AMPKγ3 200Q is more strongly associated with low pH_u. Therefore, it seems glycogen content is only indirectly related to determination of low pH_u. Metabolic enzyme capacity is altered in AMPKγ3 200Q muscle; for instance, glycogen phosphorylase and hexokinase activity are increased while lactate dehydrogenase activity is decreased (Granlund et al., 2011). Enhanced glycogen phosphorylase activity could explain elevated G6P levels frequently observed in AMPKγ3 200Q muscle. Greater glycogen phosphorylase activity could also increase rate of postmortem metabolism; however, AMPKγ3 200Q muscle typically exhibits a normal rate of metabolism and pH decline early postmortem. Regardless, glycogen does not dictate the amount of lactate generated or pH_u.

Conclusions

Capacity for postmortem glycolysis is often used to explain or predict ultimate pH. Yet, in a population lacking the AMPKγ3 200Q allele and possessing wide variation in glycolytic potential, glycolytic capacity was only weakly associated with pH_u and pork quality. Moreover, in both wild type and 200Q muscle, glycolysis stopped in the presence of residual glycogen, but muscle with 200Q possessed lower pH_u. Although glycolytic potential may be useful for crudely identifying 200Q carriers, there is little utility in glycolytic potential for predicting pH_u in populations without 200Q because glycogen content appears to be indirectly related to the extent of pH decline. Metabolic phenotype of muscle likely plays a more critical role in determining the course and culmination of pH decline.

Variable	Castrated male	Female	Significance Gender
Live weight, kg	111.2 ± 1.5	120.0 ± 1.1	***
10^{th} rib backfat, mm	23.0 ± 0.9	15.5 ± 0.6	***
Longissimus muscle area, cm^2	41.6 ± 1.1	48.0 ± 0.8	***

Table 4-1. Live weight and carcass characteristics of castrated male and female pigs. Data are least square means ± SE.

Variable	Mean	Minimum - Maximum	SD
$pH_{45\ min}$	6.39	5.55 – 6.89	0.32
$pH_{ultimate}$	5.39	5.21 – 5.62	0.07
L value	61.95	51.94 – 71.78	4.18
a value	9.25	6.54 – 13.44	1.43
b value	6.08	2.01 – 10.20	1.66
Color[a]	2.43	1.50 – 3.75	0.49
Firmness[b]	2.69	2.00 – 4.17	0.56
Drip loss, %	9.08	2.53 – 14.50	2.44

Table 4-2. Meat quality attributes of *longissimus* muscle.
[a] Subjective color: 1 = pale, pinkish gray to white and 6 = dark purplish red
[b] Subjective firmness: 1 = very soft and 5 = very firm

Genotype	Castrated Males	Females	Total
VV	5 (25)	13 (32.5)	18 (30)
IV	12 (60)	21 (52.5)	33 (55)
II	3 (15)	6 (15)	9 (15)
Total	20	40	60

Table 4-3. Number and percentage (in parentheses) of pigs with different genotypes at the AMPK γ3 V199I substitution site.

A.

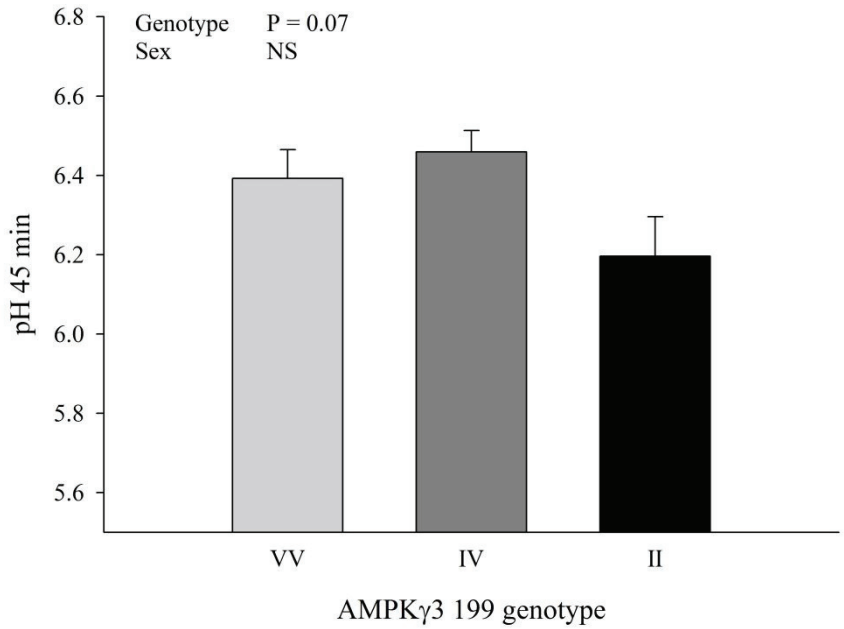

B.

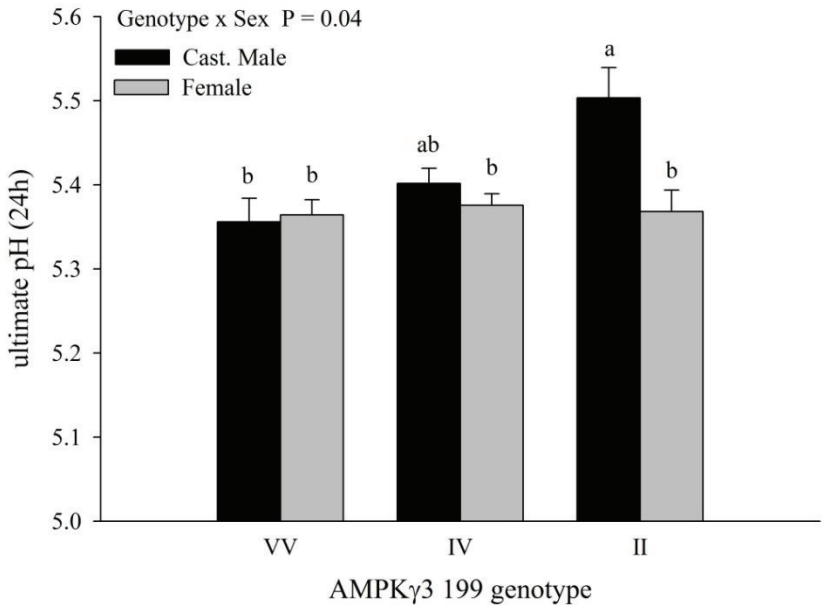

Figure 4-1. The pH of *longissimus* muscle at 45 min (A) and 24 h (pH_u; B) in AMPKγ3 199 genotypes. Data are means ± SE. [a,b] indicates significant differences between interaction classes ($P < 0.05$).

Variable	AMPKγ3 199 genotype			Significance[a]		
	VV	IV	II	Genotype	Sex	Genotype × Sex
L value				NS	NS	†
Cast. Male	65.1 ± 1.8	61.0 ± 1.2	59.0 ± 2.4			
Female	61.4 ± 1.2	62.3 ± 0.9	62.8 ± 1.7			
a value				*	NS	**
Cast. Male	10.5 ± 0.5 [b]	8.6 ± 0.4 [c]	7.5 ± 0.7 [c]			
Female	9.4 ± 0.3 [bc]	9.2 ± 0.3 [bc]	9.8 ± 0.3 [bc]			
b value				NS	NS	†
Cast. Male	7.2 ± 0.7	5.4 ± 0.4	4.4 ± 0.9			
Female	6.2 ± 0.4	6.2 ± 0.4	6.5 ± 0.9			
Color [d]	2.39 ± 0.13	2.39 ± 0.10	2.51 ± 0.18	NS	NS	NS

Table 4-4. Meat quality characteristics of *longissimus* muscle by AMPKγ3 199 genotype and sex. Data are least square means ± SE.
a NS, †, *, ** = not significant, P<0.05, P<0.01, respectively
b,c Means with differing subscripts differ (P<0.05)
d Subjective color: 1 = pale, pinkish gray to white and 6 = dark purplish red

A.

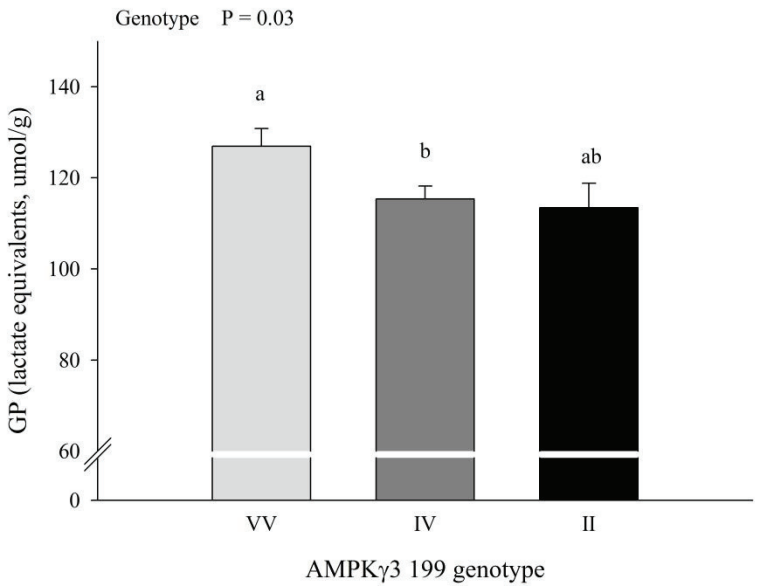

B.

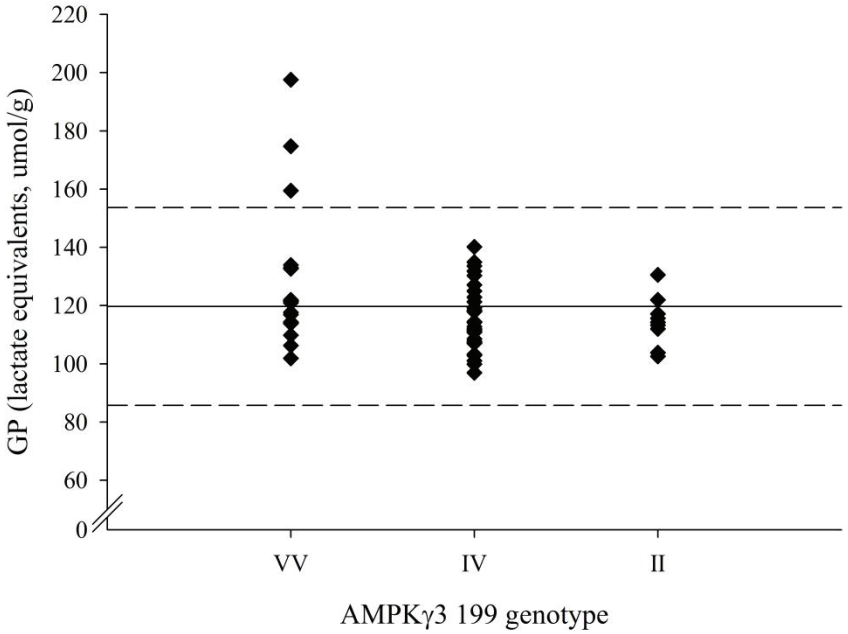

Figure 4-2. Distribution of *longissimus* muscle glycolytic potential (GP) of AMPKγ3 199 genotypes. GP was calculated as 2*(glycogen+glucose+glucose 6-phosphate) + lactate. The solid line represents the overall mean and the dashed lines represent 2 standard deviations of the mean.

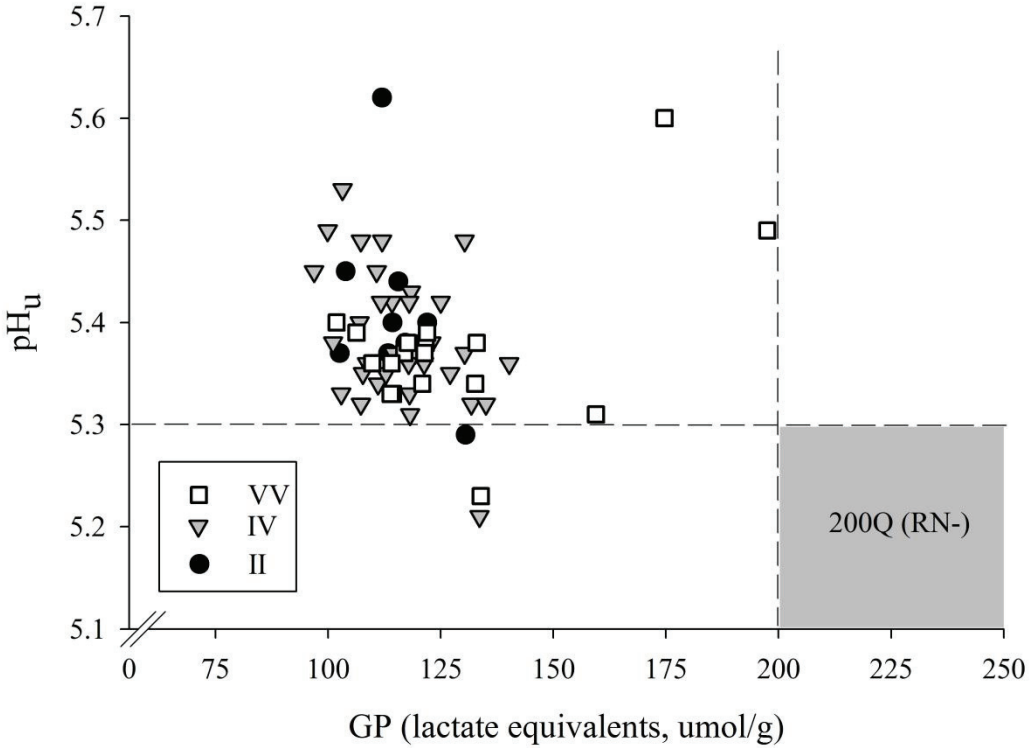

Figure 4-3. Relationship between *longissimus* muscle glycolytic potential (GP) and ultimate pH (pH_u) in AMPKγ3 199 genotypes. The dashed lines represent typical classification for low pH_u (<5.3) and high GP (>200 μmol/g). The association between high GP and low pH_u is largely based on high GP and low pH_u (shaded area) observed in pigs possessing the 200Q allele (RN- phenotype).

A.

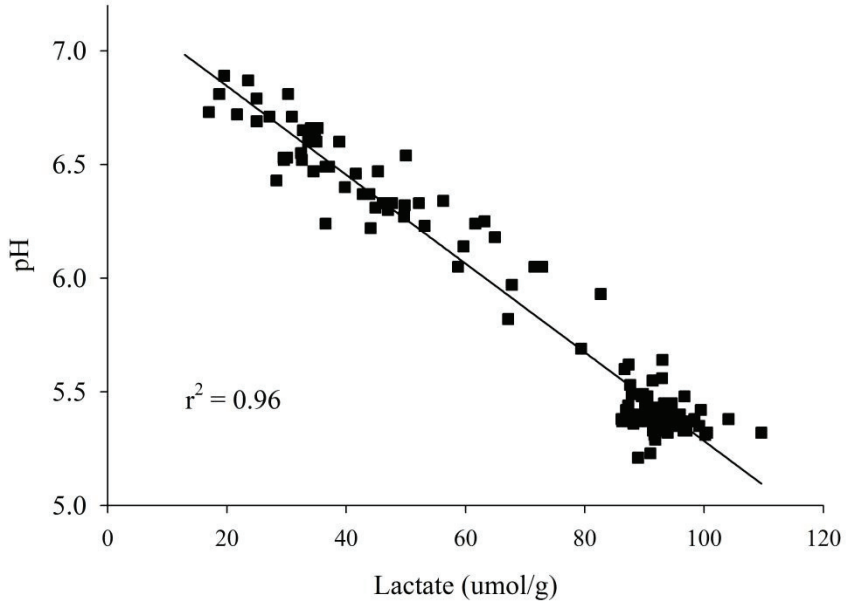

B.

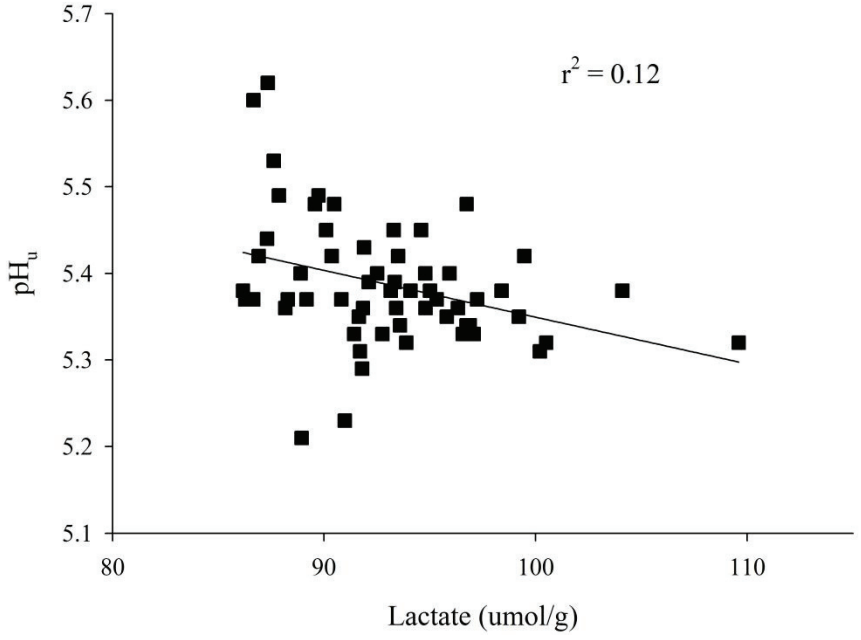

Figure 4-4. Relationship between lactate and pH in *longissimus* muscle. Lactate content and pH at 45 min and 24 h postmortem (A) exhibits a strong relationship; when only 24 h values are considered (B) the relationship is much weaker.

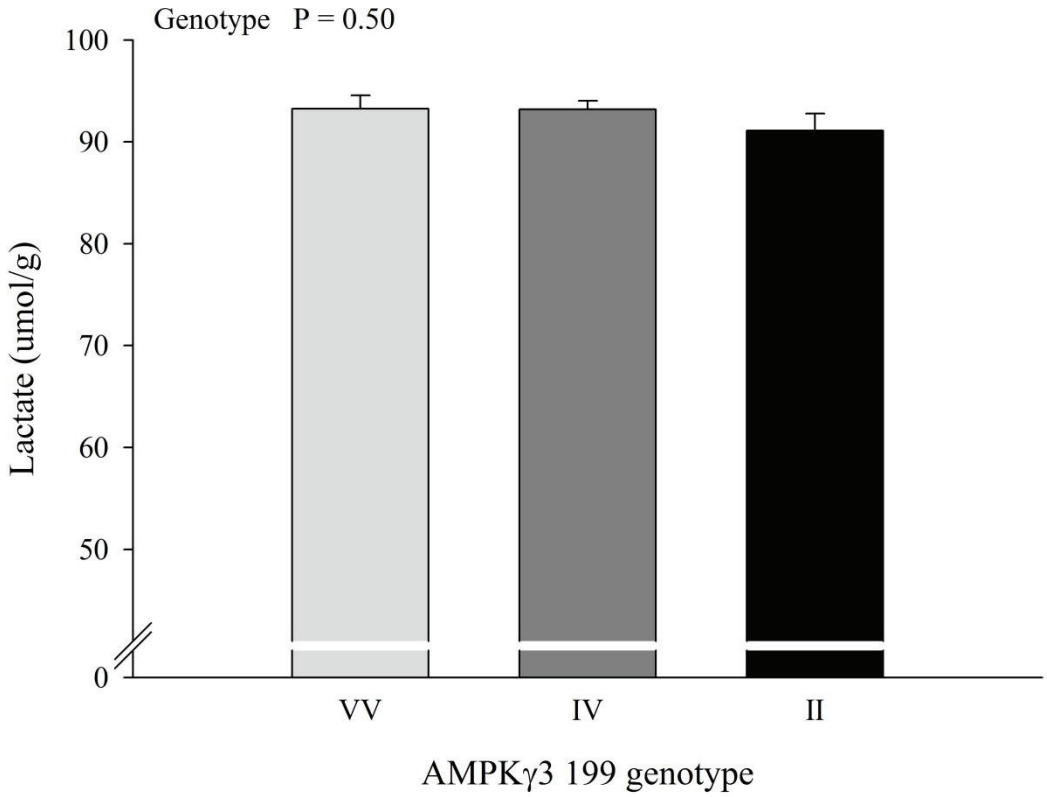

Figure 4-5. *Longissimus* muscle lactate content at 24 h postmortem in AMPKγ3 199 genotypes. Data are least square means ± SE.

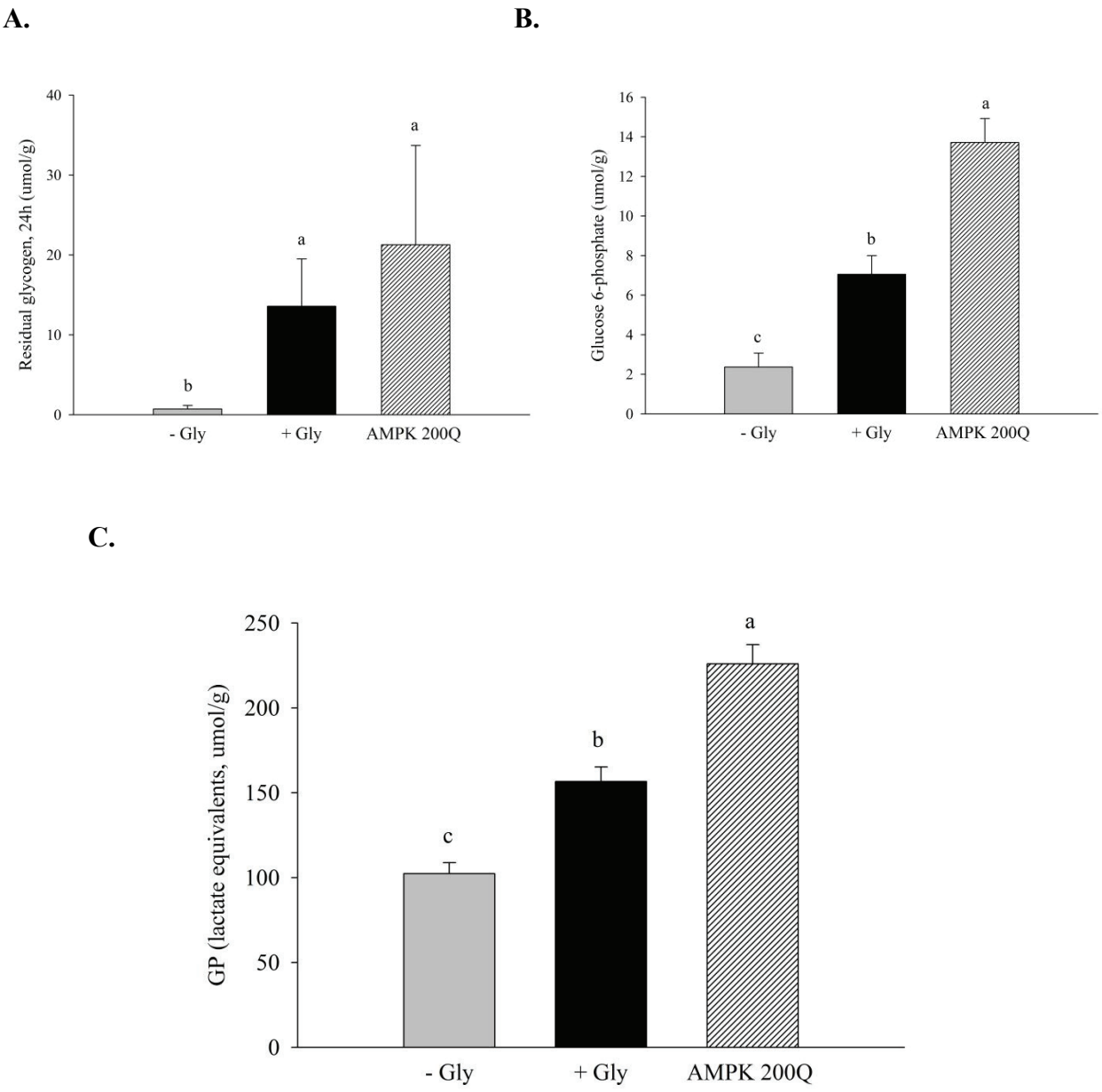

Figure 4-6. Residual glycogen content (A), glucose 6-phosphate content (B), and glycolytic potential (GP; C) in *longissimus* muscle at 24 h postmortem. Data are least square means ± SE. [a,b,c] Groups with different letters differ (P<0.05).

A.

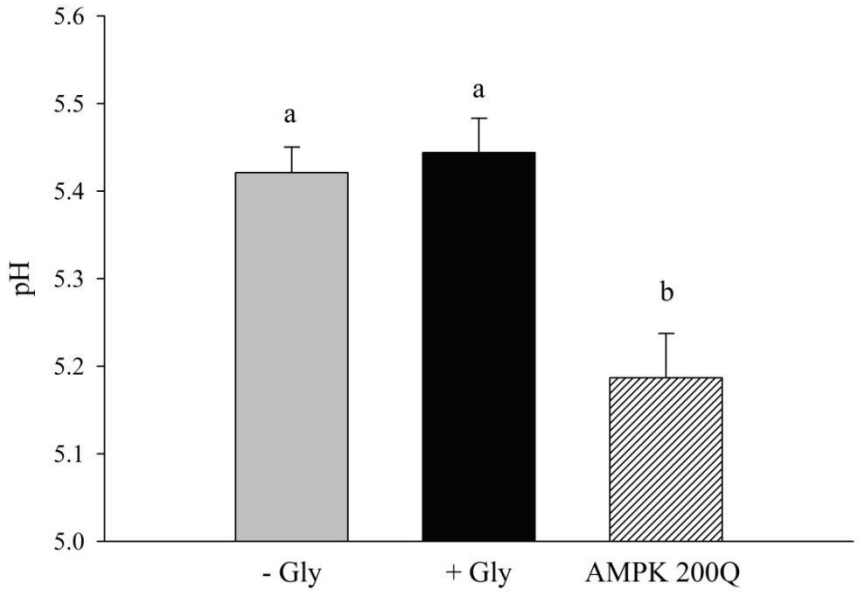

B.

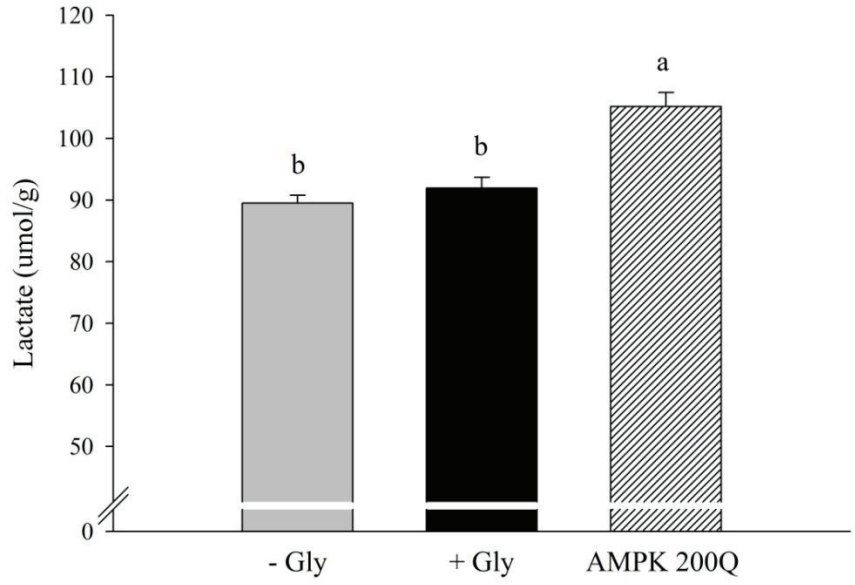

Figure 4-7. Ultimate pH (pH_u) and lactate content in *longissimus* muscle at 24 h postmortem. Data are least square means ± SE. [a,b] Groups with different letters differ (P<0.05).

References

Allison, C. P., R. O. Bates, A. M. Booren, R. C. Johnson, and M. E. Doumit. 2003. Pork quality variation is not explained by glycolytic enzyme capacity. Meat Sci. 63: 17-22.

Barnes, B. R., S. Glund, Y. C. Long, G. Hjalm, L. Andersson, and J. R. Zierath. 2005. 5'-AMP-activated protein kinase regulates skeletal muscle glycogen content and ergogenics. FASEB J. 19: 773-779.

Barnes, B. R., S. Marklund, T. L. Steiler, M. Walter, G. Hjalm, V. Amarger, M. Mahlapuu, Y. Leng, C. Johansson, D. Galuska, K. Lindgren, M. Abrink, D. Stapleton, J. R. Zierath, and L. Andersson. 2004. The 5'-AMP-activated protein kinase γ3 isoform has a key role in carbohydrate and lipid metabolism in glycolytic skeletal muscle. J. Biol. Chem. 279: 38441-38447.

Bergmeyer, H. U. 1974. Methods of enzymatic analysis. Academic Press, New York.

Ciobanu, D., J. Bastiaansen, M. Malek, J. Helm, J. Woollard, G. Plastow, and M. Rothschild. 2001. Evidence for new alleles in the protein kinase adenosine monophosphate-activated γ3-subunit gene associated with low glycogen content in pig skeletal muscle and improved meat quality. Genetics 159: 1151-1162.

Copenhafer, T. L., B. T. Richert, A. P. Schinckel, A. L. Grant, and D. E. Gerrard. 2006. Augmented postmortem glycolysis does not occur early postmortem in AMPKγ3-mutated porcine muscle of halothane positive pigs. Meat Sci. 73: 590-599.

Fontanesi, L., R. Davoli, L. Nanni Costa, F. Beretti, E. Scotti, M. Tazzoli, F. Tassone, M. Columbo, L. Buttazzoni, and V. Russo. 2008. Investigation of candidate genes for glycolytic potential of porcine skeletal muscle: association with meat quality and production traits in Italian Large White pigs. Meat Sci. 80: 780-787.

Fontanesi, L., R. Davoli, L. Nanni Costa, E. Scotti, and V. Russo. 2003. Study of candidate genes for glycolytic potential of porcine skeletal muscle: identification and analysis of mutations, linkage and physical mapping and association with meat quality traits in pigs. Cytogenet. Genome Res. 102: 145-151.

Garcia-Roves, P. M., M. E. Osler, M. H. Holmstrom, and J. R. Zierath. 2008. Gain-of-function R225Q mutation in AMP-activated protein kinase γ3 subunit increases mitochondrial biogenesis in glycolytic skeletal muscle. J. Biol. Chem. 283: 35724-35734.

Granlund, A., M. Jensen-Waern, and B. Essen-Gustavsson. 2011. The influence of the PRKAG3 mutation on glycogen, enzyme activities and fibre types in different skeletal muscles of exercise trained pigs. Acta Vet. Scand. 53: 20.

Hamilton, D. N., M. Ellis, K. D. Miller, F. K. McKeith, and D. F. Parrett. 2000. The effect of the Halothane and Rendement Napole genes on carcass and meat quality characteristics of pigs. J. Anim. Sci. 78: 2862-2867.

Hammelman, J. E., B. C. Bowker, A. L. Grant, J. C. Forrest, A. P. Schinckel, and D. E. Gerrard. 2003. Early postmortem electrical stimulation simulates PSE pork development. Meat Sci. 63: 69-77.

Immonen, K., and E. Puolanne. 2000. Variation of residual glycogen-glucose concentration at ultimate pH values below 5.75. Meat Sci. 55: 279-283.

Lindahl, G., A.-C. Enfält, G. v. Seth, Å. Joseli, I. Hedebro-Velander, H. J. Andersen, M. Braunschweig, L. Andersson, and K. Lundström. 2004. A second mutant allele (V199I) at the PRKAG3 (RN) locus--II. Effect on colour characteristics of pork loin. Meat Sci. 66: 621-627.

Mancini, R. A., and M. C. Hunt. 2005. Current research in meat color. Meat Sci. 71: 100-121.
Milan, D., J.-T. Jeon, C. Looft, V. Amarger, A. Robic, M. Thelander, C. Rogel-Gaillard, S. Paul, N. Iannuccelli, L. Rask, H. Ronne, K. Lundstrom, N. Reinsch, J. Gellin, E. Kalm, P. L. Roy, P. Chardon, and L. Andersson. 2000. A mutation in PRKAG3 associated with excess glycogen content in pig skeletal muscle. Science 288: 1248-1251.
Monin, G., and P. Sellier. 1985. Pork of low technological quality with a normal rate of muscle pH fall in the immediate post-mortem period: the case of the Hampshire breed. Meat Sci. 13: 49-63.
NPPC. 2000. Pork composition and quality assessment procedures. National Pork Producers Council, Des Moines, IA.
Otto, G., R. Roehe, H. Looft, L. Thoelking, P. W. Knap, M. F. Rothschild, G. S. Plastow, and E. Kalm. 2007. Associations of DNA markers with meat quality traits in pigs with emphasis on drip loss. Meat Sci. 75: 185-195.
Reiner, G., L. Heinricy, E. Muller, H. Geldermann, and V. Dzapo. 2002. Indications of associations of the porcine FOS proto-oncogene with skeletal muscle fibre traits. Anim. Genet. 33: 49-55.
van Laack, R. L. J. M., and R. G. Kauffman. 1999. Glycolytic potential of red, soft, exudative pork longissimus muscle. J. Anim. Sci. 77: 2971-2973.
Witczak, C. A., C. G. Sharoff, and L. J. Goodyear. 2008. AMP-activated protein kinase in skeletal muscle: from structure and localization to its role as a master regulator of cellular metabolism. Cell. Mol. Life Sci. 65: 3737-3755.

Chapter 5. Introduction and Literature Review – Skeletal Muscle Metabolism and Growth

Introduction

Skeletal muscle plays a vital role in health and quality of life. Not only is muscle responsible for support and movement, but it also significantly influences whole body metabolism. Skeletal muscle represents approximately 40% of body mass and 20% of basal energy expenditure (Levine et al., 2000). Yet, because muscle comprises a large proportion of body mass, altering muscle energy expenditure has a relatively large impact on whole body energy expenditure and substrate metabolism. In particular, oxidative capacity of muscle is a critical property associated with improvements in overall health. Greater oxidative capacity may afford protection against insulin resistance and metabolic dysregulation, attenuate muscle loss during aging, and lessen energetic deficits associated with myopathies (Barnes et al., 2004; Ljubicic et al., 2011; Wang et al., 2004; Wenz et al., 2008; Wenz et al., 2009). The protective effects of increased oxidative capacity in disease states are largely ascribed to increased mitochondrial content and enhanced mitochondrial function that increases fatty acid oxidation, augments ATP generating capacity, and protects against cellular stress.

Oxidative capacity and other muscle properties are not fixed; they can be modified to meet new conditions. This plasticity allows muscles to adapt to changes in load, exercise, hormones, and nutrition. These stimuli modulate signaling pathways that coordinate metabolic and structural modifications. Consequently, these adaptations allow muscles to cope with new demands. For instance, endurance exercise triggers pathways that promote mitochondrial biogenesis, thereby augmenting oxidative metabolism and protecting against energy stress during

subsequent exercise bouts. In order to optimize function, it may be necessary to modulate other properties, such as fiber size, capillary density, and antioxidant capacity. Thus, interplay between signaling pathways is crucial for coordinating metabolism, structure, and size to optimize muscle function.

Muscle phenotype

Skeletal muscles are functionally diverse; form and structure must be well-suited for a specific function. Accordingly, skeletal muscles vary in size, shape, and color, as well as physiological properties, in order to meet particular functional demands. In the late 1800s, French anatomist Ranvier first documented differences in muscles from the same animal, noting that some muscles appeared more red and were slower contracting than paler muscles. This overall muscle phenotype is largely described by the types of fibers contained within a muscle and their relative proportion. Overall muscle phenotype is the result of a heterogeneous composition of individual muscle cells that vary in histological, biochemical, and structural characteristics. Current classification methods describe muscles and muscle fiber types according to contractile speed (slow or fast) and predominant type of energy metabolism utilized (oxidative or glycolytic) (reviewed by Zierath and Hawley, 2004). However, these properties exist as a continuum which makes categorization into a particular type somewhat ambiguous.

Muscles and fiber types may be classified by contractile speed. The primary function of muscle is to contract or increase tension for support or locomotion. Fast-twitch fibers contract quickly and have higher maximum shortening velocities than slow-twitch fibers. Fast-twitch fibers require short bursts of high frequency contraction. The globular head or S1 fragment of myosin heavy chain (MHC) has adenosine triphosphatase (ATPase) activity and is largely

responsible for speed of contraction (Barany, 1967). Most of the functional diversity in myofibrillar ATPase activity and shortening velocity are related to MHC isoform content (Weiss et al., 1999). A fiber may contain only one MHC isoform ("pure") or it may be a hybrid of two or more MHC isoforms. On the basis of MHC isoforms in adult skeletal muscle, pure fibers are classified as "slow" type I, and the "fast" types, IIA, IIX (or IID), and IIB, with each fiber type containing the isoforms MHCIβ, MHCIIa, MHCIIx (or MHCIId), and MHCIIb, respectively (Pette and Staron, 2000). Hybrid fibers are also named on the basis of predominant MHC within the fiber (with the more abundant MHC listed first): type I/IIA, IIA/I, IIAX, IIXA, IIXB, and IIBX (Pette and Staron, 2000). In total, the presence of pure and hybrid fibers in muscle creates a continuum of slow to fast.

Muscles are also classified based on the abundance of glycolytic or oxidative enzymes. Lactate dehydrogenase activity, which converts pyruvate to lactate in anaerobic glycolysis, indicates glycolytic capacity. Succinate dehydrogenase (SDH) and nicotinamide adenine dinucleotide (NADH) histochemistry staining techniques distinguish oxidative fibers from "less" oxidative fibers in muscle cross sections. Alternatively, the activity of citrate synthase and β-hydroxy acyl coA dehydrogenase (β-HAD), key enzymes of the TCA cycle and fatty acid oxidation, respectively, may be used to quantify oxidative capacity. Certain features tend to be associated with metabolic capacity. For example, highly oxidative fibers are equipped with appropriate metabolic machinery and substrates to support oxidative metabolism, including higher mitochondrial content, greater myoglobin content, and greater lipid content. Moreover, oxidative fibers are typically smaller in diameter and have a greater capillary density; this facilitates delivery of oxygen and decreases diffusion distance. Likewise, both myoglobin and increased capillary density contribute to increased redness of fibers. In contrast, glycolytic fibers

depend on aerobic or anaerobic breakdown of glycogen for energy. These fibers possess less myoglobin and lower capillary density leading to a paler, more "white" appearance.

Metabolic properties are associated with the energetic requirements of a particular contractile type. High glycolytic capacity can supply ATP at relatively fast rates but cannot supply ATP for very long and is well-suited to fast IIB fibers. Conversely, oxidative fibers possess a slow but efficient means of ATP production; oxidative metabolism is well-suited to support posture because tension must be maintained over time but the energy demand is not great. Metabolic enzymes have been used to distinguish fast fiber types, resulting in categories: slow type I oxidative fibers, fast type IIA oxidative fibers, fast(er) IIX oxido-glycolytic fibers, and fast(est) IIB glycolytic fibers. While fibers on the extreme ends of this spectrum suggest a relationship between MHC composition and oxidative capacity, the actual relationship across fiber types is fairly weak (Pette and Staron, 2001). Intriguingly, humans do not express MHC type IIb, but this does not restrict contractile speed or glycolytic capacity (Pette and Staron, 2000).

Metabolic capacity exists as a continuum and there is overlap between MHC-based fiber types. Other characteristics contribute to fiber heterogeneity, and therefore, to the overall function of the muscle. Regulatory and structural proteins have multiple isoforms that exhibit different expression patterns across fibers; there are several isoforms of the essential and regulatory light chains of myosin, troponins (C, I and T), and sarcoplasmic reticulum Ca^{2+} ATPase (SERCA). The protein parvalbumin buffers Ca^{2+} and contributes to greater relaxation speed in fast-twitch muscles (Heizmann et al., 1982). Variation in isoforms and differential expression of non-MHC proteins further specializes fibers to meet specific functional demands.

Mitochondria in skeletal muscle

Mitochondria content and function are the principal features determining oxidative capacity of skeletal muscle fibers. Increases in mitochondrial content are associated with enhanced fatty acid oxidation and protection against insulin resistance. On the other hand, defects in ATP-generating capacity are linked to several inherited and acquired diseases. While their role in energy production is certainly appreciated, mitochondria also modulate signaling pathways and mediate apoptosis. Therefore, changing mitochondrial content and function may have far-reaching effects on overall cell physiology.

Mitochondria are unique and complex organelles. Although typically thought of as autonomous individual organelles, mitochondria are dynamic and undergo fusion and fission events (Figure 5-1). The balance of fission and fusion contributes to a range of mitochondrial morphology, from small, round-oval organelles to a branched, tubular network. Fission is a GTP-dependent process controlled by dynamin related protein 1 (Drp1) (Smirnova et al., 2001). Drp1 assembles on the mitochondrial membrane and constricts and ultimately fragments the mitochondrial tubule in a way that prevents loss of its contents. Conversely, fusion coordinates joining of the outer and inner mitochondrial membranes. Mitofusin 1 (Mfn1) and Mfn2 localize

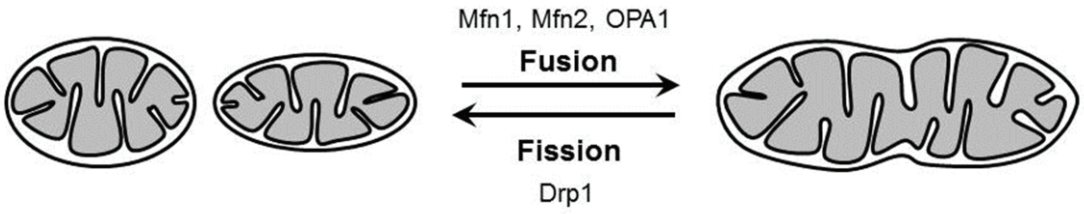

Figure 5-1. Mitochondria fusion and fission. Opposing processes of fusion and fission contribute to mitochondrial morphology. Fusion is regulated by dynamin related protein (Drp1), while fusion is mediated by mitofusins 1 and 2 (Mfn1 and Mfn2), and optic atrophy 1 (OPA1).

on the outer membrane while dynamin GTPase optic atrophy 1 (OPA1) localizes on the inner membrane, allowing mixing of matrix contents (Chen et al., 2003; Cipolat et al., 2004). Decreasing fusion results in fragmentation of mitochondria (Chen et al., 2003), whereas reducing fission leads to excessive elongation and interconnectivity of the mitochondrial network (Smirnova et al., 2001).

Mitochondria contain an inner and outer membrane, resulting in two aqueous compartments, the intermembrane space and matrix. The inner membrane contains complexes I to V of oxidative phosphorylation, whereas the matrix contains the majority of proteins, as well as copies of the mitochondrial genome. Coding information for 13 units of the oxidative phosphorylation machinery, 22 tRNAs, and 2 rRNAs is contained within the circular mitochondrial DNA (mtDNA) molecule. Transcription of mtDNA occurs independently of nuclear gene transcription, yet mtDNA is completely dependent on nuclear-encoded proteins for its maintenance and transcription. Moreover, the majority of mitochondrial proteins (~98%) are nuclear encoded, which necessitates that transcription of the mitochondrial genome must be coordinated with the nuclear genome (Ryan and Hoogenraad, 2007).

The peroxisome proliferator activated receptor γ co-activator 1 (PGC1) family is particularly important in coordinating expression of mitochondrial and nuclear encoded genes critical for mitochondrial biogenesis. Specifically, PGC1α activates multiple nuclear receptors and other transcription factors, and is considered a "master regulator" of mitochondrial biogenesis (Figure 5-2). Gain- and loss-of function studies support that PGC1α is necessary for normal expression of mitochondrial genes (Leone et al., 2005; Zechner et al., 2010). PGC1α-induced increases in mitochondrial biogenesis are proposed to occur as a result of increased

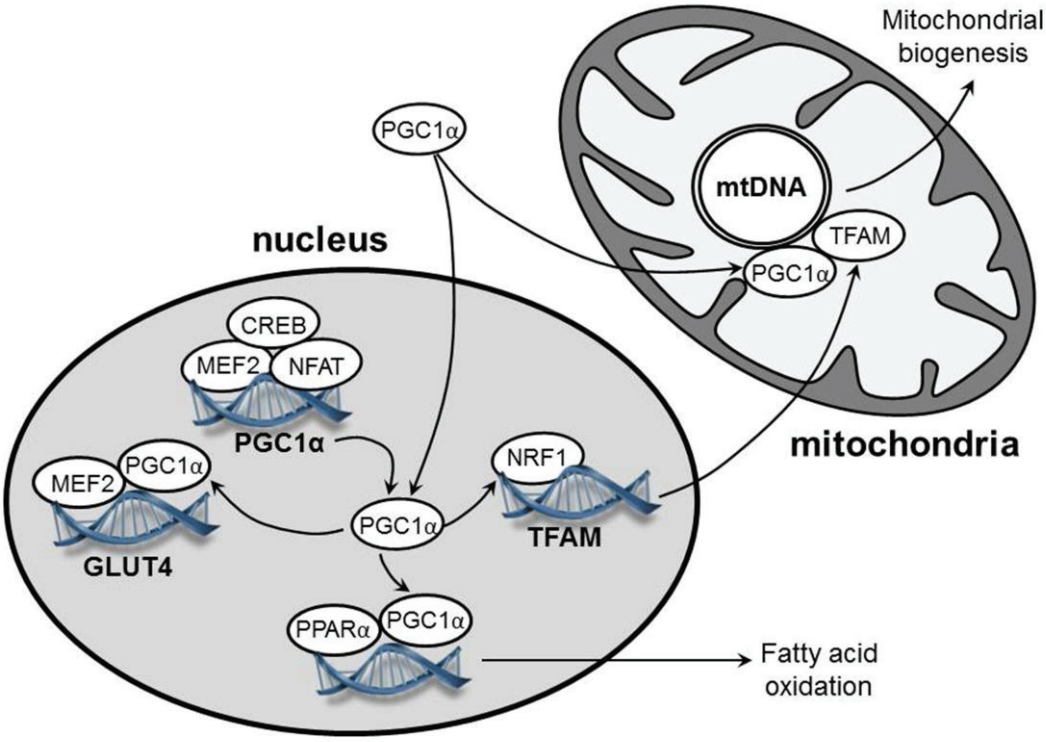

Figure 5-2. Peroxisome proliferator activated receptor γ coactivator 1α (PGC1α) regulation of gene transcription. PGC1α coordinates transcription of nuclear- and mitochondrial-encoded genes involved in oxidative metabolism. PGC1α may also regulate its own expression.

activation of PGC1α, which promotes its translocation to the nucleus and interaction with transcription factors; and through increased expression of PGC1α protein (Holloszy, 2008).

PGC1α interacts with a number of transcription factors and nuclear receptors to modulate gene expression. PGC1α coactivates nuclear respiratory factor (NRF)-1 and NRF-2, which stimulate transcription of nuclear genes required for respiration and for mtDNA transcription and replication. PGC1α also coactivates NRF-1 on the promoter for mitochondrial transcription factor A (TFAM) (Wu et al., 1999); TFAM activity is required for replication and transcription of mtDNA . Recently, Safdar et al. (2011) extended these observations by demonstrating that PGC1α can translocate to mitochondria and complex with TFAM at mtDNA transcription start sites. PGC1α interacts with several nuclear receptors, including peroxisome proliferator activated

receptor (PPAR)α and PPARδ, which augments fatty acid oxidation and oxidative phosphorylation (Vega et al., 2000; Wang et al., 2004). In addition, PGC1α promotes transcription of proteins, such as myoglobin, that help support increased oxidative capacity (Lin et al., 2002).

PGC1α activity is regulated by transcriptional and post-translational mechanisms. Transcription of PGC1α can be induced by various stimuli, such as fasting, exercise, or decreased energy charge (ATP:AMP) (Irrcher et al., 2009; Irrcher et al., 2008; Zong et al., 2002). Further, transcription factors that are regulated by PGC1α may also serve as regulators of its transcription, thus providing an autoregulatory loop that maintains increased PGC1α expression (Handschin et al., 2003). PGC1α protein has a short half-life of 2 to 3 hours, and phosphorylation (at residues T262, S265, and T298) increases its stability and transcriptional activity (Puigserver et al., 2001) and disrupts the inhibitory effects of protein p160 myb binding protein (p160MBP) on its activity (Fan et al., 2004). Moreover, deacetylation by NAD+-dependent sirtuin-1 increases PGC1α activity (Canto et al., 2009; Rodgers et al., 2005).

Mitochondrial biogenesis implies synthesis of new mitochondria; however, mitochondria are not made de novo. Rather, existing mitochondria "grow" by incorporating new proteins and then fission allows the expanding mitochondrial tubule to divide (Ryan and Hoogenraad, 2007). Mitochondrial encoded proteins are synthesized within the mitochondria whereas nuclear-encoded mitochondrial proteins must be imported into the mitochondria. These proteins must be unfolded in order to pass through the protein translocase channels, and then chaperones facilitate protein folding. Mitochondria biogenesis represents the increase in synthesis of mitochondrial proteins, while mitochondrial protein content is the net result of synthesis and degradation of these proteins.

Conventionally, energetic differences between type I compared to type II fibers have been attributed primarily to the greater mitochondrial density of type I fibers (Schwerzmann et al., 1989). Recently, others have suggested that mitochondria exhibit a certain phenotype based on fiber type (Picard et al., 2012). Mitochondrial phenotype encompasses not only ATP producing capacity, but also ROS production, and sensitivity to Ca^{2+} and apoptosis. Dissecting functional properties of mitochondria is particularly convoluted considering different methodologies, animal models, and muscles utilized. Historically, isolated mitochondria preparations have been used to assess mitochondrial function (Chance and Williams, 1955). More recently, a method using permeabilized fibers to assess mitochondrial function was developed (Saks et al., 1998). Considering the current view of mitochondria as dynamic organelles, mitochondrial isolation procedures may fragment the network and affect mitochondrial function (Picard et al., 2011).

In oxidative phosphorylation, the energy released from the oxidation of fuels is used to phosphorylate ADP to ATP. The transfer of electrons through protein complexes in the mitochondria generates a proton motive force that drives ATP synthesis (Figure 5-3). Important properties relating to ATP producing capacity of mitochondria include maximal ADP-stimulated respiration (state 3, V_{max}), basal state 4 respiration, coupling between respiration and phosphorylation, and sensitivity to ADP (K_m). The rate of oxidative phosphorylation is primarily determined by the need for ATP. Thus, high ADP concentrations stimulate maximal oxygen consumption or respiration (state 3). State 3 respiration is controlled by activity of ATP turnover and substrate oxidation, including substrate uptake, processing, electron transport chain complexes, electron acceptors and $[O_2]$ (Brand and Nicholls, 2011). State 3 respiration is one of the most common indices of mitochondrial function and does not differ between fiber types

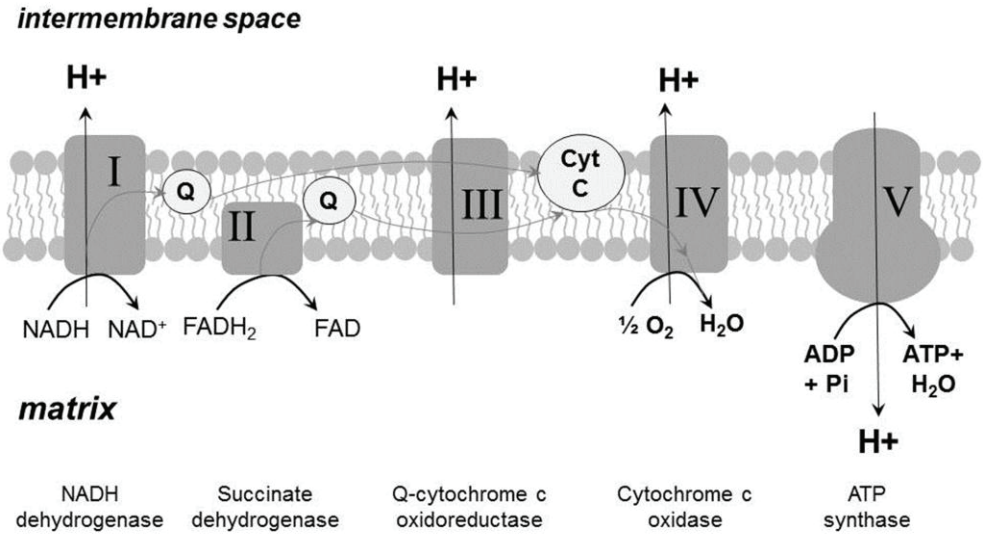

Figure 5-3. Electron transport chain in mitochondria. The transfer of electrons through protein complexes in the mitochondria generates a proton motive force that drives ATP synthesis.

(Glancy and Balaban, 2011; Leary et al., 2003; Schwerzmann et al., 1989) or isolation techniques (Picard et al., 2011). State 4 respiration is measured using an ATP synthase inhibitor to eliminate the contribution of proton flow through the ATP synthase. Thus, oxygen consumption in state 4 is indicative of proton leak across the inner membrane and represents inefficiency because oxygen consumption is not coupled to ATP synthesis. The ratio of oxygen consumption rate in state 3 relative to state 4 (respiratory control ratio, RCR) indicates the tightness of coupling between respiration and phosphorylation. Evidence supporting fiber type related differences in state 4 respiration and RCR are more limited. These properties may be measured in the presence of different substrates to determine preference and quantify specific aspects of oxidative metabolism. For example, using pyruvate + malate as substrates indicates flux through pyruvate dehydrogenase, TCA cycle, and electron transport chain, whereas using palmitoyl carnitine reveals integrity of β-oxidation and electron transport chain. Not surprisingly,

mitochondria from slow and fast fibers exhibit different capacities to oxidize fatty acids and glycerol phosphate (Jackman and Willis, 1996), likely due to inherent differences in β-HAD in slow muscle versus reliance on glycerol-phosphate shuttle in fast muscle. ADP sensitivity (K_m) is much higher (10-30 μM) in fast-twitch glycolytic muscle compared to slow (200-500 μM) and is still much higher than what would be predicted for resting muscle in vivo (Sahlin, 2007). Recently, Perry et al. (2011) demonstrated that in permeabilized fibers, inhibition of myosin ATPase and inclusion of phosphocreatine/creatine at physiological resting levels dramatically reduces the K_m for ADP to concentrations more consistent with estimates of in vivo resting respiratory rates. This also supports that contraction dramatically increases sensitivity for ADP, which provides tighter coupling of energy production with utilization when ATP demand is high (Perry et al., 2011). It is not clear, however, if different fiber types maintain different ADP sensitivity under these new conditions.

Mitochondria are the main site of production of ROS. Mitochondria appear to produce more ROS during state 4 respiration compared to ADP-stimulated state 3 respiration. During state 3 respiration, oxygen consumption is high and respiration is well-coupled to phosphorylation; electron flux is directed toward complex IV, thereby reducing ROS formation. However, in the absence of ADP, membrane potential ($\Delta\psi$) and ROS production are highest (Adhihetty et al., 2005). Therefore, ROS production is inversely related to oxygen consumption. Intriguingly, uncoupling proteins (UCPs) are a potential mechanism to decrease ROS in the resting state; UCPs allow proton influx to the matrix, which dissipates $\Delta\psi$, and uncouples oxygen consumption and ATP production (Vidal-Puig et al., 2000). At low levels, ROS are important signaling molecules. ROS modulate signaling cascades via oxidative modification of target proteins, and influence gene expression by activating redox sensitive transcription factors.

Curiously, exercise-induced increases in expression of antioxidant enzymes can be prevented by antioxidant supplementation (Ristow et al., 2009), thereby supporting that low levels of ROS are an important mechanism for triggering adaptation. Type IIB fibers possess lower antioxidant scavenging capacity and greater free radical leak, which contributes to increased ROS generation (Anderson and Neufer, 2006). An imbalance in ROS generation and removal by scavenging systems can lead to oxidative stress, loss of membrane potential, and cell death. Mitochondria are particularly susceptible to ROS-induced oxidative damage, including DNA mutations, changes in membrane fluidity, and aberrant protein function and signaling.

In fact, mtDNA has a higher mutation rate than nuclear DNA (Barja and Herrero, 2000), likely due to a lack of an efficient DNA repair system, lack of histones, and its proximity to ROS. Further, damage to mtDNA may create a "vicious cycle" whereby DNA mutations and/or deletions contribute to loss of protein function (reviewed by Alexeyev et al., 2004). Subsequently, compromised mitochondrial function results in greater ROS production and continued cycles of damage. DNA deletions are particularly harmful in post-mitotic tissues; deletions and mutations begin to accumulate in the third decade of life and also accumulate with age (Cortopassi et al., 1992). The same cell may contain mitochondria with mutated and wild-type DNA, a condition known as heteroplasmy (Fernandez-Silva et al., 2003). If the content of mutant mitochondria is high enough, it compromises cellular function. Alternatively, mitochondrial proliferation may be a mechanism to compensate for an energetic deficit. Mitochondrial proliferation can be induced by exercise (Williams et al., 1986), or by pathological circumstances involving defects in oxidative phosphorylation (Bai et al., 2004).

Mitochondria also sequester and release Ca^{2+}, which has numerous functional consequences. Ca^{2+} activates some mitochondrial enzymes, including pyruvate dehydrogenase

and isocitrate dehydrogenase. The ability of mitochondria to buffer Ca^{2+} influences the amplitude and frequency of Ca^{2+} oscillation within the cytosol. Locally high concentrations of Ca^{2+} instigate fusion-fission to redistribute Ca^{2+} in the cell. Fusion may permit mitochondria to transmit signaling throughout the cell, whereas fission impairs propagation of Ca^{2+} waves and the induction of apoptosis (Szabadkai et al., 2004). If high Ca^{2+} is sustained for a prolonged period, mitochondrial Ca^{2+} overload may occur and result in permeability transition pore opening, release of cytochrome c, and apoptosis. Fast fibers are more resistant to Ca^{2+} induced permeability transition pore opening (McMillan and Quadrilatero, 2011; Picard et al., 2008). This resistance may be necessary to tolerate the large spikes in cytosolic Ca^{2+} that occur in these fibers.

The mitochondrial matrix proteins and mtDNA are susceptible to damage but largely inaccessible to cytosolic systems for protein quality control. Thus, mitochondria have several mechanisms to counteract aggregation of damaged proteins. Mitochondria contain matrix proteases that contribute to protein quality control by degrading oxidized or misfolded proteins (Bender et al., 2011). The major matrix protease, Lon, also influences mtDNA copy number and transcription by degrading TFAM (Matsushima et al., 2010). Moreover, mitochondrial fusion-fission dynamics play an essential role in quality control of mtDNA and proteins. Fusion appears necessary for optimal mitochondrial function. Loss of either Mfn1 or Mfn2 results in embryonic lethality (Chen et al., 2003) and disruption of fusion leads to accumulation of mtDNA mutations and mitochondrial dysfunction (Chen et al., 2005). Therefore, the mixing of inner and outer membranes, matrix contents, and mtDNA during fusion is proposed to protect mitochondrial function by facilitating protein complementation, mtDNA repair, and distributing metabolites (Chen and Chan, 2009; Chen et al., 2010). Fission, on the other hand, may permit

damaged portions of mitochondria to be segregated and targeted for degradation (Twig et al., 2008).

Subcellular localization of mitochondria in muscle cells appears to impact function. Muscle mitochondria are distributed primarily either beneath the cell membrane (subsarcolemmal) or between the myofibrils (intermyofibrillar) (Muller, 1976). Although slow and fast fibers have a similar volume of intermyofibrillar mitochondria, slow fibers have a much higher volume of subsarcolemmal mitochondria (Philippi and Sillau, 1994). Subsarcolemmal and intermyofibrillar mitochondrial likely form different networks that are not connected, which contributes to distinct functional and biochemical properties. Due to their position near the cell periphery and nuclei, subsarcolemmal mitochondria likely serve important roles in providing energy for active transport of metabolites and ions across the cell membrane (Muller, 1976), influencing transcriptional adaptation (Romanello and Sandri, 2010), and acting as a protective barrier against oxidative stress inside the cell (Kuznetsov, 2007; Kuznetsov et al., 2006). Conversely, intermyofibrillar mitochondria are positioned near sites of energy consumption to supply ATP for contraction. With respect to function, intermyofibrillar mitochondria exhibit increased ADP-stimulated respiration (Cogswell et al., 1993), although this may be somewhat dependent on muscle or fiber type compositon (Philippi and Sillau, 1994). Intermyofibrillar mitochondria are also more sensitive to ROS, evidenced by greater release of cytochrome c and apoptosis-inducing factor in response to H_2O_2, whereas subsarcolemmal mitochondria have nearly 3-fold greater rates of ROS production (Adhihetty et al., 2005). This is consistent with ROS production being inversely related to oxygen consumption.

Skeletal muscle plasticity

Muscle fibers display a remarkable ability to adapt to various environmental stimuli by transitioning their phenotypes. Specifically, MHC isoforms and mitochondrial density exhibit enormous plasticity. Neuromuscular activity, mechanical loading, aging, chronic disease, and other circumstances lead to altered muscle fiber properties. Input comes from nerve activity, hormones, and other factors outside the cell, as well as intracellular messengers such as Ca^{2+} and reactive oxygen species. These cues influence signaling pathways, which can instigate changes in expression of contractile MHC proteins, mitochondrial proteins, regulatory proteins, and/or metabolic enzymes. With respect to MHC, fibers transition sequentially: I $\leftrightarrow$ I/IIA $\leftrightarrow$ IIA $\leftrightarrow$ IIAX $\leftrightarrow$ IIX $\leftrightarrow$ IIXB $\leftrightarrow$ IIB (Pette and Staron, 2001). Muscle fiber adaptation is reversible, and oxidative capacity, MHC isoforms, and other properties may not necessarily adapt in the same manner in response to environmental stimuli.

Neuromuscular activity contributes to the establishment of fiber type during development, and maintenance of fiber type thereafter. Buller et al. (1960) used cross-innervation to demonstrate that neural firing pattern significantly influences muscle fiber type; a fast muscle could become slow when innervated by tonic motor nerve activity, and vice versa. Subsequently, chronic low frequency or phasic high frequency stimulation protocols were developed to simulate slow or fast motor nerve activity, respectively. Nerve activity ultimately triggers release of Ca^{2+} from the sarcoplasmic reticulum. Disparate nerve activity patterns contribute to differences in the amplitude and duration of the cytosolic Ca^{2+} oscillation. In turn, intracellular Ca^{2+} is a potent second messenger that influences signaling pathways, enzyme activity, and metabolism.

Cytosolic Ca^{2+} levels are intimately related to twitch properties and adaptation to a particular type of exercise. Higher peak amplitude and faster rates of Ca^{2+} sequestration are well suited to short bursts of high force activity consistent with resistance training. This type of training tends to promote increased synthesis of myofibrillar proteins to increase cross sectional area and muscle force. The exact mechanisms contributing to resistance training-induced hypertrophy are not well known. Tension at the cell membrane may cause signaling events involving growth factors, cytokines, stretch activated channels, or integrin-focal adhesion complexes (reviewed by Spangenburg, 2009). Others have suggested mechanical signals are transduced from titin kinase domain within the sarcomere (Lange et al., 2005). In contrast, the sustained, low force generation during endurance training triggers transition to a more oxidative phenotype. The chronic nature of endurance exercise can result in decreased cellular energy status. Low energy charge (decreased ATP:AMP) activates AMPK, which stimulates mitochondrial biogenesis (Zong et al., 2002), thereby promoting oxidative metabolism. Continued elevation of intracellular Ca^{2+} may also promote Ca^{2+}-mediated pathways that stimulate mitochondrial biogenesis.

Training is well known to induce changes in mitochondrial density, but it also influences mitochondrial localization and quality. Greater mitochondrial density increases maximal oxygen consumption ~40% (Tonkonogi et al., 2000; Walsh et al., 2001), consistent with increases in mitochondrial protein and ATP production rate (Wibom et al., 1992). Endurance training preferentially increases mitochondria in the subsarcolemmal fraction (Krieger et al., 1980; Nielsen et al., 2011). Training increases basal substrate oxidation but does not affect ATP production, suggesting that oxidative phosphorylation is more uncoupled at rest in trained muscle (Befroy et al., 2008). Similarly, exercise trained muscle has increased capacity to remove

ROS, which protects against oxidative damage (Brooks et al., 2008; Tweedie et al., 2011), and respiration exhibits decreased sensitivity to ADP and increased sensitivity to creatine (Walsh et al., 2001). Thus, endurance training induces quantitative and qualitative adaptations in mitochondria.

However, it is not well understood how altering mitochondrial phenotype and oxidative capacity influences cell size. Increasing mitochondrial content changes the volume available for contractile proteins, suggesting there may be some limitation for increasing both power and oxidative capacity. Hickson (1980) demonstrated that training concurrently with resistance and endurance exercise resulted in less adaptation than either type of training alone. Thus, limiting cross sectional area may be an important means of maintaining optimal oxidative capacity. Correspondingly, cross-sectional area is inversely related to maximal rate of oxygen consumption (VO_{2max}) of vastly different muscle preparations; VO_{2max} is proportional to SDH activity and the number of mitochondria (van Wessel et al., 2010). This suggests the potential for fiber growth or hypertrophy may be limited if oxidative capacity is too high. Conversely, hypertrophy may sacrifice endurance capacity; that is, mitochondrial function and bioenergetics could be compromised if a fiber gets "too big." Crosstalk between signaling pathways may be an important mechanism limiting concurrent increases in mitochondria (oxidative capacity) and myofibrillar protein (hypertrophy).

Muscle protein turnover

In skeletal muscle, proteins are constantly being synthesized and degraded, and thus there is continuous protein turnover. Synthesis of new proteins and degradation of damaged or unneeded proteins contributes to growth, remodeling during adaptation, and maintenance of

phenotype. There are inherent differences in turnover of myofibrillar and mitochondrial proteins, and in the capacity for protein synthesis and degradation across fiber types. Myofibrillar proteins compromise ~55-60% of total muscle protein; sarcoplasmic proteins, which represent ~30-35% of muscle protein, include intracellular proteins and mitochondrial and other metabolic enzymes. The net balance of protein synthesis and degradation determines protein content.

The capacity for protein synthesis is influenced by templates (DNA and mRNA), availability of protein synthesis machinery, and activation of these processes by signaling pathways. Nuclear and mitochondrial DNA are transcribed into mRNA. The content of DNA template can affect the amount of mRNA available for translation. In turn, the translation of mRNA into protein requires transfer RNA (tRNA) and ribosomal RNA (rRNA). Finally, initiation and elongation factors must be activated in order for the machinery to translate mRNA into protein.

Protein synthesis

Muscle fibers are multi-nucleated, and each nucleus is proposed to control transcription for a certain amount of cytoplasm, which is referred to as DNA unit size or myonuclear domain (Hall and Ralston, 1989; Landing et al., 1974). Potential for protein synthesis is related to DNA unit size and myonuclear accretion. However, postnatal skeletal muscle cells are post-mitotic. Increases in muscle size cannot be accomplished through proliferation, so muscle growth must be achieved via hypertrophy or increases in length. Additional myonuclei may be recruited to the muscle fiber via activation of a normally quiescient population of satellite cells. These cells can divide and fuse with the myofiber (Moss and Leblond, 1970), thereby providing additional DNA and contributing to increased capacity for protein synthesis. Slower, more oxidative fibers that

have higher functional demands possess higher nuclear density and higher satellite cell content (Gibson and Schultz, 1983; Tseng et al., 1994). This suggests that slower fibers have a higher potential for transcription.

The transcription of DNA into RNA is controlled by several factors relating to access to the DNA template. Chromatin modification is necessary to provide access to DNA, and transcription factors play a key role in recruiting RNA polymerase to DNA for transcription. The proportion of MHC mRNA to total RNA does not change across fiber types (Habets et al., 1999). However, total amount of RNA differs according to fiber type, with type I fibers possessing about 5 to 6 fold greater total RNA than type IIB fibers (Habets et al., 1999). Approximately 25% of RNA polymerase II is transcriptionally active (Kimura et al., 2002), indicating that RNA polymerase II does not limit transcriptional capacity. However, transcription rate may be influenced by variability in mitochondrial content between different fiber types. Mitochondrial mass and membrane potential are positively associated with transcription rate, and RNA polymerase II is highly sensitive to ATP concentration (das Neves et al., 2010) This suggests that high mitochondrial content and ability to maintain energy homeostasis may promote transcription and hence contribute to elevated RNA content observed in slow, oxidative fibers.

Due to increased total RNA content, type I fibers should also contain more rRNA, and consequently, an increased capacity for protein synthesis. Yet, transcripts only represent potential for new proteins. The structure of mRNA influences its translation. Recently, Zid et al. (2009) showed that several nuclear encoded mitochondrial genes possessed shorter and less structured 5' untranslated regions (UTRs), which permitted increased ribosomal loading and facilitated translation. Moreover, translation is ten times more energetically costly compared to

transcription (Wagner, 2005). Translation is dependent on the availability of energy and amino acids, and precisely regulated by activation of initiation and elongation factors. Eukaryotic translation initiation factor 4E (eIF4E) binds to the 5'-cap structure of mRNA and recruits the 40S ribosome for translation. eIF4E also recruits other proteins (eIF4A, eIF4G, polyA-binding protein) to form the translation initiation factor complex. However, if eIF4E is bound to eIF4E binding protein 1 (4E-BP1), this prevents formation of the initiation complex, thus blocking protein synthesis. Phosphorylation of 4E-BP1 disrupts this interaction with eIF4E and results in activation of translation. Moreover, Miller et al. (2012) demonstrated that total 4E-BP content is increased during caloric restriction. Thus, under more chronic stress, the increase in 4E-BP contributes to overall decreases in protein synthesis initiation. P70S6 kinase (P70S6K) phosphorylates eIF4B and the 40S ribosomal subunit protein S6, which enhances RNA unwinding and translation, respectively. Subsequently, peptide elongation requires two factors, eukaryotic elongation factor (eEF) 1 and eEF2. In response to increased cellular energy demand or reduction in energy supply, eEF2 is phosphorylated, which inhibits its binding to ribosomes.

The high DNA and mRNA contents of slow muscles suggest these fibers have a high capacity for protein synthesis. In fact, type I and IIA fibers have much higher rates of protein synthesis than IIB and IIX; these differences were demonstrated within the same muscle in mice (Goodman et al., 2011). Moreover, the contrasting rates of protein synthesis had a strong relationship with size across fiber types, but not within fiber type. Yet, increased protein synthesis capacity in type I and IIA "slower" fibers is not associated with greater protein accumulation because these fibers remain relatively small. This paradox may be related to the type of protein synthesized. Fractional synthesis rates of mitochondrial and sarcoplasmic proteins are much higher than those of MHC proteins (Jaleel et al., 2008), and MHC proteins also have a

much larger mass than mitochondrial proteins. Because slow fibers generally work over a greater duration and mitochondrial proteins may be more prone to damage, it may be necessary to maintain high turnover of these proteins in order to maintain metabolic function. Thus, the high rates of protein synthesis in slower fibers coupled with their smaller size, implicate greater protein degradation and hence, greater protein turnover in these fibers.

Protein degradation

Controlled turnover of proteins is necessary to salvage amino acids from proteins that are damaged or no longer needed. These proteins must be marked for protein degradation so they can be recognized by the proteolytic systems. In skeletal muscle, several pathways contribute to protein degradation: ubiquitin-proteasome, lysosomal, calpain, and caspase proteolysis systems. The complex, proteinaceous nature of skeletal muscle requires concerted action of proteolytic systems to disassemble and degrade large, complex structural elements, as well as specificity to target only those proteins that need to be destroyed. The activation of proteolytic pathways is partly dependent on the nature of the environmental stimulus.

Ubiquitin proteasome pathway

The ubiquitin proteasome pathway is responsible for the majority of protein turnover. The 26S proteasome complex binds "tagged" poly-ubiquitinated proteins and uses ATP to unfold and move the substrates into its core for degradation. While the proteasome can degrade sarcoplasmic proteins, it cannot degrade myofibrillar proteins until they have been cut from the myofibril. Proteins are marked for degradation by attaching multiple ubiquitin proteins to lysine residues on the target protein. This process is tightly regulated and involves three enzymes:

ubiquitin activating enzyme (E1), ubiquitin conjugating enzyme (E2), and ubiquitin protein ligase (E3). While there are only a few isoforms of E1 and E2 and these enzymes have broad specificity, greater specificity is achieved by having several more specialized E3 isoforms. The muscle-specific E3 ligases, muscle atrophy F-box (MAFbx, or atrogin-1) and muscle really interesting new gene (RING) finger-1 (MuRF-1), are up-regulated during conditions that lead to atrophy, such as cancer cachexia and starvation (Lecker et al., 2004). Inhibition of either MAFbx or MuRF1 attenuates loss in muscle mass under these conditions.

Though MAFbx and MuRF-1 are considered major factors regulating protein degradation, less is known about their specific targets. MAFbx is implicated in preventing synthesis and growth pathways; it mediates ubiquitination of elongation initiation factor 3 subunit 5 (eIF3-f), as well as the muscle development factors MyoD and myogenin. In contrast, MuRF-1 is likely more involved in targeting structural and metabolic proteins. MuRF-1 binds to titin and ubiquitinates MHC, myosin light chain, nebulin, and troponins I and T. Further, MuRF-1 also targets several proteins involved in carbohydrate metabolism, including pyruvate dehydrogenase and phosphorylase β (Hirner et al., 2008). The oxidized form of cytoplasmic muscle-type creatine kinase, which is demonstrated to have low activity compared to the reduced form, is also a MuRF-1 target (Koyama et al., 2008; Zhao et al., 2007).

The activity of forkhead box O (FoxO) transcription factors regulates MAFbx and MuRF1 expression. There are three FoxO family members in skeletal muscle: FoxO1, FoxO3a and FoxO4. Dominant negative FoxO3a prevents increases in MAFbx and MuRF-1 mRNA and blocks atrophy of slow (soleus) and fast (tibialis anterior) muscles during cachexia and sepsis (Reed et al., 2011). Remarkably, under normal conditions, dominant negative FoxO instigates increases in satellite cell proliferation, and induces muscle hypertrophy and de novo protein

synthesis (Reed et al., 2011), suggesting that FoxO transcriptional activity also plays an important role in limiting growth under normal conditions.

Lysosomal proteolysis

Lysosomes are membrane bound vesicles responsible the degradation of various cellular and extracellular components. Lysosomal hydrolases degrade organelles and proteins, as well as components which may enter the cell by endocytosis. Within the acidic lumen, there are various enzymes – proteases (cathepsins), lipases, nucleases, glycosidases – responsible for degradation of macromolecules. Lysosomal-dependent degradation of cytoplasmic contents involves sequestration of targets to the lysosome and their degradation by enzymes. Therefore, delivery of proteins to the lysosome is a key step in lysosomal proteolysis.

Several pathways are utilized to bring cytoplasmic targets to the lysosome: microautophagy, chaperone-mediated autophagy, or macroautophagy. Microautophagy involves the lysosomal membrane engulfing small portions of the cytosol; however, the significance of this method in skeletal muscle is not well established (Bechet et al., 2005). In the chaperone mediated pathway, protein targets are recognized by the heat shock cognate of 70 kDa. The substrate protein complex binds a receptor on the lysosome and is subsequently internalized for degradation. Finally, macroautophagy, which is commonly referred to as autophagy, involves formation of a double membrane structure or pre-autophagosome. This structure sequesters portions of cytoplasm or organelles, and expands to form an autophagosome. Expansion of the pre-autophagosome is mediated by microtubule associated protein 1 light chain 3 (LC3). Shortly after its synthesis, pro-LC3 is cleaved to generate the cytosolic form, LC3-I. Addition of phosphatidylethanolamine to LC3-I produces LC3-II, which is associated with the expanding

autophagosome membrane (Mizushima et al., 2010). The protein p62 recognizes poly-ubiquitinated proteins and binds directly to LC3-II, supporting that p62 is important for targeting protein aggregates for autophagy (Pankiv et al., 2007). LC3-II remains on the autophagosome until it fuses with a lysosome. Then, the inner membrane of the autophagosome lyses, and its contents are broken down by the lysosomal enzymes.

Turnover of mitochondrial proteins and autophagy of entire mitochondria (mitophagy) is mediated by the lysosomal system. Mieap, a p53 inducible protein, plays a key role in mitochondrial quality control and induction of mitophagy. The interaction of mieap with the outer mitochondrial membrane protein BCL2/adenovirus E1B 19 kDa interacting protein (Bnip3) may be critical for inducing the translocation of lysosomal proteins from the cytosol to the mitochondrial matrix (Miyamoto et al., 2011). The lysosome like organelles within the matrix then degrade damaged and oxidized mitochondrial proteins in order to maintain mitochondrial integrity (Miyamoto et al., 2011; Nakamura et al., 2012). Moreover, mieap can induce the formation of vacuole like structures that recruit lysosomes and result in mitophagy of dysfunctional mitochondria (Miyamoto et al., 2011). ROS may be a key factor mediating recruitment of lysosomal proteins to the matrix.

Lysosomal systems are an important means of removing damaged proteins and long-lived cytosolic and transmembrane proteins, and also support organelle turnover. Moreover, during nutrient stress, upregulation of the lysosomal system is a key mechanism for providing additional metabolic intermediates. Under basal conditions, impairment of lysosomal degradation results in accumulation of misfolded proteins and altered organelles, which impairs normal cellular function; conversely, excessive activation of lysosomal degradation can contribute to loss of muscle mass and decreased function. While Dufour et al. (1989) demonstrated that cathepsins

can degrade myosin in vitro, this may not be biologically relevant as lysosomes are likely not large enough to engulf myosin and other large proteins (Goll et al., 2008). In agreement, Furuno et al. (1990) demonstrated that inhibition of lysosomal function failed to block myofibrillar degradation during atrophy. Consistent with observations that cathepsin expression is higher in tissues with high protein turnover, cathepsins are more highly expressed in slow oxidative muscles (Bechet et al., 2005). FoxO transcriptional activity also enhances cathepsin L and Bnip3 expression (Mammucari et al., 2007).

Calpain-mediated proteolysis

The calpain system, a family of Ca^{2+} dependent proteases, includes 14 members. The isoforms m-calpain and μ-calpain, are dependent on millimolar and micromolar Ca^{2+} concentrations, respectively, for activity. Calpain activity is also influenced by its inhibitor, calpastatin, and autolysis, which enhances Ca^{2+} sensitivity and weakens Ca^{2+} sensitivity of calpastatin binding. In contrast to other proteolytic systems, calpains do not degrade polypeptides; rather, they provide the first means of disassembling proteins from the myofibril, so that they may be degraded by "bulk" degradation systems. Calpain targets include the cytoskeletal proteins titin, nebulin, desmin, and talin, among others; calpain degrades a few cellular kinases and phosphatases as well. Calpain activity tends to be higher in slower, more oxidative fibers (McMillan and Quadrilatero, 2011).

Caspases

Caspases are involved with protein degradation during apoptosis. External and internal signals can activate caspases, which propagate the cell death signal by cleaving and activating

other caspases. Caspase activation can be facilitated via receptor-mediated mechanisms or by the release of proapoptotic factors from opening of the mitochondrial permeability transition pore. As myofibers are long-lived, terminally differentiated cells, muscle cells generally are rather resistant to apoptosis unless subjected to myopathic conditions or muscle wasting. Although apoptosis per se is not typical for muscle, atrophying fibers may lose nuclei (myonuclear apoptosis) in order to preserve constant myonuclear domain. In this situation, caspases may mediate DNA fragmentation and loss of nuclei (Powers et al., 2007).

Signaling pathways controlling muscle phenotype

Clearly, there are inherent differences in protein synthesis and turnover in slow oxidative fibers compared to their fast, glycolytic counterparts. High oxidative fibers exhibit high rates of protein synthesis but high rates of degradation as well. There is likely competition between turnover rates of myofibrillar protein and metabolic/mitochondrial proteins. Moreover, if mitochondrial function is not optimal, compromised energetic status activates signaling for adaptation and survival. A complex network of signaling pathways is responsible for regulating protein turnover and metabolism. These pathways integrate information regarding nerve and muscle activity, calcium oscillations, and energy status, with growth factors and cytokines, in order to modulate phenotype.

Akt/mTOR

Akt is an important regulator of protein synthesis, glycogen synthesis, and cell proliferation and survival. There are 3 isoforms of Akt (1, 2, and 3), with Akt1 playing the most significant role in muscle. Certain growth factors, such as insulin like growth factor-1, lead to

Akt activation via the phosphatidyl inositol triphosphate pathway. Akt is phosphorylated on separate residues (Thr^{308} and Ser^{473}) by at least two different kinases. Akt content and activation change with atrophic and hypertrophic stimuli, implicating Akt as a major player in muscle growth. In hindlimb immobilization model of disuse, Akt protein and phosphorylation levels decrease during atrophy (Bodine et al., 2001). In contrast, constitutively active Akt induces hypertrophy in regenerating muscle, whereas a dominant negative Akt partially inhibits increases in fiber size (Pallafacchina et al., 2002). Akt has three major downsteam effectors: mammalian target of rapamycin (mTOR), glycogen synthase kinase 3β (GSK3β) and FoxO pathways.

The kinase mTOR integrates information about the nutrient and energy status of the cell with growth signals to modulate key steps in protein synthesis and degradation. mTOR is part of two distinct complexes, mTORC1 (contains raptor) and mTORC2 (contains rictor); mTORC1 is nutrient and rapamycin-sensitive whereas mTORC2 is rapamycin insensitive (Wullschleger et al., 2006). Akt's effect on muscle growth is largely mediated through phosphorylation of mTORC1, which, in turn, regulates several players involved in peptide translation initiation and elongation. Activated mTOR phosphorylates 4E-BP1, P70S6K, and eEF2K, which releases inhibition of translation initiation, promotes protein synthesis, and enhances translation, respectively (Wang and Proud, 2006). In support, inhibition of mTOR with rapamycin during compensatory hypertrophy blocks virtually all adaptive hypertrophy (Bodine et al., 2001). In response to limiting nutrients, mTOR also induces autophagy as a means of providing energy to the cell.

Akt phosphorylates and inactivates glycogen synthase kinase 3β (GSK3β), a negative regulator of translation initiation factor eIF2B. Inactive GSK3β augments protein synthesis by increasing mRNA translation (Rommel et al., 2001; Vyas et al., 2002). Along these same lines,

recently Verhees et al. (2011) demonstrated that expression of MAFbx depends on GSK3β activity. Other targets of Akt include FoxO transcription factors and GTPase activating protein tuberin sclerosis complex (TSC2). Akt phosphorylates FoxO factors, resulting in their translocation from the nucleus and concomitant reduction in expression of MAFbx and MuRF1. Meanwhile, phosphorylation of TSC2 blocks its GTPase activity, allowing the protein Rheb to remain active and promote protein synthesis through its interaction with mTORC1.

AMPK-PGC1α

Whereas Akt/mTOR is a critical regulator of protein turnover, AMP-activated protein kinase (AMPK), dubbed the "fuel gauge" of the cell, is a major regulator of skeletal muscle metabolism. AMPK promotes both acute responses and adaptive mechanisms in response to energetic stress. AMPK, a heterotrimeric serine-threonine kinase, is composed of a regulatory β

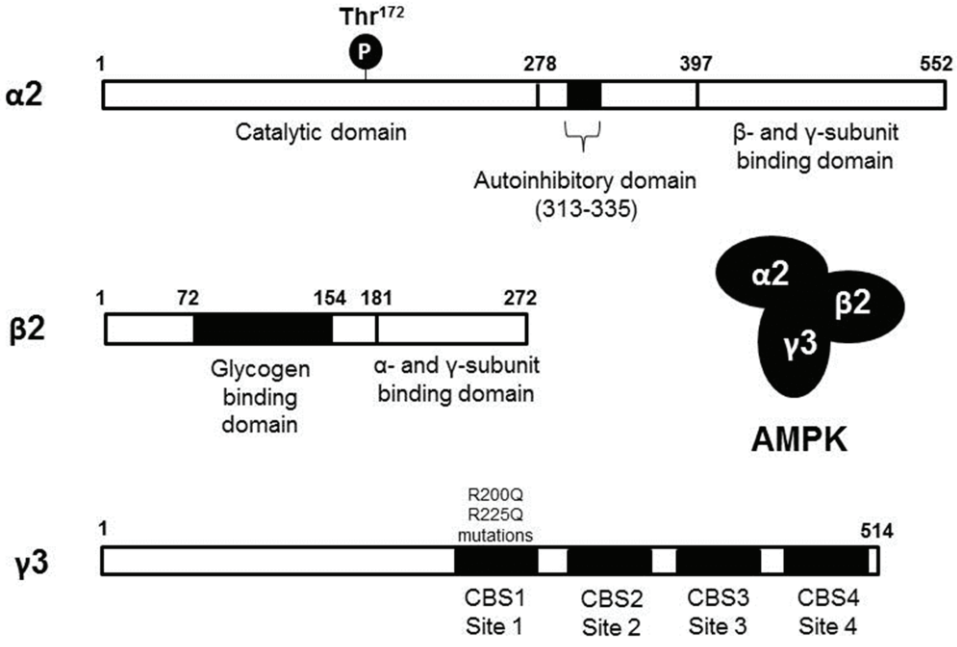

Figure 5-4. Structure of AMPK. AMPK is a heterotrimer composed of an α, β, and γ subunit. Adapted from Witczak et al. (2008) and Milan et al. (2000).

(β1 or β2) and γ (γ1, γ2, or γ3) subunit and a catalytic α (α1 or α2) subunit (Figure 5-4). The β subunit functions as a scaffold and contains a glycogen binding domain (Polekhina et al., 2003). The γ subunit possesses four potential adenine nucleotide binding sites. One site contains a permanently bound AMP, and another site is unoccupied; the two remaining sites (sites 1 and 3) competitively bind AMP, ADP, or ATP, and are involved in detecting energy status and regulating AMPK activity.

Cellular energy status regulates activation of AMPK by several mechanisms (Figure 5-5). Binding of AMP causes conformational changes that enhance AMPK activity by (1) promoting phosphorylation of Thr^{172} on the α-subunit, the main site required for activation of AMPK by upstream kinases (Oakhill et al., 2010; Stein et al., 2000); (2) allosteric activation (Suter et al., 2006); and (3) protection from dephosphorylation by phosphatases 2A and 2C (Sanders et al.,

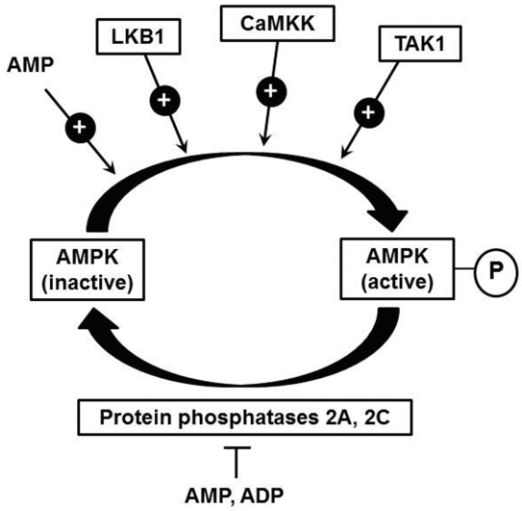

Figure 5-5. Regulation of AMPK activity by upstream kinases, allosteric activation, and phosphatases. AMPK activity is increased by phosphorylation at Thr^{172} by the upstream kinases LKB1, calcium/calmodulin dependent protein kinase kinase (CaMKK), and transforming growth factor β activating kinase 1 (TAK1); and AMP-induced allosteric activation. AMP or ADP binding also causes conformational changes that protect against dephosphorylation by phosphatases. Adapted from Witczak et al. (2000).

2007; Suter et al., 2006). Increasing AMP:ATP is considered the main stimulus inciting AMPK activity. However, ADP was recently shown to have similar stimulatory effects on AMPK, except ADP does not allosterically activate AMPK (Oakhill et al., 2011; Xiao et al., 2011). The major upstream kinase implicated in Thr^{172} phosphorylation is the tumor supressor LKB1, accompanied by its accessory proteins, STRAD and MO25 (Hawley et al., 2003). However, LKB1 appears to be constitutively active in skeletal muscle (Sakamoto et al., 2004), indicating that it is not the primary mode for regulating AMPK activity. Ca^{2+}/calmodulin-dependent protein kinase kinase (CaMKKβ) acts upstream of AMPK in a Ca^{2+}, AMP-independent manner, thus providing a means of connecting contraction, Ca^{2+}, and AMPK activity (Hawley et al., 2005). Another upstream kinase, transforming growth factor β activated kinase (TAK1), is activated by cytokines, but its physiological relevance is not clear (reviewed by Witczak et al., 2008). Thus, regulation by adenine nucleotides (energy status) appears the key mechanism regulating AMPK activity. Compromised energy charge may result from either decreasing ATP generation or accelerating ATP consumption. Several experimental and pharmacological compounds activate AMPK by interfering with energy production via inhibition of the respiratory chain, ATP synthase, or glycolysis (Hawley et al., 2010), whereas other compounds, such as 5-aminoimidizole-4-carboxamide 1-β-D ribonucleoside (AICAR), are AMP analogs (Merrill et al., 1997). In contrast, exercise and muscle contraction enhance AMPK activation by enhancing ATP utilization.

In response to decreased energy charge, AMPK stimulates energy producing pathways and down-regulates energy consuming pathways in order to preserve cellular ATP (Figure 5-6). Increased AMPK activity promotes translocation of the GLUT4 transporter to the cell membrane, demonstrating that AMPK is responsible for mediating contraction-induced, insulin-

independent glucose uptake (Jorgensen et al., 2004b; Kurth-Kraczek et al., 1999). AMPK also enhances lipid oxidation by inactivating acetyl CoA carboxylase, which reduces malonyl-CoA levels and relieves inhibition of carnitine palmitoyl transferase-1. This results in greater fatty acid uptake into the mitochondria and enhanced lipid oxidation for greater energy production. During exercise, impaired ability to activate AMPK results in decreased glucose uptake and reduced mitochondrial function, supporting that AMPK is essential for metabolic response to exercise (Lee-Young et al., 2009; O'Neill et al., 2011).

AMPK also facilitates longer lasting effects on metabolism by influencing gene

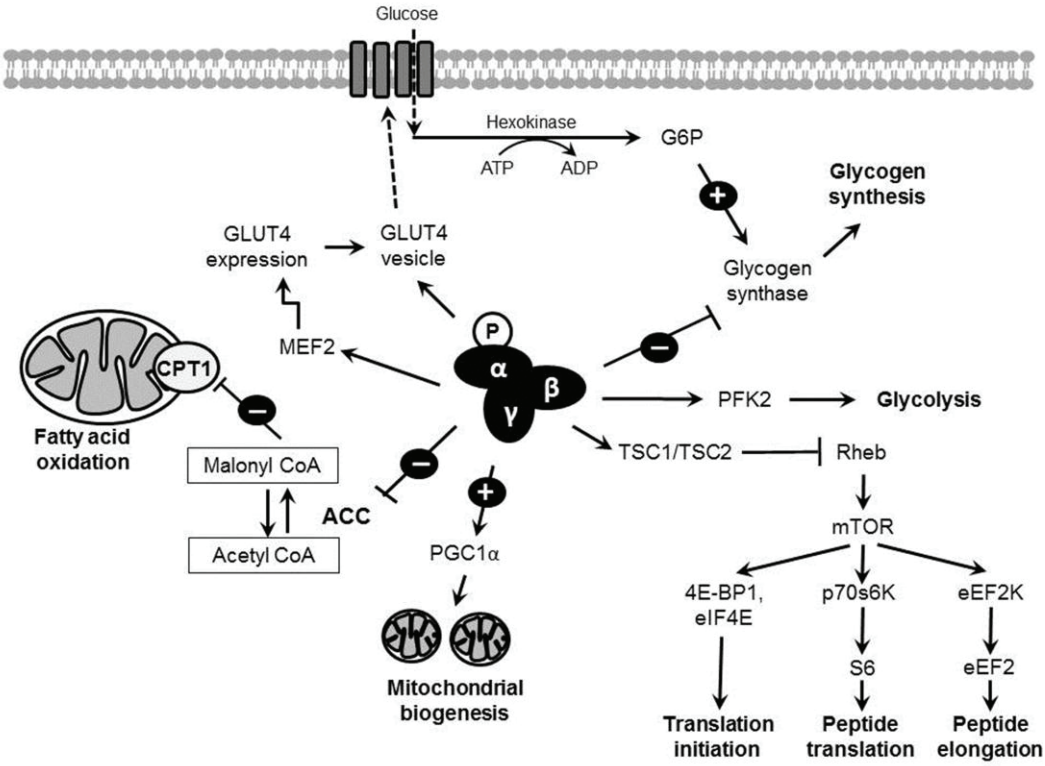

Figure 5-6. Role of AMP-activated protein kinase (AMPK) in regulation of metabolism. AMPK alters protein activity and gene and protein expression; and influences multiple pathways, including fatty acid oxidation, glucose transport, glycolysis, and protein synthesis.

transcription, protein expression, and adaptation. Chronic activation of AMPK increases GLUT4 transcription (Zheng et al., 2001), hexokinase and GLUT4 protein content and muscle glycogen (Holmes et al., 1999), and mitochondrial biogenesis (Zong et al., 2002). AMPK promotes the adaptive response to chronic energy deprivation by directly activating PGC1α (Jager et al., 2007), which initiates many of AMPK's effects on gene regulation and promotes oxidative metabolism. Further, Rockl et al. (2007) revealed that AMPK mediates the exercise induced transformation of muscle to a more oxidative phenotype. In contrast, greatly diminished AMPK activation in α2-kinase dead mice results in lower intermyofibrillar mitochondria content and exercise intolerance (O'Neill et al., 2011).

AMPK's regulation of metabolism is more complex when the roles of specific isoforms and muscle fiber types are considered. Of the 12 possible heterotrimer combinations, only three are significantly expressed in human skeletal muscle: α2β2γ1, α2β2γ3, and α1β2γ1 (Birk and Wojtaszewski, 2006). Exercise preferentially activates heterotrimers containing the α2 subunit, particularly α2β2γ3 (Birk and Wojtaszewski, 2006). While α1 complexes are cytosolic, α2 complexes are at least partly nuclear and likely play a direct role in regulating gene and protein expression via direct interactions in the nucleus (McGee et al., 2003; Salt et al., 1998). A conserved glycogen binding domain on the β subunit allows AMPK to associate with glycogen in cultured cells (Polekhina et al., 2003) and may be another means by which AMPK detects cellular energy stores. Key mutations in the β subunit's glycogen binding domain abolish AMPK's capacity to bind glycogen and reduce inhibition of AMPK by glycogen (McBride et al., 2009). This, coupled with fact that contraction-induced AMPK activity is inversely related to glycogen content (Barnes et al., 2005a), suggests that glycogen may exhibit some feedback control on AMPK activity or may sequester AMPK and prevent its interaction with substrates.

The γ subunit plays a major role in modulating AMPK activation and metabolism. Mahlapuu et al. (2004) found that γ3 is specific to skeletal muscle and is more highly expressed in fast "white" muscles. This corroborated earlier observations that swine with the $\gamma3^{R200Q}$ mutation possess a 70% increase in glycogen in muscle, but not in liver and heart (Milan et al., 2000). Although Milan et al. (2000) indicated that AMPK activity is lower in $\gamma3^{R200Q}$ pigs, this is unlikely for several reasons. The R200Q mutation is in the domain of γ3 responsible for AMP binding. A similar mutation in the γ1 subunit, R70Q, results in constitutive AMPK activity and loss of AMP dependence (Adams et al., 2004). Further, Costford et al. (2007) identified a $\gamma3^{R225W}$ mutation in humans, which is homologous to R200Q. Differentiated satellite cells from $\gamma3^{R225W}$ carriers possess nearly a two-fold increase in basal and AMP-activated AMPK activity; muscle from these subjects contains a 90% increase in glycogen and 30% decrease in triglycerides. This, along with the dominant nature of the mutation, is convincing evidence that $\gamma3^{R200Q}$ is an activating mutation. Constitutive activation of AMPK and persistent glucose transport likely contribute to elevated glycogen in $\gamma3^{R200Q}$ muscle. It may be argued AMPK activation decreases glycogen synthesis because heterotrimers containing activated α2-AMPK can phosphorylate glycogen synthase (GS) at site 2 (Ser^7), thereby inactivating GS (Jorgensen et al., 2004a). However, increased glucose transport due to chronic AMPK activation would result in increased levels of glucose-6 phosphate (G6P); this allosteric activator can 'overrule' the inactivation of GS by phosphorylation, resulting in increased glycogen synthesis.

Despite its elevated glycogen, white muscle of $\gamma3^{R200Q}$ mutant pigs has a more oxidative phenotype (Lebret et al., 1999) and possesses a greater proportion of 'slower' myosin heavy chain isoform (Park et al., 2009b). Mice with an equivalent mutation ($\gamma3^{R225Q}$) maintain higher rates of fatty acid oxidation when exposed to a high fat diet, thereby protecting them against

triglyceride accumulation in muscle and insulin resistance (Barnes et al., 2004). After contraction, transgenic mice overexpressing $\gamma3^{R225Q}$ show decreased glucose oxidation (Barnes et al., 2005a), greater ACC inactivation, and lower muscle triglyceride content than control mice (Barnes et al., 2005b). Moreover, opposite transcriptional changes occur in transgenic $\gamma3^{R225Q}$ compared to γ3 knock-out mice; numerous genes involved in glucose and fat metabolism and muscle ergogenics are affected (Nilsson et al., 2006). The γ3 mutations increase oxidative capacity in glycolytic skeletal muscle by increasing mitochondrial biogenesis, which is associated with increased expression of PGC1α and several transcription factors that regulate mitochondrial proteins (Garcia-Roves et al., 2008). This evidence supports that γ3 regulates fuel repartitioning and muscle adaptation to facilitate lipid oxidation.

Calcium

Ca^{2+} is a potent signaling mechanism that affects enzyme activity, growth, and adaptation in skeletal muscle. Neural activation and membrane depolarization lead to the release of Ca^{2+} from the sarcoplasmic reticulum, which elicits force production. Because Ca^{2+} is intimately linked to the contraction-relaxation cycle, it is well-suited to serve as a "feed-forward" signal to increase metabolism and ATP production. Frequency and duration of stimulation influence the amplitude and duration of the Ca^{2+} signal; thus the type of Ca^{2+} transient likely dictates the physiological response. Prolonged activity or chronic conditions may lead to changes in gene and protein expression aimed at promoting adaptation.

Ca^{2+} signals are detected by the Ca^{2+} binding protein, calmodulin (CaM). Calmodulin has four Ca^{2+} binding sites and undergoes conformational changes before activating downstream proteins. Several classes of protein kinases and certain phosphatases, such as calcineurin,

contain a Ca^{2+}/CaM binding domain. For example, Ca^{2+}/CaM increases the activity of phosphorylase kinase, which converts glycogen phosphorylase *b* to its more active *a* form. Therefore, Ca^{2+} coordinates increased glycogen breakdown with the increased energy demand of contraction. While phosphorylase kinase is a 'dedicated' Ca^{2+}/calmodulin dependent kinase (CaMK) with only one known substrate, there are several multifunctional CaMKs that possess broad substrate specificity. Mainly, Ca^{2+}/CaM modulates muscle growth, adaptation, and metabolism via calcineurin, CaMKs (CaMKI, CaMKII, CaMKIV), and CaMK kinases (CaMKKs).

The serine/threonine phosphatase calcineurin plays a major role in muscle adaptation. Specifically, tonic motor neuron activation results in sustained, low amplitude levels (100-300 nM) of Ca^{2+} that are sufficient to enhance calcineurin activity. Increased calcineurin activity promotes the slow fiber program, including increased expression of myoglobin and type I MHC (Chin et al., 1998; Naya et al., 2000), whereas inhibition of calcineurin results in a slow to fast transition (Chin et al., 1998). Activated calcineurin dephosphorylates nuclear factor of activated T cells (NFAT) transcription factors, which promotes their translocation to the nucleus. Different motor activity/stimulation patterns induce activation of certain NFAT family members; in turn, the combination of NFAT isoforms present in the nucleus determines which MHC and metabolic genes are transcribed (Calabria et al., 2009). Several "slow" genes contain binding sites for NFAT and myocyte enhancer factor 2 (MEF2), and these transcription factors appear to work together to promote the slow fiber program. Accordingly, transgenic mice overexpressing active calcineurin exhibit a muscle phenotype similar to that induced by chronic endurance training. Activated calcineurin increases expression of genes for lipid metabolism and mitochondrial oxidative phosphorylation, concordant with decreased expression of glycolytic

enzymes; altogether, this results in increased fatty acid oxidation, decreased glucose utilization, and enhanced glycogen storage (Long et al., 2007). Moreover, transgenic mice show increased energy expenditure and mitochondrial oxidative function, which supports increased endurance performance (Jiang et al., 2010) and contributes to protection against diet-induced glucose intolerance (Ryder et al., 2003).

The multifunctional CaMKII may be important in regulation of muscle phenotype. CaMKII is encoded by distinct but homologous genes (α, β, γ, δ) and gives rise to numerous splice variants with different expression patterns and subcellular localization. A unique property of CaMKII is that upon Ca^{2+}/CaM binding, CaMKII undergoes intersubnit phosphorylation which results in Ca^{2+} independent activity. Therefore, CaMKII can retain activity in the absence of Ca^{2+}/CaM (autonomous activity), yet its maximal Ca^{2+}/CaM-stimulated activity is unaffected (reviewed by Hudmon and Schulman, 2002). This complex regulation is thought to permit CaMKII to detect the frequency of Ca^{2+} oscillations and adjust kinase activity accordingly. CaMKII is implicated in acute responses and long-term muscle adaptation. Exercise increases autonomous but not maximal activity of CaMKII (Rose and Hargreaves, 2003), and activity is maintained during continuous exercise (Rose et al., 2006). Importantly, CaMKII may partly mediate contraction-induced glucose transport (Wright et al., 2004) and increased GLUT4 protein content (Ojuka et al., 2002). However, chronic exposure to Ca^{2+} abrogates AICAR induced AMPK activation and GLUT4 expression in myotubes; AMPK activation is recovered by knockdown of CaMKII (Park et al., 2009a). CaMKII activation influences GLUT4 expression via modification of MEF binding site in the GLUT4 promoter. Caffeine reduces the amount of histone deacetylases in the nucleus, and this is prevented by dantrolene or CaMKII inhibitor (Mukwevho et al., 2008). The translocation of deacetylases allows hyperacetylation of histones

near the MEF2 binding site and increased MEF2A binding to the GLUT4 gene (Mukwevho et al., 2008; Smith et al., 2007; Smith et al., 2008). Ca^{2+} independent CaMKII activity is also involved in muscle adaptation to divergent stimuli. Voluntary wheel running and stretch overload-induced hypertrophy are associated with increased Ca^{2+}-independent activity of CaMKII (Fluck et al., 2000). In turn, CaMKII activity phosphorylates serum response factor, which activates α-actin gene expression. While the evidence for CaMKII involvement in skeletal muscle hypertrophy is limited, there is support for CaMKII contributing to cardiac hypertrophy. The variation in CaMKII isoforms may contribute to the diverse responses (metabolic versus hypertrophy) and differences between tissues.

In contrast to CaMKII, CaMKIV is regulated by upstream kinases and phosphatases. Overexpression of CaMKIV in skeletal muscle is linked to increased mtDNA replication and biogenesis, augmented expression of genes in fatty acid oxidation and oxidative phosphorylation, and reduced susceptibility to fatigue (Wu et al., 2002). Additionally, Zong et al. (2002) showed that CaMKIV expression increased in mice treated with the creatine analog β-guanidinopropionic acid, but not AMPK knockout mice, suggesting that AMPK was important for CaMKIV upregulation. Yet, Akimoto et al. (2004) showed that CaMKIV knockout mice display a skeletal muscle phenotype similar to that of wild type mice, with no changes in fiber type composition or metabolic enzyme content, thus supporting that CaMKIV is dispensable for normal muscle adaptation and function. Further, presence of CaMKIV expression was seriously questioned; CaMKIV is not detectable in human muscle (Rose and Hargreaves, 2003) or rodent skeletal muscle (Akimoto et al., 2004; Chin, 2004).

CaMK kinases (CaMKKs) in skeletal muscle may also integrate Ca^{2+} signaling pathways with metabolism. Although CaMKKα expression in muscle is well documented (Witczak et al.,

2007), the expression of CaMKKβ in muscle is more controversial. While CaMKKα is dependent on Ca^{2+}, CaMKKβ exhibits Ca^{2+}/CaM independent activity. CaMKKs may act upstream of AMPK, therefore connecting muscle contraction with energy producing pathways (Abbott et al., 2009; Jensen et al., 2007a; Jensen et al., 2007b).

Disturbances in calcium metabolism can profoundly affect muscle function and metabolism. Specifically, the skeletal muscle ryanodine receptor (RyR1), a 565 kDa protein, assembles in tetramers to form Ca^{2+} release channels. There are over 300 mutations identified in RyR1, with most mutations being found in three separate regions (Lanner et al., 2010). While the most severe phenotype is associated with mutations in the pore of the channel, the majority of mutations are mapped to inter-domain and inter-subunit interfaces (reviewed by Capes et al., 2011). Two phenotypes, central core disease and malignant hyperthermia (MH), are associated with these mutations. Central core disease, which is more severe, is characterized by muscle weakness, reduced muscle mass, and delayed motor development; proposed mechanisms include constitutively active channels or impaired Ca^{2+} release. In contrast, MH susceptible individuals are typically more sensitive to agents that cause channel opening (reviewed by Mickelson and Louis, 1996). Rapid and increased Ca^{2+} release results in hypermetabolism, elevated body temperature, and muscle rigidity (MacLennan and Phillips, 1992).

A RyR1 mutation in the pig causes MH and has proven a valuable model to understand RyR1 function and Ca^{2+} metabolism. Only one mutation has been documented in porcine RyR1: a single nucleotide polymorphism (T→C) at nucleotide 1843, resulting in an amino acid change from arginine to cysteine ($RyR1^{R615C}$) (Fujii et al., 1991). Ca^{2+} release channels of MH susceptible swine are more sensitive to agents that stimulate channel opening, thus allowing longer open time probability and enhanced Ca^{2+} release (Mickelson et al., 1988; Mickelson et al.,

1989). The high amplitude Ca^{2+} release contributes to greater twitch tension and stimulation of metabolism. Further, enhanced Ca^{2+} release into the cytosol is associated with an increase in peak amplitude of Ca^{2+} in mitochondria in cells transfected with $RyR1^{R615C}$ (Brini et al., 2005). Jiang et al. (2008) further elaborated the molecular mechanism of $RyR1^{R615C}$ by demonstrating that $RyR1^{R615C}$ lowers the threshold for store overload induced Ca^{2+} release, which is the propensity for spontaneous Ca^{2+} release during Ca^{2+} overload in the lumen of the sarcoplasmic reticulum. Porcine $RyR1^{R615C}$ is associated with increased fiber size, decreased capillary density, and rapid metabolism (Essen-Gustavsson et al., 1992). RyR1 mutations do not appear to be linked to hypertrophy in humans; however, the cardiac RyR2 mutation R176Q accelerates development of pressure overload-induced cardiac hypertrophy by calcineurin/NFAT pathway (van Oort et al., 2010).

Changes in cytosolic and mitochondrial Ca^{2+} transients significantly alter metabolism, yet the cellular mechanisms and consequences are not completely understood. Recently, Giulivi et al. (2011) demonstrated that the $RyR1^{R163C}$ mutation causes increases in mitochondrial matrix Ca^{2+}, which contributes to mitochondrial proliferation, augmented ROS production, and lower expression of mitochondrial proteins. Moreover, $RyR1^{R163C}$ muscle exhibits low oxidative phosphorylation, glucose transport, and glycolysis, indicative of a compromised bioenergetic state. Inadequate capacity to maintain homeostasis is evident in MH susceptible human muscle exposed to caffeine or exercise; stimulation causes rapid consumption of ATP, decreases intracellular pH, and extends the period necessary to recover phosphocreatine (Monsieurs et al., 1997; Textor et al., 2003). Another MH-associated mutation, $RyR1^{Y522S}$, causes leaky Ca^{2+} release channels, which increases reactive nitrogen species production and oxidative stress and is associated with swollen, misshaped mitochondria (Durham et al., 2008). Although oxidative

stress is commonly observed in MH mutated muscle, the precise mechanisms and phenotype may be different given that the mutations have disparate effects on Ca^{2+} oscillation. Nonetheless, these mutations provide an interesting model to understand the influence of Ca^{2+} on mitochondrial function and cellular bioenergetics.

MAPK pathways

Mitogen activated protein kinase (MAPK) signaling pathways are conserved across eukaryotes and are important in the regulation of cellular proliferation, differentiation, and development. These pathways are organized in a hierarchy of three kinases, designated as a MAPK kinase kinase, MAPK kinase, and MAPK. The MAPK family includes extracellular regulated kinase (ERK1/2), 38 kDa stress activated protein kinase (p38), c-Jun N-terminal kinase (JNK), and ERK5. ERK5 function is relatively unknown, but it appears to be involved in muscle cell differentiation and fusion (Dinev et al., 2001; Kramer and Goodyear, 2007; Sunadome et al., 2011). The MAPKs coordinate acute and chronic responses to cellular stressors by targeting cytosolic proteins and nuclear transcription factors. MAPKs appear to be regulated by either mechanical or metabolic-related stimuli.

The ERK 1/2 pathway is implicated in muscle fiber type specific hypertrophy and the inhibition of atrophy. Specifically, ERK may mediate IGF-1 induced hypertrophy (Haddad and Adams, 2004; Lantier et al., 2010), as well as β-agonist-induced hypertrophy and fiber type transition (Shi et al., 2007). Hypertrophy may be accomplished via greater activation of ERK2 in fast muscle; fast gastrocnemius possesses greater ERK1/2 activity than soleus, which is due to a greater relative abundance of ERK2 versus ERK1 and a greater proportion of activated ERK2 (Shi et al., 2008). In contrast, attenuation of ERK1/2 induces atrophy by increasing protein

degradation and decreasing protein synthesis, perhaps via indirect effects on Akt (Shi et al., 2009). Curiously, Winter et al. (2011) recently showed that ERK and Akt signaling pathways phosphorylate distinct sites on TSC2, which may have synergistic effects on mTORC1 signaling and protein metabolism. ERK1/2 is also activated in response to Ca^{2+} induced oxidative stress, and may be important in cell survival (Espinosa et al., 2006; Giulivi et al., 2011). ERK1/2 signaling may increase fatty acid uptake and oxidation during low to moderate intensity contraction (Raney and Turcotte, 2006).

On the other hand, p38 MAPK contributes to adaptation to a more oxidative phenotype. There are four isoforms of p38 (α, β, γ, and δ), with p38α and p38γ being the most abundantly expressed in skeletal muscle. Exercise stimulates activation of p38, and p38 signals through activating transcription factor 2 (ATF-2) to increase PGC1α expression (Akimoto et al., 2005). In particular, p38γ is critical for exercise induced metabolic adaptations, including angiogenesis and mitochondrial biogenesis, but is not linked to MHC transformation (Pogozelski et al., 2009). Ca^{2+} signaling may also contribute to activation of p38-induced increases in PGC1α expression (Wright et al., 2007). TNFα and oxidative stress induce general activation of p38, ERK1/2, and JNK, only p38 was associated with increased expression of MAFbx (Li et al., 2005).

The role of JNK in skeletal muscle growth and metabolism is less well defined, but JNK likely is the predominant MAPK involved in cell death signaling. Because ROS themselves are not able to initiate caspases, a cell death signaling pathway such as JNK is needed (reviewed by Powers et al., 2007). Oxidative stress activates apoptosis signal regulating kinase 1, which is a MAPK kinase kinase. Although both JNK and p38 have been implicated in apoptosis, JNK appears to mediate oxidative stress induced decreases in insulin sensitivity. Overexpression of a

dominant negative mutant JNK provides some resistance to oxidative stress, suggesting that JNK may be the pathway that links ROS with cell death (Berdichevsky et al., 2010).

Nuclear factor-κB (NF-κB)

NFκB is an integral point or "central switch" in multiple signaling pathways that coordinate the responses to cellular stress. Not only is NFκB activated by various stimuli, but it also regulates the expression of over 150 target genes, including cytokines, antioxidants, growth factors, and regulators of apoptosis (reviewed by Pahl, 1999). The NFκB /Rel family members include p50, p52, p65, RelB and c-Rel; these proteins form heterodimers or homodimers. Inactive NFκB dimers are sequestered in the cytoplasm by inhibitor of nuclear factor-κBα (IκBα). Phosphorylation of IκBα by IκB kinase (IKK) targets it for degradation, thus releasing the NFκB dimers and allowing their translocation to the nucleus for NFκB mediated gene transcription.

The physiological response to NFκB activation appears dependent on duration of the stress stimulus. Chronic activation of NFκB is associated with pathological conditions, including muscle wasting and insulin resistance, whereas acute activation of NFκB by exercise may have beneficial effects. Atrophy induced by forced expression of MAPK phosphatase increases NFκB activity to a greater extent in slow soleus muscle, whereas the ubiquitin proteasome plays a larger role in proteolysis in gastrocnemius (Shi et al., 2009). Chronic activation of NFκB caused by overexpression of IKK in transgenic mice instigates profound muscle protein breakdown mediated by MuRF-1, ultimately resulting in a cachetic like phenotype (Cai et al., 2004). Moreover, NFκB mediates the decrease of PGC1α in skeletal muscle cells exposed to palmitate (Coll et al., 2006) as well as the reduced mitochondrial protein content and content and MHC I

mRNA caused by chronic TNFα treatment (Remels et al., 2010). Curiously, ERK may modulate palmitate-induced activation of NFκB, and, in turn, ERK activation can be blunted by AMPK (Green et al., 2011). However, the insulin resistant phenotype persists even when NFκB signaling was prevented, suggesting that development of insulin resistance may not be dependent on NFκB inflammatory signaling. Thus, NFκB seems to play a larger role in proteolysis and metabolism in slow muscle, and may contribute to perturbed metabolism and pathological physiology by downregulating genes crucial to oxidative capacity.

In contrast, acute or intermittent increases in NFκB may help instigate adaptations that are physiologically beneficial. Although ROS are generally considered harmful to the cell, small or transient increases may be useful for activating signaling pathways that increase expression of antioxidants and other defenses, thus providing a protective mechanism against additional insults. Exercise increases phosphorylation of IKK during exercise, which is paralleled by IκBα phosphorylation, and stimulation of NFκB activity (Ho et al., 2005; Ji et al., 2004). In fact, acute exercise is associated with NFκB binding to the MnSOD gene, which is followed by an increase in MnSOD mRNA and protein (Hollander et al., 2001). Exercise-induced enhancement of NFκB activity may be partly mediated by MAPKs (Ho et al., 2005; Kefaloyianni et al., 2006) or redox status (Ji et al., 2004).

Antagonism between AMPK/PGC1α and Akt/mTOR

Akt and AMPK are critical modulators of growth and energy metabolism, respectively. Akt mediates changes in protein synthesis and degradation thus impacting cell growth, whereas the energy sensor AMPK promotes pathways that increase glucose transport, mitochondrial biogenesis, and fatty acid oxidation. While Akt modulates energy consuming pathways, AMPK

is involved in conserving energy and promoting ATP production. Due to their contrasting roles in regulating cell phenotype and homeostasis, there is antagonism between Akt and AMPK signaling pathways. These signaling pathways play an important role in determining the balance between muscle cell hypertrophy and oxidative capacity.

Concurrent with its role in increasing energy production, AMPK also blocks energy consuming pathways. AMPK activates TSC2, which is dominant over phosphorylation by Akt, and leads to inactivation of mTOR (Inoki et al., 2003). Additionally, AMPK attenuates the growth signaling response downstream of mTOR by decreasing 4E-BP1 and p70S6K1 phosphorylation, thereby preventing initiation and translation (Thomson et al., 2008); and increasing phosphorylation of eEF2, which inhibits its binding to ribosomes (Mounier et al., 2009). In contrast, AMPKα1/α2 knockout mice possess fibers with greater cross sectional area and higher levels of p70S6K phosphorylation (Lantier et al., 2010). Furthermore, overload-induced muscle hypertrophy is accelerated in AMPKα1 knockout mice, evidencing a role for AMPK in limiting skeletal muscle hypertrophy (Mounier et al., 2009).

An AMPK-Akt "switch" is proposed to be a mechanism that partially mediates specific adaptations to endurance and resistance exercise (Atherton et al., 2005). In rodent muscle, low frequency stimulation increases AMPK phosphorylation and prevents protein translation initiation and elongation, whereas high frequency stimulation does not affect AMPK phosphorylation, but activates Akt/mTOR dependent protein synthesis (Atherton et al., 2005). However, when endurance trained human subjects undergo resistance exercise, markers of protein synthesis are increased; and, when strength-trained subjects perform endurance exercise, AMPK activation is increased (Coffey et al., 2006). Prior training also attenuates exercise-specific signaling response (Coffey et al., 2006). Together, this suggests that AMPK or Akt may

be preferentially activated by a specific signal, and continued single mode training promotes adaptation that weakens that response. However, muscle maintains plasticity to activate pathways associated with the contrasting type of exercise. Although muscle maintains plasticity to adapt to a new impetus, this still does not clarify how training or prolonged exposure to both types of stimuli (ie, endurance and strength), regulates these signaling pathways to modulate muscle phenotype.

In addition, AMPK has been implicated in protein degradation pathways. AMPK activates FoxO3, but only when FoxO3 is already in the nucleus (Greer et al., 2007), and may increase expression of the FoxO3 targets, MAFbx and MuRF-1 following AICAR treatment (Krawiec et al., 2007; Nakashima and Yakabe, 2007). FoxO3 is a proposed target of both Akt and AMPK; while Akt promotes FoxO3 translocation from the nucleus and thus inhibits its activity, AMPK appears to activate FoxO3. Thus, during situations of low nutrient availability and low cellular energy, FoxO3 activity would likely be maximized by the combined effects of high AMPK activity and low Akt activity. Although AMPK appears to activate E3 ligases, Viana et al. (2008) showed that AMPK inhibits proteasome activity; AMPK may inhibit this process because it is ATP-dependent.

In contrast, autophagy is not energy dependent and is divergently regulated by AMPK and mTORC1. A complex of UNC-51-like kinase-1 (ULK1), autophagy related gene (Atg13), and focal adhesion kinase family interacting protein of 200 kD (FIP200) is essential for autophagy, with ULK1 being a critical initiator that localizes to the autophagosome. AMPK and mTORC1 have opposing regulatory effects on ULK1 via phosphorylation at different regulatory sites. In the presence of growth factors and abundant nutrients, mTORC1 associates with ULK1/Atg13/FIP200 and phosphorylates ULK1, which inhibits ULK1 activity and autophagy

(Ganley et al., 2009; Hosokawa et al., 2009; Jung et al., 2009). There is some evidence suggesting AMPK associates with ULK1 and that basal AMPK activity may contribute to ULK1 inhibition (Shang et al., 2011). Upon starvation, ULK1 is dephosphorylated at mTOR dependent phosphorylation sites, and subsequently phosphorylated and activated by AMPK (Kim et al., 2011). AMPK activation may also indirectly contribute to autophagy by inducing phosphorylation of raptor, which inactivates mTORC1, and releases its inhibition of ULK1 (Lee et al., 2010). More importantly, AMPK appears to be necessary for mitochondrial homeostasis; loss of AMPK or ULK1 leads to abnormal accumulation of autophagy adaptor protein p62 and defective mitophagy, which adversely affects mitochondrial morphology and function (Egan et al., 2011).

AMPK activation seems to enhance protein degradation, yet its downstream target PGC1α is positively associated with maintenance of muscle protein. Sandri et al. (2006) demonstrated that in mice overexpressing PGC1α, denervation and fasting induce a smaller decrease in fiber size and smaller induction of atrogin-1 and MuRF-1 than in control mice. Similarly, overexpression of PGC1α improves muscle energy status (ATP) by enhancing oxidative capacity, and thus prevents muscle apoptosis, autophagy, and proteasome degradation in mouse models of mitochondrial myopathy and metabolic disease (Wenz et al., 2008; Wenz et al., 2009). PGC1α may prevent protein degradation in these disease states because the additional oxidative capacity protects against mitochondrial dysfunction, which decreases oxidative stress and attenuates activation of inflammatory or apoptotic pathways that increase proteolysis.

Summary

Mitochondrial oxidative capacity enhances ability of muscle to cope with energetic stress and thus affords protection against metabolic disease and age-related decline in muscle function. Increasing the quantity of mitochondria augments ATP producing capacity whereas improving quality of mitochondria is associated with increased basal oxidation rates and protection against oxidative stress and mitochondrial dysfunction. Yet, improvements in muscle oxidative capacity are thought to limit muscle hypertrophy. Limiting cell size may be an important aspect that optimizes oxygen delivery and diffusion. Promoting oxidative capacity and growth concurrently could sacrifice aspects of mitochondrial function. Furthermore, there are inherent differences in turnover of mitochondrial and myofibrillar protein. Several signaling networks contribute to mitochondrial biogenesis and cell growth; specifically, the AMPK/PGC1α and Akt/mTOR pathways may have antagonistic effects. Using an animal model that exhibits both increased mitochondrial biogenesis and fiber hypertrophy may enhance our understanding of the control of muscle phenotype.

References

Abbott, M. J., A. M. Edelman, and L. P. Turcotte. 2009. CaMKK is an upstream signal of AMP-activated protein kinase in regulation of substrate metabolism in contracting skeletal muscle. Am. J. Physiol. Regul. Integr. Comp. Physiol. 297: R1724-1732.

Adams, J., Z. P. Chen, B. J. Van Denderen, C. J. Morton, M. W. Parker, L. A. Witters, D. Stapleton, and B. E. Kemp. 2004. Intrasteric control of AMPK via the γ1 subunit AMP allosteric regulatory site. Protein Sci. 13: 155-165.

Adhihetty, P. J., V. Ljubicic, K. J. Menzies, and D. A. Hood. 2005. Differential susceptibility of subsarcolemmal and intermyofibrillar mitochondria to apoptotic stimuli. Am. J. Physiol. Cell Physiol. 289: C994-C1001.

Akimoto, T., S. C. Pohnert, P. Li, M. Zhang, C. Gumbs, P. B. Rosenberg, R. S. Williams, and Z. Yan. 2005. Exercise stimulates PGC-1α transcription in skeletal muscle through activation of the p38 MAPK pathway. J. Biol. Chem. 280: 19587-19593.

Akimoto, T., T. J. Ribar, R. S. Williams, and Z. Yan. 2004. Skeletal muscle adaptation in response to voluntary running in Ca^{2+}/calmodulin-dependent protein kinase IV-deficient mice. Am. J. Physiol. Cell Physiol. 287: C1311-1319.

Alexeyev, M. F., S. P. Ledoux, and G. L. Wilson. 2004. Mitochondrial DNA and aging. Clin. Sci. 107: 355-364.

Anderson, E. J., and P. D. Neufer. 2006. Type II skeletal myofibers possess unique properties that potentiate mitochondrial H_2O_2 generation. Am. J. Physiol. Cell Physiol. 290: C844-851.

Atherton, P. J., J. Babraj, K. Smith, J. Singh, M. J. Rennie, and H. Wackerhage. 2005. Selective activation of AMPK-PGC-1α or PKB-TSC2-mTOR signaling can explain specific adaptive responses to endurance or resistance training-like electrical muscle stimulation. FASEB J. 19: 786-788.

Bai, R. K., C. L. Perng, C. H. Hsu, and L. J. Wong. 2004. Quantitative PCR analysis of mitochondrial DNA content in patients with mitochondrial disease. Ann. N. Y. Acad. Sci. 1011: 304-309.

Barany, M. 1967. ATPase activity of myosin correlated with speed of muscle shortening. J. Gen. Physiol. 50: Suppl:197-218.

Barja, G., and A. Herrero. 2000. Oxidative damage to mitochondrial DNA is inversely related to maximum life span in the heart and brain of mammals. FASEB J. 14: 312-318.

Barnes, B. R., S. Glund, Y. C. Long, G. Hjalm, L. Andersson, and J. R. Zierath. 2005a. 5'-AMP-activated protein kinase regulates skeletal muscle glycogen content and ergogenics. FASEB J. 19: 773-779.

Barnes, B. R., Y. C. Long, T. L. Steiler, Y. Leng, D. Galuska, J. F. Wojtaszewski, L. Andersson, and J. R. Zierath. 2005b. Changes in exercise-induced gene expression in 5'-AMP-activated protein kinase γ3-null and γ3 R225Q transgenic mice. Diabetes 54: 3484-3489.

Barnes, B. R., S. Marklund, T. L. Steiler, M. Walter, G. Hjalm, V. Amarger, M. Mahlapuu, Y. Leng, C. Johansson, D. Galuska, K. Lindgren, M. Abrink, D. Stapleton, J. R. Zierath, and L. Andersson. 2004. The 5'-AMP-activated protein kinase γ3 isoform has a key role in carbohydrate and lipid metabolism in glycolytic skeletal muscle. J. Biol. Chem. 279: 38441-38447.

Bechet, D., A. Tassa, D. Taillandier, L. Combaret, and D. Attaix. 2005. Lysosomal proteolysis in skeletal muscle. Int. J. Biochem. Cell Biol. 37: 2098-2114.

Befroy, D. E., K. F. Petersen, S. Dufour, G. F. Mason, D. L. Rothman, and G. I. Shulman. 2008. Increased substrate oxidation and mitochondrial uncoupling in skeletal muscle of endurance-trained individuals. Proc. Natl. Acad. Sci. USA 105: 16701-16706.

Bender, T., I. Lewrenz, S. Franken, C. Baitzel, and W. Voos. 2011. Mitochondrial enzymes are protected from stress-induced aggregation by mitochondrial chaperones and the Pim1/LON protease. Mol. Biol. Cell 22: 541-554.

Berdichevsky, A., L. Guarente, and A. Bose. 2010. Acute oxidative stress can reverse insulin resistance by inactivation of cytoplasmic JNK. J. Biol. Chem. 285: 21581-21589.

Birk, J. B., and J. F. Wojtaszewski. 2006. Predominant α2/β2/γ3 AMPK activation during exercise in human skeletal muscle. J. Physiol. 577: 1021-1032.

Bodine, S. C., T. N. Stitt, M. Gonzalez, W. O. Kline, G. L. Stover, R. Bauerlein, E. Zlotchenko, A. Scrimgeour, J. C. Lawrence, D. J. Glass, and G. D. Yancopoulos. 2001. Akt/mTOR pathway is a crucial regulator of skeletal muscle hypertrophy and can prevent muscle atrophy in vivo. Nat. Cell Biol. 3: 1014-1019.

Brand, M. D., and D. G. Nicholls. 2011. Assessing mitochondrial dysfunction in cells. Biochem. J. 435: 297-312.

Brini, M., S. Manni, N. Pierobon, G. G. Du, P. Sharma, D. H. MacLennan, and E. Carafoli. 2005. Ca^{2+} signaling in HEK-293 and skeletal muscle cells expressing recombinant ryanodine receptors harboring malignant hyperthermia and central core disease mutations. J. Biol. Chem. 280: 15380-15389.

Brooks, S. V., A. Vasilaki, L. M. Larkin, A. McArdle, and M. J. Jackson. 2008. Repeated bouts of aerobic exercise lead to reductions in skeletal muscle free radical generation and nuclear factor κB activation. J. Physiol. 586: 3979-3990.

Buller, A. J., J. C. Eccles, and R. M. Eccles. 1960. Interactions between motoneurones and muscles in respect of the characteristic speeds of their responses. J. Physiol. 150: 417-439.

Cai, D., J. D. Frantz, N. E. Tawa, Jr., P. A. Melendez, B. C. Oh, H. G. Lidov, P. O. Hasselgren, W. R. Frontera, J. Lee, D. J. Glass, and S. E. Shoelson. 2004. IKKβ/NF-κB activation causes severe muscle wasting in mice. Cell 119: 285-298.

Calabria, E., S. Ciciliot, I. Moretti, M. Garcia, A. Picard, K. A. Dyar, G. Pallafacchina, J. Tothova, S. Schiaffino, and M. Murgia. 2009. NFAT isoforms control activity-dependent muscle fiber type specification. Proc. Natl. Acad. Sci. USA 106: 13335-13340.

Canto, C., Z. Gerhart-Hines, J. N. Feige, M. Lagouge, L. Noriega, J. C. Milne, P. J. Elliott, P. Puigserver, and J. Auwerx. 2009. AMPK regulates energy expenditure by modulating NAD+ metabolism and SIRT1 activity. Nature 458: 1056-1060.

Capes, E. M., R. Loaiza, and H. H. Valdivia. 2011. Ryanodine receptors. Skelet. Muscle 1: 18.

Chance, B., and G. R. Williams. 1955. Respiratory enzymes in oxidative phosphorylation J. Biol. Chem. 217: 383-394.

Chen, H., and D. C. Chan. 2009. Mitochondrial dynamics--fusion, fission, movement, and mitophagy--in neurodegenerative diseases. Hum. Mol. Genet. 18: R169-176.

Chen, H., A. Chomyn, and D. C. Chan. 2005. Disruption of fusion results in mitochondrial heterogeneity and dysfunction. J. Biol. Chem. 280: 26185-26192.

Chen, H., S. A. Detmer, A. J. Ewald, E. E. Griffin, S. E. Fraser, and D. C. Chan. 2003. Mitofusins Mfn1 and Mfn2 coordinately regulate mitochondrial fusion and are essential for embryonic development. J. Cell Biol. 160: 189-200.

Chen, H., M. Vermulst, Y. E. Wang, A. Chomyn, T. A. Prolla, J. M. McCaffery, and D. C. Chan. 2010. Mitochondrial fusion is required for mtDNA stability in skeletal muscle and tolerance of mtDNA mutations. Cell 141: 280-289.

Chin, E. R. 2004. The role of calcium and calcium/calmodulin-dependent kinases in skeletal muscle plasticity and mitochondrial biogenesis. Proc. Nutr. Soc. 63: 279-286.

Chin, E. R., E. N. Olson, J. A. Richardson, Q. Yang, C. Humphries, J. M. Shelton, H. Wu, W. Zhu, R. Bassel-Duby, and R. S. Williams. 1998. A calcineurin-dependent transcriptional pathway controls skeletal muscle fiber type. Genes Dev. 12: 2499-2509.

Cipolat, S., O. Martins de Brito, B. Dal Zilio, and L. Scorrano. 2004. OPA1 requires mitofusin 1 to promote mitochondrial fusion. Proc. Natl. Acad. Sci. USA 101: 15927-15932.

Coffey, V. G., Z. Zhong, A. Shield, B. J. Canny, A. V. Chibalin, J. R. Zierath, and J. A. Hawley. 2006. Early signaling responses to divergent exercise stimuli in skeletal muscle from well-trained humans. FASEB J. 20: 190-192.

Cogswell, A. M., R. J. Stevens, and D. A. Hood. 1993. Properties of skeletal muscle mitochondria isolated from subsarcolemmal and intermyofibrillar regions. Am. J. Physiol. 264: C383-389.

Coll, T., M. Jove, R. Rodriguez-Calvo, E. Eyre, X. Palomer, R. M. Sanchez, M. Merlos, J. C. Laguna, and M. Vazquez-Carrera. 2006. Palmitate-mediated downregulation of peroxisome proliferator-activated receptor-gamma coactivator 1alpha in skeletal muscle cells involves MEK1/2 and nuclear factor-kappaB activation. Diabetes 55: 2779-2787.

Cortopassi, G. A., D. Shibata, N. W. Soong, and N. Arnheim. 1992. A pattern of accumulation of a somatic deletion of mitochondrial DNA in aging human tissues. Proc. Natl. Acad. Sci. USA 89: 7370-7374.

Costford, S. R., N. Kavaslar, N. Ahituv, S. N. Chaudhry, W. S. Schackwitz, R. Dent, L. A. Pennacchio, R. McPherson, and M. E. Harper. 2007. Gain-of-function R225W mutation in human AMPKγ3 causing increased glycogen and decreased triglyceride in skeletal muscle. PLoS ONE 2: e903.

das Neves, R. P., N. S. Jones, L. Andreu, R. Gupta, T. Enver, and F. J. Iborra. 2010. Connecting variability in global transcription rate to mitochondrial variability. PLoS Biol. 8: e1000560.

Dinev, D., B. W. Jordan, B. Neufeld, J. D. Lee, D. Lindemann, U. R. Rapp, and S. Ludwig. 2001. Extracellular signal regulated kinase 5 (ERK5) is required for the differentiation of muscle cells. EMBO Rep. 2: 829-834.

Dufour, E., A. Ouali, A. Obled, C. Deval, and C. Valin. 1989. Lysosomal proteinase-sensitive regions in fast and slow skeletal muscle myosins. Biochimie 71: 625-632.

Durham, W. J., P. Aracena-Parks, C. Long, A. E. Rossi, S. A. Goonasekera, S. Boncompagni, D. L. Galvan, C. P. Gilman, M. R. Baker, N. Shirokova, F. Protasi, R. Dirksen, and S. L. Hamilton. 2008. RyR1 S-nitrosylation underlies environmental heat stroke and sudden death in Y522S RyR1 knockin mice. Cell 133: 53-65.

Egan, D. F., D. B. Shackelford, M. M. Mihaylova, S. Gelino, R. A. Kohnz, W. Mair, D. S. Vasquez, A. Joshi, D. M. Gwinn, R. Taylor, J. M. Asara, J. Fitzpatrick, A. Dillin, B. Viollet, M. Kundu, M. Hansen, and R. J. Shaw. 2011. Phosphorylation of ULK1 (hATG1) by AMP-activated protein kinase connects energy sensing to mitophagy. Science 331: 456-461.

Espinosa, A., A. Leiva, M. Pena, M. Muller, A. Debandi, C. Hidalgo, M. A. Carrasco, and E. Jaimovich. 2006. Myotube depolarization generates reactive oxygen species through

NAD(P)H oxidase; ROS-elicited Ca^{2+} stimulates ERK, CREB, early genes. J. Cell. Physiol. 209: 379-388.
Essen-Gustavsson, B., K. Karlstrom, and K. Lundstrom. 1992. Muscle fibre characteristics and metabolic response at slaughter in pigs of different halothane genotypes and their relation to meat quality. Meat Sci. 31: 1-11.
Fan, M., J. Rhee, J. St-Pierre, C. Handschin, P. Puigserver, J. Lin, S. Jaeger, H. Erdjument-Bromage, P. Tempst, and B. M. Spiegelman. 2004. Suppression of mitochondrial respiration through recruitment of p160 myb binding protein to PGC-1α: modulation by p38 MAPK. Genes Dev. 18: 278-289.
Fernandez-Silva, P., J. A. Enriquez, and J. Montoya. 2003. Replication and transcription of mammalian mitochondrial DNA. Exp. Physiol. 88: 41-56.
Fluck, M., M. N. Waxham, M. T. Hamilton, and F. W. Booth. 2000. Skeletal muscle Ca^{2+}-independent kinase activity increases during either hypertrophy or running. J. Appl. Physiol. 88: 352-358.
Fujii, J., K. Otsu, F. Zorzato, S. D. Leon, V. K. Khanna, J. E. Weiler, P. J. O'Brien, and D. H. MacLennan. 1991. Identification of a mutation in porcine ryanodine receptor associated with malignant hyperthermia. Science 253: 448-451.
Furuno, K., M. N. Goodman, and A. L. Goldberg. 1990. Role of different proteolytic systems in the degradation of muscle proteins during denervation atrophy. J. Biol. Chem. 265: 8550-8557.
Ganley, I. G., H. Lam du, J. Wang, X. Ding, S. Chen, and X. Jiang. 2009. ULK1.ATG13.FIP200 complex mediates mTOR signaling and is essential for autophagy. J. Biol. Chem. 284: 12297-12305.
Garcia-Roves, P. M., M. E. Osler, M. H. Holmstrom, and J. R. Zierath. 2008. Gain-of-function R225Q mutation in AMP-activated protein kinase γ3 subunit increases mitochondrial biogenesis in glycolytic skeletal muscle. J. Biol. Chem. 283: 35724-35734.
Gibson, M. C., and E. Schultz. 1983. Age-related differences in absolute numbers of skeletal muscle satellite cells. Muscle Nerve 6: 574-580.
Giulivi, C., C. Ross-Inta, A. Omanska-Klusek, E. Napoli, D. Sakaguchi, G. Barrientos, P. D. Allen, and I. N. Pessah. 2011. Basal bioenergetic abnormalities in skeletal muscle from ryanodine receptor malignant hyperthermia susceptible R163C knock-in mice. J. Biol. Chem. 286: 99-113.
Glancy, B., and R. S. Balaban. 2011. Protein composition and function of red and white skeletal muscle mitochondria. Am. J. Physiol. Cell Physiol. 300: C1280-1290.
Goll, D. E., G. Neti, S. W. Mares, and V. F. Thompson. 2008. Myofibrillar protein turnover: the proteasome and the calpains. J. Anim. Sci. 86: E19-35.
Goodman, C. A., D. M. Mabrey, J. W. Frey, M. H. Miu, E. K. Schmidt, P. Pierre, and T. A. Hornberger. 2011. Novel insights into the regulation of skeletal muscle protein synthesis as revealed by a new nonradioactive in vivo technique. FASEB J. 25: 1028-1039.
Green, C. J., K. Macrae, S. Fogarty, D. G. Hardie, K. Sakamoto, and H. S. Hundal. 2011. Counter-modulation of fatty acid-induced pro-inflammatory nuclear factor κB signalling in rat skeletal muscle cells by AMP-activated protein kinase. Biochem. J. 435: 463-474.
Greer, E. L., P. R. Oskoui, M. R. Banko, J. M. Maniar, M. P. Gygi, S. P. Gygi, and A. Brunet. 2007. The energy sensor AMP-activated protein kinase directly regulates the mammalian FOXO3 transcription factor. J. Biol. Chem. 282: 30107-30119.

Habets, P. E., D. Franco, J. M. Ruijter, A. J. Sargeant, J. A. Pereira, and A. F. Moorman. 1999. RNA content differs in slow and fast muscle fibers: implications for interpretation of changes in muscle gene expression. J. Histochem. Cytochem. 47: 995-1004.

Haddad, F., and G. R. Adams. 2004. Inhibition of MAP/ERK kinase prevents IGF-I-induced hypertrophy in rat muscles. J. Appl. Physiol. 96: 203-210.

Hall, Z. W., and E. Ralston. 1989. Nuclear domains in muscle cells. Cell 59: 771-772.

Handschin, C., J. Rhee, J. Lin, P. T. Tarr, and B. M. Spiegelman. 2003. An autoregulatory loop controls peroxisome proliferator-activated receptor gamma coactivator 1α expression in muscle. Proc. Natl. Acad. Sci. USA 100: 7111-7116.

Hawley, S., J. Boudeau, J. Reid, K. Mustard, L. Udd, T. Makela, D. Alessi, and D. G. Hardie. 2003. Complexes between the LKB1 tumor suppressor, STRADα/β and MO25α/β are upstream kinases in the AMP-activated protein kinase cascade. J. Biol. 2: 28.

Hawley, S. A., D. A. Pan, K. J. Mustard, L. Ross, J. Bain, A. M. Edelman, B. G. Frenguelli, and D. G. Hardie. 2005. Calmodulin-dependent protein kinase kinase-β is an alternative upstream kinase for AMP-activated protein kinase. Cell Metab. 2: 9-19.

Hawley, S. A., F. A. Ross, C. Chevtzoff, K. A. Green, A. Evans, S. Fogarty, M. C. Towler, L. J. Brown, O. A. Ogunbayo, A. M. Evans, and D. G. Hardie. 2010. Use of cells expressing γ subunit variants to identify diverse mechanisms of AMPK activation. Cell Metab. 11: 554-565.

Heizmann, C. W., M. W. Berchtold, and A. M. Rowlerson. 1982. Correlation of parvalbumin concentration with relaxation speed in mammalian muscles. Proc. Natl. Acad. Sci. USA 79: 7243-7247.

Hickson, R. C. 1980. Interference of strength development by simultaneously training for strength and endurance. Eur. J. Appl. Physiol. Occup. Physiol. 45: 255-263.

Hirner, S., C. Krohne, A. Schuster, S. Hoffmann, S. Witt, R. Erber, C. Sticht, A. Gasch, S. Labeit, and D. Labeit. 2008. MuRF1-dependent regulation of systemic carbohydrate metabolism as revealed from transgenic mouse studies. J. Mol. Biol. 379: 666-677.

Ho, R. C., M. F. Hirshman, Y. Li, D. Cai, J. R. Farmer, W. G. Aschenbach, C. A. Witczak, S. E. Shoelson, and L. J. Goodyear. 2005. Regulation of IκB kinase and NF-κB in contracting adult rat skeletal muscle. Am. J. Physiol. Cell Physiol. 289: C794-801.

Hollander, J., R. Fiebig, M. Gore, T. Ookawara, H. Ohno, and L. L. Ji. 2001. Superoxide dismutase gene expression is activated by a single bout of exercise in rat skeletal muscle. Pflugers Arch. 442: 426-434.

Holloszy, J. O. 2008. Regulation by exercise of skeletal muscle content of mitochondria and GLUT4. J. Physiol. Pharmacol. 59 Suppl 7: 5-18.

Holmes, B. F., E. J. Kurth-Kraczek, and W. W. Winder. 1999. Chronic activation of 5'-AMP-activated protein kinase increases GLUT-4, hexokinase, and glycogen in muscle. J. Appl. Physiol. 87: 1990-1995.

Hosokawa, N., T. Hara, T. Kaizuka, C. Kishi, A. Takamura, Y. Miura, S. Iemura, T. Natsume, K. Takehana, N. Yamada, J. L. Guan, N. Oshiro, and N. Mizushima. 2009. Nutrient-dependent mTORC1 association with the ULK1-Atg13-FIP200 complex required for autophagy. Mol. Biol. Cell 20: 1981-1991.

Hudmon, A., and H. Schulman. 2002. Structure-function of the multifunctional Ca^{2+}/calmodulin-dependent protein kinase II. Biochem. J. 364: 593-611.

Inoki, K., T. Zhu, and K. L. Guan. 2003. TSC2 mediates cellular energy response to control cell growth and survival. Cell 115: 577-590.

Irrcher, I., V. Ljubicic, and D. A. Hood. 2009. Interactions between ROS and AMP kinase activity in the regulation of PGC-1α transcription in skeletal muscle cells. Am. J. Physiol. Cell Physiol. 296: C116-123.

Irrcher, I., V. Ljubicic, A. F. Kirwan, and D. A. Hood. 2008. AMP-activated protein kinase-regulated activation of the PGC-1α promoter in skeletal muscle cells. PLoS ONE 3: e3614.

Jackman, M. R., and W. T. Willis. 1996. Characteristics of mitochondria isolated from type I and type IIb skeletal muscle. Am. J. Physiol. 270: C673-678.

Jager, S., C. Handschin, J. St.-Pierre, and B. M. Spiegelman. 2007. AMP-activated protein kinase (AMPK) action in skeletal muscle via direct phosphorylation of PGC-1α. Proc. Natl. Acad. Sci. USA 104: 12017-12022.

Jaleel, A., K. R. Short, Y. W. Asmann, K. A. Klaus, D. M. Morse, G. C. Ford, and K. S. Nair. 2008. In vivo measurement of synthesis rate of individual skeletal muscle mitochondrial proteins. Am. J. Physiol. Endocrinol. Metab. 295: E1255-1268.

Jensen, T. E., A. J. Rose, Y. Hellsten, J. F. Wojtaszewski, and E. A. Richter. 2007a. Caffeine-induced Ca^{2+} release increases AMPK-dependent glucose uptake in rodent soleus muscle. Am. J. Physiol. Endocrinol. Metab. 293: E286-292.

Jensen, T. E., A. J. Rose, S. B. Jorgensen, N. Brandt, P. Schjerling, J. F. Wojtaszewski, and E. A. Richter. 2007b. Possible CaMKK-dependent regulation of AMPK phosphorylation and glucose uptake at the onset of mild tetanic skeletal muscle contraction. Am. J. Physiol. Endocrinol. Metab. 292: E1308-1317.

Ji, L. L., M. C. Gomez-Cabrera, N. Steinhafel, and J. Vina. 2004. Acute exercise activates nuclear factor (NF)-κB signaling pathway in rat skeletal muscle. FASEB J. 18: 1499-1506.

Jiang, D., W. Chen, J. Xiao, R. Wang, H. Kong, P. P. Jones, L. Zhang, B. Fruen, and S. R. Chen. 2008. Reduced threshold for luminal Ca^{2+} activation of RyR1 underlies a causal mechanism of porcine malignant hyperthermia. J. Biol. Chem. 283: 20813-20820.

Jiang, L. Q., P. M. Garcia-Roves, T. de Castro Barbosa, and J. R. Zierath. 2010. Constitutively active calcineurin in skeletal muscle increases endurance performance and mitochondrial respiratory capacity. Am. J. Physiol. Endocrinol. Metab. 298: E8-E16.

Jorgensen, S. B., J. N. Nielsen, J. B. Birk, G. S. Olsen, B. Viollet, F. Andreelli, P. Schjerling, S. Vaulont, D. G. Hardie, and B. F. Hansen. 2004a. The α2-5'AMP-activated protein kinase is a site 2 glycogen synthase kinase in skeletal muscle and is responsive to glucose loading. Diabetes 53: 3074-3081.

Jorgensen, S. B., B. Viollet, F. Andreelli, C. Frosig, J. B. Birk, P. Schjerling, S. Vaulont, E. A. Richter, and J. F. P. Wojtaszewski. 2004b. Knockout of the α2 but not α1 5'-AMP-activated protein kinase isoform abolishes 5-aminoimidazole-4-carboxamide-1-β-4-ribofuranoside but not contraction-induced glucose uptake in skeletal muscle. J. Biol. Chem. 279: 1070-1079.

Jung, C. H., C. B. Jun, S. H. Ro, Y. M. Kim, N. M. Otto, J. Cao, M. Kundu, and D. H. Kim. 2009. ULK-Atg13-FIP200 complexes mediate mTOR signaling to the autophagy machinery. Mol. Biol. Cell 20: 1992-2003.

Kefaloyianni, E., C. Gaitanaki, and I. Beis. 2006. ERK1/2 and p38-MAPK signalling pathways, through MSK1, are involved in NF-κB transactivation during oxidative stress in skeletal myoblasts. Cell. Signal. 18: 2238-2251.

Kim, J., M. Kundu, B. Viollet, and K. L. Guan. 2011. AMPK and mTOR regulate autophagy through direct phosphorylation of Ulk1. Nat. Cell Biol. 13: 132-141.
Kimura, H., K. Sugaya, and P. R. Cook. 2002. The transcription cycle of RNA polymerase II in living cells. J. Cell Biol. 159: 777-782.
Koyama, S., S. Hata, C. C. Witt, Y. Ono, S. Lerche, K. Ojima, T. Chiba, N. Doi, F. Kitamura, K. Tanaka, K. Abe, S. H. Witt, V. Rybin, A. Gasch, T. Franz, S. Labeit, and H. Sorimachi. 2008. Muscle RING-finger protein-1 (MuRF1) as a connector of muscle energy metabolism and protein synthesis. J. Mol. Biol. 376: 1224-1236.
Kramer, H. F., and L. J. Goodyear. 2007. Exercise, MAPK, and NF-kappaB signaling in skeletal muscle. J. Appl. Physiol. 103: 388-395.
Krawiec, B. J., G. J. Nystrom, R. A. Frost, L. S. Jefferson, and C. H. Lang. 2007. AMP-activated protein kinase agonists increase mRNA content of the muscle-specific ubiquitin ligases MAFbx and MuRF1 in C2C12 cells. Am. J. Physiol. Endocrinol. Metab. 292: E1555-1567.
Krieger, D. A., C. A. Tate, J. McMillin-Wood, and F. W. Booth. 1980. Populations of rat skeletal muscle mitochondria after exercise and immobilization. J. Appl. Physiol. 48: 23-28.
Kurth-Kraczek, E. J., M. F. Hirshman, L. J. Goodyear, and W. W. Winder. 1999. 5' AMP-activated protein kinase activation causes GLUT4 translocation in skeletal muscle. Diabetes 48: 1667-1671.
Kuznetsov, A. 2007. Structural organization and dynamics of mitochondria in the cells in vivo. In: V. Saks (ed.) Molecular Systems Bioenergetics. Wiley, Weinheim.
Kuznetsov, A. V., J. Troppmair, R. Sucher, M. Hermann, V. Saks, and R. Margreiter. 2006. Mitochondrial subpopulations and heterogeneity revealed by confocal imaging: possible physiological role? Biochim. Biophys. Acta 1757: 686-691.
Landing, B. H., L. G. Dixon, and T. R. Wells. 1974. Studies on isolated human skeletal muscle fibers, including a proposed pattern of nuclear distribution and a concept of nuclear territories. Hum. Pathol. 5: 441-461.
Lange, S., F. Xiang, A. Yakovenko, A. Vihola, P. Hackman, E. Rostkova, J. Kristensen, B. Brandmeier, G. Franzen, B. Hedberg, L. G. Gunnarsson, S. M. Hughes, S. Marchand, T. Sejersen, I. Richard, L. Edstrom, E. Ehler, B. Udd, and M. Gautel. 2005. The kinase domain of titin controls muscle gene expression and protein turnover. Science 308: 1599-1603.
Lanner, J. T., D. K. Georgiou, A. D. Joshi, and S. L. Hamilton. 2010. Ryanodine receptors: structure, expression, molecular details, and function in calcium release. Cold Spring Harb Perspect Biol 2: a003996.
Lantier, L., R. Mounier, J. Leclerc, M. Pende, M. Foretz, and B. Viollet. 2010. Coordinated maintenance of muscle cell size control by AMP-activated protein kinase. FASEB J. 24: 3555-3561.
Leary, S. C., C. N. Lyons, A. G. Rosenberger, J. S. Ballantyne, J. Stillman, and C. D. Moyes. 2003. Fiber-type differences in muscle mitochondrial profiles. Am. J. Physiol. Regul. Integr. Comp. Physiol. 285: R817-826.
Lebret, B., P. Le Roy, G. Monin, L. Lefaucheur, J. C. Caritez, A. Talmant, J. M. Elsen, and P. Sellier. 1999. Influence of the three RN genotypes on chemical composition, enzyme activities, and myofiber characteristics of porcine skeletal muscle. J. Anim. Sci. 77: 1482-1489.

Lecker, S. H., R. T. Jagoe, A. Gilbert, M. Gomes, V. Baracos, J. Bailey, S. R. Price, W. E. Mitch, and A. L. Goldberg. 2004. Multiple types of skeletal muscle atrophy involve a common program of changes in gene expression. FASEB J. 18: 39-51.

Lee-Young, R. S., S. R. Griffee, S. E. Lynes, D. P. Bracy, J. E. Ayala, O. P. McGuinness, and D. H. Wasserman. 2009. Skeletal muscle AMP-activated protein kinase is essential for the metabolic response to exercise in vivo. J. Biol. Chem. 284: 23925-23934.

Lee, J. W., S. Park, Y. Takahashi, and H. G. Wang. 2010. The association of AMPK with ULK1 regulates autophagy. PLoS ONE 5: e15394.

Leone, T. C., J. J. Lehman, B. N. Finck, P. J. Schaeffer, A. R. Wende, S. Boudina, M. Courtois, D. F. Wozniak, N. Sambandam, C. Bernal-Mizrachi, Z. Chen, J. O. Holloszy, D. M. Medeiros, R. E. Schmidt, J. E. Saffitz, E. D. Abel, C. F. Semenkovich, and D. P. Kelly. 2005. PGC-1α deficiency causes multi-system energy metabolic derangements: muscle dysfunction, abnormal weight control and hepatic steatosis. PLoS Biol. 3: e101.

Levine, J. A., W. T. Donahoo, and E. L. Melanson. 2000. Cellular and Whole-Animal Energetics. In: M. H. Stipanuk (ed.) Biochemical, Physiological, and Molecular Aspects of Human Nutrition. p 593-617. Saunders, Philadelpha.

Li, Y. P., Y. Chen, J. John, J. Moylan, B. Jin, D. L. Mann, and M. B. Reid. 2005. TNF-alpha acts via p38 MAPK to stimulate expression of the ubiquitin ligase atrogin1/MAFbx in skeletal muscle. FASEB J. 19: 362-370.

Lin, J., H. Wu, P. T. Tarr, C. Y. Zhang, Z. Wu, O. Boss, L. F. Michael, P. Puigserver, E. Isotani, E. N. Olson, B. B. Lowell, R. Bassel-Duby, and B. M. Spiegelman. 2002. Transcriptional co-activator PGC-1α drives the formation of slow-twitch muscle fibres. Nature 418: 797-801.

Ljubicic, V., P. Miura, M. Burt, L. Boudreault, S. Khogali, J. A. Lunde, J. M. Renaud, and B. J. Jasmin. 2011. Chronic AMPK activation evokes the slow, oxidative myogenic program and triggers beneficial adaptations in mdx mouse skeletal muscle. Hum. Mol. Genet. 20: 3478-3493.

Long, Y. C., S. Glund, P. M. Garcia-Roves, and J. R. Zierath. 2007. Calcineurin regulates skeletal muscle metabolism via coordinated changes in gene expression. J. Biol. Chem. 282: 1607-1614.

MacLennan, D. H., and M. S. Phillips. 1992. Malignant hyperthermia. Science 256: 789-794.

Mahlapuu, M., C. Johansson, K. Lindgren, G. Hjalm, B. R. Barnes, A. Krook, J. R. Zierath, L. Andersson, and S. Marklund. 2004. Expression profiling of the γ-subunit isoforms of AMP-activated protein kinase suggests a major role for γ3 in white skeletal muscle. Am. J. Physiol. Endocrinol. Metab. 286: E194-200.

Mammucari, C., G. Milan, V. Romanello, E. Masiero, R. Rudolf, P. Del Piccolo, S. J. Burden, R. Di Lisi, C. Sandri, J. Zhao, A. L. Goldberg, S. Schiaffino, and M. Sandri. 2007. FoxO3 controls autophagy in skeletal muscle in vivo. Cell Metab. 6: 458-471.

Matsushima, Y., Y. Goto, and L. S. Kaguni. 2010. Mitochondrial Lon protease regulates mitochondrial DNA copy number and transcription by selective degradation of mitochondrial transcription factor A (TFAM). Proc. Natl. Acad. Sci. USA 107: 18410-18415.

McBride, A., S. Ghilagaber, A. Nikolaev, and D. G. Hardie. 2009. The glycogen-binding domain on the AMPK beta subunit allows the kinase to act as a glycogen sensor. Cell Metab. 9: 23-34.

McGee, S. L., K. F. Howlett, R. L. Starkie, D. Cameron-Smith, B. E. Kemp, and M. Hargreaves. 2003. Exercise increases nuclear AMPK α2 in human skeletal muscle. Diabetes 52: 926-928.

McMillan, E. M., and J. Quadrilatero. 2011. Differential apoptosis-related protein expression, mitochondrial properties, proteolytic enzyme activity, and DNA fragmentation between skeletal muscles. Am. J. Physiol. Regul. Integr. Comp. Physiol. 300: R531-543.

Merrill, G. F., E. J. Kurth, D. G. Hardie, and W. W. Winder. 1997. AICA riboside increases AMP-activated protein kinase, fatty acid oxidation, and glucose uptake in rat muscle. Am. J. Physiol. 273: E1107-1112.

Mickelson, J. R., E. M. Gallant, L. A. Litterer, K. M. Johnson, W. E. Rempel, and C. F. Louis. 1988. Abnormal sarcoplasmic reticulum ryanodine receptor in malignant hyperthermia. J. Biol. Chem. 263: 9310-9315.

Mickelson, J. R., E. M. Gallant, W. E. Rempel, K. M. Johnson, L. A. Litterer, B. A. Jacobson, and C. F. Louis. 1989. Effects of the halothane-sensitivity gene on sarcoplasmic reticulum function. Am. J. Physiol. 257: C787-794.

Mickelson, J. R., and C. F. Louis. 1996. Malignant hyperthermia: excitation-contraction coupling, Ca^{2+} release channel, and cell Ca^{2+} regulation defects. Physiol. Rev. 76: 537-592.

Milan, D., J.-T. Jeon, C. Looft, V. Amarger, A. Robic, M. Thelander, C. Rogel-Gaillard, S. Paul, N. Iannuccelli, L. Rask, H. Ronne, K. Lundstrom, N. Reinsch, J. Gellin, E. Kalm, P. L. Roy, P. Chardon, and L. Andersson. 2000. A mutation in PRKAG3 associated with excess glycogen content in pig skeletal muscle. Science 288: 1248-1251.

Miller, B. F., M. M. Robinson, M. D. Bruss, M. Hellerstein, and K. L. Hamilton. 2012. A comprehensive assessment of mitochondrial protein synthesis and cellular proliferation with age and caloric restriction. Aging Cell 11: 150-161.

Miyamoto, Y., N. Kitamura, Y. Nakamura, M. Futamura, T. Miyamoto, M. Yoshida, M. Ono, S. Ichinose, and H. Arakawa. 2011. Possible existence of lysosome-like organella within mitochondria and its role in mitochondrial quality control. PLoS ONE 6: e16054.

Mizushima, N., T. Yoshimori, and B. Levine. 2010. Methods in mammalian autophagy research. Cell 140: 313-326.

Monsieurs, K., L. Heytens, C. Kloeck, J. J. Martin, F. Wuyts, and L. Bossaert. 1997. Slower recovery of muscle phosphocreatine in malignant hyperthermia-susceptible individuals assessed by 31P-MR spectroscopy. J. Neurol. 244: 651-656.

Moss, F. P., and C. P. Leblond. 1970. Nature of dividing nuclei in skeletal muscle of growing rats. J. Cell Biol. 44: 459-462.

Mounier, R., L. Lantier, J. Leclerc, A. Sotiropoulos, M. Pende, D. Daegelen, K. Sakamoto, M. Foretz, and B. Viollet. 2009. Important role for AMPKα1 in limiting skeletal muscle cell hypertrophy. FASEB J. 23: 2264-2273.

Mukwevho, E., T. A. Kohn, D. Lang, E. Nyatia, J. Smith, and E. O. Ojuka. 2008. Caffeine induces hyperacetylation of histones at the MEF2 site on the Glut4 promoter and increases MEF2A binding to the site via a CaMK-dependent mechanism. Am. J. Physiol. Endocrinol. Metab. 294: E582-588.

Muller, W. 1976. Subsarcolemmal mitochondria and capillarization of soleus muscle fibers in young rats subjected to an endurance training. A morphometric study of semithin sections. Cell Tissue Res. 174: 367-389.

Nakamura, Y., N. Kitamura, D. Shinogi, M. Yoshida, O. Goda, R. Murai, H. Kamino, and H. Arakawa. 2012. BNIP3 and NIX Mediate Mieap-Induced Accumulation of Lysosomal Proteins within Mitochondria. PLoS ONE 7: e30767.

Nakashima, K., and Y. Yakabe. 2007. AMPK activation stimulates myofibrillar protein degradation and expression of atrophy-related ubiquitin ligases by increasing FOXO transcription factors in C2C12 myotubes. Biosci Biotechnol Biochem 71: 1650-1656.

Naya, F. J., B. Mercer, J. Shelton, J. A. Richardson, R. S. Williams, and E. N. Olson. 2000. Stimulation of slow skeletal muscle fiber gene expression by calcineurin in vivo. J. Biol. Chem. 275: 4545-4548.

Nielsen, J., H. C. Holmberg, H. D. Schroder, B. Saltin, and N. Ortenblad. 2011. Human skeletal muscle glycogen utilization in exhaustive exercise: role of subcellular localization and fibre type. J. Physiol. 589: 2871-2885.

Nilsson, E. C., Y. C. Long, S. Martinsson, S. Glund, P. Garcia-Roves, L. T. Svensson, L. Andersson, J. R. Zierath, and M. Mahlapuu. 2006. Opposite transcriptional regulation in skeletal muscle of AMP-activated protein kinase γ3 R225Q transgenic versus knock-out mice. J. Biol. Chem. 281: 7244-7252.

O'Neill, H. M., S. J. Maarbjerg, J. D. Crane, J. Jeppesen, S. B. Jorgensen, J. D. Schertzer, O. Shyroka, B. Kiens, B. J. van Denderen, M. A. Tarnopolsky, B. E. Kemp, E. A. Richter, and G. R. Steinberg. 2011. AMP-activated protein kinase (AMPK) beta1beta2 muscle null mice reveal an essential role for AMPK in maintaining mitochondrial content and glucose uptake during exercise. Proc. Natl. Acad. Sci. USA 108: 16092-16097.

Oakhill, J. S., Z. P. Chen, J. W. Scott, R. Steel, L. A. Castelli, N. Ling, S. L. Macaulay, and B. E. Kemp. 2010. β-Subunit myristoylation is the gatekeeper for initiating metabolic stress sensing by AMP-activated protein kinase (AMPK). Proc. Natl. Acad. Sci. USA 107: 19237-19241.

Oakhill, J. S., R. Steel, Z. P. Chen, J. W. Scott, N. Ling, S. Tam, and B. E. Kemp. 2011. AMPK is a direct adenylate charge-regulated protein kinase. Science 332: 1433-1435.

Ojuka, E. O., T. E. Jones, L. A. Nolte, M. Chen, B. R. Wamhoff, M. Sturek, and J. O. Holloszy. 2002. Regulation of GLUT4 biogenesis in muscle: evidence for involvement of AMPK and Ca^{2+}. Am. J. Physiol. Endocrinol. Metab. 282: E1008-1013.

Pahl, H. L. 1999. Activators and target genes of Rel/NF-κB transcription factors. Oncogene 18: 6853-6866.

Pallafacchina, G., E. Calabria, A. L. Serrano, J. M. Kalhovde, and S. Schiaffino. 2002. A protein kinase B-dependent and rapamycin-sensitive pathway controls skeletal muscle growth but not fiber type specification. Proc. Natl. Acad. Sci. USA 99: 9213-9218.

Pankiv, S., T. H. Clausen, T. Lamark, A. Brech, J. A. Bruun, H. Outzen, A. Overvatn, G. Bjorkoy, and T. Johansen. 2007. p62/SQSTM1 binds directly to Atg8/LC3 to facilitate degradation of ubiquitinated protein aggregates by autophagy. J. Biol. Chem. 282: 24131-24145.

Park, S., T. L. Scheffler, A. M. Gunawan, H. Shi, C. Zeng, K. M. Hannon, A. L. Grant, and D. E. Gerrard. 2009a. Chronic elevated calcium blocks AMPK-induced GLUT-4 expression in skeletal muscle. Am. J. Physiol. Cell Physiol. 296: C106-115.

Park, S. K., A. M. Gunawan, T. L. Scheffler, A. L. Grant, and D. E. Gerrard. 2009b. Myosin heavy chain isoform content and energy metabolism can be uncoupled in pig skeletal muscle. J. Anim. Sci. 87: 522-531.

Perry, C. G., D. A. Kane, C. T. Lin, R. Kozy, B. L. Cathey, D. S. Lark, C. L. Kane, P. M. Brophy, T. P. Gavin, E. J. Anderson, and P. D. Neufer. 2011. Inhibiting myosin-ATPase reveals a dynamic range of mitochondrial respiratory control in skeletal muscle. Biochem. J. 437: 215-222.

Pette, D., and R. S. Staron. 2000. Myosin isoforms, muscle fiber types, and transitions. Microsc. Res. Tech. 50: 500-509.

Pette, D., and R. S. Staron. 2001. Transitions of muscle fiber phenotypic profiles. Histochem. Cell Biol. 115: 359-372.

Philippi, M., and A. H. Sillau. 1994. Oxidative capacity distribution in skeletal muscle fibers of the rat. J. Exp. Biol. 189: 1-11.

Picard, M., K. Csukly, M. E. Robillard, R. Godin, A. Ascah, C. Bourcier-Lucas, and Y. Burelle. 2008. Resistance to Ca^{2+}-induced opening of the permeability transition pore differs in mitochondria from glycolytic and oxidative muscles. Am. J. Physiol. Regul. Integr. Comp. Physiol. 295: R659-668.

Picard, M., R. T. Hepple, and Y. Burelle. 2012. Mitochondrial functional specialization in glycolytic and oxidative muscle fibers: tailoring the organelle for optimal function. Am. J. Physiol. Cell Physiol. 302: C629-641.

Picard, M., T. Taivassalo, D. Ritchie, K. J. Wright, M. M. Thomas, C. Romestaing, and R. T. Hepple. 2011. Mitochondrial structure and function are disrupted by standard isolation methods. PLoS ONE 6: e18317.

Pogozelski, A. R., T. Geng, P. Li, X. Yin, V. A. Lira, M. Zhang, J. T. Chi, and Z. Yan. 2009. p38γ mitogen-activated protein kinase is a key regulator in skeletal muscle metabolic adaptation in mice. PLoS ONE 4: e7934.

Polekhina, G., A. Gupta, B. J. Michell, B. van Denderen, S. Murthy, S. C. Feil, I. G. Jennings, D. J. Campbell, L. A. Witters, M. W. Parker, B. E. Kemp, and D. Stapleton. 2003. AMPK β subunit targets metabolic stress sensing to glycogen. Curr. Biol. 13: 867-871.

Powers, S. K., A. N. Kavazis, and J. M. McClung. 2007. Oxidative stress and disuse muscle atrophy. J. Appl. Physiol. 102: 2389-2397.

Puigserver, P., J. Rhee, J. Lin, Z. Wu, J. C. Yoon, C. Y. Zhang, S. Krauss, V. K. Mootha, B. B. Lowell, and B. M. Spiegelman. 2001. Cytokine stimulation of energy expenditure through p38 MAP kinase activation of PPARgamma coactivator-1. Mol. Cell 8: 971-982.

Raney, M. A., and L. P. Turcotte. 2006. Regulation of contraction-induced FA uptake and oxidation by AMPK and ERK1/2 is intensity dependent in rodent muscle. Am. J. Physiol. Endocrinol. Metab. 291: E1220-1227.

Reed, S. A., P. B. Sandesara, S. M. Senf, and A. R. Judge. 2011. Inhibition of FoxO transcriptional activity prevents muscle fiber atrophy during cachexia and induces hypertrophy. FASEB J.

Remels, A. H., H. R. Gosker, P. Schrauwen, P. P. Hommelberg, P. Sliwinski, M. Polkey, J. Galdiz, E. F. Wouters, R. C. Langen, and A. M. Schols. 2010. TNF-α impairs regulation of muscle oxidative phenotype: implications for cachexia? FASEB J. 24: 5052-5062.

Ristow, M., K. Zarse, A. Oberbach, N. Kloting, M. Birringer, M. Kiehntopf, M. Stumvoll, C. R. Kahn, and M. Bluher. 2009. Antioxidants prevent health-promoting effects of physical exercise in humans. Proc. Natl. Acad. Sci. USA 106: 8665-8670.

Rockl, K. S., M. F. Hirshman, J. Brandauer, N. Fujii, L. A. Witters, and L. J. Goodyear. 2007. Skeletal muscle adaptation to exercise training: AMP-activated protein kinase mediates muscle fiber type shift. Diabetes 56: 2062-2069.

Rodgers, J. T., C. Lerin, W. Haas, S. P. Gygi, B. M. Spiegelman, and P. Puigserver. 2005. Nutrient control of glucose homeostasis through a complex of PGC-1α and SIRT1. Nature 434: 113-118.

Romanello, V., and M. Sandri. 2010. Mitochondrial biogenesis and fragmentation as regulators of muscle protein degradation. Curr. Hypertens. Rep. 12: 433-439.

Rommel, C., S. C. Bodine, B. A. Clarke, R. Rossman, L. Nunez, T. N. Stitt, G. D. Yancopoulos, and D. J. Glass. 2001. Mediation of IGF-1-induced skeletal myotube hypertrophy by PI(3)K/Akt/mTOR and PI(3)K/Akt/GSK3 pathways. Nat. Cell Biol. 3: 1009-1013.

Rose, A. J., and M. Hargreaves. 2003. Exercise increases Ca^{2+}-calmodulin-dependent protein kinase II activity in human skeletal muscle. J. Physiol. 553: 303-309.

Rose, A. J., B. Kiens, and E. A. Richter. 2006. Ca^{2+}-calmodulin-dependent protein kinase expression and signalling in skeletal muscle during exercise. J. Physiol. 574: 889-903.

Ryan, M. T., and N. J. Hoogenraad. 2007. Mitochondrial-nuclear communications. Annu. Rev. Biochem. 76: 701-722.

Ryder, J. W., R. Bassel-Duby, E. N. Olson, and J. R. Zierath. 2003. Skeletal muscle reprogramming by activation of calcineurin improves insulin action on metabolic pathways. J. Biol. Chem. 278: 44298-44304.

Safdar, A., J. P. Little, A. J. Stokl, B. P. Hettinga, M. Akhtar, and M. A. Tarnopolsky. 2011. Exercise increases mitochondrial PGC-1α content and promotes nuclear-mitochondrial cross-talk to coordinate mitochondrial biogenesis. J. Biol. Chem. 286: 10605-10617.

Sahlin, K. 2007. Mitochondrial Adaptation to Exercise and Training: A Physiological Approach. In: V. Saks (ed.) Molecular Systems Bioenergetics. p 457-478. Wiley, Weinheim.

Sakamoto, K., O. Goransson, D. G. Hardie, and D. R. Alessi. 2004. Activity of LKB1 and AMPK-related kinases in skeletal muscle: effects of contraction, phenformin, and AICAR. Am. J. Physiol. Endocrinol. Metab. 287: 310-317.

Saks, V. A., V. I. Veksler, A. V. Kuznetsov, L. Kay, P. Sikk, T. Tiivel, L. Tranqui, J. Olivares, K. Winkler, F. Wiedemann, and W. S. Kunz. 1998. Permeabilized cell and skinned fiber techniques in studies of mitochondrial function in vivo. Mol. Cell. Biochem. 184: 81-100.

Salt, I., J. W. Celler, S. A. Hawley, A. Prescott, A. Woods, D. Carling, and D. G. Hardie. 1998. AMP-activated protein kinase: greater AMP dependence, and preferential nuclear localization, of complexes containing the α2 isoform. Biochem. J. 334 (Pt 1): 177-187.

Sanders, M. J., P. O. Grondin, B. D. Hegarty, M. A. Snowden, and D. Carling. 2007. Investigating the mechanism for AMP activation of the AMP-activated protein kinase cascade. Biochem. J. 403: 139-148.

Sandri, M., J. Lin, C. Handschin, W. Yang, Z. P. Arany, S. H. Lecker, A. L. Goldberg, and B. M. Spiegelman. 2006. PGC1α protects skeletal muscle from atrophy by suppressing FoxO3 action and atrophy-specific gene transcription. Proc. Natl. Acad. Sci. USA 103: 16260-16265.

Schwerzmann, K., H. Hoppeler, S. R. Kayar, and E. R. Weibel. 1989. Oxidative capacity of muscle and mitochondria: correlation of physiological, biochemical, and morphometric characteristics. Proc. Natl. Acad. Sci. USA 86: 1583-1587.

Shang, L., S. Chen, F. Du, S. Li, L. Zhao, and X. Wang. 2011. Nutrient starvation elicits an acute autophagic response mediated by Ulk1 dephosphorylation and its subsequent dissociation from AMPK. Proc. Natl. Acad. Sci. USA 108: 4788-4793.

Shi, H., J. M. Scheffler, J. M. Pleitner, C. Zeng, S. Park, K. M. Hannon, A. L. Grant, and D. E. Gerrard. 2008. Modulation of skeletal muscle fiber type by mitogen-activated protein kinase signaling. FASEB J. 22: 2990-3000.

Shi, H., J. M. Scheffler, C. Zeng, J. M. Pleitner, K. M. Hannon, A. L. Grant, and D. E. Gerrard. 2009. Mitogen-activated protein kinase signaling is necessary for the maintenance of skeletal muscle mass. Am. J. Physiol. Cell Physiol. 296: C1040-1048.

Shi, H., C. Zeng, A. Ricome, K. M. Hannon, A. L. Grant, and D. E. Gerrard. 2007. Extracellular signal-regulated kinase pathway is differentially involved in β-agonist-induced hypertrophy in slow and fast muscles. Am. J. Physiol. Cell Physiol. 292: C1681-1689.

Smirnova, E., L. Griparic, D. L. Shurland, and A. M. van der Bliek. 2001. Dynamin-related protein Drp1 is required for mitochondrial division in mammalian cells. Mol. Biol. Cell 12: 2245-2256.

Smith, J. A., M. Collins, L. A. Grobler, C. J. Magee, and E. O. Ojuka. 2007. Exercise and CaMK activation both increase the binding of MEF2A to the Glut4 promoter in skeletal muscle in vivo. Am. J. Physiol. Endocrinol. Metab. 292: E413-420.

Smith, J. A., T. A. Kohn, A. K. Chetty, and E. O. Ojuka. 2008. CaMK activation during exercise is required for histone hyperacetylation and MEF2A binding at the MEF2 site on the Glut4 gene. Am. J. Physiol. Endocrinol. Metab. 295: E698-704.

Spangenburg, E. E. 2009. Changes in muscle mass with mechanical load: possible cellular mechanisms. Appl Physiol Nutr Metab 34: 328-335.

Stein, S. C., A. Woods, N. A. Jones, M. D. Davison, and D. Carling. 2000. The regulation of AMP-activated protein kinase by phosphorylation. Biochem. J. 345: 437-443.

Sunadome, K., T. Yamamoto, M. Ebisuya, K. Kondoh, A. Sehara-Fujisawa, and E. Nishida. 2011. ERK5 regulates muscle cell fusion through Klf transcription factors. Dev. Cell 20: 192-205.

Suter, M., U. Riek, R. Tuerk, U. Schlattner, T. Wallimann, and D. Neumann. 2006. Dissecting the role of 5 '-AMP for allosteric stimulation, activation, and deactivation of AMP-activated protein kinase. J. Biol. Chem. 281: 32207-32216.

Szabadkai, G., A. M. Simoni, M. Chami, M. R. Wieckowski, R. J. Youle, and R. Rizzuto. 2004. Drp-1-dependent division of the mitochondrial network blocks intraorganellar Ca^{2+} waves and protects against Ca^{2+}-mediated apoptosis. Mol. Cell 16: 59-68.

Textor, Z., M. Beer, M. Anetseder, H. Kostler, E. Kagerbauer, W. Kenn, D. Hahn, and N. Roewer. 2003. Caffeine impairs intramuscular energy balance in patients susceptible to malignant hyperthermia. Muscle Nerve 28: 353-358.

Thomson, D. M., C. A. Fick, and S. E. Gordon. 2008. AMPK activation attenuates S6K1, 4E-BP1, and eEF2 signaling responses to high-frequency electrically stimulated skeletal muscle contractions. J. Appl. Physiol. 104: 625-632.

Tonkonogi, M., B. Walsh, M. Svensson, and K. Sahlin. 2000. Mitochondrial function and antioxidative defence in human muscle: effects of endurance training and oxidative stress. J. Physiol. 528 Pt 2: 379-388.

Tseng, B. S., C. E. Kasper, and V. R. Edgerton. 1994. Cytoplasm-to-myonucleus ratios and succinate dehydrogenase activities in adult rat slow and fast muscle fibers. Cell Tissue Res. 275: 39-49.

Tweedie, C., C. Romestaing, Y. Burelle, A. Safdar, M. A. Tarnopolsky, S. Seadon, S. L. Britton, L. G. Koch, and R. T. Hepple. 2011. Lower oxidative DNA damage despite greater ROS

production in muscles from rats selectively bred for high running capacity. Am. J. Physiol. Regul. Integr. Comp. Physiol. 300: R544-553.
Twig, G., A. Elorza, A. J. Molina, H. Mohamed, J. D. Wikstrom, G. Walzer, L. Stiles, S. E. Haigh, S. Katz, G. Las, J. Alroy, M. Wu, B. F. Py, J. Yuan, J. T. Deeney, B. E. Corkey, and O. S. Shirihai. 2008. Fission and selective fusion govern mitochondrial segregation and elimination by autophagy. EMBO J. 27: 433-446.
van Oort, R. J., J. L. Respress, N. Li, C. Reynolds, A. C. De Almeida, D. G. Skapura, L. J. De Windt, and X. H. Wehrens. 2010. Accelerated development of pressure overload-induced cardiac hypertrophy and dysfunction in an RyR2-R176Q knockin mouse model. Hypertension 55: 932-938.
van Wessel, T., A. de Haan, W. van der Laarse, and R. Jaspers. 2010. The muscle fiber type–fiber size paradox: hypertrophy or oxidative metabolism? Eur. J. Appl. Physiol. 110: 665-694.
Vega, R. B., J. M. Huss, and D. P. Kelly. 2000. The coactivator PGC-1 cooperates with peroxisome proliferator-activated receptor alpha in transcriptional control of nuclear genes encoding mitochondrial fatty acid oxidation enzymes. Mol. Cell. Biol. 20: 1868-1876.
Verhees, K. J., A. M. Schols, M. C. Kelders, C. M. Op den Kamp, J. L. van der Velden, and R. C. Langen. 2011. Glycogen synthase kinase-3β is required for the induction of skeletal muscle atrophy. Am. J. Physiol. Cell Physiol. 301: C995-C1007.
Viana, R., C. Aguado, I. Esteban, D. Moreno, B. Viollet, E. Knecht, and P. Sanz. 2008. Role of AMP-activated protein kinase in autophagy and proteasome function. Biochem. Biophys. Res. Commun. 369: 964-968.
Vidal-Puig, A. J., D. Grujic, C. Y. Zhang, T. Hagen, O. Boss, Y. Ido, A. Szczepanik, J. Wade, V. Mootha, R. Cortright, D. M. Muoio, and B. B. Lowell. 2000. Energy metabolism in uncoupling protein 3 gene knockout mice. J. Biol. Chem. 275: 16258-16266.
Vyas, D. R., E. E. Spangenburg, T. W. Abraha, T. E. Childs, and F. W. Booth. 2002. GSK-3β negatively regulates skeletal myotube hypertrophy. Am. J. Physiol. Cell Physiol. 283: C545-551.
Wagner, A. 2005. Energy constraints on the evolution of gene expression. Mol. Biol. Evol. 22: 1365-1374.
Walsh, B., M. Tonkonogi, and K. Sahlin. 2001. Effect of endurance training on oxidative and antioxidative function in human permeabilized muscle fibres. Pflugers Arch. 442: 420-425.
Wang, X., and C. G. Proud. 2006. The mTOR pathway in the control of protein synthesis. Physiology (Bethesda) 21: 362-369.
Wang, Y. X., C. L. Zhang, R. T. Yu, H. K. Cho, M. C. Nelson, C. R. Bayuga-Ocampo, J. Ham, H. Kang, and R. M. Evans. 2004. Regulation of muscle fiber type and running endurance by PPARδ. PLoS Biol. 2: e294.
Weiss, A., S. Schiaffino, and L. A. Leinwand. 1999. Comparative sequence analysis of the complete human sarcomeric myosin heavy chain family: implications for functional diversity. J. Mol. Biol. 290: 61-75.
Wenz, T., F. Diaz, B. M. Spiegelman, and C. T. Moraes. 2008. Activation of the PPAR/PGC-1α pathway prevents a bioenergetic deficit and effectively improves a mitochondrial myopathy phenotype. Cell Metab. 8: 249-256.

Wenz, T., S. G. Rossi, R. L. Rotundo, B. M. Spiegelman, and C. T. Moraes. 2009. Increased muscle PGC-1α expression protects from sarcopenia and metabolic disease during aging. Proc. Natl. Acad. Sci. USA 106: 20405-20410.

Wibom, R., E. Hultman, M. Johansson, K. Matherei, D. Constantin-Teodosiu, and P. G. Schantz. 1992. Adaptation of mitochondrial ATP production in human skeletal muscle to endurance training and detraining. J. Appl. Physiol. 73: 2004-2010.

Williams, R. S., S. Salmons, E. A. Newsholme, R. E. Kaufman, and J. Mellor. 1986. Regulation of nuclear and mitochondrial gene expression by contractile activity in skeletal muscle. J. Biol. Chem. 261: 376-380.

Winter, J. N., L. S. Jefferson, and S. R. Kimball. 2011. ERK and Akt signaling pathways function through parallel mechanisms to promote mTORC1 signaling. Am. J. Physiol. Cell Physiol. 300: C1172-1180.

Witczak, C. A., N. Fujii, M. F. Hirshman, and L. J. Goodyear. 2007. Ca^{2+}/calmodulin-dependent protein kinase kinase-α regulates skeletal muscle glucose uptake independent of AMP-activated protein kinase and Akt activation. Diabetes 56: 1403-1409.

Witczak, C. A., C. G. Sharoff, and L. J. Goodyear. 2008. AMP-activated protein kinase in skeletal muscle: from structure and localization to its role as a master regulator of cellular metabolism. Cell. Mol. Life Sci. 65: 3737-3755.

Wright, D. C., P. C. Geiger, D. H. Han, T. E. Jones, and J. O. Holloszy. 2007. Calcium induces increases in peroxisome proliferator-activated receptor γ coactivator-1α and mitochondrial biogenesis by a pathway leading to p38 mitogen-activated protein kinase activation. J. Biol. Chem. 282: 18793-18799.

Wright, D. C., K. A. Hucker, J. O. Holloszy, and D. H. Han. 2004. Ca^{2+} and AMPK both mediate stimulation of glucose transport by muscle contractions. Diabetes 53: 330-335.

Wu, H., S. B. Kanatous, F. A. Thurmond, T. Gallardo, E. Isotani, R. Bassel-Duby, and R. S. Williams. 2002. Regulation of mitochondrial biogenesis in skeletal muscle by CaMK. Science 296: 349-352.

Wu, Z., P. Puigserver, U. Andersson, C. Zhang, G. Adelmant, V. Mootha, A. Troy, S. Cinti, B. Lowell, R. C. Scarpulla, and B. M. Spiegelman. 1999. Mechanisms controlling mitochondrial biogenesis and respiration through the thermogenic coactivator PGC-1. Cell 98: 115-124.

Wullschleger, S., R. Loewith, and M. N. Hall. 2006. TOR signaling in growth and metabolism. Cell 124: 471-484.

Xiao, B., M. J. Sanders, E. Underwood, R. Heath, F. V. Mayer, D. Carmena, C. Jing, P. A. Walker, J. F. Eccleston, L. F. Haire, P. Saiu, S. A. Howell, R. Aasland, S. R. Martin, D. Carling, and S. J. Gamblin. 2011. Structure of mammalian AMPK and its regulation by ADP. Nature 472: 230-233.

Zechner, C., L. Lai, J. F. Zechner, T. Geng, Z. Yan, J. W. Rumsey, D. Collia, Z. Chen, D. F. Wozniak, T. C. Leone, and D. P. Kelly. 2010. Total skeletal muscle PGC-1 deficiency uncouples mitochondrial derangements from fiber type determination and insulin sensitivity. Cell Metab. 12: 633-642.

Zhao, T. J., Y. B. Yan, Y. Liu, and H. M. Zhou. 2007. The generation of the oxidized form of creatine kinase is a negative regulation on muscle creatine kinase. J. Biol. Chem. 282: 12022-12029.

Zheng, D., P. S. MacLean, S. C. Pohnert, J. B. Knight, A. L. Olson, W. W. Winder, and G. L. Dohm. 2001. Regulation of muscle GLUT4 transcription by AMP-activated protein kinase. J. Appl. Physiol. 91: 1073-1083.

Zid, B. M., A. N. Rogers, S. D. Katewa, M. A. Vargas, M. C. Kolipinski, T. A. Lu, S. Benzer, and P. Kapahi. 2009. 4E-BP extends lifespan upon dietary restriction by enhancing mitochondrial activity in Drosophila. Cell 139: 149-160.

Zierath, J. R., and J. A. Hawley. 2004. Skeletal muscle fiber type: influence on contractile and metabolic properties. PLoS Biol. 2: e348.

Zong, H., J. M. Ren, L. H. Young, M. Pypaert, J. Mu, M. J. Birnbaum, and G. I. Shulman. 2002. AMP kinase is required for mitochondrial biogenesis in skeletal muscle in response to chronic energy deprivation. Proc. Natl. Acad. Sci. USA 99: 15983-15987.

Chapter 6. Fiber hypertrophy and increased oxidative capacity can occur simultaneously in pig glycolytic skeletal muscle

Abstract

An inverse relationship exists between skeletal muscle fiber cross-sectional area (CSA) and oxidative capacity, which suggests muscle fibers hypertrophy at the expense of oxidative capacity. Therefore, our objective was to utilize pigs possessing mutations associated with increased oxidative capacity (AMP-activated protein kinase, AMPK$\gamma3^{R200Q}$) or fiber hypertrophy (ryanodine receptor 1, RyR1^{R615C}) to determine if these events occur in parallel. Longissimus muscle was collected from wild type (control), AMPK$\gamma3^{R200Q}$, RyR1^{R615C}, and AMPK$\gamma3^{R200Q}$-RyR1^{R615C} pigs. Regardless of AMPK genotype, RyR^{R615C} increased fiber CSA by 35%. In contrast, $\gamma3^{R200Q}$ pig muscle exhibited greater citrate synthase and β-hydroxyacyl coA dehydrogenase activity. Isolated mitochondria from AMPK$\gamma3^{R200Q}$ muscle had greater maximal, ADP-stimulated oxygen consumption rate. Additionally, AMPK$\gamma3^{R200Q}$ muscle contained increased (~50%) content of mitochondrial proteins succinate dehydrogenase and cytochrome c oxidase and greater mitochondrial DNA. Surprisingly, RyR1^{R615C} increased mitochondrial proteins and DNA, but this was not associated with improved oxidative capacity, suggesting that altered energy metabolism in RyR1^{R615C} muscle influences mitochondrial proliferation and protein turnover. Thus, pigs that possess both $\gamma3^{R200Q}$ and RyR^{R615C} exhibit increased muscle fiber CSA as well as greater oxidative capacity. Altogether, this supports that hypertrophy and enhanced oxidative capacity can occur simultaneously in skeletal muscle, and suggests the signaling mechanisms controlling these events are independently regulated.

Introduction

Skeletal muscle, which comprises approximately 40% of body mass, plays fundamental roles in support, movement, and whole body energy metabolism. Functional and phenotypic diversity of skeletal muscle is ascribed to heterogeneous composition of fibers that vary in histological, biochemical, and structural characteristics. Fibers are typically classified according to contractile speed (slow or fast) and predominant type of energy metabolism (oxidative or glycolytic). Type I fibers are slow-contracting and highly oxidative, whereas type II fibers (IIa, IIx, and IIb) are considered fast-contracting, yet vary widely in capacity for oxidative or glycolytic metabolism (Pette and Staron, 2001). Among these properties, oxidative capacity is strongly associated with muscle health and overall well-being. Enhanced oxidative capacity affords protection against insulin resistance and metabolic dysregulation (Barnes et al., 2004; Wang et al., 2004), attenuates muscle loss during aging (Wenz et al., 2009), and lessens energetic deficits associated with myopathies (Ljubicic et al., 2011; Wenz et al., 2008). The protective effects of increased oxidative capacity in disease states are largely attributed to increased mitochondrial content and enhanced mitochondrial function, which increases fatty acid oxidation, augments ATP generating capacity, and protects against cellular stress.

Muscle displays a remarkable ability to adapt phenotype in response to environmental stimuli. Endurance training readily promotes increases in maximal oxygen consumption and metabolic adaptations that enhance oxidative capacity, whereas resistance training stimulates increases in muscle fiber size. Curiously, combining resistance and endurance training results in less adaptation than either type of training alone (Hickson, 1980). The concurrent training phenomenon is not necessarily related to contractile phenotype because mitochondrial biogenesis can be augmented without changes in myosin heavy chain (Garcia-Roves et al., 2008; Geng et

al., 2010). Instead, oxidative capacity appears more closely associated with fiber size. Correspondingly, CSA is inversely related to maximal rate of oxygen consumption of vastly different muscle preparations; in turn, maximal oxygen consumption is proportional to succinate dehydrogenase activity and mitochondrial content (van Wessel et al., 2010). Thus, limiting fiber hypertrophy may be a means for maintaining optimal oxidative capacity.

Concomitant increases in size and oxidative capacity are likely limited by interaction between intracellular signaling pathways. Specifically, an AMP-activated protein kinase (AMPK)/Akt "switch" may mediate specific adaptations to endurance or resistance exercise (Atherton et al., 2005). The cellular energy sensor AMPK is a heterotrimeric serine/threonine kinase composed of catalytic α and regulatory β and γ subunits; in response to low cellular energy status, AMPK inhibits energy consuming pathways, including protein synthesis. In fact, AMPK attenuates growth signaling by inactivating the major signaling network for protein synthesis, the Akt /mammalian target of rapamycin pathway (Inoki et al., 2003). Moreover, AMPKα1/α2 knockout mice possess fibers with greater CSA (Lantier et al., 2010), further supporting that AMPK negatively influences muscle growth. Meanwhile, AMPK mediates metabolic adaptation by enhancing activity and expression of peroxisome proliferator activator receptor γ coactivator 1α (PGC1α), which coordinates expression of nuclear and mitochondrial encoded genes critical for mitochondrial biogenesis and increased oxidative capacity (Zong et al., 2002).

Thus, activation of AMPK induces shift to a more oxidative phenotype, while likely simultaneously limiting muscle growth. The porcine R200Q mutation in the AMPKγ3 subunit, and the equivalent mutation in the mouse (R225Q), result in constitutive AMPK activation, thereby contributing to increased mitochondrial protein content and enhanced oxidative capacity

in glycolytic skeletal muscle (Barnes et al., 2004; Garcia-Roves et al., 2008). While activated AMPK would be expected to limit growth, AMPKγ3^{R200Q} does not appear to affect muscle or overall growth in pigs (Carr et al., 2006). Considering pigs have a high potential for lean growth, this suggests that it may be possible to increase both fiber size and oxidative capacity in AMPKγ3^{R200Q} pig muscle. We used a genetic approach to determine if we could stimulate fiber hypertrophy in conjunction with AMPKγ3^{R200Q}. The porcine R615C mutation in the skeletal muscle ryanodine receptor (RyR1) increases muscle fiber size (Essen-Gustavsson et al., 1992), although the exact mechanism is not known. The RyR1 protein assembles in tetramers to form Ca^{2+} release channels which modulate the frequency and amplitude of Ca^{2+} release into the cytosol. Mechanistically, RyR1^{R615C} increases sensitivity to agents that stimulate channel opening and enhances luminal Ca^{2+} activation of RyR1 (Jiang et al., 2008; Mickelson et al., 1989). Aberrant Ca^{2+} homeostasis profoundly influences muscle function and energy metabolism. In fact, RyR1^{R615C} pig muscle exhibits lower resting glycogen and phosphocreatine levels and rapid glycolysis and ATP hydrolysis (Klont et al., 1994). Although increasing the oxidative capacity of RyR1^{R615C} muscle might prevent hypertrophy, it would also be expected to improve energy homeostasis. Therefore, our objective was to utilize pigs possessing AMPKγ3^{R200Q} and RyR1^{R615C} mutations to investigate the relationship between fiber size and metabolic phenotype. Herein, we show that muscle fibers can hypertrophy in parallel with increased oxidative capacity.

Materials and Methods

Animals. Animals were bred and reared at the Virginia Tech Swine Center and all procedures were carried out in accordance with the guidelines of the Institutional Animal Care and Use

Committee. Pigs heterozygous at the RyR1 and AMPKγ3 loci were bred to generate all possible genotype combinations. Female and castrated male pigs were reared under standard conditions and fed ad libitum. At approximately 120 kg, animals were transported to the Virginia Tech Meat Science Center and harvested. Immediately after exsanguination, muscle samples (~5-10 g) were collected from the lumbar region of the longissimus muscle. Samples were immediately frozen in liquid nitrogen and stored at -80°C until further analysis. Muscle samples for histology were mounted on cork with TissueTek, placed in isopentane cooled by liquid nitrogen, and stored at -80°C.

Genotype determination. Genotypes were determined using polymerase chain reaction (PCR) restriction fragment length polymorphism technique. DNA was isolated from blood or tissue and used for PCR amplification. PCR products were digested with appropriate restriction enzyme overnight and fragments were separated on an agarose gel stained with ethidium bromide for visualization. Pigs were evaluated for RyR1 genotype (Fujii et al., 1991) following the procedures outlined by O'Brien et al. (1993). For determination of AMPKγ3 genotype, the primers were (5' – 3') AAATGTGCAGACAAGGATCTC (forward) and CCCACGAAGCTCTGCTT (reverse). AMPKγ3 products were digested with restriction enzyme BsrBI. Those that were homozygous "normal" (wild type) at both RyR1 and AMPK loci were considered control, while those pigs designated $RyR1^{R615C}$ were homozygous mutant. RyR1 heterozygotes were excluded because they tend to exhibit an intermediate phenotype. In contrast, AMPKγ3 mutation is dominant, so both homozygous mutant and heterozygotes were utilized (designated $AMPK\gamma3^{R200Q}$). Finally, pigs denoted as AMPKγ3-RyR1 mutants were either

heterozygous or homozygous mutant at AMPKγ3 locus, and homozygous mutant at the RyR1 locus.

Histology. Skeletal muscle cross sections (10 μm) were placed on silane-coated microscope slides and stored at -80°C until analysis. Wheat germ agglutinin tagged with Alexa Fluor® conjugate (Invitrogen, Carlsbad, CA, USA) was used to label membranes for cross sectional area (CSA). Mean fiber CSA was determined from at least 100 fibers (range 100-400) per pig. For succinate dehydrogenase (SDH) staining, sections were incubated at 37°C for 1 h in 0.2 M phosphate buffer containing sodium succinate and nitro blue tetrazolium. Sections were washed in water, treated with increasing concentrations of acetone, rinsed, and mounted. Images were captured with a Nikon Eclipse Ti inverted microscope and CoolSNAP HQ2 monochrome camera and analyzed using NIS Elements AR3.1 software.

Enzyme Activity. Citrate synthase catalyzes the formation of citrate and CoASH from acetyl-CoA and oxaloactetate. CoASH reduces 5,5'-dithiobis-2-nitrobenzoic acid (DTNB) and citrate synthase activity was determined from the reduction of DTMB over time. Briefly, ten microliters of a 1:5 diluted muscle homogenate was added, in duplicate, to 170 μl of a solution containing Tris buffer (0.1M, pH 8.3), DNTB (1mM, in 0.1M in Tris buffer) and oxaloacetate (0.01M, in 0.1M Tris buffer). Following a 2 min background reading, the spectrophotometer (SPECTRAmax ME, Molecular Devices Corporation, Sunnyvale, CA, USA) was calibrated and 30μl of 3 mM acetyl CoA was added to initiate the reaction. Absorbance was measured at 405nm at 37C every 12 seconds for 7 minutes. Maximum citrate synthase activity was calculated and reported as nmol/min/mg.

For the determination of β-hydroxyacyl-CoA dehydrogenase (β-HAD), oxidation of NADH to NAD was measured. In triplicate, 35 µl of whole muscle homogenate was added to 190µl of a buffer containing 0.1M liquid triethanolamine, 5mM EDTA tetrasodium salt dihydrate, and 0.45mM NADH. The spectrophotometer was calibrated and 15µl of 2mM acetoacetyl CoA was added to initiate the reaction. Absorbance was measured at 340 nm every 12 seconds for 6 minutes at 37C. Maximum β-HAD activity was calculated and reported as nmol/min/mg.

Mitochondrial Respiration. Mitochondria were isolated by differential centrifugation. Briefly, freshly dissected longissimus muscle was placed in ice-cold homogenization buffer (5 ml/g fresh muscle) (100 mM sucrose, 180 mM KCl, 50 mM Tris, 10 mM EDTA, 5 mM $MgCl_2$, 1 mM K-ATP, pH 7.4) and visible connective tissue and fat were removed. Muscle (~300 mg) was finely minced in 1.5 ml homogenization buffer, and following addition of protease (subtilisin A, 5 mg/ml), muscle was homogenized using a glass-teflon homogenizer. Homogenate was diluted to ~6 ml with homogenization buffer, filtered through cheesecloth, and centrifuged at 450 x g for 2 min at 4°C. Supernatant was filtered again and centrifuged at 6000 x g for 15 min at 4°C. The resulting mitochondrial pellet was resuspended in mannitol-sucrose medium (220 mM mannitol, 70 mM sucrose, 10 mM Tris-HCl, 1 mM EGTA; pH 7.4). Protein concentration was determined using BCA protein assay kit (Pierce, Rockford, IL). Equal amounts of mitochondrial protein were plated in triplicate and the Seahorse Bioscience Flux Analyzer (North Billerica, MA) was used to measure mitochondrial oxygen consumption rate (OCR). After initial mixing and equilibration, OCR measurements were taken to determine baseline rates. Assessment of state 3 (active, maximum phosphorylating) respiration through complex I was determined in the presence of pyruvate (10 mM), malate (5 mM), and ADP (5 mM). Complex II-driven respiration was determined in the presence of succinate (20 mM) and ADP (5 mM), and rotenone (2 µM)

was used to block complex I. Evaluation of β-oxidation and electron transport chain function was made in the presence of palmitoyl carnitine (40 μM) and malate (2 μM). State 4 non-phosphorylating, maximal leak-dependent respiration was quantified following the addition of oligomycin (2 μM). Maximum uncoupled respiration was determined following addition FCCP (0.3 μM).

Mitochondrial DNA Copy Number. Total genomic DNA was isolated from longissimus muscle and treated with RNase. DNA concentration was determined using a Nanodrop spectrophotometer (Thermo Scientific, Waltham, MA, USA), and samples were diluted to yield equal DNA concentrations. Primers were designed using Primer Blast (NCBI) for mtDNA (cytochrome c oxidase subunit III, AJ002189.1) and nuclear DNA (β-actin, DQ452569.1). Final reaction mix included 1X SYBR green master mix (Applied Biosystems, Foster City, CA, USA), 500 nM of each primer, and 2 ng of DNA. Mitochondrial DNA (mtDNA) was compared with nuclear DNA using relative expression, determined by $2^{-(\Delta CT)}$ where ΔC_T represents $C_{T\ mtDNA}$-$C_{Tnuclear\ DNA}$.

Transcript abundance using real-time PCR. Total RNA was isolated from longissimus muscle using TRIzol according to the manufacturer's instructions (Life Technologies, Grand Island, NY, USA). RNA was treated with recombinant DNase (Life Technologies) and RNA concentration was quantified using Nanodrop spectrophotometer. RNA was reverse transcribed to cDNA using reverse transcriptase (Promega, Madison, WI, USA) according to the manufacturer's instructions. Reactions (15 μl) were performed in triplicate in a 96-well format using 7900 Fast Real-Time PCR system (Applied Biosystems). Final reaction mix included 1X fast SYBR green

master mix (Applied Biosystems), 670 nM of each primer, and 50 ng cDNA. Target specific primer sets were designed using Primer-BLAST (NCBI) for PGC1α (NM_213963), cytochrome c oxidase subunit 5B (Cox5B, NM_001007517.1); succinate dehydrogenase A (SDH-A, XM_003362140.1); NADH dehydrogenase subunit 1 (ND1, GQ339894.1); and cytochrome B (GU937818.1). Genes were normalized to eukaryotic elongation factor 1 α1 (eEF1a1, NM_001097418). Relative standard curves containing 0.2 to 200 ng cDNA were used to determine primer efficiency, which ranged between 97-106%. Relative expression was determined by $2^{-(\Delta CT)}$ where ΔC_T represents $C_{T\ target}$-$C_{T\ endogenous\ control}$.

Western blotting. Longissimus muscle tissue was powdered in liquid nitrogen and homogenized in ice cold RIPA buffer (50 mM Tris-HCl, pH 74; 150 mM NaCl, 1 mM EDTA, 1% NP-40, 1 mM PMSF, 0.25% sodium deoxycholate, 1 mM sodium orthovanadate, 1 mM sodium fluroide, and 1 μg/ml aprotinin, leupeptin, and pepstatin). Samples were centrifuged at 10,000 x g for 10 min at 4°C, and the supernatant was collected. Protein concentration was determined using BCA protein assay kit (Pierce, Rockford, IL) and samples were diluted to yield equal protein concentration and mixed with Laemmli buffer. Protein samples (25 μg) were separated using SDS-PAGE and transferred to polyvinylidene difluoride or nitrocellulose membranes. Membranes were blocked in StartingBlock Blocking Buffer (Thermo Scientific). Blots were probed with primary antibody (cytochrome c oxidase subunit IV, troponin I and light chain 3, Cell Signaling, Beverly, MA, USA; and SDH-A, Novus, Litteton, CO, USA) prepared in blocking buffer with 0.05% tween and washed in tris buffered saline with 0.05% tween. Then, blots were incubated with the appropriate IRDye® 680 or 800 conjugated anti-IgG antibody (LI-

COR® Biosciences, Lincoln, NE, USA). Bands were visualized using Odyssey ® Infrared Imaging System (LI-COR® Biosciences) and quantified using the manufacturer's software.

Statistical Analysis. Data were analyzed using SAS JMP. Model analyzed the main effects of AMPK and RyR1 genotype and the interaction (AMPK*RyR1). Main effect of gender (female and castrated male) was tested but was only included in the model if significant. For interactions, differences in LSM were determined using Tukey's adjustment for multiple comparisons. $P<0.05$ was considered significant.

Results

AMPK$\gamma3^{R200Q}$ and RyR1^{R615C} mutations are associated with increased oxidative capacity and fiber size, respectively; therefore quantifying these characteristics in pigs possessing both AMPK$\gamma3^{R200Q}$ and RyR1^{R615C} should indicate if increased CSA and oxidative capacity can occur simultaneously. We chose the longissimus muscle because AMPKγ3 is more highly expressed in glycolytic muscle (Mahlapuu et al., 2004), and the highly glycolytic nature of longissimus muscle in pigs provides a large potential for augmenting mitochondrial biogenesis and oxidative enzyme activity. Thus, using pigs with both AMPK$\gamma3^{R200Q}$ and RyR1^{R615C} mutations would allow us to determine if an increase in muscle fiber size sacrifices oxidative capacity, or alternatively, if increased oxidative capacity prevents hypertrophy.

RyR1 ^{R615C} contributes to muscle hypertrophy

RyR1^{R615C} increases fiber size as much as 50% (Essen-Gustavsson et al., 1992). Thus, our first objective was to confirm the effect of RyR1^{R615C} genotype on fiber CSA, and identify

AMPK genotype effects or genotype interactions. First, we determined CSA of longissimus muscle fibers from control, AMPKγ3^{R200Q}, RyR1^{R615C}, AMPKγ3^{R200Q} - RyR1^{R615C} pigs (representative images, Figure 6-1A). RyR1^{R615C} increased mean fiber CSA approximately 35% (*P*=0.0003, Figure 6-1B). A genotype interaction was not detected, supporting that regardless of AMPK genotype, RyR1^{R615C} is associated with muscle hypertrophy. Moreover, RyR1 is expressed in all skeletal muscle fibers regardless of contractile or metabolic phenotype, suggesting that RyR1^{R615C} should increase fiber size across the entire fiber population. In accord, RyR1^{R615C} shifted the frequency distribution for CSA (Figure 6-1C). Next, we examined if fiber hypertrophy resulted in overall increases in muscle size by determining total area of the longissimus muscle between the 10th and 11th ribs. Curiously, the combination of AMPKγ3^{R200Q} and RyR1^{R615C} robustly increased muscle area (17%) when compared to AMPKγ3^{R200Q}, yet muscle area was not different in RyR1^{R615C} compared to control pigs (AMPKγ3* RyR1 interaction, *P*=0.05; Figure 6-1D). These results were similar if longissimus muscle area was evaluated relative to body weight. Altogether, this supports that RyR1^{R615C} induces hypertrophy of fibers, but fiber hypertrophy does not necessarily correspond to overall increases in total muscle size.

AMPKγ3 ^{R200Q} increases oxidative capacity

Muscle oxidative capacity represents the ability of fibers to generate ATP through aerobic metabolism. Enhanced oxidative capacity typically parallels increases in mitochondrial density and protein content (Wibom et al., 1992). Therefore, increased oxidative enzyme activity in tissue homogenates may be more reflective of increased mitochondrial content, whereas enzyme activity measured in mitochondrial fractions (activity per unit mitochondrial protein)

reveals qualitative improvements in function. We employed histological staining for SDH activity as an indicator of mitochondrial content and activity (Figure 6-2A). SDH, an inner mitochondrial membrane protein, converts succinate to fumarate in the TCA cycle and delivers electrons to the electron transport chain. SDH activity staining appeared weakest in muscle from control pigs, whereas darker staining in AMPKγ3^{R200Q} –containing muscle corroborated that AMPKγ3^{R200Q} enhances mitochondrial content and oxidative capacity. To confirm this, we utilized muscle homogenates to quantify citrate synthase and β-hydroxyacyl coA dehydrogenase (β-HAD) activity, key enzymes in the TCA cycle and fatty acid β-oxidation, respectively. AMPKγ3^{R200Q} increased citrate synthase activity nearly 50% (P=0.002, Figure 6-2B) while β-HAD activity increased roughly 40% (P=0.02, Figure 6-2C). Therefore, AMPKγ3^{R200Q} enhances oxidative capacity irrespective of RyR1 genotype.

In addition, we used isolated mitochondria from longissimus muscle to assess functional aspects of mitochondria. Important properties relating to ATP producing capacity of mitochondria include maximal ADP-stimulated respiration (state 3), basal state 4 respiration, coupling between respiration and phosphorylation. The rate of oxidative phosphorylation is primarily determined by the need for ATP. Therefore, high concentrations of ADP stimulate maximal oxygen consumption (state 3), and greater ADP-stimulated respiration indicates a greater capacity for oxidative phosphorylation. To determine state 4 respiration, ATP synthase is inhibited in order to eliminate the contribution of proton flow through ATP synthase. Oxygen consumption in state 4 indicates proton leak across the inner membrane and represents inefficiency because oxygen consumption does not result in phosphorylation of ADP. Thus, the ratio between state 3 and state 4, referred to as respiratory control ratio (RCR), represents the coupling between respiration and phosphorylation. We monitored oxygen consumption rate in

the presence of various substrates and inhibitors to determine state 3 (active, maximum phosphorylating respiration), state 4 (resting respiration), and uncoupled respiration. Function of pyruvate dehydrogenase and complex I was assessed using pyruvate, malate, and ADP, whereas complex II driven respiration was determined using succinate and ADP, along with rotenone to block complex I. Lastly, β-oxidation and electron transport function were determined using palmitoyl carnitine and malate. AMPK$\gamma3^{R200Q}$ increased state 3 respiration regardless of substrate, as evidenced by enhanced oxygen consumption rate per μg mitochondrial protein (Figure 6-3). There also tended to be a genotype interaction, demonstrated by the low state 3 respiration of RyR^{R615C} mitochondria yet relatively high state 3 of AMPK$\gamma3^{R200Q}$ - RyR^{R615C} mitochondria. Unfortunately, there was only 1 RyR^{R615C} sample for analysis, and thus the error for this observation is relatively high. However, considering the response of AMPK$\gamma3^{R200Q}$ - RyR^{R615C} mitochondria, it seems that RyR^{R615C} certainly does not negatively influence mitochondria function when present with AMPK$\gamma3^{R200Q}$. Overall, oligomycin greatly decreased oxygen consumption, indicating low proton leak and resulting in similar state 4 respiration among all genotypes (data not shown). RCRs (Table 6-1) were not significantly different, although values for genotypes followed a similar trend as OCR for state 3 respiration. In total, AMPK$\gamma3^{R200Q}$ increased capacity for oxidative phosphorylation in isolated mitochondria without significantly altering other functional parameters. Because mitochondrial function assays were conducted using the same concentrations of mitochondrial protein, we infer that AMPK$\gamma3^{R200Q}$ affects mitochondrial functional quality. In conjunction with CSA, this supports that oxidative capacity and fiber size can be increased simultaneously.

Mitochondrial content

Gene dosage, or mtDNA content, is considered the primary regulatory mechanism governing mitochondrial gene and protein expression (Williams, 1986). Thus, we used the ratio between copy number of mtDNA and nuclear DNA to examine differences in mitochondrial content between genotypes. AMPKγ3^{R200Q} contributed to a ~60% increase in mitochondrial content (Figure 6-4). This is consistent with ~50% increase in mitochondrial content observed in white gastrocnemius of transgenic mice with AMPKγ3^{R225Q}, which is analogous to the pig mutation (Garcia-Roves et al., 2008). Mitochondria proliferation is a mechanism to compensate for energy deficit, and may be induced by contractile activity (Williams et al., 1986). Exercise can activate AMPK, which promotes adaptation via mitochondrial biogenesis (Zong et al., 2002). Thus, the increase in mtDNA attributed to AMPKγ3^{R200Q} can likely be considered a "healthy" adaptation. Unexpectedly, RyR1^{R615C} enhanced mtDNA content by ~40%. Mitochondrial proliferation can also be caused by pathological circumstances involving defects in oxidative metabolism (Bai et al., 2004). RyR1^{R615C} -induced mitochondrial proliferation may be a compensatory mechanism to cope with rapid metabolism and challenged energy homeostasis in RyR1 mutant muscle. Similarly, murine skeletal muscle with RyR1^{R163C} exhibits compromised capacity to generate ATP and possesses higher mtDNA copy number (Giulivi et al., 2011).

Content of mitochondrial mRNA generally parallels increases in mtDNA and oxidative capacity (Williams, 1986). Therefore, we determined mRNA expression of activators of mitochondrial biogenesis and expression of nuclear and mitochondrial encoded genes. PGC1α coordinates mitochondrial and nuclear gene expression to promote mitochondrial biogenesis; it interacts with a number of transcription factors and nuclear receptors to modulate gene expression and contributes to an autoregulatory loop that promotes its own expression

(Handschin et al., 2003). Although genotype significantly influenced mtDNA content, PGC1α was not affected (Figure 6-5A). Transcript abundance is an important mechanism contributing to PGC1α content (Atherton et al., 2005; Irrcher et al., 2008). However, PGC1α activity is also determined by protein turnover, phosphorylation (Puigserver et al., 2001), and protein-binding interactions (Fan et al., 2004). While AMPKγ3^{R225Q} is associated with both enhanced PGC1α mRNA and protein (Garcia-Roves et al., 2008), it appears that PGC1α activity in mutant pigs is likely controlled by post-translational modifications and/or protein turnover.

Because mitochondrial biogenesis requires coordinated expression of mitochondrial and nuclear genomes, we also evaluated mRNA expression of mitochondrial and nuclear encoded genes. Genotype did not alter expression of nuclear encoded genes, cytochrome c oxidase subunit 5B (Cox5B), and succinate dehydrogenase A (SDH-A) (Figure 6-5B); expression of mitochondrial encoded cytochrome B was not affected either (Figure 6-5C). However, AMPKγ3^{R200Q} increased transcript abundance of mitochondrial encoded NADH dehydrogenase subunit 1 (complex I) by ~30% (Figure 6-5C). Overall, AMPKγ3 and RyR1 genotypes do not appear to alter transcription, indicating that translational mechanisms may be important means contributing to mitochondrial content.

Improvements in oxidative capacity generally parallel increases in mitochondrial density and protein content (Wibom et al., 1992). We employed succinate dehydrogenase A (SDH-A) and cytochrome c oxidase (complex IV) subunit IV as markers of mitochondrial protein content (representative images, Figure 6-6A). AMPKγ3^{R200Q} augmented protein levels of both SDH-A and CoxIV by roughly 45% (Figure 6-6B, 6C). Curiously, RyR1^{R615C} also increased mitochondrial protein content, though to a lesser extent (~20%). To our knowledge, there is no evidence indicating that porcine RyR1^{R615C} increases content of mitochondrial proteins, nor did

we expect that RyR1 genotype would influence protein content. Mitochondrial protein content of RyR1^{R615C} muscle is not consistent with oxidative capacity assessed by citrate synthase or β-HAD activities or state 3 respiration. This contradiction suggests that protein function may be reduced in RyR1^{R615C} muscle, which could be caused by protein damage, improper folding, or altered turnover.

Mitochondrial protein turnover

RyR1^{R615C} is associated with increases in mitochondrial proteins but not oxidative enzyme activity. This indicates a possible defect in protein quality control; that is, damaged proteins may not be degraded as quickly in RyR1 mutants. In skeletal muscle, several pathways contribute to protein degradation: ubiquitin proteasome, lysosomal, calpain, and caspase proteolysis systems. Because ubiquitin proteasome pathway is responsible for the majority of cellular protein degradation, we first investigated the E3 ubiquitin ligase, muscle really interesting gene finger 1 (MuRF-1). MuRF-1 targets certain metabolic proteins, including pyruvate dehydrogenase (Hirner et al., 2008) and muscle-type creatine kinase (Koyama et al., 2008), for degradation. However, genotype did not influence MuRF-1 protein content (data not shown).

Although the lysosomal system is responsible for a much lower proportion of total protein degradation, it mediates turnover of mitochondrial proteins and autophagy of entire mitochondria (mitophagy). Proteins or organelles targeted for degradation are engulfed by a double-membraned vesicle called the autophagosome. Subsequently, the autophagosome fuses with a lysosome, resulting in degradation of targets as well as the inner autophagosomal membrane (Mizushima et al., 2010). Microtubule associated protein 1 light chain 3 (LC3) and

p62 are markers of autophagy. Pro-LC3 is cleaved, generating the cytosolic LC3-I form. Addition of phosphatidylethanolamine to LC3-I produces LC3-II, which is associated with the expanding autophagosome membrane (Mizushima et al., 2010). Meanwhile, p62 recognizes poly-ubiquitinated proteins and binds directly to LC3-II on the autophagosome, thereby mediating protein degradation; p62 is subsequently degraded during autophagy (Pankiv et al., 2007). Thus, p62 content is inversely correlated with autophagic activity. Genotype did not affect p62 protein levels (data not shown). LC3-II generally correlates with the number of autophagosomes (Kabeya et al., 2000). Although not significant, RyR1^{R615C} tended (P=0.09) to decrease LC3-II content. However, there is some difficulty in interpreting LC3 immunoblotting because there are differences in reactivity for LC3-II versus LC3-I; and an increase in LC3-II can indicate autophagic flux, or it can signify inhibition of autophagy (Mizushima and Yoshimori, 2007). Yet, conversion of LC3-I to LC3-II also implies increased autophagic flux. Both AMPKγ3^{R200Q} and RyR1^{R615C} decreased the ratio of LC3-II to LC3-I (Figure 6-7), suggesting that the conversion of cytosolic LC3-I to the autophagosomal LC3-II form may be reduced; thus decreased autophagic flux could contribute to elevated mitochondrial protein content in these genotypes. Regulatory mechanisms controlling autophagy, particularly in mammalian cells, are not well understood. For example, AMPK has been shown to have contrasting roles under basal conditions (Shang et al., 2011) compared to starvation (Kim et al., 2011), and the mechanisms are still under debate.

Discussion

Enhanced skeletal muscle oxidative capacity protects against insulin resistance, sarcopenia, and energetic deficits. Clearly, muscle oxidative capacity benefits muscle health and

overall well-being, yet the ability to augment aerobic capacity may be limited by fiber size. Oxidative capacity and muscle fiber size are inversely related (van Wessel et al., 2010), and interaction between signaling pathways largely prevents concurrent increases in fiber size and oxidative metabolism (Atherton et al., 2005; Coffey et al., 2006). Yet, we clearly demonstrate that both muscle fiber size and oxidative capacity can be increased simultaneously. RyR1^{R615C} contributed to ~35% increase in fiber size, while AMPKγ3^{R200Q} enhanced mitochondrial content and enzyme activity. Given that RyR1^{R615C} muscle is susceptible to rapid metabolism, it is particularly remarkable that RyR1^{R615C} did not appear to have any adverse effects on oxidative capacity of AMPKγ3^{R200Q} – RyR1^{R615C} muscle. This is consistent with concept that mitochondrial biogenesis and increased oxidative capacity have protective effects for muscle health.

There are over 300 mutations identified in RyR1, with most mutations being found in three separate regions (Lanner et al., 2010). While the most severe phenotype is associated with mutations in the pore of the calcium release channel, the majority of mutations are mapped to inter-domain and inter-subunit interfaces (reviewed by Capes et al., 2011). Several knock-in mouse models of other RyR1 mutations have been developed, but are not synonymous with RyR1^{R615C}, which is the only known porcine mutation (Fujii et al., 1991). RyR1 mutations have disparate effects on Ca^{2+} release, which differentially influences energy homeostasis, muscle phenotype, and viability (Brini et al., 2005). For example, homozygosity for RyR1^{R163C} in mice causes embryonic lethality (Feng et al., 2011), whereas RyR1^{R615C} homozygous pigs are stress-susceptible but viable, and heterozygous pigs exhibit an intermediate phenotype. RyR1^{R615C} increases sensitivity to agents that stimulate channel opening, contributing to enhanced Ca^{2+} release (Mickelson et al., 1988; Mickelson et al., 1989); RyR1^{R615C} also lowers the threshold for

store overload induced Ca^{2+} release (Jiang et al., 2008). Rapid and increased Ca^{2+} release results in hypermetabolism, elevated body temperature, and muscle rigidity (MacLennan and Phillips, 1992).

Although RyR1 mutations do not appear to be linked with hypertrophy in humans, porcine $RyR1^{R615C}$ increases fiber size (Essen-Gustavsson et al., 1992). Greater CSA in $RyR1^{R615C}$ pigs muscle is usually referred to as a work-induced hypertrophy, but the signaling mechanisms are not known. $RyR1^{R163C}$ induces a slow to fast fiber transition, which is associated with a relative decrease in calcineurin relative to calcineurin inhibitor and activation of extracellular regulated kinase (ERK)-1/2 signaling (Giulivi et al., 2011). Activation of ERK1/2 is implicated in muscle hypertrophy (Haddad and Adams, 2004; Lantier et al., 2010; Shi et al., 2008; Shi et al., 2007). However, in our hands, $RyR1^{R615C}$ did not affect ERK1/2 phosphorylation (data not shown).

Despite AMPK's role in limiting protein synthesis, $AMPK\gamma3^{R200Q}$ did not seem to hinder muscle growth. On a chronic basis, nutrient signals or adaptive mechanisms would likely override this negative effect. Intriguingly, $AMPK\gamma3^{R200Q}$ increases total Akt protein (Granlund et al., 2010), and Akt content is positively related to muscle growth (Bodine et al., 2001). We also found increased Akt protein levels in $AMPK\gamma3^{R200Q}$ longissimus muscle (data not shown), suggesting that increased Akt expression may be a means of compensating for downregulation of protein synthesis by activated AMPK.

Notably, the increase in fiber size in $RyR1^{R615C}$ pig muscle did not contribute to an overall increase in longissimus muscle area. However, $AMPK\gamma3^{R200Q}$ - $RyR1^{R615C}$ pigs possessed greater fiber size and greater muscle area than their $AMPK\gamma3^{R200Q}$ counterparts. This raises an intriguing possibility: $RyR1^{R615C}$ pigs may possess fewer muscle fibers, and $AMPK\gamma3^{R200Q}$ in the

presence of RyR1^{R615C} may partially ameliorate loss of fibers. We did not observe any obvious histological defects or myopathic features in RyR1^{R615C} muscle that would suggest post-natal loss of fibers. Moreover, because muscle fibers are post-mitotic, this further supports that a developmental phenomenon could be responsible. Alternatively, other quantitative trait loci associated with muscle development are linked with RyR1 (Cherel et al., 2011), implying that RyR1^{R615C} may only partly explain changes in muscle development and/or fiber size.

Increased fiber CSA in RyR1^{R615C} increases the diffusion distance for oxygen to mitochondria and contributes to decreased capillary density (Essen-Gustavsson et al., 1992), which could exacerbate rapid metabolism. Yet, oxidative enzyme activity is not different in RyR1^{R615C} versus control muscle, supporting that oxidative capacity is not significantly impacted. In agreement, isolated mitochondria (Campion et al., 1975; Rasmussen et al., 1996) and permeabilized myofibers (Werner et al., 2010) from RyR1^{R615C} muscle exhibit similar respiratory activities as control. While oxidative enzyme activity in RyR1^{R615C} muscle is similar to control, RyR1^{R615C} muscle does exhibit mitochondrial proliferation and increased mitochondrial protein content. This may be a mechanism to cope with energetic stress. In contrast, mitochondria from RyR1^{R163C} muscle have lower state 3 and state 4 respiration, mitochondrial proliferation, and increased oxidative stress (Giulivi et al., 2011). Ca^{2+} amplitude is higher in RyR1^{R615C} mitochondria, and spikes in mitochondrial matrix Ca^{2+} increase generation of reactive oxygen species (Brini et al., 2005). Thus, oxidative stress could explain why increased mitochondrial protein does not result in concomitant improvements in oxidative capacity in RyR1^{R615C} pigs. Moreover, mtDNA is particularly susceptible to oxidative damage due to its location and lack of histones. Spikes in mitochondrial matrix Ca^{2+} increase generation of reactive oxygen species, and mtDNA is particularly susceptible to oxidative damage due to its

location and lack of histones. Increased reactive oxygen species production could also damage mitochondrial proteins, potentially explaining why increased mitochondrial protein does not result in concomitant improvements in oxidative capacity in $RyR1^{R615C}$ pigs.

The increase in mitochondrial content and oxidative capacity in $AMPK\gamma3^{R200Q}$ - $RyR1^{R615C}$ muscle could have several advantages. Most obviously, increased oxidative capacity augments ATP generating ability, which would improve maintenance of resting cytosolic Ca^{2+} levels and membrane potentials. Additionally, mitochondria act as a high capacity, low affinity transient Ca^{2+} store (Camello-Almaraz et al., 2006), thereby providing a larger Ca^{2+} "sink" to help buffer fluctuations in cytosolic and mitochondrial matrix Ca^{2+}. Given that subsarcolemmal and intermyofibrillar populations of mitochondria exhibit different properties, functional improvements may be related to which mitochondrial population is affected. Intermyofibrillar mitochondria exhibit increased ADP-stimulated respiration (Cogswell et al., 1993) but are more sensitive to reactive oxygen species (Adhihetty et al., 2005), while subsarcolemmal mitochondria are important for transport of metabolites and ions across the cell membrane (Muller, 1976).

AMPK plays a key role in modulating muscle metabolism in response to acute and chronic energy stress. Intriguingly, the expression of AMPKγ subunit is not necessarily important for AMPK to influence adaptation (Garcia-Roves et al., 2008); instead, γ3 mutations appear to have the most profound effects on energy substrates and metabolism in skeletal muscle. In addition to the aforementioned influence of $AMPK\gamma3^{R200Q}$ in the pig, $AMPK\gamma3^{R225W}$ mutation in humans confers a 90% increase in muscle glycogen and a 30% decrease in triglycerides (Costford et al., 2007); and the $\gamma3^{R225Q}$ in mice increases glycogen ~2 fold and enhances fatty acid oxidation (Barnes et al., 2004). These γ3 mutations are considered gain-of-function mutations that result in constitutive activity. We have previously demonstrated that

RyR1^{R615C} blunts AMPK phosphorylation in pigs with AMPKγ3^{R200Q} (Park et al., 2009), suggesting that Ca^{2+} induced abrogation of AMPK would prevent increases in oxidative capacity and glycogen content. Although RyR1^{R615C} - AMPKγ3^{R200Q} pig muscle has decreased content of the muscle specific glucose transporter GLUT4 compared to pigs possessing only AMPKγ3^{R200Q} (Park et al., 2009), the AMPK-RyR1 mutant muscle still possesses dramatically increased glycogen (Copenhafer et al., 2006). This verifies that the AMPK mutation may be more important than its expression or activity per se, further supporting that we could expect both fiber hypertrophy and increased oxidative metabolism in AMPKγ3^{R200Q} - RyR1^{R615C} muscle.

AMPKγ3^{R200Q} clearly improved oxidative capacity regardless of RyR1 genotype. AMPK is well-documented to modulate the master mitochondrial regulator PGC1α, but we did not detect differences in PGC1α mRNA expression. Yet, in a chronic situation, mRNA likely would not be the primary means of regulation. It would be more efficient to modulate phenotype at the protein level by increasing synthesis, reducing degradation, or affecting stability and activity via post-translational mechanisms. We did, however, detect differences in mitochondrial-encoded ND1. Because electrons enter the electron transport chain at complex I or complex II, this eludes to the possibility that AMPKγ3^{R200Q} may improve mitochondrial quality by altering protein stoichiometry; that is, AMPKγ3^{R200Q} enhances function by preferentially increasing expression of certain metabolic enzymes. While mRNA expression appears fairly stable in AMPKγ3^{R200Q} muscle, mitochondrial protein content is increased. AMPKγ3^{R200Q} elicits similar effects on metabolic phenotype regardless of RyR1 genotype, indicating that AMPKγ3^{R200Q} supports mitochondrial biogenesis and upregulation of fatty acid oxidation irrespective of AMPK phosphorylation. It is possible the activating properties of the mutation impact cellular

localization or how AMPK interacts with other proteins, but additional work will be necessary to show this.

In summary, we have demonstrated that hypertrophy and oxidative adaptation both occur in AMPKγ3^{R200Q} - RyR1^{R615C} muscle. AMPKγ3^{R200Q} increases muscle oxidative capacity, evidenced by enhanced citrate synthase, β-HAD activity, and state 3 respiration, as well as augmented mitochondrial content. Conversely, RyR1^{R615C} contributes to muscle hypertrophy, which is corroborated by increased muscle fiber CSA. Although RyR1^{R615C} also contributes to increases in mtDNA and mitochondrial protein, these changes are not associated with improvements in function. Nonetheless, increased oxidative capacity in RyR1^{R615C} pigs possessing the AMPKγ3 mutation supports that AMPK-induced mitochondrial and metabolic adaptations improve ATP generating capacity despite aberrant Ca^{2+} metabolism and increased fiber CSA. This highlights the important role of muscle mitochondria content and quality, and further substantiates that oxidative capacity protects against energetic defects and is a critical determinant of muscle health and whole body metabolism. In total, this supports that hypertrophy and enhanced oxidative capacity can occur simultaneously in skeletal muscle, and the signaling mechanisms controlling these events appear to be independently regulated.

A.

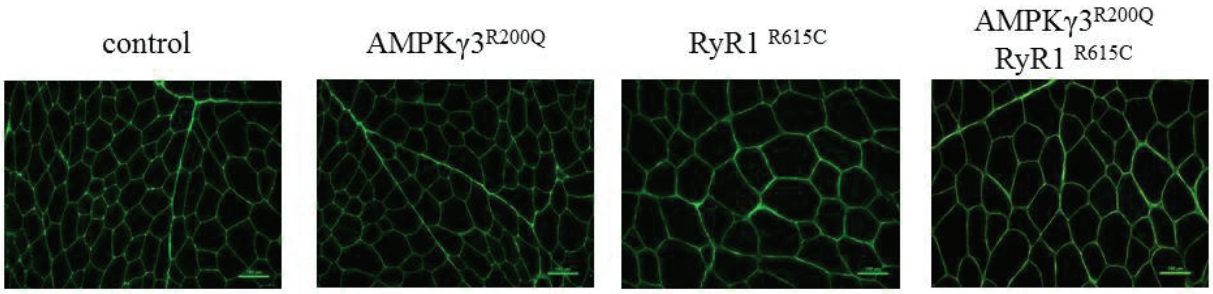
control
AMPKγ3R200Q
RyR1 R615C
AMPKγ3R200Q
RyR1 R615C

B.

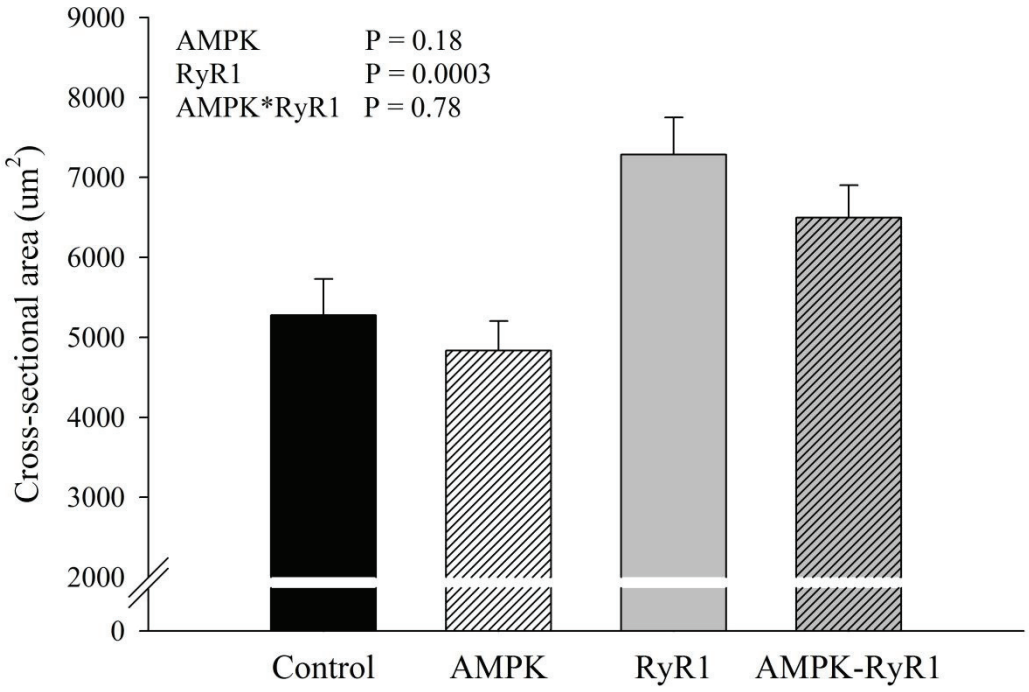
AMPK P = 0.18
RyR1 P = 0.0003
AMPK*RyR1 P = 0.78
Cross-sectional area (um2)
9000
8000
7000
6000
5000
4000
3000
2000
0
Control
AMPK
RyR1
AMPK-RyR1

C.

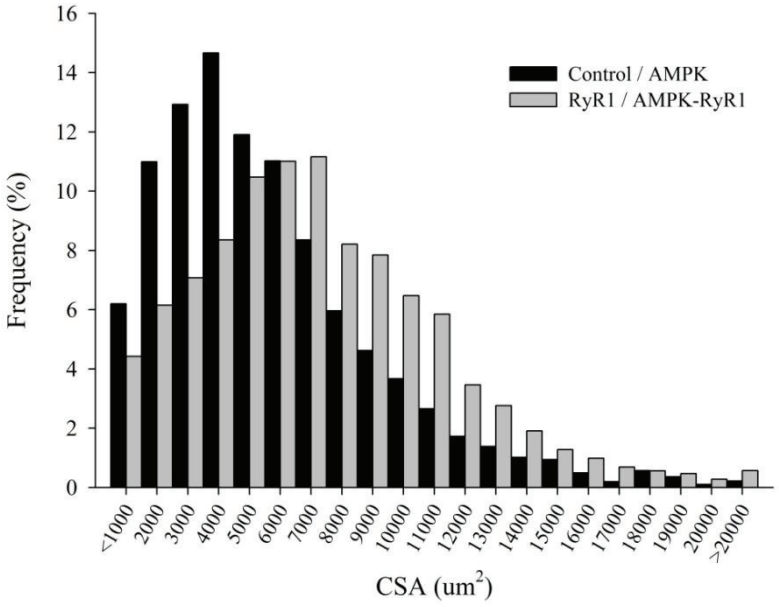

D.

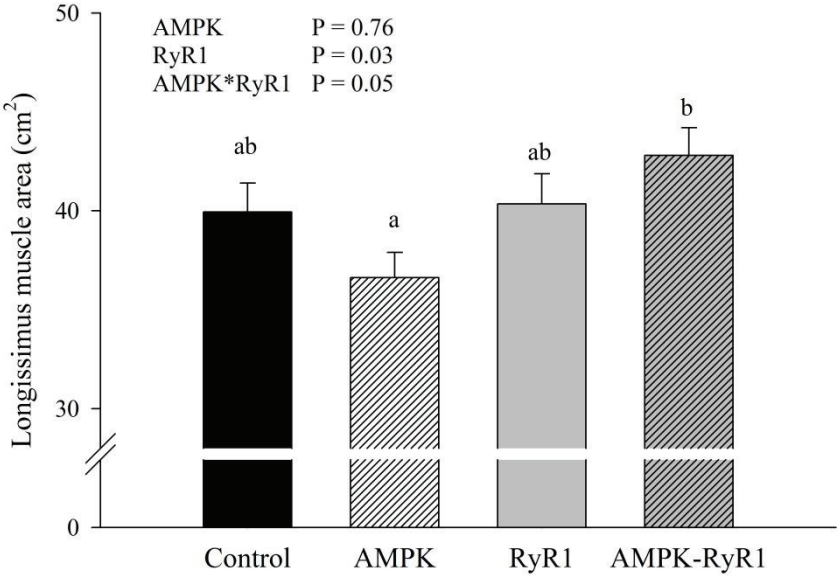

Figure 6-1. RyR1 mutation increases cross-sectional area (CSA) of longissimus muscle fibers but does not necessarily increase total muscle area. Fluorescent-tagged wheat germ agglutinin was used to label membranes of muscle fibers. (A) Representative images (inset bar = 100 μm) indicating fiber CSA of different genotypes. (B) Mean CSA was determined from 100-400 fibers per pig. Values represent LSM ± SE (n = 7-11 pigs per genotype). (C) Frequency distribution of fiber CSA comparing RyR1 normal (control and AMPK) versus RyR1^{R615C} (RyR1 and AMPK-RyR1) pigs. (D) Total longissimus muscle cross-sectional area (cm2) was determined caudal to the 10th costa. Values represent LSM ± SE (n = 7-11 pigs per genotype).

A.

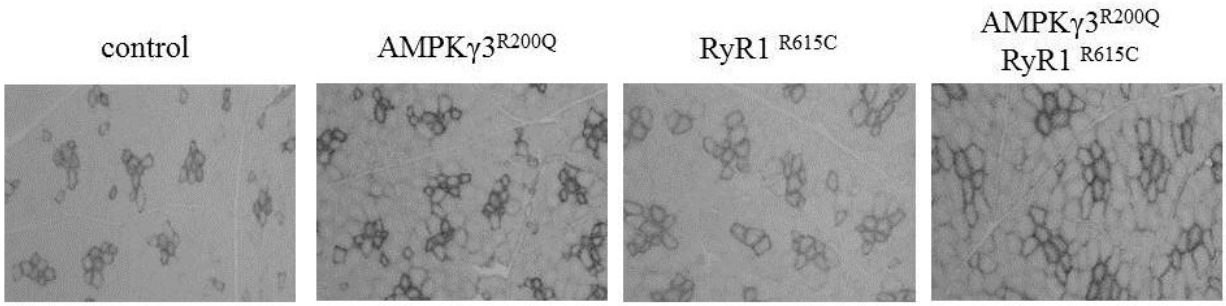

B.

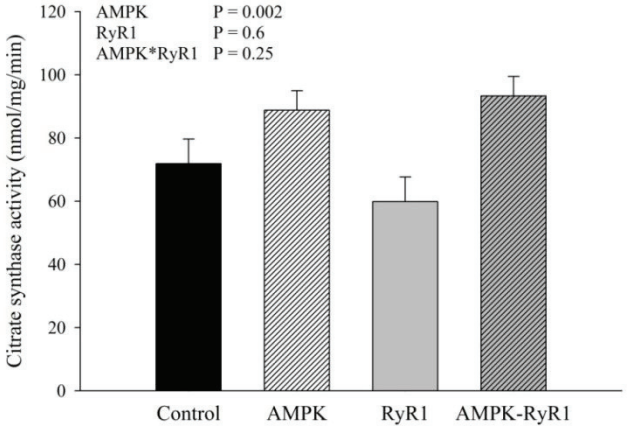

C.

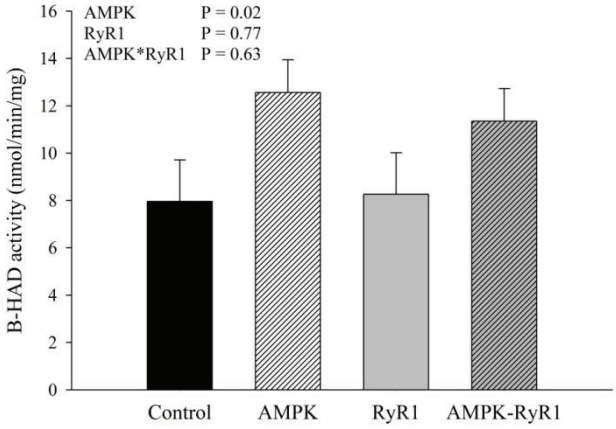

Figure 6-2. AMPKγ3^{R200Q} increases activity of key oxidative enzymes in longissimus muscle. (A) Muscle histological sections stained for succinate dehydrogenase activity. Activity of (B) citrate synthase and (C) β-hydroxyacyl coA dehydrogenase (β-HAD) assessed in muscle homogenates. AMPK genotype significantly ($P<0.05$) influences citrate synthase and β-HAD activity. Data are means ± SE (n = 5-6 pigs per genotype).

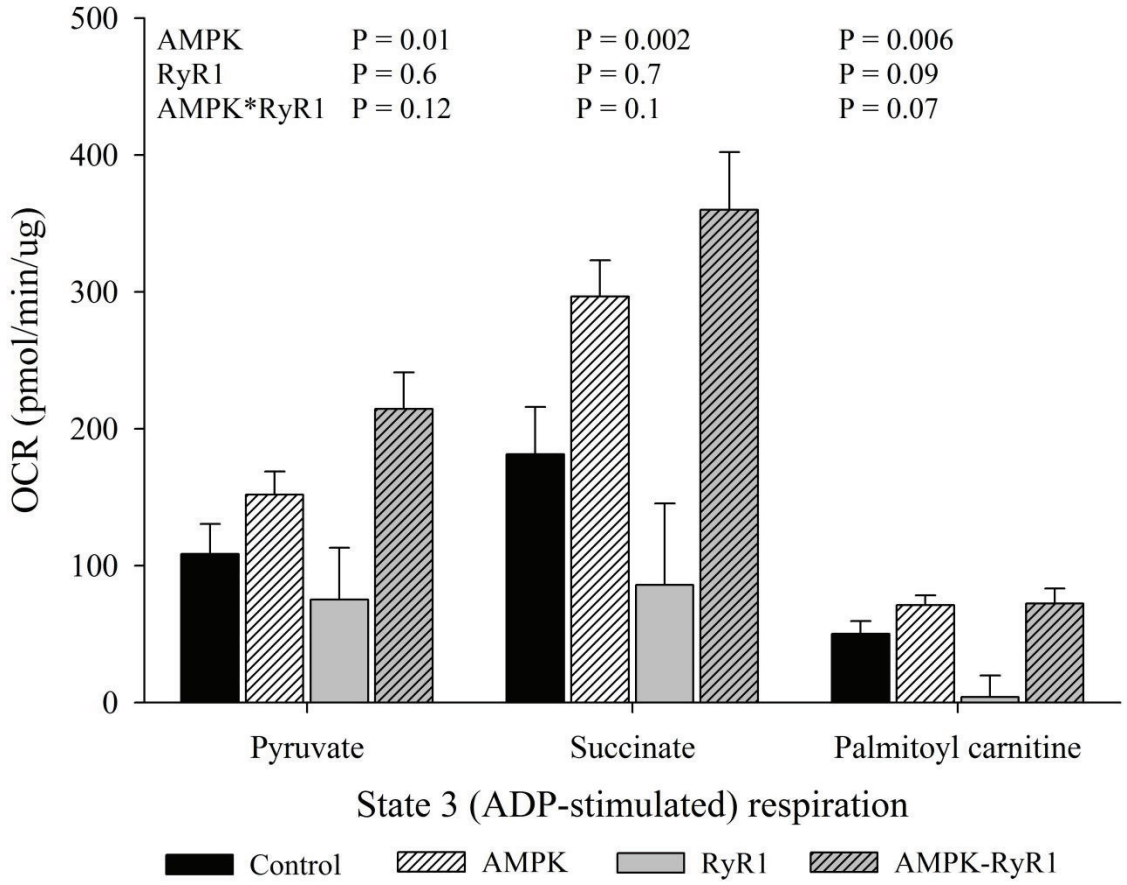

Figure 6-3. AMPKγ3^{R200Q} increases state 3 respiration in isolated mitochondria. Oxygen consumption rate (OCR) was measured in isolated mitochondria from longissimus muscle. Assessment of state 3 (active, maximum phosphorylating) respiration through complex I was determined in the presence of pyruvate, malate, and ADP. Complex II-driven respiration was determined in the presence of succinate and ADP, and rotenone was used to block complex I. Evaluation of β-oxidation and electron transport function was made in the presence of palmitoyl carnitine, malate, and ADP. Data are means ± SE.

Genotype	RCR
Control	2.33 ± 0.5
AMPK	2.76 ± 0.4
RyR1	1.92 ± 0.8
AMPK-RyR1	3.60 ± 0.6

Table 6-1. Respiratory control ratio (RCR) values of isolated mitochondria from different pig genotypes. Values represent the ratio of oxygen consumption rate in (OCR) the presence of ADP, pyruvate and malate (state 3) to OCR after addition of the ATP synthase inhibitor, oligomycin. Data are means ± SE.

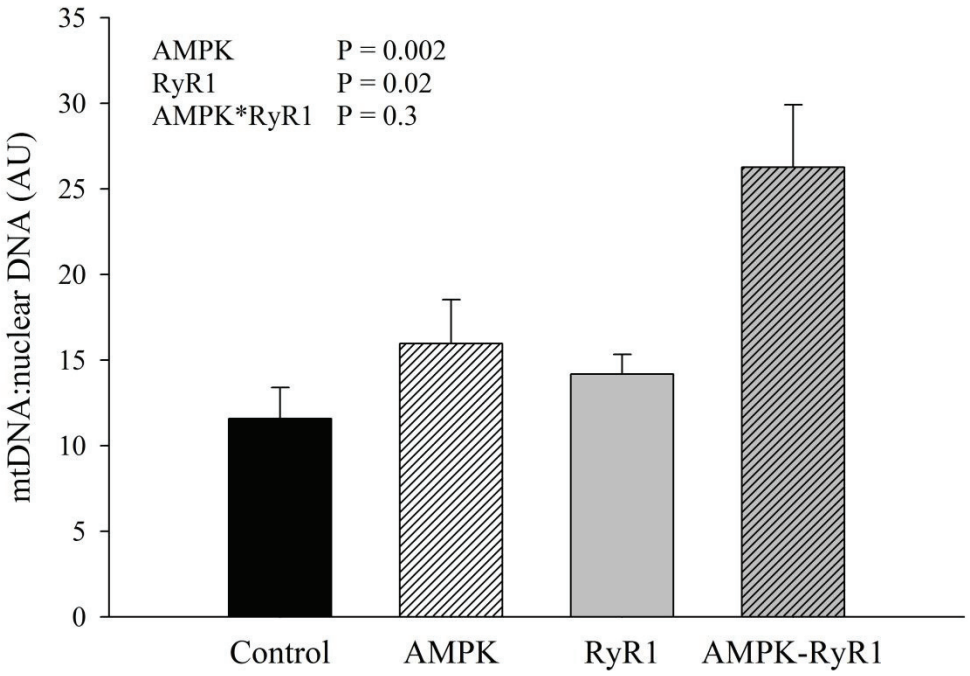

Figure 6-4. Mitochondrial DNA (mtDNA) content of longissimus muscle from control and AMPK^{R200Q} and RyR1^{R615C} mutant pigs. Mitochondrial content was estimated using the ratio of copy number of mitochondrial DNA versus nuclear DNA (β-actin). There were significant main effects of AMPK and RyR1 genotype (n = 3-5 pigs per genotype).

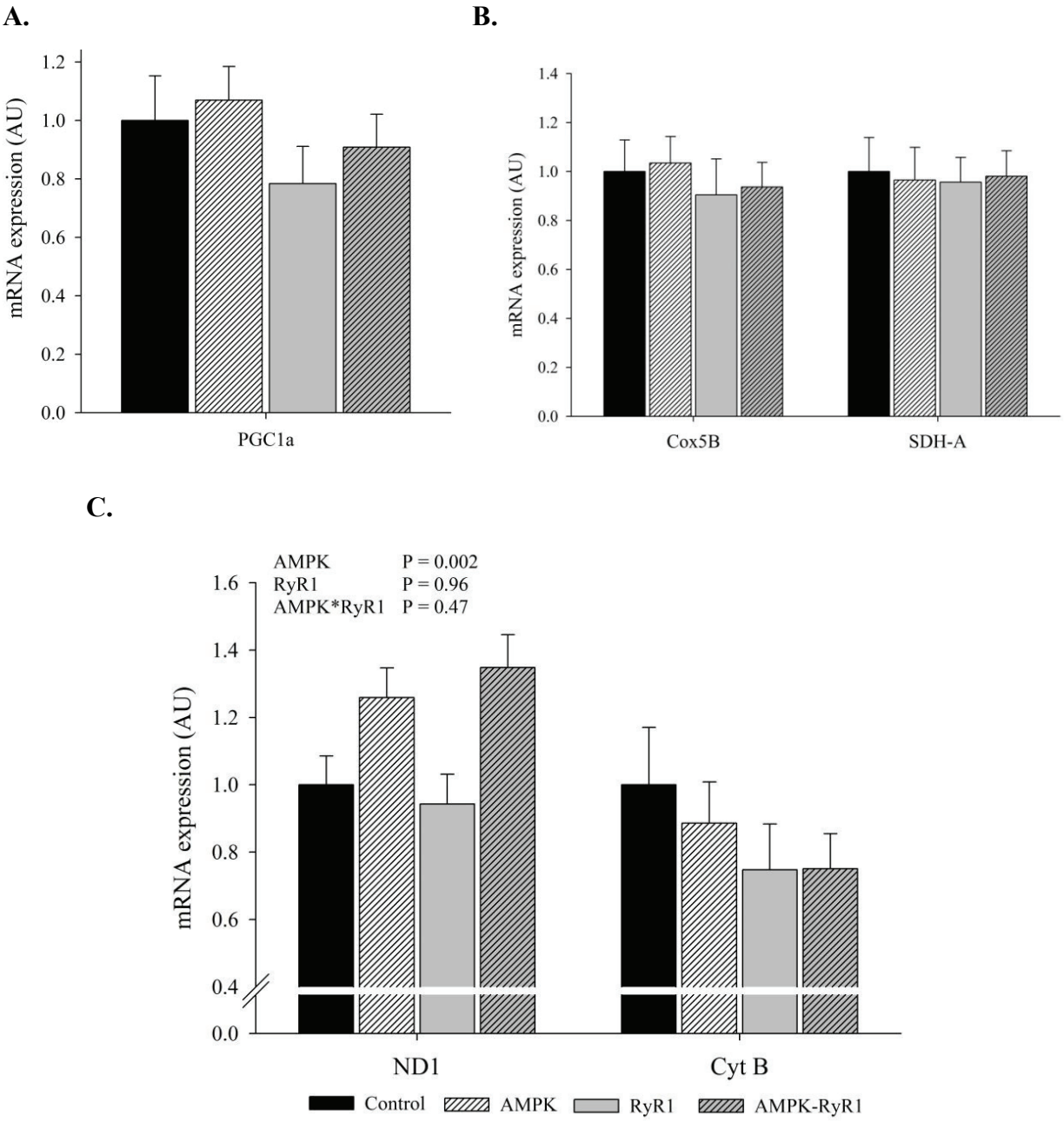

Figure 6-5. Transcript levels of key regulators of mitochondrial biogenesis and nuclear DNA- and mitochondrial DNA-encoded proteins. Transcript levels of each gene were normalized to eukaryotic translation elongation factor 1 alpha 1 (eEF1a1) and expressed relative to control. Transcript levels of (A) mitochondrial biogenesis regulator, PGC1α; (B) nuclear-encoded proteins, Cox5B and SDH-A; and (C) mitochondrial-encoded proteins ND1 and Cyt B. Abbreviations used are PGC1a, peroxisome proliferator activated receptor γ coactivator 1α; TFAM, mitochondrial transcription factor A; Cox5B, cytochrome c oxidase subunit 5B; SDH-A, succinate dehydrogenase A; ND1, NADH dehydrogenase subunit 1; and Cyt B, cytochrome B. Main effects of genotype were significant for TFAM and ND1 and are indicated above the bars for that gene. (n = 7-12 pigs per genotype).

A.

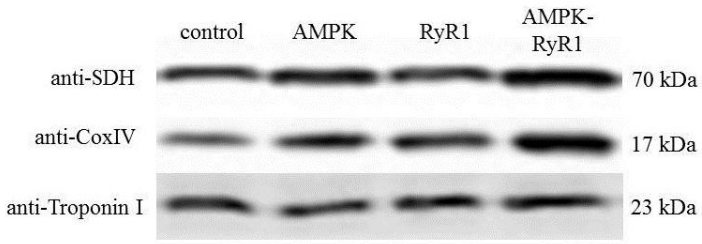

B.

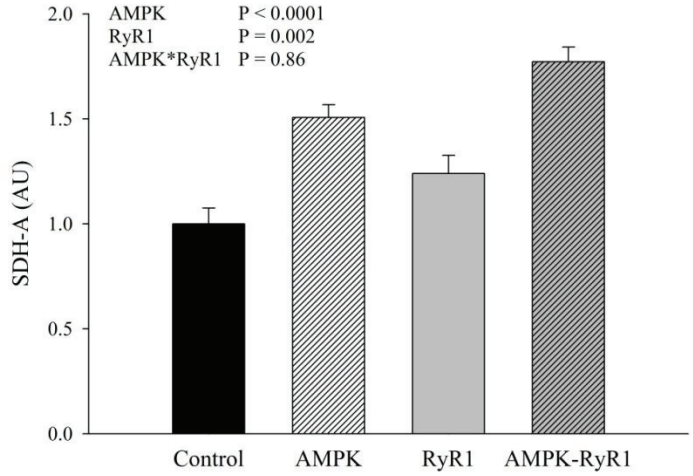

C.

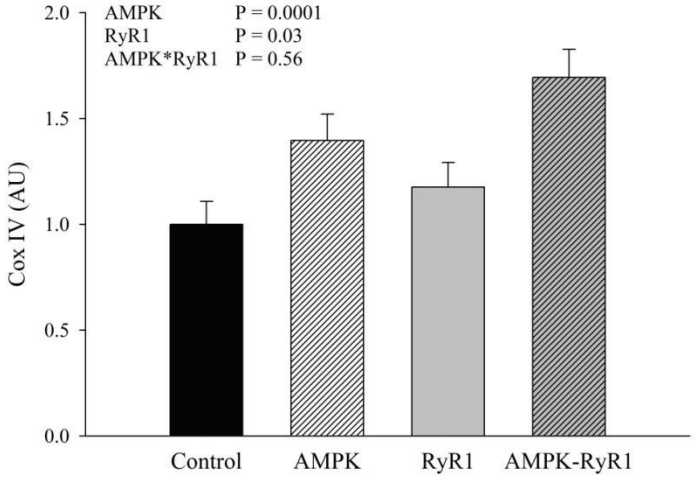

Figure 6-6. Mitochondrial protein expression in longissimus muscle. (A) Representative immunoblots for mitochondrial proteins and troponin I. Troponin I was not different between genotypes. Levels of (B) succinate dehydrogenase subunit A (SDH) and (C) cytochrome c oxidase subunit IV (CoxIV) quantified by Western blotting. There were significant ($P<0.05$) main effects of AMPK and RyR1 genotype. (n = 7-11 pigs per genotype)

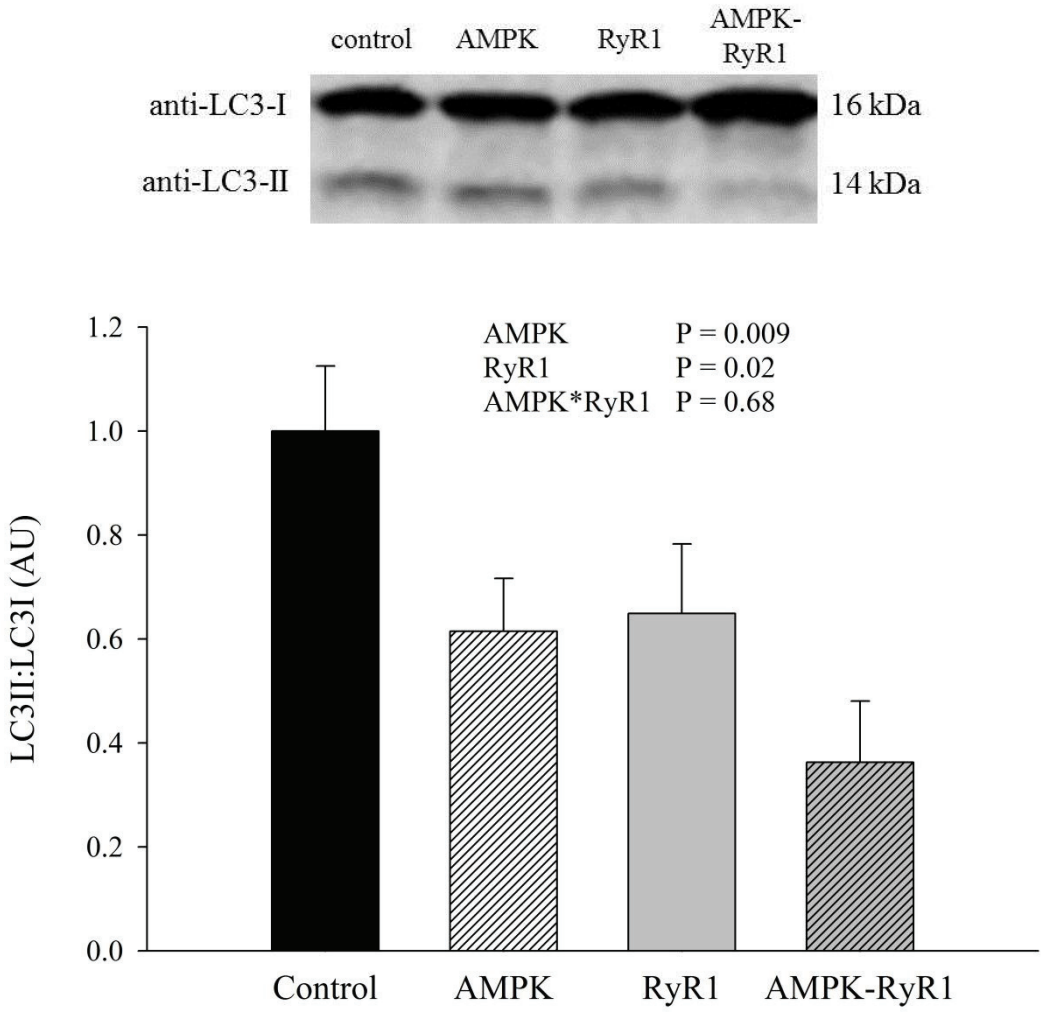

Figure 6-7. Ratio of LC3-II to LC3-I in longissimus muscle from AMPKγ3 and RyR1 genotypes. Microtubule associated protein light chain 3 (LC3) is involved in autophagic flux. Pro-LC3 is cleaved, generating the cytosolic 16 kDa LC3-I form. Addition of phosphatidylethanolamine produces LC3-II, which associates with the autophagosome and is subsequently degraded during autophagy. Greater proportion of LC3-II:LC3-I suggests greater activation of autophagy.

References

Adhihetty, P. J., V. Ljubicic, K. J. Menzies, and D. A. Hood. 2005. Differential susceptibility of subsarcolemmal and intermyofibrillar mitochondria to apoptotic stimuli. Am. J. Physiol. Cell Physiol. 289: C994-C1001.

Atherton, P. J., J. Babraj, K. Smith, J. Singh, M. J. Rennie, and H. Wackerhage. 2005. Selective activation of AMPK-PGC-1α or PKB-TSC2-mTOR signaling can explain specific adaptive responses to endurance or resistance training-like electrical muscle stimulation. FASEB J. 19: 786-788.

Bai, R. K., C. L. Perng, C. H. Hsu, and L. J. Wong. 2004. Quantitative PCR analysis of mitochondrial DNA content in patients with mitochondrial disease. Ann. N. Y. Acad. Sci. 1011: 304-309.

Barnes, B. R., S. Marklund, T. L. Steiler, M. Walter, G. Hjalm, V. Amarger, M. Mahlapuu, Y. Leng, C. Johansson, D. Galuska, K. Lindgren, M. Abrink, D. Stapleton, J. R. Zierath, and L. Andersson. 2004. The 5'-AMP-activated protein kinase γ3 isoform has a key role in carbohydrate and lipid metabolism in glycolytic skeletal muscle. J. Biol. Chem. 279: 38441-38447.

Bodine, S. C., T. N. Stitt, M. Gonzalez, W. O. Kline, G. L. Stover, R. Bauerlein, E. Zlotchenko, A. Scrimgeour, J. C. Lawrence, D. J. Glass, and G. D. Yancopoulos. 2001. Akt/mTOR pathway is a crucial regulator of skeletal muscle hypertrophy and can prevent muscle atrophy in vivo. Nat. Cell Biol. 3: 1014-1019.

Brini, M., S. Manni, N. Pierobon, G. G. Du, P. Sharma, D. H. MacLennan, and E. Carafoli. 2005. Ca^{2+} signaling in HEK-293 and skeletal muscle cells expressing recombinant ryanodine receptors harboring malignant hyperthermia and central core disease mutations. J. Biol. Chem. 280: 15380-15389.

Camello-Almaraz, C., P. J. Gomez-Pinilla, M. J. Pozo, and P. J. Camello. 2006. Mitochondrial reactive oxygen species and Ca2+ signaling. Am. J. Physiol. Cell Physiol. 291: C1082-1088.

Campion, D. R., J. C. Olson, D. G. Topel, L. L. Christian, and D. L. Kuhlers. 1975. Mitochondrial traits of muscle from stress-susceptible pigs. J. Anim. Sci. 41: 1314-1317.

Capes, E. M., R. Loaiza, and H. H. Valdivia. 2011. Ryanodine receptors. Skelet. Muscle 1: 18.

Carr, C. C., J. B. Morgan, E. P. Berg, S. D. Carter, and F. K. Ray. 2006. Growth performance, carcass composition, quality, and enhancement treatment of fresh pork identified through deoxyribonucleic acid marker-assisted selection for the Rendement Napole gene. J. Anim. Sci. 84: 910-917.

Cherel, P., J. Pires, J. Glenisson, D. Milan, N. Iannuccelli, F. Herault, M. Damon, and P. Le Roy. 2011. Joint analysis of quantitative trait loci and major-effect causative mutations affecting meat quality and carcass composition traits in pigs. BMC Genet 12: 76.

Coffey, V. G., Z. Zhong, A. Shield, B. J. Canny, A. V. Chibalin, J. R. Zierath, and J. A. Hawley. 2006. Early signaling responses to divergent exercise stimuli in skeletal muscle from well-trained humans. FASEB J. 20: 190-192.

Cogswell, A. M., R. J. Stevens, and D. A. Hood. 1993. Properties of skeletal muscle mitochondria isolated from subsarcolemmal and intermyofibrillar regions. Am. J. Physiol. 264: C383-389.

Copenhafer, T. L., B. T. Richert, A. P. Schinckel, A. L. Grant, and D. E. Gerrard. 2006. Augmented postmortem glycolysis does not occur early postmortem in AMPKγ3-mutated porcine muscle of halothane positive pigs. Meat Sci. 73: 590-599.

Costford, S. R., N. Kavaslar, N. Ahituv, S. N. Chaudhry, W. S. Schackwitz, R. Dent, L. A. Pennacchio, R. McPherson, and M. E. Harper. 2007. Gain-of-function R225W mutation in human AMPKγ3 causing increased glycogen and decreased triglyceride in skeletal muscle. PLoS ONE 2: e903.

Essen-Gustavsson, B., K. Karlstrom, and K. Lundstrom. 1992. Muscle fibre characteristics and metabolic response at slaughter in pigs of different halothane genotypes and their relation to meat quality. Meat Sci. 31: 1-11.

Fan, M., J. Rhee, J. St-Pierre, C. Handschin, P. Puigserver, J. Lin, S. Jaeger, H. Erdjument-Bromage, P. Tempst, and B. M. Spiegelman. 2004. Suppression of mitochondrial respiration through recruitment of p160 myb binding protein to PGC-1α: modulation by p38 MAPK. Genes Dev. 18: 278-289.

Feng, W., G. C. Barrientos, G. Cherednichenko, T. Yang, I. T. Padilla, K. Truong, P. D. Allen, J. R. Lopez, and I. N. Pessah. 2011. Functional and biochemical properties of ryanodine receptor type 1 channels from heterozygous R163C malignant hyperthermia-susceptible mice. Mol. Pharmacol. 79: 420-431.

Fujii, J., K. Otsu, F. Zorzato, S. D. Leon, V. K. Khanna, J. E. Weiler, P. J. O'Brien, and D. H. MacLennan. 1991. Identification of a mutation in porcine ryanodine receptor associated with malignant hyperthermia. Science 253: 448-451.

Garcia-Roves, P. M., M. E. Osler, M. H. Holmstrom, and J. R. Zierath. 2008. Gain-of-function R225Q mutation in AMP-activated protein kinase γ3 subunit increases mitochondrial biogenesis in glycolytic skeletal muscle. J. Biol. Chem. 283: 35724-35734.

Geng, T., P. Li, M. Okutsu, X. Yin, J. Kwek, M. Zhang, and Z. Yan. 2010. PGC-1α plays a functional role in exercise-induced mitochondrial biogenesis and angiogenesis but not fiber-type transformation in mouse skeletal muscle. Am. J. Physiol. Cell Physiol. 298: C572-579.

Giulivi, C., C. Ross-Inta, A. Omanska-Klusek, E. Napoli, D. Sakaguchi, G. Barrientos, P. D. Allen, and I. N. Pessah. 2011. Basal bioenergetic abnormalities in skeletal muscle from ryanodine receptor malignant hyperthermia susceptible R163C knock-in mice. J. Biol. Chem. 286: 99-113.

Granlund, A., O. Kotova, B. Benziane, D. Galuska, M. Jensen-Waern, A. V. Chibalin, and B. Essén-Gustavsson. 2010. Effects of exercise on muscle glycogen synthesis signalling and enzyme activities in pigs carrying the PRKAG3 mutation. Exp. Physiol. 95: 541-549.

Haddad, F., and G. R. Adams. 2004. Inhibition of MAP/ERK kinase prevents IGF-I-induced hypertrophy in rat muscles. J. Appl. Physiol. 96: 203-210.

Handschin, C., J. Rhee, J. Lin, P. T. Tarr, and B. M. Spiegelman. 2003. An autoregulatory loop controls peroxisome proliferator-activated receptor gamma coactivator 1α expression in muscle. Proc. Natl. Acad. Sci. USA 100: 7111-7116.

Hickson, R. C. 1980. Interference of strength development by simultaneously training for strength and endurance. Eur. J. Appl. Physiol. Occup. Physiol. 45: 255-263.

Hirner, S., C. Krohne, A. Schuster, S. Hoffmann, S. Witt, R. Erber, C. Sticht, A. Gasch, S. Labeit, and D. Labeit. 2008. MuRF1-dependent regulation of systemic carbohydrate metabolism as revealed from transgenic mouse studies. J. Mol. Biol. 379: 666-677.

Inoki, K., T. Zhu, and K. L. Guan. 2003. TSC2 mediates cellular energy response to control cell growth and survival. Cell 115: 577-590.
Irrcher, I., V. Ljubicic, A. F. Kirwan, and D. A. Hood. 2008. AMP-activated protein kinase-regulated activation of the PGC-1α promoter in skeletal muscle cells. PLoS ONE 3: e3614.
Jiang, D., W. Chen, J. Xiao, R. Wang, H. Kong, P. P. Jones, L. Zhang, B. Fruen, and S. R. Chen. 2008. Reduced threshold for luminal Ca^{2+} activation of RyR1 underlies a causal mechanism of porcine malignant hyperthermia. J. Biol. Chem. 283: 20813-20820.
Kabeya, Y., N. Mizushima, T. Ueno, A. Yamamoto, T. Kirisako, T. Noda, E. Kominami, Y. Ohsumi, and T. Yoshimori. 2000. LC3, a mammalian homologue of yeast Apg8p, is localized in autophagosome membranes after processing. EMBO J. 19: 5720-5728.
Kim, J., M. Kundu, B. Viollet, and K. L. Guan. 2011. AMPK and mTOR regulate autophagy through direct phosphorylation of Ulk1. Nat. Cell Biol. 13: 132-141.
Klont, R. E., E. Lambooy, and J. G. van Logtestijn. 1994. Effect of dantrolene treatment on muscle metabolism and meat quality of anesthetized pigs of different halothane genotypes. J. Anim. Sci. 72: 2008-2016.
Koyama, S., S. Hata, C. C. Witt, Y. Ono, S. Lerche, K. Ojima, T. Chiba, N. Doi, F. Kitamura, K. Tanaka, K. Abe, S. H. Witt, V. Rybin, A. Gasch, T. Franz, S. Labeit, and H. Sorimachi. 2008. Muscle RING-finger protein-1 (MuRF1) as a connector of muscle energy metabolism and protein synthesis. J. Mol. Biol. 376: 1224-1236.
Lanner, J. T., D. K. Georgiou, A. D. Joshi, and S. L. Hamilton. 2010. Ryanodine receptors: structure, expression, molecular details, and function in calcium release. Cold Spring Harb Perspect Biol 2: a003996.
Lantier, L., R. Mounier, J. Leclerc, M. Pende, M. Foretz, and B. Viollet. 2010. Coordinated maintenance of muscle cell size control by AMP-activated protein kinase. FASEB J. 24: 3555-3561.
Ljubicic, V., P. Miura, M. Burt, L. Boudreault, S. Khogali, J. A. Lunde, J. M. Renaud, and B. J. Jasmin. 2011. Chronic AMPK activation evokes the slow, oxidative myogenic program and triggers beneficial adaptations in mdx mouse skeletal muscle. Hum. Mol. Genet. 20: 3478-3493.
MacLennan, D. H., and M. S. Phillips. 1992. Malignant hyperthermia. Science 256: 789-794.
Mahlapuu, M., C. Johansson, K. Lindgren, G. Hjalm, B. R. Barnes, A. Krook, J. R. Zierath, L. Andersson, and S. Marklund. 2004. Expression profiling of the γ-subunit isoforms of AMP-activated protein kinase suggests a major role for γ3 in white skeletal muscle. Am. J. Physiol. Endocrinol. Metab. 286: E194-200.
Mickelson, J. R., E. M. Gallant, L. A. Litterer, K. M. Johnson, W. E. Rempel, and C. F. Louis. 1988. Abnormal sarcoplasmic reticulum ryanodine receptor in malignant hyperthermia. J. Biol. Chem. 263: 9310-9315.
Mickelson, J. R., E. M. Gallant, W. E. Rempel, K. M. Johnson, L. A. Litterer, B. A. Jacobson, and C. F. Louis. 1989. Effects of the halothane-sensitivity gene on sarcoplasmic reticulum function. Am. J. Physiol. 257: C787-794.
Mizushima, N., and T. Yoshimori. 2007. How to interpret LC3 immunoblotting. Autophagy 3: 542-545.
Mizushima, N., T. Yoshimori, and B. Levine. 2010. Methods in mammalian autophagy research. Cell 140: 313-326.

Muller, W. 1976. Subsarcolemmal mitochondria and capillarization of soleus muscle fibers in young rats subjected to an endurance training. A morphometric study of semithin sections. Cell Tissue Res. 174: 367-389.

Pankiv, S., T. H. Clausen, T. Lamark, A. Brech, J. A. Bruun, H. Outzen, A. Overvatn, G. Bjorkoy, and T. Johansen. 2007. p62/SQSTM1 binds directly to Atg8/LC3 to facilitate degradation of ubiquitinated protein aggregates by autophagy. J. Biol. Chem. 282: 24131-24145.

Park, S., T. L. Scheffler, A. M. Gunawan, H. Shi, C. Zeng, K. M. Hannon, A. L. Grant, and D. E. Gerrard. 2009. Chronic elevated calcium blocks AMPK-induced GLUT-4 expression in skeletal muscle. Am. J. Physiol. Cell Physiol. 296: C106-115.

Pette, D., and R. S. Staron. 2001. Transitions of muscle fiber phenotypic profiles. Histochem. Cell Biol. 115: 359-372.

Puigserver, P., J. Rhee, J. Lin, Z. Wu, J. C. Yoon, C. Y. Zhang, S. Krauss, V. K. Mootha, B. B. Lowell, and B. M. Spiegelman. 2001. Cytokine stimulation of energy expenditure through p38 MAP kinase activation of PPARgamma coactivator-1. Mol. Cell 8: 971-982.

Rasmussen, U. F., H. N. Rasmussen, A. J. Andersen, P. Fogd Jorgensen, and B. Quistorff. 1996. Characterization of mitochondria from pig muscle: higher activity of exo-NADH oxidase in animals suffering from malignant hyperthermia. Biochem. J. 315 (Pt 2): 659-663.

Shang, L., S. Chen, F. Du, S. Li, L. Zhao, and X. Wang. 2011. Nutrient starvation elicits an acute autophagic response mediated by Ulk1 dephosphorylation and its subsequent dissociation from AMPK. Proc. Natl. Acad. Sci. USA 108: 4788-4793.

Shi, H., J. M. Scheffler, J. M. Pleitner, C. Zeng, S. Park, K. M. Hannon, A. L. Grant, and D. E. Gerrard. 2008. Modulation of skeletal muscle fiber type by mitogen-activated protein kinase signaling. FASEB J. 22: 2990-3000.

Shi, H., C. Zeng, A. Ricome, K. M. Hannon, A. L. Grant, and D. E. Gerrard. 2007. Extracellular signal-regulated kinase pathway is differentially involved in β-agonist-induced hypertrophy in slow and fast muscles. Am. J. Physiol. Cell Physiol. 292: C1681-1689.

van Wessel, T., A. de Haan, W. van der Laarse, and R. Jaspers. 2010. The muscle fiber type–fiber size paradox: hypertrophy or oxidative metabolism? Eur. J. Appl. Physiol. 110: 665-694.

Wang, Y. X., C. L. Zhang, R. T. Yu, H. K. Cho, M. C. Nelson, C. R. Bayuga-Ocampo, J. Ham, H. Kang, and R. M. Evans. 2004. Regulation of muscle fiber type and running endurance by PPARδ. PLoS Biol. 2: e294.

Wenz, T., F. Diaz, B. M. Spiegelman, and C. T. Moraes. 2008. Activation of the PPAR/PGC-1α pathway prevents a bioenergetic deficit and effectively improves a mitochondrial myopathy phenotype. Cell Metab. 8: 249-256.

Wenz, T., S. G. Rossi, R. L. Rotundo, B. M. Spiegelman, and C. T. Moraes. 2009. Increased muscle PGC-1α expression protects from sarcopenia and metabolic disease during aging. Proc. Natl. Acad. Sci. USA 106: 20405-20410.

Werner, C., R. Natter, K. Schellander, and M. Wicke. 2010. Mitochondrial respiratory activity in porcine longissimus muscle fibers of different pig genetics in relation to their meat quality. Meat Sci. 85: 127-133.

Wibom, R., E. Hultman, M. Johansson, K. Matherei, D. Constantin-Teodosiu, and P. G. Schantz. 1992. Adaptation of mitochondrial ATP production in human skeletal muscle to endurance training and detraining. J. Appl. Physiol. 73: 2004-2010.

Williams, R. S. 1986. Mitochondrial gene expression in mammalian striated muscle. Evidence that variation in gene dosage is the major regulatory event. J. Biol. Chem. 261: 12390-12394.

Williams, R. S., S. Salmons, E. A. Newsholme, R. E. Kaufman, and J. Mellor. 1986. Regulation of nuclear and mitochondrial gene expression by contractile activity in skeletal muscle. J. Biol. Chem. 261: 376-380.

Zong, H., J. M. Ren, L. H. Young, M. Pypaert, J. Mu, M. J. Birnbaum, and G. I. Shulman. 2002. AMP kinase is required for mitochondrial biogenesis in skeletal muscle in response to chronic energy deprivation. Proc. Natl. Acad. Sci. USA 99: 15983-15987.